Cellular Interaction in Cell-based Cartilage Repair

Yao Fu

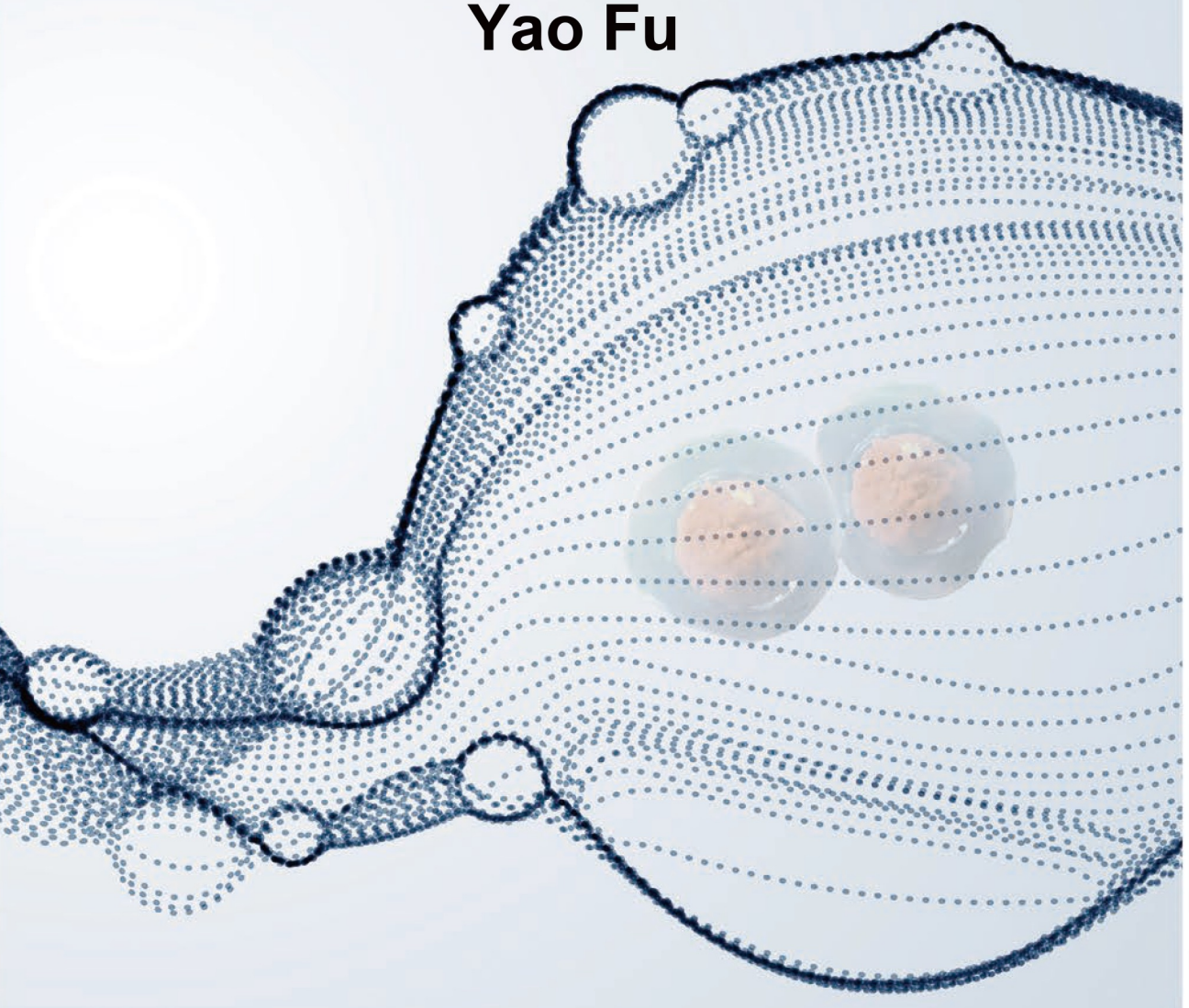

CELLULAR INTERACTIONS IN CELL-BASED CARTILAGE REPAIR

Yao Fu

This dissertation has been approved by:

Supervisor
prof. dr. ir. H.B.J. Karperien

Co-supervisors:
dr. S.K. Both
dr. B. Zoetebier

Cover design: Yao Fu. The numbers of each chapter were draw by Mengya Jiao. The abstract vector particles shape and Stem cells of the thesis cover were designed by Sylverarts Vectors and Yurchanka Siarhei from Shutterstock (www.shuttertock.com).
Printed by: Ipskampprinting
ISBN: 978-90-365-5290-5
DOI: 10.3990/1.9789036552905

CELLULAR INTERACTIONS IN CELL-BASED CARTILAGE REPAIR

DISSERTATION

to obtain
the degree of doctor at the Universiteit Twente,
on the authority of the rector magnificus,
prof. dr. ir. A. Veldkamp,
on account of the decision of the Doctorate Board
to be publicly defended
on Wednesday 10 November 2021 at 12.45 hours

by

Yao Fu

born on the 24th of March, 1989
in Suzhou, P.R.China

Graduation Committee:

Chair / secretary:	prof.dr. J.L. Herek
Supervisor:	prof.dr.ir. H.B.J. Karperien
Co-supervisors:	dr. S.K. Both dr. B. Zoetebier

Committee Members:

Prof. Dr. A. Kocer (University of Twente)

Prof. Dr. M.C. Kruijt (University of Twente)

Prof. Dr. A. Van Wijnen (University of Vermont)

Prof. Dr. T. Welting (University of Maastricht)

Dr. L. Vonk (Co.Don A.G.)

To my beloved family and Cecilia

虽然他们也没帮上什么忙

Summary

Interactions of cells with their surrounding cells and matrix, which most likely involves cell-cell communication, are vital for successful tissue development and regeneration. These interactions are complex due to the involvement of multiple signaling pathways, such as mediated by gap-junctions, direct cell-cell contacts and growth factor signaling which often simultaneously are activated in the same cell. Understanding the cellular communication mechanisms and the regulation of complex intercellular interactions in co-cultures are thus of great importance in cartilage tissue regeneration. To mimic the hydrated environment of articular cartilage injectable hydrogels can be used to facilitate cell proliferation, differentiation, and matrix production by encapsulated cells. Moreover, a hybrid injectable hydrogel can combine multiple functionalities, such as tunable physical properties, proteolytic degradation properties, and enhanced extracellular matrix production, into one gel system. Therefore, the optimal concentration and the ratio of polymers-based hybrid hydrogels for cell growth and matrix formation are essential for the application of cell encapsulated injectable bio-constructs for cartilage regeneration.

This thesis describes: i) the fundamental knowledge regarding how mesenchymal stem cells act as a mediator in Chondrocyte-MSC co-cultures and how MSCs can regulate cellular behavior and chondro-induction features in co-cultures; ii) potential cell death mechanisms regulating Chondrocyte-MSC co-cultures and the cellular interactions in co-cultures; and iii) the modification of injectable hydrogels with optimal hybrid polymers and encapsulated cells to improve upon cartilage regeneration strategies.

In Chapter 3, we selected a panel of MSCs from 18 distinct donors and investigated their propensity to undergo chondrogenesis. Monoculture and co-culture pellets were formed to sketch inter-donor variability and to evaluate whether the beneficial effect of the MSCs is relying on their donor variation. After four weeks, species-specific qPCR analysis of human GAPDH demonstrated the near-complete loss of MSCs in all the co-culture pellets. However, enhanced cartilage matrix deposition in co-culture groups was confirmed by histology staining and GAG quantification assay. Besides, although widely distributed among different donors, average bovine chondrogenic mRNA was expressed higher compared to the pure bCH group. Moreover, both the matrix formation and GAG content show no correlation with donor variation of MSCs. Together with previous results, these results demonstrate

that the beneficial effects of MSC in the chondrocyte-MSC co-cultures are a general phenomenon independent of MSCs donor variation, culture conditions, and the origin of the MSCs. To further investigate the mechanism underlying this observation, in Chapter 4, we tested whether the beneficial effect of the MSCs was dependent on intercellular communication. For this work, we utilized a micro-aggregates system formed through a high throughput platform to study cellular interaction during the co-cultures. Enhanced cartilage matrix deposition was confirmed in micro-aggregates encapsulated constructs and direct MSC-Chondrocyte contact co-cultures. Via the indirect cell-cell contact, it was observed that the presence of MSCs promotes the proliferation of chondrocytes in the co-cultures. Simultaneously preferential apoptosis of MSCs was induced through indirect MSC-Chondrocyte contact. Besides, cell viability was increased significantly in the direct cell-cell contact environment. Based on the data from Chapter 4, we concluded that both direct and indirect MSC-Chondrocyte contact is involved in the cellular behavior changes in micro-aggregate co-cultures. Direct MSC-Chondrocyte contact maintains the cell proliferation and consequently promotes matrix production, which is essential for increased chondro-induction in co-cultures.

In Chapter 4, along with previous studies, we showed that MSCs in co-cultures disappeared over time. In Chapter 5, we set up experiments to elucidate the mechanism. Monoculture and co-culture pellets were cultured for seven days in chondrocyte proliferation media in hypoxia conditions. RNA sequencing was performed to assess differences in gene expression between monocultures and co-culture. The expression level of Caspase-3, LC3B, and P62 were quantified by immune fluorescence assays. RNA sequencing revealed significant up-regulation of more than 90 genes in the co-cultures when compared to monocultures. Remarkably, 75% of these genes play a role in cell death pathways, such as apoptosis and autophagy. Moreover, immunofluorescence results show an evident up-regulation of the autophagic machinery while there is no substantial activation of the apoptotic pathway. To further investigate the autophagic activity in the co-cultures, different cell conditions cultured in a starvation environment were exposed to different inhibitors and activators of the apoptotic and autophagic pathways in Chapter 6. The enhanced protein expression level of autophagy markers in the MSCs monoculture was confirmed by western blot and immunofluorescence staining. This result indicated that the starvation environment induces autophagy in the MSCs, which

can be regulated by chemical stimuli. Meanwhile, chondrocytes responded differently to the surrounding environment and external chemical stimuli. The results indicated that autophagy in chondrocytes was not utterly actived by the starvation condition. However, in the starvation environment, the co-culture did not induce the autophagy pathway as rarely protein expression was observed despite that the majority of cells consisted of MSCs. On the contrary, intercellular interaction in the co-cultures of chondrocytes and MSCs down-regulated the autophagic activity in each cell. Furthermore, interaction between the cells modified impact of cell death pathways modulators when compared with their effect in monocultures. Results from these chapters indicated that in co-cultures in hypoxia the autophagy pathway is mostly activated while in the starvation environment, both apoptosis and autophagy appear to be involved in cell death. We propose that this sacrificial cell death may contribute to the trophic effects of MSCs on cartilage formation.

To further investigate the application of a cell-based injectable hydrogel for a cartilage regenerative approach, in Chapter 7, different ratios of Hyaluronic acid (HA)- and dextran (Dex)-based hybrid hydrogels at both 10%w/v and 5%w/v were prepared with a designed mold to investigate the property changes and their effects on the cellular behavior and cartilage matrix formation. The results from this chapter indicated that the rheology and compression analysis indicated that 5%w/v hydrogels laden with cells exhibit a significant increase in the mechanical properties after 21 days. Based on the data from Chapter 7, we concluded that 5%w/v HA and Dex hybrid hydrogels with a higher concentration of Dextran-TA were demonstrated to provide a mechanically stable environment, maintain the cell viability, and promote the cartilaginous specific matrix deposition *in vitro*. 5%w/v hybrid hydrogels were then combined with different types of cells and subcutaneously implanted in the back of male and female nude rats to assess the biocompatibility and safety of cells encapsulated hydrogels in Chapter 8. Subcutaneous implantation of these biomaterials revealed highly satisfactory results since the histology evidenced the integration of the gels within the host tissue with no sign of acute or chronic inflammatory response. Enhanced tissue invasion and some giant cells infiltration were observed in the HA/Dex hydrogels with encapsulated monoculture cells. Moreover, Chondrocyte-MSC co-cultures show beneficial interaction with the biomaterials, for instance be enhancing cell proliferation and matrix deposition. Taken together all these results, along with

previous data, we concluded that 5%w/v hydrogels with a higher concentration of Dextran-TA encapsulated with Chondrocyte-MSC co-cultures are adequate for injectable applications and *in situ* cell delivery in cartilage regeneration approaches. Besides, in this work, gender difference shows an impact on the performance of chondrocytes encapsulated HA/Dextran-TA hydrogels.

Together, this thesis introduces a set of cellular interactions investigation and innovative hybrid injectable hydrogel modifications. The findings presented in this thesis could facilitate the development of new therapeutic strategies and contribute to the clinical translation of cartilage tissue engineering applications.

Samenvatting

Interacties van cellen met de omringende cellen en matrix, die hoogstwaarschijnlijk cel-cel communicatie met zich meebrengt, zijn van vitaal belang voor een succesvolle weefselontwikkeling en regeneratie. Deze interacties zijn complex vanwege de betrokkenheid van meerdere signaalroutes, zoals gemedieerd door gap-junctions, directe cel-celcontacten en groeifactorsignalering die vaak gelijktijdig in dezelfde cel worden geactiveerd. Het begrijpen van de cellulaire communicatiemechanismen en de regulering van complexe intercellulaire interacties in co-culturen zijn dus van groot belang bij de regeneratie van kraakbeenweefsel. Ondertussen wordt bij onderzoek naar regeneratie van kraakbeenweefsel de injecteerbare hydrogel gebruikt om de gehydrateerde omgeving van gewrichtskraakbeen na te bootsen en celproliferatie, differentiatie en matrixproductie door ingekapselde cellen te vergemakkelijken. Bovendien kan een hybride injecteerbare hydrogel meerdere functionaliteiten combineren, zoals afstembare fysische eigenschappen, proteolytische afbraakeigenschappen en verbeterde extracellulaire matrixproductie, tot één gelsysteem. Daarom zijn de optimale concentratie en de verhouding van op polymeren gebaseerde hybride hydrogels voor celgroei en matrixvorming essentieel voor de toepassing van in cellen ingekapselde injecteerbare bio-constructen voor kraakbeenregeneratie.

Dit proefschrift beschrijft: i) de fundamentele kennis over hoe mesenchymale stamcellen optreden als mediator in co-culturen van Chondrocyte-MSC en hoe MSC's cellulair gedrag en chondro-inductie-eigenschappen in co-culturen kunnen reguleren; ii) mogelijke celdoodmechanismen die Chondrocyte-MSC-co-culturen en de cellulaire interacties in co-culturen reguleren; en iii) de modificatie van injecteerbare hydrogels met optimale hybride polymeren en ingekapselde cellen om de kraakbeenregeneratiestrategieën te verbeteren.

In hoofdstuk 3 selecteerden we een panel van MSC's van 18 verschillende donoren en onderzochten ze hun neiging om chondrogenese te ondergaan. Er werden monocultuur- en co-kweekpellets gevormd om de variabiliteit tussen donoren te schetsen en om te evalueren of het gunstige effect van de MSC's afhankelijk is van de donorvariatie. Na vier weken toonde soortspecifieke qPCR-analyse van humaan GAPDH het bijna volledige verlies van MSC's in alle co-kweekpellets aan. Verbeterde depositie van kraakbeenmatrix in co-kweekgroepen werd echter bevestigd door histologische kleuring en GAG-kwantificeringstest. Bovendien, hoewel wijd verspreid onder verschillende donoren, werd het chondrogeen mRNA

van runderen gemiddeld hoger uitgedrukt in vergelijking met de groep bestaande uit alleen bCH. Bovendien vertonen zowel de matrixvorming als het GAG-gehalte geen correlatie met donorvariatie van de MSC's. Samen met eerdere resultaten tonen deze resultaten aan dat de gunstige effecten van MSC in de chondrocyten-MSC-co-culturen een algemeen fenomeen zijn dat onafhankelijk is van de donorvariatie van MSC's, kweekomstandigheden of de oorsprong van de MSC's. Om het mechanisme achter deze waarneming verder te onderzoeken, hebben we in hoofdstuk 4 vervolgens getest of het gunstige effect van de MSC's afhankelijk was van intercellulaire communicatie. In dit werk gebruikten we een microaggregaatsysteem gevormd via een platform met hoge doorvoer om cellulaire interactie tijdens de co-culturen te bestuderen. Verbeterde depositie van kraakbeenmatrix werd bevestigd in micro-aggregaten ingekapselde constructen en directe co-culturen van MSC-chondrocyten. Via het indirecte cel-celcontact werd waargenomen dat de aanwezigheid van MSC's de proliferatie van chondrocyten in de co-culturen bevordert. Tegelijkertijd werd preferentiële apoptose van MSC's geïnduceerd door indirect MSC-chondrocytencontact. Bovendien was de levensvatbaarheid van cellen significant verhoogd in de directe cel-cel contactomgeving. Op basis van de gegevens uit hoofdstuk 4 concludeerden we dat zowel direct als indirect MSC-chondrocytencontact betrokken is bij cellulaire gedragsveranderingen in micro-aggregaat co-culturen. Direct MSC-chondrocytcontact houdt de celproliferatie in stand en bevordert daardoor de matrixproductie, wat essentieel is voor verhoogde chondro-inductie in co-culturen.

In hoofdstuk 4 toonden we, zoals ook in eerdere studies, aan dat MSC's in co-culturen in de loop van de tijd verdwenen. In hoofdstuk 5 hebben we experimenten opgezet om het mechanisme op te helderen. Monocultuur- en co-kweekpellets werden gedurende zeven dagen gekweekt in chondrocytproliferatiemedia onder hypoxie-omstandigheden. RNA-sequencing werd uitgevoerd om verschillen in genexpressie tussen monoculturen en co-cultuur te beoordelen. Het expressieniveau van Caspase-3, LC3B en P62 werd gekwantificeerd door middel van immuunfluorescentietests. RNA-sequencing toonde een significante verhoogde regulering van meer dan 90 genen in de co-culturen in vergelijking met monoculturen. Opvallend is dat 75% van deze genen een rol spelen bij celdoodroutes, zoals apoptose en autofagie. Bovendien laten immunofluorescentieresultaten een duidelijke verhoogde regulatie van de autofagische activiteit zien, terwijl er geen substantiële activering van de

apoptotische route is. Om de autofagische activiteit in de co-culturen verder te onderzoeken, werden verschillende celcondities gekweekt in een verhongeringsomgeving blootgesteld aan verschillende remmers en activatoren van de apoptotische en autofagische routes in Hoofdstuk 6. Het verhoogde proteïne-expressieniveau van autofagiemarkers in de MSC-monocultuur werd bevestigd door western blot en immunofluorescentie kleuring. Dit resultaat gaf aan dat de verhongeringsomgeving autofagie induceert in de MSC's, die kan worden gereguleerd door chemische stimuli. Ondertussen reageerden chondrocyten anders op de omgeving en externe chemische stimuli. Dit resultaat geeft aan dat autofagy in chondorcyten niet volledig wordt geactiveerd door de uithongeringsconditie. In de verhongeringsomgeving induceerde de co-cultuur echter niet de autofagieroute, aangezien zelden eiwitexpressie werd waargenomen, ondanks het feit dat de meerderheid van de cellen uit MSC's bestond. Integendeel, intercellulaire interactie in de co-culturen van chondrocyten en MSC's reguleerde de autofagische activiteit in elke cel naar beneden. Bovendien veranderde de interactie tussen de cellen de impact van modulatoren van celdoodroutes in vergelijking met hun effect in monoculturen. De resultaten van deze hoofdstukken gaven aan dat in co-culturen in hypoxie de autofagieroute meestal wordt geactiveerd, terwijl in de verhongeringsomgeving zowel apoptose als autofagie betrokken lijken te zijn bij celdood. We stellen voor dat deze opofferende celdood kan bijdragen aan de trofische effecten van MSC's op de vorming van kraakbeen.

Om de toepassing van een op cellen gebaseerde injecteerbare hydrogel voor regeneratie van kraakbeen verder te onderzoeken, hebben we in hoofdstuk 7 verschillende verhoudingen van een op hyaluronzuur (HA) - en dextran (Dex) gebaseerde hybride hydrogels bij zowel 10% w/v als 5% w/v gemaakt met een ontworpen mal om de veranderingen in eigenschappen en hun effecten op het cellulaire gedrag en de vorming van kraakbeenmatrix te onderzoeken. De resultaten van dit hoofdstuk gaven door middel van reologie en compressieanalyse dat 5% w/v hydrogels beladen met cellen na 21 dagen een significante toename van de mechanische eigenschappen vertoonden. Op basis van de gegevens uit hoofdstuk 7 concludeerden we dat 5% w/v HA en Dex hybride hydrogels met een hogere concentratie Dextran-TA een mechanisch stabiele omgeving bleken te bieden, de levensvatbaarheid van de cellen te behouden en de kraakbeenspecifieke matrixafzetting te bevorderen in vitro. Hybride hydrogels met 5% w/v werden vervolgens gecombineerd met verschillende soorten cellen en subcutaan

geïmplanteerd in de rug van mannelijke en vrouwelijke naakte ratten, om de biocompatibiliteit en veiligheid van in cellen ingekapselde hydrogels in hoofdstuk 8 te beoordelen. Subcutane implantatie van deze biomaterialen leverde zeer bevredigende resultaten op, aangezien de histologie de integratie van de gels in het gastheerweefsel aantoonde zonder tekenen van acute of chronische ontstekingsreactie. Verbeterde weefselinvasie en enkele infiltratie van reuzencellen werden waargenomen in de HA/Dex-hydrogels met ingekapselde monocultuurcellen. Bovendien vertonen chondrocyten-MSC-co-culturen een gunstige interactie met de biomaterialen, bijvoorbeeld door celproliferatie en matrixafzetting te verbeteren. Wanneer al deze resultaten worden samengenomen, in combinatie met eerdere gegevens, dan concludeerden we dat 5% w/v hydrogels met een hogere concentratie van Dextran-TA ingekapseld met Chondrocyte-MSC co-culturen geschikt zijn voor injecteerbare toepassingen en in situ celafgifte bij kraakbeenregeneratiebenaderingen. Bovendien toont het geslachtsverschil in deze studie aan dat dit van invloed is op de prestaties van in chondrocyten ingekapselde HA/Dextran-TA-hydrogels.

Samengenomen levert dit proefschrift een reeks onderzoeken naar cellulaire interacties en innovatieve hybride injecteerbare hydrogelmodificaties. De bevindingen in dit proefschrift kunnen de ontwikkeling van nieuwe therapeutische strategieën vergemakkelijken en bijdragen aan de klinische vertaling van toepassingen van kraakbeenweefseltechniek.

Contents

Summary / Samenvatting		ix/xi
Chapter 1	General introduction and thesis outline	1
Chapter 2	Trophic effects of mesenchymal stem cells in tissue regeneration	9
Chapter 3	Beneficial effects of MSCs on co-cultured chondrocytes are independent of inter-donor chondrogenesis variation	55
Chapter 4	High throughput generated micro-aggregates of MSCs and chondrocytes as a model to investigate cell to cell communication	83
Chapter 5	Autophagy Is Involved in Mesenchymal Stem Cell Death in Coculture with Chondrocytesdocx	123
Chapter 6	Interaction between MSCs and Chondrocyte modifies impact of signal modulators	173
Chapter 7	Engineering of optimized hydrogel formulations for cartilage repair	197
Chapter 8	Preliminary in vivo evaluation Hyaluronic acid and Dextran hybrid injectable hydrogels for cartilage tissue engineering application	231
Chapter 9	Reflection and Outlook	261
Acknowledgements		281
Biography		284
Scientific output		285

Chapter 1

General introduction and thesis outline

1.1 Trophic function of MSCs in cartilage tissue regeneration

Mesenchymal stem cells (MSCs) hold great potential for regenerative medicine because of their ability for self-renewal and differentiation into tissue-specific cells such as osteoblasts, chondrocytes, and adipocytes[1]. The research on MSCs is evolving and continuously expanding with a recent boost of interest in clinical applications. Differentiation properties of MSCs are essential for tissue repair strategies and cell-based therapies. However, the clinical potential of the trophic effects of MSCs is recently gaining significant traction as the basis for new stem cell therapies[2-5]. The trophic function of MSCs refers to their functional capacity to secrete a broad array of bioactive factors that support regenerative processes in damaged tissues[6]. These factors can have a distinct impact on the processes they regulate and collectively generate a microenvironment that enables injured tissues to mount a self-regulated regenerative response[7, 8].

1.2 MSCs death modulation in co-cultures

The mechanisms governing the beneficial effects of MSCs imply that MSCs improve cellular behavior by cell-to-cell contact and/or secretion of bioactive factors. A group of factors essential from the viewpoint of regeneration processes is factors with cell death regulative effect. From this aspect, cell death modulation appears as a crucial biological function that could carry a significant part of the therapeutic effects of MSCs. Indeed, MSCs were reported to decrease significantly after culturing with chondrocytes[9]. Cell death is a fundamental process in maintaining cellular homeostasis, which can be either accidental or programed. Programmed cell death, also known as apoptosis, requires a cascade of cysteine-aspartic proteases known as caspases to respond to the activation of the death signal. The intrinsic mitochondrial pathways and the extrinsic pathway are two distinct pathways for apoptosis[10]. Autophagy is a catabolic process that leads to cellular degradation and the recycling of proteins and organelles by lysosomal digestion. A basal level of autophagy is considered as cytoprotective, since it contributes to removing misfolded or unnecessary proteins, allowing a balance in cell homeostasis[11].

The interfaces between apoptosis and autophagy were reviewed in recent publications[12, 13]. Although apoptosis was considered as the most well-characterized and prevalent form of controlled cell death, it has been indicated the central importance of autophagy as a stress response that influences decisions of cell life

and cell death. The autophagy machinery has been associated with the execution of specific forms of cell death triggered either by hyperactivation of the autophagy flux or by its inhibition. Thus, although autophagy and apoptosis are distinct cellular processes, with different biochemical and morphological appearances, the actual protein networks that control their respective regulation and execution are highly interconnected.

1.3 Injectable hydrogels as unique biomedical materials for cartilage tissue regeneration

Injectable hydrogels offer the advantages of proper alignment with irregularly shaped defects and allow easy cell incorporation. Moreover, from the clinical viewpoint, implantation surgery can be avoided and replaced by a simple *in situ* injection procedure. Another considerable advantage is the utilization of hydrogels as a factor-delivery platform[14]. Compared to systemic co-delivery systems, injectable hydrogel-based factor-delivery systems allow for simultaneous delivery of multiple agents at the damaged sites with a relatively high concentration in a sustained manner, without or with reduced systemic toxic side effects[15]. Injectable hydrogels can be formed by physical or chemical crosslinking. Previously, we designed injectable biomimetic hydrogels based on mixtures of polysaccharide-tyramine conjugates such as hyaluronic Acid-tyramine (HA-TA) and dextran-tyramine (Dex-TA) using enzymatic crosslinking[16]. Based on this unique gel-forming feature, various properties of formed hydrogels, such as gelation time, stiffness, and degradation rate, can be easily manipulated, thereby regulate the cellular behavior and chondro-induction features.

1.4 Aims and outline of this thesis

This thesis focuses on: i) acquisition of fundamental knowledge regarding how mesenchymal stem cells act as a mediator in Chondrocyte-MSC co-cultures and how MSCs are able to regulate cellular behavior and chondro-induction features in co-cultures, ii) determine which cell death mechanisms are affected in Chondrocyte-MSC co-cultures and iii) pioneer novel approaches with optimal hybrid injectable hydrogels to improve upon cartilage regeneration strategies.

The current chapter gives a general introduction that allows the reader to understand the scope and aims of the thesis. Chapter two gives an overview of the beneficial effects of MSCs in tissue regeneration and summarizes the various underlying mechanisms used by MSCs to act as trophic mediators, including the secretion of

growth factors, production of extracellular vesicles, and the formation of membrane nanotubes. Furthermore, we postulate that apoptosis of the MSCs is an integral part of the trophic effect during tissue repair.

Chapter three provides further evidence that beneficial effects of MSCs in the Chondrocyte-MSC co-culture system are independent of MSCs donor variation, which indicates that this beneficial effect in co-cultures is a general phenomenon with potential implications for use in cartilage repair strategies. Chapter four investigates the way of cellular interaction during Chondrocyte-MSC co-cultures using a micro-aggregation approach. This chapter demonstrates that both direct and indirect MSC-Chondrocyte contact are involved in the cellular behavior changes of these cells, whereas these contact methods affect differently in co-cultures.

In chapter five, we revealed that the autophagy pathway, rather than the apoptosis, probably is the principal regulator in the death of MSCs in Chondrocyte-MSC co-cultures. We propose that this sacrificial cell death may perhaps contribute to the trophic effects of MSCs on cartilage formation. Chapter six aims to further elucidate the underlying mechanism by using various modulators of both the apoptotic and autophagy pathways.

Chapters seven and eight investigate the optimal hybrid hydrogels to improve cartilage regeneration strategies *in vitro* and *in vivo*. Remarkably, compared to higher concentration hydrogels, 5% w/v hydrogels laden with cells exhibit a significant increase in the mechanical properties and the deposition of cartilage matrix *in vitro*. Moreover, in chapter eight, 5%w/v hybrid hydrogels were combined with different types of cells to assess the biocompatibility and safety of cells encapsulated hydrogels and characterize the reaction of the neighboring tissues. Chapter nine reflects upon the results presented in this thesis and provides directions for further research.

Reference

1. Caplan A.I. Mesenchymal stem cells. J Orthop Res 9, 641, 1991.

2. Yang X., Balakrishnan, I., Torok-Storb, B., and Pillai, M.M. Marrow stromal cell infusion rescues hematopoiesis in lethally irradiated mice despite rapid clearance after infusion. Adv Hematol 2012, 142530, 2012.

3. Mora-Lee S., Sirerol-Piquer, M.S., Gutiérrez-Pérez, M., Gomez-Pinedo, U., Roobrouck, V.D., López, T., et al. Therapeutic effects of hMAPC and hMSC transplantation after stroke in mice. PLoS One 7, e43683, 2012.

4. Nakamura T., Sekiya, I., Muneta, T., Hatsushika, D., Horie, M., Tsuji, K., et al. Arthroscopic, histological and MRI analyses of cartilage repair after a minimally invasive method of transplantation of allogeneic synovial mesenchymal stromal cells into cartilage defects in pigs. Cytotherapy 14, 327, 2012.

5. de Windt T.S., Vonk, L.A., Slaper-Cortenbach, I.C., van den Broek, M.P., Nizak, R., van Rijen, M.H., et al. Allogeneic mesenchymal stem cells stimulate cartilage regeneration and are safe for single-stage cartilage repair in humans upon mixture with recycled autologous chondrons. Stem Cells 35, 256, 2017.

6. Skalnikova H.K. Proteomic techniques for characterisation of mesenchymal stem cell secretome. Biochimie 95, 2196, 2013.

7. Attar-Schneider O., Zismanov, V., Drucker, L., and Gottfried, M. Secretome of human bone marrow mesenchymal stem cells: an emerging player in lung cancer progression and mechanisms of translation initiation. Tumor Biol 37, 4755, 2016.

8. Marfy-Smith S.J., and Clarkin, C.E. Are mesenchymal stem cells so bloody great after all? Stem Cells Transl Med 6, 3, 2017.

9. Wu L., Leijten, J.C., Georgi, N., Post, J.N., van Blitterswijk, C.A., and Karperien, M. Trophic effects of mesenchymal stem cells increase chondrocyte proliferation and matrix formation. Tissue Eng Part A 17, 1425, 2011.

10. Elmore S. Apoptosis: a review of programmed cell death. Toxicol Pathol 35, 495, 2007.

11. Ryter S.W., Cloonan, S.M., and Choi, A.M. Autophagy: a critical regulator of cellular metabolism and homeostasis. Mol Cells 36, 7, 2013.

12. Booth L.A., Roberts, J.L., and Dent, P. The role of cell signaling in the crosstalk between autophagy and apoptosis in the regulation of tumor cell survival in response to sorafenib and neratinib. Semin Cancer Biol 19, 30024, 2019.

13. Napoletano F., Baron, O., Vandenabeele, P., Mollereau, B., and Fanto, M. Intersections between regulated cell death and autophagy. Trends Cell Biol 29, 323, 2019.

14. Talebian S., Foroughi, J., Wade, S.J., Vine, K.L., Dolatshahi-Pirouz, A., Mehrali, M., et al. Biopolymers for antitumor implantable drug delivery systems: recent advances and future outlook. Adv Mater 30, 1706665, 2018.

15. He C., Kim, S.W., and Lee, D.S. In situ gelling stimuli-sensitive block copolymer hydrogels for drug delivery. J Controlled Release 127, 189, 2008.

16. Jin R., Teixeira, L.M., Dijkstra, P.J., Van Blitterswijk, C., Karperien, M., and Feijen, J. Enzymatically-crosslinked injectable hydrogels based on biomimetic dextran–hyaluronic acid conjugates for cartilage tissue engineering. Biomaterials 31, 3103, 2010.

Chapter 2

Trophic effects of mesenchymal stem cells in tissue regeneration

Yao Fu, Lisanne Karbaat, Sanne K. Both, Ling Wu, Jeroen Leijten, and Marcel Karperien

Abstract

Mesenchymal stem cells (MSCs) are considered to hold great therapeutic value for cell-based therapy and for tissue regeneration in particular. Recent evidence indicates that the main underlying mechanism for MSCs' beneficial effects in tissue regeneration is based on their capability to produce a large variety of bioactive trophic factors that stimulate neighboring parenchymal cells to start repairing damaged tissues. These new findings could potential replace the classical paradigm of MSC differentiation and cell replacement. These bioactive factors have diverse actions like modulating the local immune system, enhancing angiogenesis, preventing cell apoptosis, and stimulating survival, proliferation and differentiation of resident tissue specific cells. Therefore, MSCs are referred to as conductors of tissue repair and regeneration by secreting trophic mediators. In this review article, we have summarized the studies that focused on the trophic effects of MSC within the context of tissue regeneration. We will also highlight the various underlying mechanisms employed by MSCs to act as trophic mediators. Besides the secretion of growth factors, we discuss two additional mechanisms that are likely to mediate MSC's beneficial effects in tissue regeneration, namely the production of extracellular vesicles (EVs) and the formation of membrane nanotubes (MNTs), which can both connect different cells and transfer a variety of trophic factors varying from proteins to mRNAs and miRNAs. Furthermore, we postulate that apoptosis of the MSCs is an integral part of the trophic effect during tissue repair.

2.1 Introduction

The traditional approach of regenerating biologically functional tissues, the triad of cells, scaffolds and growth factors, has resulted in promising strategies[1]. In this approach, mesenchymal stem cells (MSCs) have been considered as potential therapeutic cells. MSCs can be readily isolated from a variety of adult tissues throughout the body, including bone marrow[2, 3], adipose tissue[4] and muscle[5]. They can also be derived from fetal tissues that can be collected during gestation and delivery, such as the amniotic fluid[6] or the umbilical cord[7]. MSCs have a high proliferation potential and can differentiate into various committed cell types, including bone, cartilage, muscle, tendon/ligament, fat, dermis, and other connective tissues[8-10].

In the tissue engineering field, researchers have sought ways to exploit the multilineage differentiation potential of these culture expanded MSCs to regenerate lost or worn out tissue. For example, a working hypothesis is that MSCs would generate *de novo* tissue themselves by incorporating specific biological cues into scaffolds that combined with the cells would stimulate their differentiation into the desired cell type (Fig. 2.1A). This strategy is currently explored in preclinical studies[11-13]. In another strategy, MSCs are injected either at the site of the injured tissue or in the blood stream. It is believed that the MSCs would subsequently home to the diseased tissue and induce tissue repair. Indeed this concept is under investigation in a large number of preclinical trials for treating a wide range of diseases[14-16]. While beneficial effects of this approach have been reported there is much uncertainty with respect of the mechanism of action. In fact, only a small fraction of the injected cells are actually homing to damaged tissues and even less cells can be found back in the tissue in long term follow up of days to weeks[17-21]. After transplantation into the heart, the exogenous MSC showed poor survival and do not persist in the infarcted area[22]. Other investigators have even failed to detect permanent engraftment of transplanted MSCs in infarcted hearts[23]. MSC have been

found to home preferentially to the ischemic boundary in stroke studies[24]. However, it has been shown that cells disappeared progressively and were no longer detected 4 weeks after transplantation[25]. Similar findings were reported in another study, in which human adipose tissue-derived MSCs in a mouse model of hind limb ischemia. Indeed the injected cells improved neovascularization, but the incorporation of MSCs into the vascular structures resulted quite low (less than 1%), indicating that other effects, rather than direct differentiation of MSCs in neovasculature, likely accounted for the observed beneficial effects[26]. All this evidence suggests that in many tissue engineering approaches the contribution of MSC to support the repair process by directly differentiating in *de novo* repair tissue is fairly limited due to poor engraftment and survival of cells[27]. Since in many of these studies beneficial effects have been reported this raises the question how the injected cells exert their effect.

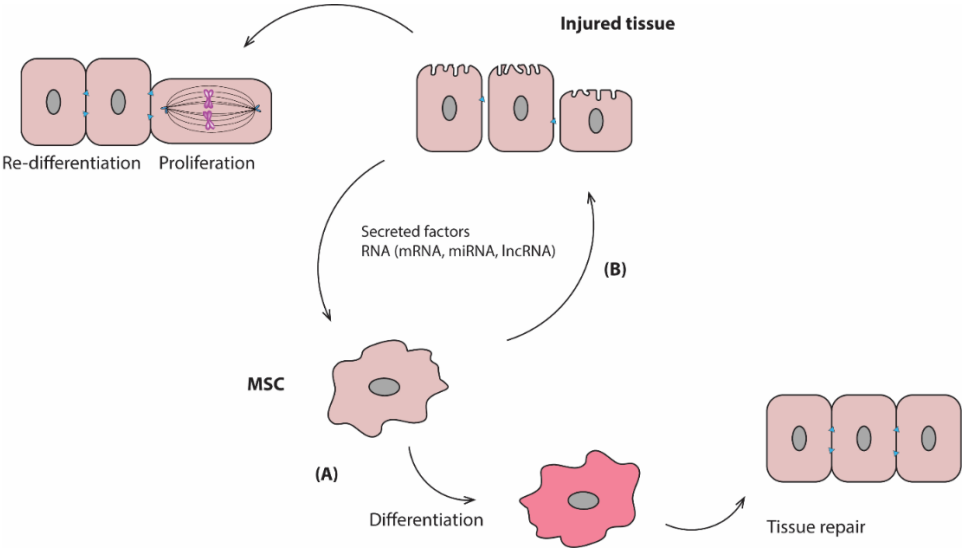

Figure 2.1 Mechanisms through which MSCs mediate tissue repair. *(A) MSCs directly differentiate into tissue specific cells that are enforced by specific biological cues released from the injured tissue and microenvironment, which improves the generation of de novo tissue. (B) Trophic effect of MSCs support tissue regeneration by delivering bioactive*

molecules and genetic information that enhance the activity of tissue-resident cells.

Besides their multilineage differentiation capacity, MSCs have shown to be capable of reducing inflammation by modulating the immune system[28-35], promoting angiogenesis[36-40], and inducing both cell migration, proliferation[41-44], differentiation and extracellular matrix formation[39, 45, 46] (Table 2.1). Therefore, it has been proposed that the functional benefits observed after MSC transplantation in experimental models of tissue regeneration might be related to the trophic effects of MSCs (Fig. 2.1B)[47-49]. This specific role of MSCs is the main focus of this review. In particular, we will discuss the possible mechanisms behind this effect.

Table 2.1 Paracrine factors secreted by MSCs.

Secreted factors	Proposed function
Basic fibroblast growth factor (bFGF)[39, 93, 182]	Cell survival and Proliferation
Granulocyte/macrophage colony stimulating factor (G/M-CSF)[38]	
Insulin-like growth factor (IGF)[38, 183]	
Secreted frizzled-related protein-1 (SFRP1)[43]	
Secreted frizzled-related protein-2 (SFRP2)[41]	
Stanniocalcin-1 (STC-1)[44]	Remodeling of extracellular matrix
Transforming growth factor β (TGF-β)[38, 184]	
Metalloproteinase-1 (MMP1)[39]	
Metalloproteinase-2 (MMP2)[45]	
Metalloproteinase-9 (MMP9)[46]	
Plasminogen activator (PA)[39]	Angiogenesis

Tumor necrosis factor-α (TNF- α)[39] Angiopoietins (ANGs)[36] Fibroblast growth factor-2 (FGF-2)[37, 53, 184] Transforming growth factor- β (TGF-β)[38, 39] Vascular endothelial growth factor (VEGF)[37, 40, 185] Hepatocyte growth factor (HGF)[29, 49] Human leukocyte antigen-G5 (HLA-G5)[34, 35] Indoleamine 2,3-dioxygenase (IDO)[28, 32, 186] Inducible nitric oxide synthase (iNOS)[187] Interleukin-6 (IL-6)[102] Interleukin-10 (IL-10)[33, 188] Leukemia inhibitory factor (LIF)[189] Prostaglandin E2 (PGE2)[28, 190-192] Transforming growth factor- β (TGF-β)[28, 29, 33, 193]	Immunomodulatory

2.2 MSCs act as trophic mediators in tissue regeneration

MSCs exhibit the capacity to migrate to injured sites and can therefore contribute to tissue repair[50]. The trophic effect of MSCs in tissue repair was first proposed by Arnold Caplan[51]. There is a dynamic regulation and interplay of stem cell derived cytokines that influence tissue survival, repair, and regeneration, including the

activation of resident and circulating stem cells[27]. Currently, researchers are increasingly integrating the trophic roles of MSCs as a prominent feature in tissue repair strategies[52]. One engrafted MSC has the potential to modulate the activity of many surrounding cells via inter-cellular communication. This hypothesis is supported by the *in vitro* observation that MSC-conditioned medium (CM) improves tissue repair[27, 53]. MSC-CM acts as a chemoattractant for tissue-specialized cells[54]. Analyses of MSC-conditioned medium indicate that MSCs secrete many known mediators of tissue repair including growth factors, cytokines, and chemokines[53]. This evidence suggests that the therapeutic effect of MSCs may largely depend on their capacity to secrete soluble factors that promote several key biological activities.

2.2.1 MSCs in osteoarthritis (OA) and other cartilage defects repair

Partial replacement of chondrocytes with stem cells in autologous chondrocyte implantation (ACI) has been proposed as an effective strategy to limit or even omit the *in vitro* expansion phase of chondrocytes[55]. Indeed, *in vitro* studies have shown that cartilage matrix deposition and chondrogenic gene expression in MSCs could be improved by co-culture of MSCs and chondrocytes[56, 57]. Based on these studies, it was assumed that the beneficial effects of co-culturing MSCs and chondrocytes in cartilage matrix formation were largely due to the differentiation of MSCs into chondrocytes. However, using cell tracking experiments it was later shown that DiI-labeled allogeneic MSCs in cartilage defects were present after 1 week, but not after 4 or 12 weeks post-implantation, while the cartilage repair progress lasted for at least three months[58]. This implies that the transplantation of allogeneic MSCs could only have acted at the beginning of the repair process. Importantly, this experiment indicated that MSCs did not contribute significantly to wound healing by differentiating into the newly formed tissue[58, 59, 60].

In a study performed by our group[61] human mesenchymal stem cells (hMSCs) were used in pellet co-culture with human primary chondrocytes (hPCs) or bovine primary chondrocytes (bPCs) and the role of the individual cell populations in

matrix formation was studied. This revealed that these co-culture systems outperformed monoculture systems of either hPCs or hMSCs in terms of cartilage formation. Interestingly, the increase in matrix deposition was mainly achieved by increasing the matrix production of hPCs. Furthermore, we observed a significant decrease in MSC overtime, most probably caused by apoptosis, which may play an important role in the cartilage matrix formation of pellet co-culture system[62, 63]. The beneficial effects of the pellet co-culture model were largely due to the stimulation of proliferation and the matrix formation of chondrocytes induced by a trophic effect of the MSCs. This trophic role of MSCs in cartilage formation is furthermore supported by independent studies performed by others[64-66]. These studies point to a dominant role of the MSCs in stimulating resident or co-implanted chondrocytes to initiate a regenerative response. One can interpret the role of the MSC in these systems as the initiator or even as the conductor of the repair process by activating cell and tissue autonomous repair mechanisms, such as the induction of chondrocyte proliferation and matrix production. Once activated, the cartilage regeneration becomes self-reliant and chondrocyte-driven and is largely independent of MSC-based stimulation. Moreover, the trophic effect of MSCs is independent of culture conditions and the origin of the MSCs[66, 67]. These studies suggested that the supportive trophic role in tissue repair and regeneration might not be limited to MSCs but could also be displayed by other stem cell populations or even non-stem cells such as dermal fibroblasts[56]. These findings starting from observations *in vitro* have been confirmed in animal studies and recently also in a clinical trial[68, 69].

2.2.2 MSCs in renal regeneration

The role of MSCs in the recovery of acute kidney injury (AKI) has been extensively studied. It has been reported that MSCs administration effectively counteracted the detrimental effects of experimental AKI[70-72] and induced functional improvements in chronic kidney disease[73]. Initially, it was thought that MSCs would home to the kidney to replace damaged renal cells. However, after initial accumulation of

systemically administered MSCs in the injured kidney, only a few of these cells permanently engraft within the tubules and without obvious evidence of cell differentiation into tubular cells[70-72]. In a rat AKI model, the iron-labeled MSCs were predominantly located in the glomerular capillaries, while kidney tubular cells showed no iron labeling, indicating the absence of trans-differentiation into tubular cells[74]. It has been suggested that MSCs do not replace renal tubular cells, but mitigate the damage by providing paracrine support for repair. MSCs achieve this by releasing growth factors that modulate the immune response and subsequently stimulate tissue repair[75, 76]. The kidneys of MSC-treated rats revealed a decrease in gene expression of pro-inflammatory cytokines and an increase in several growth factors with mitogenic, pro-survival, and anti-apoptotic effects[77]. In particular, insulin-like growth factor (IGF-1) and vascular endothelial growth factor (VEGF) were suggested as critical mediators[42, 78]. In an *in vivo* model of lung injury, a decline in the levels of tumor necrosis factor (TNF), interleukin (IL)-6, and interferon-gamma (IFN-γ) was also detected in the group pre-treated with MSCs[79]. This hypothesis is supported by a mouse model of tubular injury showing that injection of conditioned medium from murine MSCs resulted in a significant decrease of tubular cell apoptosis, increased survival and renal function improvement[80]. Therefore, it can be concluded that the regenerative response of MSCs in this model depends on secreted bio-active factors.

2.2.3 MSCs in myocardial repair and regeneration

Injection of MSCs has been demonstrated to have therapeutic effects after myocardial infarction. Similar to the mechanism of MSCs promoting kidney repair, current data suggests that the direct differentiation of allogeneic MSCs into cardiomyocytes is very limited. Instead, the MSCs secrete factors and regulate the function of cardiomyocytes and immature cells during repair[81-84]. In support of this paracrine hypothesis, many studies have observed that MSCs secrete cytokines, chemokines, and growth factors that could potentially repair damaged cardiac tissue.

VEGF, transforming growth factor beta 1 (TGF-β1), fibroblast growth factor 2 (FGF-2), hepatocyte growth factor (HGF) and granulocyte colony stimulating factor (G-CSF) have all been identified as key factors released by MSCs[85]. These factors have been demonstrated to exert beneficial effects on the heart, including neovascularization, attenuation of ventricular remodeling and increased angiogenesis[39]. Anti-inflammatory action is also exerted by MSC in a murine acute myocarditis model[86]. Furthermore, MSC-conditioned medium can reduce apoptosis and necrosis of cardiomyocytes exposed to low oxygen tension[87]. The injection of MSC-CM into animal myocardial infarction models limited infarct size, reduced cardiomyocytes apoptosis and ventricular remodeling and resulted in improved cardiac function compared with controls[49, 88, 89]. Meanwhile, extra cardiac administration of MSCs provided clear evidence that cardiac repair can be achieved through MSC's trophic actions, and did not rely on their presence in the infarcted myocardium[90]. Though, it should be emphasized that many of these positive effects of MSCs in AKI and myocardial infarction were found in animal models. Replication of these beneficial effects in human patients is the subject of many clinical trials and is subject of an intense scientific debate.

2.2.4 MSCs in wound healing and vascularization

Neovascularization is another important biological process positively influenced by stem cells in a paracrine fashion. Co-culture of endothelial cells and MSCs can simulate and stabilize endothelial microvascular networks and promote cell functions[91]. A study with co-application of MSCs and endothelial cells resulted in improved angiogenesis which was largely due to the secretion of angiogenic cytokines by the MSCs stimulating the endothelial cells[92]. Another mechanism by which MSCs contribute to wound healing is by reducing inflammation, and by inducing migration and proliferation of resident tissue specific cells[27]. Many of these effects can be replicated by using MSC-conditioned medium both *in vitro*[93] and *in vivo*[53]. Indeed, the CM acted as a chemoattractant recruiting macrophages and

endothelial cells to the wound. The MSC-CM has a similar effect as MSCs on a wound both accelerating epithelialization[53, 94, 95]. Studies have indicated that many cell types in the wound area, including epithelial cells, endothelial cells, keratinocytes, and fibroblasts, are responsive to factors secreted by MSCs[96]. The trophic function of MSCs in the wound-healing environment has been further elucidated in animal models. In a diabetic rat model of ulcerating wounds, researchers evaluated the function of MSCs in the context of improved collagen metabolism[97]. Overall, this data suggests that MSCs released soluble factors that stimulated proliferation and migration of the predominant cell types in the wound in therapeutically relevant concentrations.

2.2.5 MSCs in neurological disorders

MSCs have been reported to provide a potential therapeutic benefit in the treatment of neurological disease and injury[98]. MSCs are able to exert neurotrophic effects by releasing a variety of molecules that directly or indirectly promote endogenous repair. Such molecules may include neurotrophic growth factors, chemokines, cytokines, and extracellular matrix proteins[99]. Increased levels of IGF-1 as well as VEGF, bFGF, and epidermal growth factor (EGF) were observed in the brain of treated rats, as compared with controls[48]. Paracrine effects of such factors involve direct neurotrophic and/or neuroprotective activity on resident progenitor cells, hence inducing neurogenesis, oligodendrogenesis[100], neurite outgrowth[101, 102], angiogenesis[103], or anti-apoptotic effects[48] on neurons and glia cells. Furthermore, MSCs have been shown to improve gain-of-functions in brain stroked rats without differentiating into a neuronal phenotype[104]. It is assumed that the MSCs were able to achieve this by secreting a cocktail of factors into the neural niche microenvironment that mediated neural repair and protection.

2.3 Mechanisms behind the trophic effects

In each of these disease models discussed above, the MSCs secreted factors stimulated neighboring cells. It has been proposed that the interaction of stem cells

with their microenvironment, also named niche, has a critical role in defining the phenotype of the stem cell but also determines their secretory profile[105]. This has suggested that the selection in the production of the paracrine factors produced by the MSCs is in part orchestrated by the injured tissue. Indeed, MSCs appear to enhance the regenerative potential of multiple tissues types as a result of various mechanisms that become activated when exposed to the biochemical factors that are characteristic of an injured environment *in vivo*[106].

In a living tissue, cells constantly interact with each other and their ECM. This interaction influences the proliferation and differentiation of cells within the tissue and organ[107, 108]. Cell-cell communication is required to guarantee effective coordination among different cell types within tissues. Classical means of cell communication (Fig. 2.2) are represented by cell junctions, cell adhesion molecules, and signaling through secreted and soluble factors which all connect neighboring cells acting in a paracrine or even endocrine manner[109-111].

More recently, communication by extracellular vesicles (EVs) and membrane nanotubes (MNTs) have been identified as possible mechanisms. Furthermore, we postulate that apoptosis is an integral part of the trophic effect of MSCs in tissue repair. It seems likely that each of these mechanisms can contribute to the trophic role of the MSC in tissue regeneration. The extent to which each of these mechanisms can contribute to the therapeutic effect is likely dependent on the context such as tissue type, type of tissue damage, and inflammation degree. Recent articles summarized the mechanisms of the more classical ways of cell communication[109, 111]. In this review, we will emphasize on the latter three mechanisms.

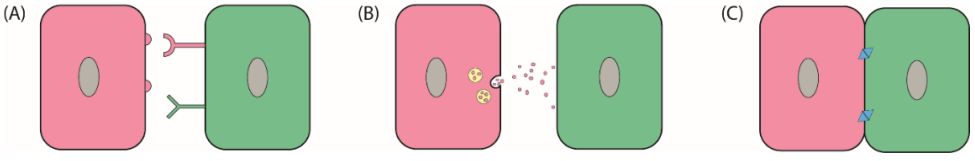

Figure 2.2 Classical forms of cellular communication. *(A) Signal molecules, adhesion molecules, and irons can bind to specific intracellular and cell surface receptors that can trigger a variety of cellular responses, depending on the receptor. (B) Signals can be transmitted from one cell to its neighboring cells via signal transmission, especially in neural synapse. (C) Two cells in direct contact with each other may send signals across gap junctions.*

2.3.1 Extracellular vesicles

EVs are cytosol fragments with a spherical morphology, surrounding by a membrane composed of a lipid bilayer and hydrophilic proteins, similar to the cell plasma membrane (Fig. 2.3)[112]. Such vesicles are released from most cells and can be isolated from most body fluids such as serum, plasma, urine and cerebrospinal fluid[113-115]. EVs are a heterogeneous group of vesicles and includes exosomes, microvesicles, and apoptotic bodies. It has proven to be a challenge to experimentally distinguish between these vesicles due to their overlapping biophysical characteristics and lack of discriminating markers[116, 117]. Therefore, the term EVs will be used in this review to refer to a mixed population of vesicles.

2.3.1.1 Formation of EVs

Exosomes are 30-100 nm in size and are secreted when multivesicular bodies (MVBs), a late endosomal compartment, fuse with the plasma membrane[118, 119]. Exosome production is generally regarded as a constitutive membrane vesicle pathway, although it can increase as a result of stimulation with e.g. Ca^{2+} ionophore[112]. Microvesicles, also termed shedding vesicles, tend to be 100 nm to 1 µm in diameter and are directly derived from the cell membrane of activated cells through the disruption of the cortical cytoskeleton. These vesicles shed into the extracellular space in a calcium flux- and calpain-dependent manner[120]. Apoptotic

bodies are larger than 1 μm and are derived from dying cells. They result from of budding of the plasma membrane, and contain cytoplasm with organelles[121].

These apoptotic bodies are a special class in the EVs. In tissue regeneration studies, cell death was considered as a consequence of injury, lack of oxygen and not as a regenerative factor, until recently. Researchers proposed the concept of "altruistic cell suicide" based on their observation that dying cells could induce proliferation of their neighboring cells[122]. The apoptotic cells release a variety of signals, including apoptotic bodies, which induce cellular responses over short and/or long-range distances. During apoptosis, apoptotic bodies containing biological information are transferred from apoptotic to non-apoptotic cells. Indeed, endothelial cell–derived apoptotic bodies convey paracrine signals to recipient vascular cells that trigger the production of CXCL12[123]. This data indicates that the apoptotic bodies likely play an important role in paracrine signaling supporting tissue repair and regeneration. Thus the disappearance over time of MSCs from the injured tissue could reflect the death of MSCs. The extent to which MSC's cell death contributes to tissue regeneration as well as the underlying mechanism of this "altruistic cell death" deserves further study. As mentioned before, also in the pellet co-culture model of MSCs and primary chondrocytes an association was found between MSC disappearance from the pellets likely by apoptosis and the stimulation of chondrocyte proliferation and matrix formation. It is presently unclear whether the cell death of MSCs in these pellet co-cultures with primary chondrocytes contributes to the improved cartilage formation in this model.

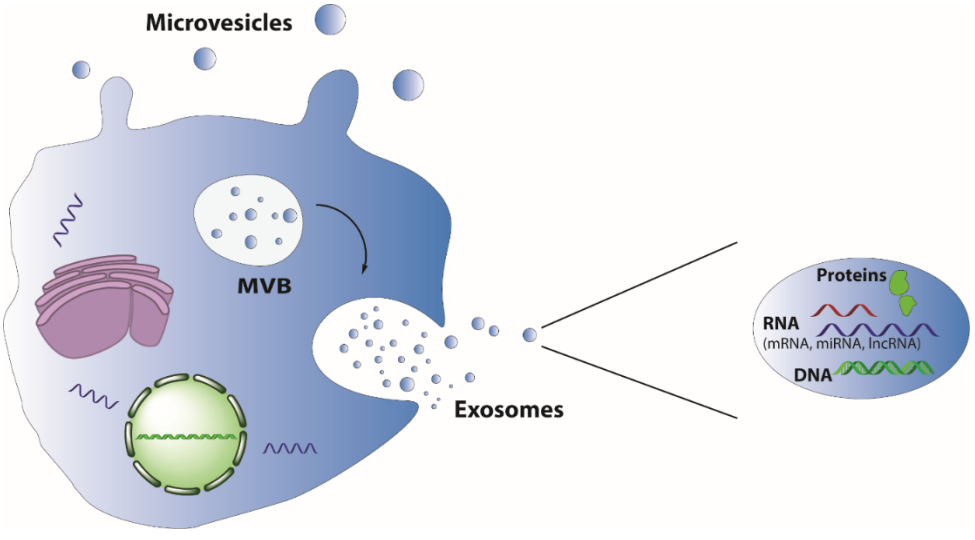

Figure 2.3 Mechanisms involved in the formation of microvesicles (MVs) and exosomes. *Exosomes are formed from multivesicular bodies (MVBs) and are released by fusion of MVBs with the plasma membrane, whereas MVs bud directly from the plasma membrane. The extracellular vesicles (EVs) contain a variety of proteins, RNA and DNA species.*

2.3.1.2 EVs biological activities

Cell communication by means of EVs is considered to be a universal way for cells to interact with each other and influence the behavior of other neighboring cells by exchanging material and information. Indeed, EVs can stimulate target cells and induce alterations in the phenotype and behavior of recipient cells[124, 125]. EVs influence the fate of target cells in numerous ways. First, they may directly stimulate the cells by interaction with membrane bound receptors or ligands[126]. Indeed, EVs express surface molecules and several types of receptors, including transforming growth factor β (TGFβ), CD95L, MHC class Ⅰ / Ⅱ molecules and the CCR5 chemokine receptor[126, 127]. After ligand interaction, they may then modulate the functional target cell by delivering intracellular proteins[128, 129]. Secondly, EVs can transfer receptors, bioactive lipids or nucleic acids between cells after fusion with target cell membrane. Of particular interest is the involvement of EV in the horizontal transfer of genetic information. Subsets of mRNAs, miRNAs and long

noncoding RNAs (lncRNAs) can be transferred via EVs to recipient cells, inducing functional and phenotypic changes[130, 131]. In particular, the horizontal transfer of miRNAs has been proposed as a new form of intercellular communication, representing a means by which donor cells can regulate the gene expression of recipient cells[132]. EVs extend the trophic repertoire of MSCs from the classical secreted growth factors to now include as well mRNAs, miRNAs, lipids, and membrane bound proteins.

Stem cells and differentiated cells communicate with each other to regulate the self-renewal and differentiation processes related to tissue repair[133]. In this process, stem cells and differentiated cells may establish bi-directional communication during the reparative process. EVs, by transferring selected patterns of proteins, lipids, mRNAs and miRNAs to recipient cells, may be considered as potent paracrine mediators of signaling between stem cells and differentiated cells[110]. In the first scenario, EVs released from injured tissue may help to reprogram the phenotype of stem cells to acquire tissue-specific features. The other way around, EVs derived from stem cells may induce cell cycle re-entry of cells survived an injury allowing tissue regeneration[110]. In this context, the stem cell-derived EVs could participate in the repair process[105] by provoking genetic and epigenetic changes in target cells thereby activating critical cell processes for tissue regeneration e.g. by inducing cell proliferation, differentiation, and extracellular matrix production. Meanwhile, EVs released from damaged tissues may organize adult resident stem cells into a reparative program[134]. With the progress of tissue repair, the demands of the regenerating tissue will change and may request a different type of support from the MSC. Paracrine signaling, for example by EVs, back and forth between tissue specific cells and the stem cells may keep the trophic role of the MSCs in pace with the regenerative process. EVs may exert these functions next to classical ways of communication by means of secreted growth factors. In fact, the beneficial effect of MSC conditioned medium as reported in many studies cannot only be attributed to the presence of secreted growth factors but could have been mediated at least in part

by the presence of EVs which are in most protocols also present in the conditioned medium. It would be of great interest to repeat the CM experiments with medium deprived from EVs to determine the contribution of either secreted growth factors or the EVs to the beneficial effects in tissue repair.

EVs contain diverse species of RNAs that reflect the functional state of the cell of origin, and could represent an important therapeutic tool, since these RNA subsets impact directly or indirectly protein translation when taken up by the target cells[135]. Therefore, several studies have evaluated whether stem-cell-derived EVs perform similar to MSCs in tissue regeneration *in vivo*[136-138]. The use of MSC derived EVs rather than the cells themselves may avoid possible long-term mal-differentiation of engrafted cells and attenuate many of the safety concerns related to the use of living cells.

2.3.1.3 Role of EVs in tissue regeneration

Proteomics analysis of MSC-derived EVs has shown that they contain the factors influencing angiogenesis such as FGF, VEGF, HGF, EGF and IL-8[139, 140]. Thus MSCs release not only growth factors directly into medium but also as an integral part of EVs. It is at present unclear whether growth factors embedded in an EV have distinct biological activity compared to the same growth factors directly released into the extracellular space. This requires more research. Nevertheless it is clear that release of growth factors in EVs represents another way for cellular communication and transportation in the extracellular space[141].

EVs have been shown that they are the mediators of the cardio-protective effects of MSCs and that they diminish the size of the infarct in an ischemic mouse model[142]. A similar model showed that MSC-derived EVs enhanced blood flow recovery, reduced the infract size and preserved cardiac systolic and diastolic performance by promoting angiogenesis[143]. Currently it is hypothesized that the cardio-protective effects of EVs are resulting from a combination of improved angiogenesis, anti-apoptotic effects, anti-inflammatory effects and anti-cardiac remodeling factors

showing a clear overlap with the proposed actions of MSC-CM. Recently, researchers showed that CXCR4 overexpressing MSCs produced EVs with increased concentrations of VEGF and IGF-1α. They loaded MSCs with EVs, which were produced in CXCR4 overexpressing MSCs, and proved that these exosomes were delivered *in vivo* upon implantation of a cell sheet, leading to increased angiogenesis, reduced infarct size, and improved cardiac remodeling[144].

Bruno *et al.* wrote an extensive review on the use of MSC-derived EVs on renal regeneration[119]. MSC-derived EVs were first tested for their renal regenerative potential in a model of AKI[134]. A meta-analysis on the studies using MSC-derived EVs in AKI concluded that MSC-derived EVs have a more profound therapeutic potential than conditioned medium, and that early administration of EVs in AKI has the most effect[145]. Besides AKI, MSC-derived EVs have been tested in chronic diabetic nephropathy, where they were found to be as effective as conditioned medium[146]. The exosomes were found to suppress the invasion of bone marrow derived cells (the source of inflammatory cytokines) by downregulating their adhesion molecules (ICAM-1). This resulted in a decreased the expression of TNF-α. Besides this, activation of renal inflammatory pathways via p38-MAPK was reversed. TGF-β1 expression was downregulated and tight junction protein expression (e.g., ZO-1) was persevered. Consequently, TGF-β mediated epithelial-to-mesenchymal transition was inhibited.

Recent studies compared the effect of injected MSCs and MSC-derived EVs on the neural functional recovery after ischemia or apoplexy[137, 147]. Both studies found equally positive therapeutic effects of MSCs and EVs. Improvement of neurological impairment, neuroprotection and neurogenesis and angiogenesis were equally stimulated by the presence of either MSCs or EVs. Although the composition of the EVs was not within the scope of these studies, other research has shown that the neurotrophic effect of injected MSCs results from a variety of molecules that directly or indirectly promote endogenous repair (reviewed in *chapter 2.5*). Hofer

et al. reviewed the role of MSCs secreted trophic factors in never repair[148]. Neurotrophic brain-derived neurotrophic factor (BDNF), nerve growth factor (NGF), and glial cell line-derived neurotrophic factor (GDNF), ciliary neurotrophic factor (CNTF) as well as angiogenic VEGF and angiopoietin-1 (Ang1) work as neuroprotective factors. It is assumed that the MSCs are able to achieve their therapeutic effects by secreting a cocktail of these factors in EVs into the neural niche microenvironment that mediates neural repair and protection. However, to date, the molecular definition of their cargo remains unknown. Also these studies suggest a large overlap in the activity of MSC-CM and MSC-derived EVs which may suggest that EVs rather than secreted growth factors and cytokines play a more dominant role in the mechanism of action by which MSCs induce tissue regeneration.

Based on the anti-inflammatory, anti-apoptotic, anti-fibrotic and pro-regenerative properties of MSC-derived EVs it was long speculated that EVs might exert a positive effect on osteoarthritis (OA) or rheumatoid diseases[149, 150]. Zhang *et al.* showed that the addition of MSC-derived exosomes led to complete restoration of cartilage and subchondral bone. Hyaline cartilage with a good surface regularity, complete bonding to the adjacent cartilage was formed after 12 weeks in 5 out of 6 rats[150].

Based on all examples above EVs can have numerous positive effect on tissue regeneration due to their anti-apoptotic, angiogenesis promoting and pro-proliferative effects. In spite of all these positive results many of the animal models used, do not resemble a realistic pathological situation. Many of the models inject the EVs directly after injury, to prevent development of tissue damage, even when the disease is chronic and progressive like OA[119, 143, 144, 150]. There are studies where the administration of EVs is delayed, but these are the minority. In the studies for chronic kidney disease (CKD) there is one paper using EVs to cure already established damage[151]. In this study they compared EVs and conditioned medium

and found that EVs do not have a curative effect. One other paper describes the regenerative effect of EVs in established chronic diabetic nephropathy[146]. The exosomes were found to suppress the invasion of bone marrow derived cells by downregulating their adhesion molecules. Clearly more work is needed whether MSCs, MSC-CM or MSC-derived EVs can play a role in the reversion or even regeneration of established disease and whether there are specific windows for opportunities in which treatment is most beneficial.

2.3.2 Membrane nanotubes

Rustom and co-workers[152] were the first to describe an as yet unknown type of intercellular connection. They noticed some straight lines connecting two adjacent cells that were not in direct cell-cell contact. With regards to dimensions and morphology, these structures were termed membrane nanotubes (MNTs) or tunneling nanotubes (TNTs). MNTs are long thin F-actin-based membranous channels connecting cells (Fig. 2.4). These structures were observed between many eukaryotic cells[153-156], suggesting that these connections represent common mechanism of functional intercellular connectivity and cell-to-cell communication. MNTs are widely considered a neotype of cell communication through its ability to transport many components and signals from one cell to another[157].

2.3.2.1 Structural characteristics of MNTs

Electron transmission and scanning microscopes were used to reveal the surface and formation of MNTs. Meanwhile, fluorescence studies can give information about the structure of MNTs, as well as their function in intercellular transfer[158, 159]. To study the latter process, dyes such as DiD, DiO, fluorescent proteins like GFP, and selected cell compartments markers are widely used. The diameter of MNTs ranges from 50 to 200 nm and some are as long as the diameter of a few cells[152]. Findings suggest that the thickness and length of MNTs might be related to the components exchanged through the tunnels, as well as their quantity[160].

Two types of MNTs have been distinguished, open-ended and closed-ended. For open-ended MNTs, intercellular cargo or larger organelles such as mitochondria or vesicles may be transported from the MNTs to the target cell[160, 161]. For the closed-ended structures membranous cargo can enter into the target cell as a result of endocytic forces[162]. Their functions could apply to various specific topologies, depending on the types of signals.

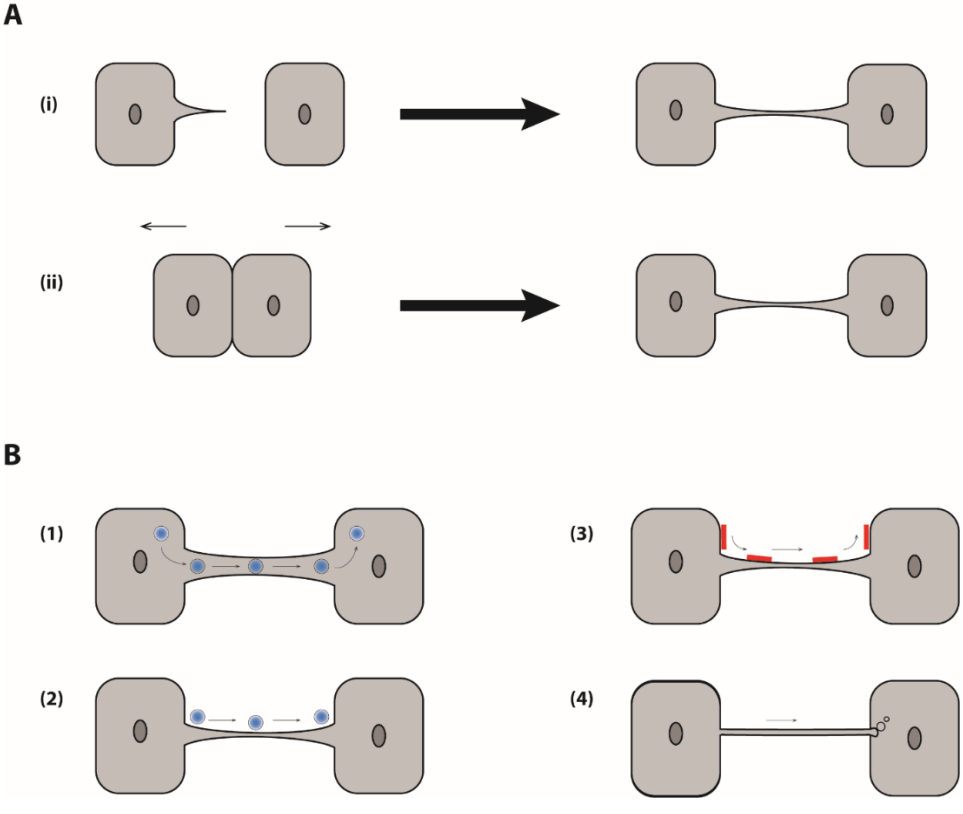

Figure 2.4 Mechanisms of membrane nanotube (MNT) formation and potential functions*. (A) MNTs can be derived from filopodia-like protrusions (i) and prior cell-cell contacts (ii). (B) Organelles and proteins can transport via MNTs, either inside (1) or along their surface (2). Patches of surface membranes and activation signals could be transmitted between connected cells (3). Membranous cargo can enter into the target cell by endocytic forces from the end of closed-ended nanotubes (4).*

2.3.2.2 Formation of MNTs

Until now, two mechanisms of MNTs formation are known[162-164] (Fig. 2.4A). In the first mechanism, linkages form after a cell extends a *de novo* filopodia-like bridge that is then bound and tightly anchored to a neighboring cell. Filopodia are dynamic exploratory and sensory organelles that can direct cell migration towards specific sources, including nearby cells. These structures can be maintained to form a long-lived stable filopodial bridge, or alternatively, function as structural intermediates to more complex cell-cell interfaces[165]. The second mechanism of MNTs formation is connected with prior cell-cell contact, after which the cells are separated and a nanotube is formed between them. These mechanisms may vary per cell type. Indeed, most immobile cell types, such as neuronal-like PC12, form tubes by the outgrowth of filopodia[166]. Mobile cells, such as kidney cells and T cells, which easily connect with other cells, form tubes by the second method[156, 167]. However, it is important to note that the two mechanisms could occur in the same cell type. Despite the two possible mechanisms of formation, it's accepted that actin polymerization is required for MNTs formation. This specific feature of MNTs helps to distinguish them from other similar structures such as membrane tubules formed by neutrophils[168].

Little has been done to investigate the signaling pathways involved in MNTs formation. Since actin polymerization is required, it has been proposed that some proteins involved in actin polymerization, such as Cdc42, will also be important for nanotube formation. Indeed, Cdc42, Rac1, ezrin and N-WASP are all present in MNTs, but the requirement of these factors in MNTs formation has so far not been assessed[169]. Using expression of dominant negative constructs in HeLa cells, inhibition of Cdc42 resulted in decreased MNTs formation, but Rac1 inhibition showed no effect[170]. It's suggests that the signaling requirements for MNTs formation may be different depending on the mechanisms of formation.

2.3.2.3 Biological significance of MNTs

Many studies have investigated the biological function of this recently discovered structure that connects two distant cells (Fig. 2.4B). A common function of MNTs is the propagation of an electrical signal[167]. Organelles and proteins transport via MNTs also seems to play an important role especially when cells are damaged or undergo premature senescence[171-173]. Ca^{2+} and intercellular vesicles could also be transported via MNTs between cells[161, 174, 175]. Transfer of miRNA through MNTs has been described in cancer cells, but if this function is also present in immune cells or in MSCs has to be investigated[176]. MNTs were found to transport porous silicon microparticles, so they may be involved in the dispersion of therapeutic agents at the site of diseased tissue[177]. MNTs have also been suggested to provide cell-contact dependent communication over long distances[158]. Recently, MNTs have been observed between MSCs and vascular smooth muscle cells (VSMCs), which promoted the proliferation but not differentiation of MSCs by transfer of mitochondria from VSMCs into MSCs[178], as well as between MSCs and osteoclast precursors, which was found to be essential for osteoclastogenesis[179]. Overall, MNTs are novel candidates to explain how direct cell-to-cell communication occurs and play an important role in many (patho)physiological processes by transporting molecular signals and cell organelles from one cell to another[180]. We propose that communication via nanotubes could be an additional mechanism by which MSCs exert their positive effect in tissue regeneration.

2.4 Conclusions

The beneficial function of transplanted MSCs has already been proven in many therapeutic domains. Recently, the trophic effect of MSCs is being considered as the most important player in the observed reparative effects of these cells. In the case of severe tissue damage, MSCs can be attracted to the site where they secrete a broad repertoire of trophic factors that function to assist the repair and regeneration process[51]. The trophic hypothesis of MSCs action changed the perspective of the therapeutic use of MSCs in regenerative medicine[181]. The mechanisms governing

this trophic activity are quite distinct from those used in tissue engineering functional substitutes for replacement of damaged or lost tissue. There is strong evidence showing that the effect is at least partly mediated by secretion of growth factors, cytokines and other secreted proteins affecting resident cells stimulating tissue repair, but it is likely that more mechanisms exist. In this review, we have discussed two additional mechanisms that could be employed by the MSCs in support of their trophic role, extracellular vesicles (EVs) and membrane nanotubes (MNTs), which can connect different cells and deliver their trophic factors. These structures are defined as important forms of intercellular communication, and are involved in many physiological processes. As they may influence the behavior of recipient cells by delivering their bioactive cargo, it may be possible to exploit this effect in tissue regeneration and repair. The extent to which these additional mechanisms contribute to the trophic effect of MSCs in tissue repair and regeneration deserves further study. Indeed gaining a solid understanding of these mechanisms may lead to development of new strategies and /or therapeutic tools for tissue regeneration.

References

1. Cancedda R., Giannoni P., Mastrogiacomo M. A tissue engineering approach to bone repair in large animal models and in clinical practice. Biomaterials **28,** 4240, 2007.

2. Barry F., Boynton R. E., Liu B., Murphy J. M. Chondrogenic differentiation of mesenchymal stem cells from bone marrow: differentiation-dependent gene expression of matrix components. Exp Cell Res **268,** 189, 2001.

3. Johnstone B., Hering T. M., Caplan A. I., Goldberg V. M., Yoo J. U. In Vitro Chondrogenesis of Bone Marrow-Derived Mesenchymal Progenitor Cells. Exp Cell Res **238,** 265, 1998.

4. Guilak F., Awad H. A., Fermor B., Leddy H. A., Gimble J. M. Adipose-derived adult stem cells for cartilage tissue engineering. Biorheology **41,** 389, 2004.

5. Usas A., Huard J. Muscle-derived stem cells for tissue engineering and regenerative therapy. Biomaterials **28,** 5401, 2007.

6. De Coppi P., Bartsch G., Siddiqui M. M., Xu T., Santos C. C., Perin L.*, et al.* Isolation of amniotic stem cell lines with potential for therapy. Nat Biotechnol **25,** 100, 2007.

7. Weiss M. L., Troyer D. L. Stem cells in the umbilical cord. Stem Cell Rev **2,** 155, 2006.

8. Caplan A. I. Cell delivery and tissue regeneration. J Control Release **11,** 157, 1990.

9. Caplan A. I. Mesenchymal stem cells. J Orthop Res **9,** 641, 1991.

10. Caplan A. I. Review: mesenchymal stem cells: cell-based reconstructive therapy in orthopedics. Tissue Eng **11,** 1198, 2005.

11. Buda R., Vannini F., Cavallo M., Baldassarri M., Luciani D., Mazzotti A.*, et al.* One-step arthroscopic technique for the treatment of osteochondral lesions of the knee with bone-marrow-derived cells: three years results. Musculoskelet Surg **97,** 145, 2013.

12. Chen W., Liu J., Manuchehrabadi N., Weir M. D., Zhu Z., Xu H. H. K. Umbilical cord and bone marrow mesenchymal stem cell seeding on macroporous calcium phosphate for bone regeneration in rat cranial defects. Biomaterials **34,** 9917, 2013.

13. Haleem A. M., Singergy A. A., Sabry D., Atta H. M., Rashed L. A., Chu C. R.*, et al.* The Clinical Use of Human Culture-Expanded Autologous Bone Marrow Mesenchymal Stem Cells Transplanted on Platelet-Rich Fibrin Glue in the Treatment of Articular Cartilage Defects: A Pilot Study and Preliminary Results. Cartilage **1,** 253, 2010.

14. Jung K. H., Shin H. P., Lee S., Lim Y. J., Hwang S. H., Han H.*, et al.* Effect of human umbilical cord blood-derived mesenchymal stem cells in a cirrhotic rat model. Liver Int **29,** 898, 2009.

15. Oksuz S., Ulkur E., Oncul O., Kose G. T., Kucukodaci Z., Urhan M. The effect of subcutaneous mesenchymal stem cell injection on statis zone and apoptosis in an experimental burn model. Plast Reconstr Surg **131,** 463, 2013.

16. van Ramshorst J., Bax J. J., Beeres S. L., Dibbets-Schneider P., Roes S. D., Stokkel M. P.*, et al.* Intramyocardial bone marrow cell injection for chronic myocardial ischemia: a randomized controlled trial. JAMA **301,** 1997, 2009.

17. Devine S. M., Bartholomew A. M., Mahmud N., Nelson M., Patil S., Hardy W.*, et al.* Mesenchymal stem cells are capable of homing to the bone marrow of non-human primates following systemic infusion. Exp Hematol **29,** 244, 2001.

18. Ji J. F., He B. P., Dheen S. T., Tay S. S. Interactions of chemokines and chemokine receptors mediate the migration of mesenchymal stem cells to the impaired site in the brain after hypoglossal nerve injury. Stem Cells **22,** 415, 2004.

19. Lange C., Brunswig-Spickenheier B., Cappallo-Obermann H., Eggert K., Gehling U. M., Rudolph C.*, et al.* Radiation rescue: mesenchymal stromal cells protect from lethal irradiation. PLoS One **6,** e14486, 2011.

20. Shi M., Li J., Liao L., Chen B., Li B., Chen L.*, et al.* Regulation of CXCR4 expression in human mesenchymal stem cells by cytokine treatment: role in homing efficiency in NOD/SCID mice. Haematologica **92,** 897, 2007.

21. Yang X., Balakrishnan I., Torok-Storb B., Pillai M. M. Marrow Stromal Cell Infusion Rescues Hematopoiesis in Lethally Irradiated Mice despite Rapid Clearance after Infusion. Adv Hematol **2012,** 142530, 2012.

22. Terrovitis J. V., Smith R. R., Marban E. Assessment and optimization of cell engraftment after transplantation into the heart. Circ Res **106,** 479, 2010.

23. Muller-Ehmsen J., Krausgrill B., Burst V., Schenk K., Neisen U. C., Fries J. W.*, et al.* Effective engraftment but poor mid-term persistence of mononuclear and mesenchymal bone marrow cells in acute and chronic rat myocardial infarction. J Mol Cell Cardiol **41,** 876, 2006.

24. Kang S. K., Lee D. H., Bae Y. C., Kim H. K., Baik S. Y., Jung J. S. Improvement of neurological deficits by intracerebral transplantation of human adipose tissue-derived stromal cells after cerebral ischemia in rats. Exp Neurol **183,** 355, 2003.

25. Mora-Lee S., Sirerol-Piquer M. S., Gutierrez-Perez M., Gomez-Pinedo U., Roobrouck V. D., Lopez T.*, et al.* Therapeutic effects of hMAPC and hMSC transplantation after stroke in mice. PLoS One **7,** e43683, 2012.

26. Moon M. H., Kim S. Y., Kim Y. J., Kim S. J., Lee J. B., Bae Y. C.*, et al.* Human adipose tissue-derived mesenchymal stem cells improve postnatal neovascularization in a mouse model of hindlimb ischemia. Cell Physiol Biochem **17,** 279, 2006.

27. Gnecchi M., Zhang Z., Ni A., Dzau V. J. Paracrine mechanisms in adult stem cell signaling and therapy. Circ Res **103,** 1204, 2008.

28. Aggarwal S., Pittenger M. F. Human mesenchymal stem cells modulate allogeneic immune cell

responses. Blood **105,** 1815, 2005.

29. Di Nicola M., Carlo-Stella C., Magni M., Milanesi M., Longoni P. D., Matteucci P.*, et al.* Human bone marrow stromal cells suppress T-lymphocyte proliferation induced by cellular or nonspecific mitogenic stimuli. Blood **99,** 3838, 2002.

30. English K. Mechanisms of mesenchymal stromal cell immunomodulation. Immunol Cell Biol **91,** 19, 2013.

31. Klinker M. W., Wei C. H. Mesenchymal stem cells in the treatment of inflammatory and autoimmune diseases in experimental animal models. World J Stem Cells **7,** 556, 2015.

32. Krampera M., Cosmi L., Angeli R., Pasini A., Liotta F., Andreini A.*, et al.* Role for interferon-gamma in the immunomodulatory activity of human bone marrow mesenchymal stem cells. Stem Cells **24,** 386, 2006.

33. Nasef A., Chapel A., Mazurier C., Bouchet S., Lopez M., Mathieu N.*, et al.* Identification of IL-10 and TGF-beta transcripts involved in the inhibition of T-lymphocyte proliferation during cell contact with human mesenchymal stem cells. Gene Expr **13,** 217, 2007.

34. Nasef A., Mathieu N., Chapel A., Frick J., Francois S., Mazurier C.*, et al.* Immunosuppressive effects of mesenchymal stem cells: involvement of HLA-G. Transplantation **84,** 231, 2007.

35. Selmani Z., Naji A., Zidi I., Favier B., Gaiffe E., Obert L.*, et al.* Human leukocyte antigen-G5 secretion by human mesenchymal stem cells is required to suppress T lymphocyte and natural killer function and to induce CD4+CD25highFOXP3+ regulatory T cells. Stem Cells **26,** 212, 2008.

36. Sun L., Cui M., Wang Z., Feng X., Mao J., Chen P.*, et al.* Mesenchymal stem cells modified with angiopoietin-1 improve remodeling in a rat model of acute myocardial infarction. Biochem Biophys Res Commun **357,** 779, 2007.

37. Spanholtz T. A., Theodorou P., Holzbach T., Wutzler S., Giunta R. E., Machens H. G. Vascular endothelial growth factor (VEGF165) plus basic fibroblast growth factor (bFGF) producing cells induce a mature and stable vascular network--a future therapy for ischemically challenged tissue. J Surg Res **171,** 329, 2011.

38. Rehman J., Traktuev D., Li J., Merfeld-Clauss S., Temm-Grove C. J., Bovenkerk J. E.*, et al.* Secretion of angiogenic and antiapoptotic factors by human adipose stromal cells. Circulation **109,** 1292, 2004.

39. Kinnaird T., Stabile E., Burnett M. S., Lee C. W., Barr S., Fuchs S.*, et al.* Marrow-derived stromal cells express genes encoding a broad spectrum of arteriogenic cytokines and promote in vitro and in vivo arteriogenesis through paracrine mechanisms. Circ Res **94,** 678, 2004.

40. Beckermann B. M., Kallifatidis G., Groth A., Frommhold D., Apel A., Mattern J.*, et al.* VEGF expression by mesenchymal stem cells contributes to angiogenesis in pancreatic carcinoma. Br J Cancer **99,** 622, 2008.

41. Mirotsou M., Zhang Z., Deb A., Zhang L., Gnecchi M., Noiseux N., *et al.* Secreted frizzled related protein 2 (Sfrp2) is the key Akt-mesenchymal stem cell-released paracrine factor mediating myocardial survival and repair. Proc Natl Acad Sci U S A **104,** 1643, 2007.

42. Imberti B., Morigi M., Tomasoni S., Rota C., Corna D., Longaretti L., *et al.* Insulin-Like Growth Factor-1 Sustains Stem Cell–Mediated Renal Repair. J Am Soc Nephrol **18,** 2921, 2007.

43. Dufourcq P., Descamps B., Tojais N. F., Leroux L., Oses P., Daret D., *et al.* Secreted frizzled-related protein-1 enhances mesenchymal stem cell function in angiogenesis and contributes to neovessel maturation. Stem Cells **26,** 2991, 2008.

44. Block G. J., Ohkouchi S., Fung F., Frenkel J., Gregory C., Pochampally R., *et al.* Multipotent stromal cells are activated to reduce apoptosis in part by upregulation and secretion of stanniocalcin-1. Stem Cells **27,** 670, 2009.

45. Kuchroo P., Dave V., Vijayan A., Viswanathan C., Ghosh D. Paracrine factors secreted by umbilical cord-derived mesenchymal stem cells induce angiogenesis in vitro by a VEGF-independent pathway. Stem Cells Dev **24,** 437, 2015.

46. Kim Y., Kim H., Cho H., Bae Y., Suh K., Jung J. Direct comparison of human mesenchymal stem cells derived from adipose tissues and bone marrow in mediating neovascularization in response to vascular ischemia. Cell Physiol Biochem **20,** 867, 2007.

47. Morigi M., De Coppi P. Cell therapy for kidney injury: different options and mechanisms--mesenchymal and amniotic fluid stem cells. Nephron Exp Nephrol **126,** 59, 2014.

48. Wakabayashi K., Nagai A., Sheikh A. M., Shiota Y., Narantuya D., Watanabe T., *et al.* Transplantation of human mesenchymal stem cells promotes functional improvement and increased expression of neurotrophic factors in a rat focal cerebral ischemia model. J Neurosci Res **88,** 1017, 2010.

49. Gnecchi M., He H., Noiseux N., Liang O. D., Zhang L., Morello F., *et al.* Evidence supporting paracrine hypothesis for Akt-modified mesenchymal stem cell-mediated cardiac protection and functional improvement. FASEB J **20,** 661, 2006.

50. Newman R. E., Yoo D., LeRoux M. A., Danilkovitch-Miagkova A. Treatment of inflammatory diseases with mesenchymal stem cells. Inflamm Allergy Drug Targets **8,** 110, 2009.

51. Caplan A. I., Dennis J. E. Mesenchymal stem cells as trophic mediators. J Cell Biochem **98,** 1076, 2006.

52. Kassis I., Vaknin-Dembinsky A., Karussis D. Bone marrow mesenchymal stem cells: agents of immunomodulation and neuroprotection. Curr Stem Cell Res Ther **6,** 63, 2011.

53. Chen L., Tredget E. E., Wu P. Y., Wu Y. Paracrine factors of mesenchymal stem cells recruit macrophages and endothelial lineage cells and enhance wound healing. PloS one **3,** e1886, 2008.

54. Gurtner G. C., Werner S., Barrandon Y., Longaker M. T. Wound repair and regeneration. Nature

453, 314, 2008.

55. Ochs B. G., Muller-Horvat C., Albrecht D., Schewe B., Weise K., Aicher W. K.*, et al.* Remodeling of articular cartilage and subchondral bone after bone grafting and matrix-associated autologous chondrocyte implantation for osteochondritis dissecans of the knee. Am J Sports Med **39,** 764, 2011.

56. Hendriks J. A., Miclea R. L., Schotel R., de Bruijn E., Moroni L., Karperien M.*, et al.* Primary chondrocytes enhance cartilage tissue formation upon co-culture with a range of cell types. Soft Matter **6,** 5080, 2010.

57. Vadala G., Studer R. K., Sowa G., Spiezia F., Iucu C., Denaro V.*, et al.* Coculture of bone marrow mesenchymal stem cells and nucleus pulposus cells modulate gene expression profile without cell fusion. Spine (Phila Pa 1976) **33,** 870, 2008.

58. Nakamura T., Sekiya I., Muneta T., Hatsushika D., Horie M., Tsuji K.*, et al.* Arthroscopic, histological and MRI analyses of cartilage repair after a minimally invasive method of transplantation of allogeneic synovial mesenchymal stromal cells into cartilage defects in pigs. Cytotherapy **14,** 327, 2012.

59. Baraniak P. R., McDevitt T. C. Stem cell paracrine actions and tissue regeneration. Regen Med **5,** 121, 2010.

60. Meirelles Lda S., Fontes A. M., Covas D. T., Caplan A. I. Mechanisms involved in the therapeutic properties of mesenchymal stem cells. Cytokine Growth Factor Rev **20,** 419, 2009.

61. Wu L., Leijten J. C., Georgi N., Post J. N., van Blitterswijk C. A., Karperien M. Trophic effects of mesenchymal stem cells increase chondrocyte proliferation and matrix formation. Tissue Eng Part A **17,** 1425, 2011.

62. Fujihara Y., Takato T., Hoshi K. Macrophage-inducing FasL on chondrocytes forms immune privilege in cartilage tissue engineering, enhancing in vivo regeneration. Stem Cells **32,** 1208, 2014.

63. Xie G. H., Wang S. J., Wang Y., Zhang Y., Zhang H. Z., Jin S.*, et al.* Fas Ligand gene transfer enhances the survival of tissue-engineered chondrocyte allografts in mini-pigs. Transpl Immunol **19,** 145, 2008.

64. Acharya C., Adesida A., Zajac P., Mumme M., Riesle J., Martin I.*, et al.* Enhanced chondrocyte proliferation and mesenchymal stromal cells chondrogenesis in coculture pellets mediate improved cartilage formation. J Cell Physiol **227,** 88, 2012.

65. Meretoja V. V., Dahlin R. L., Kasper F. K., Mikos A. G. Enhanced chondrogenesis in co-cultures with articular chondrocytes and mesenchymal stem cells. Biomaterials **33,** 6362, 2012.

66. Wang M., Rahnama R., Cheng T., Grotkopp E., Jacobs L., Limburg S.*, et al.* Trophic stimulation of articular chondrocytes by late‐passage mesenchymal stem cells in coculture. J Orthop Res **31,** 1936, 2013.

67. Wu L., Prins H.-J., Helder M. N., van Blitterswijk C. A., Karperien M. Trophic effects of

mesenchymal stem cells in chondrocyte co-cultures are independent of culture conditions and cell sources. Tissue Eng Part A **18,** 1542, 2012.

68. Dahlin R. L., Kinard L. A., Lam J., Needham C. J., Lu S., Kasper F. K.*, et al.* Articular chondrocytes and mesenchymal stem cells seeded on biodegradable scaffolds for the repair of cartilage in a rat osteochondral defect model. Biomaterials **35,** 7460, 2014.

69. de Windt T. S., Vonk L. A., Slaper-Cortenbach I. C., van den Broek M. P., Nizak R., van Rijen M. H.*, et al.* Allogeneic Mesenchymal Stem Cells Stimulate Cartilage Regeneration and Are Safe for Single-Stage Cartilage Repair in Humans upon Mixture with Recycled Autologous Chondrons. Stem Cells **35,** 256, 2017.

70. Morigi M., Imberti B., Zoja C., Corna D., Tomasoni S., Abbate M.*, et al.* Mesenchymal stem cells are renotropic, helping to repair the kidney and improve function in acute renal failure. J Am Soc Nephrol **15,** 1794, 2004.

71. Duffield J. S., Park K. M., Hsiao L.-L., Kelley V. R., Scadden D. T., Ichimura T.*, et al.* Restoration of tubular epithelial cells during repair of the postischemic kidney occurs independently of bone marrow-derived stem cells. J Clin Invest **115,** 1743, 2005.

72. Herrera M. B., Bussolati B., Bruno S., Fonsato V., Romanazzi G. M., Camussi G. Mesenchymal stem cells contribute to the renal repair of acute tubular epithelial injury. Int J Mol Med **14,** 1035, 2004.

73. Choi S., Park M., Kim J., Hwang S., Park S., Lee Y. The role of mesenchymal stem cells in the functional improvement of chronic renal failure. Stem Cells Dev **18,** 521, 2009.

74. Lange C., Togel F., Ittrich H., Clayton F., Nolte-Ernsting C., Zander A. R.*, et al.* Administered mesenchymal stem cells enhance recovery from ischemia/reperfusion-induced acute renal failure in rats. Kidney Int **68,** 1613, 2005.

75. Humphreys B. D., Bonventre J. V. Mesenchymal stem cells in acute kidney injury. Annu Rev Med **59,** 311, 2008.

76. Wise A. F., Ricardo S. D. Mesenchymal stem cells in kidney inflammation and repair. Nephrology (Carlton) **17,** 1, 2012.

77. Togel F., Hu Z., Weiss K., Isaac J., Lange C., Westenfelder C. Administered mesenchymal stem cells protect against ischemic acute renal failure through differentiation-independent mechanisms. Am J Physiol Renal Physiol **289,** F31, 2005.

78. Tögel F., Zhang P., Hu Z., Westenfelder C. VEGF is a mediator of the renoprotective effects of multipotent marrow stromal cells in acute kidney injury. J Cell Mol Med **13,** 2109, 2009.

79. Yagi H., Soto-Gutierrez A., Navarro-Alvarez N., Nahmias Y., Goldwasser Y., Kitagawa Y.*, et al.* Reactive bone marrow stromal cells attenuate systemic inflammation via sTNFR1. Mol Ther **18,** 1857, 2010.

80. Bi B., Schmitt R., Israilova M., Nishio H., Cantley L. G. Stromal cells protect against acute tubular

injury via an endocrine effect. J Am Soc Nephrol **18,** 2486, 2007.

81. Wollert K. C., Drexler H. Cell-based therapy for heart failure. Curr Opin Cardiol **21,** 234, 2006.

82. Pittenger M. F., Martin B. J. Mesenchymal stem cells and their potential as cardiac therapeutics. Circ Res **95,** 9, 2004.

83. Iso Y., Spees J. L., Serrano C., Bakondi B., Pochampally R., Song Y.-H.*, et al.* Multipotent human stromal cells improve cardiac function after myocardial infarction in mice without long-term engraftment. Biochem Biophys Res Commun. **354,** 700, 2007.

84. Hatzistergos K. E., Quevedo H., Oskouei B. N., Hu Q., Feigenbaum G. S., Margitich I. S.*, et al.* Bone marrow mesenchymal stem cells stimulate cardiac stem cell proliferation and differentiation. Circ Res **107,** 913, 2010.

85. Crisostomo P. R., Wang M., Markel T. A., Lahm T., Abarbanell A. M., Herrmann J. L.*, et al.* Stem cell mechanisms and paracrine effects: potential in cardiac surgery. Shock **28,** 375, 2007.

86. Van Linthout S., Savvatis K., Miteva K., Peng J., Ringe J., Warstat K.*, et al.* Mesenchymal stem cells improve murine acute coxsackievirus B3-induced myocarditis. Eur Heart J **32,** 2168, 2011.

87. Gnecchi M., He H., Liang O. D., Melo L. G., Morello F., Mu H.*, et al.* Paracrine action accounts for marked protection of ischemic heart by Akt-modified mesenchymal stem cells. Nat Med **11,** 367, 2005.

88. Danieli P., Malpasso G., Ciuffreda M. C., Cervio E., Calvillo L., Copes F.*, et al.* Conditioned medium from human amniotic mesenchymal stromal cells limits infarct size and enhances angiogenesis. Stem Cells Transl Med **4,** 448, 2015.

89. Lim B. K., Choi J. H., Nam J. H., Gil C. O., Shin J. O., Yun S. H.*, et al.* Virus receptor trap neutralizes coxsackievirus in experimental murine viral myocarditis. Cardiovasc Res **71,** 517, 2006.

90. Shabbir A., Zisa D., Suzuki G., Lee T. Heart failure therapy mediated by the trophic activities of bone marrow mesenchymal stem cells: a noninvasive therapeutic regimen. Am J Physiol Heart Circ Physiol **296,** H1888, 2009.

91. Pedersen T. O., Blois A. L., Xue Y., Xing Z., Cottler-Fox M., Fristad I.*, et al.* Osteogenic stimulatory conditions enhance growth and maturation of endothelial cell microvascular networks in culture with mesenchymal stem cells. J Tissue Eng **3,** 2041731412443236, 2012.

92. Tateishi-Yuyama E., Matsubara H., Murohara T., Ikeda U., Shintani S., Masaki H.*, et al.* Therapeutic angiogenesis for patients with limb ischaemia by autologous transplantation of bone-marrow cells: a pilot study and a randomised controlled trial. The Lancet **360,** 427, 2002.

93. Kinnaird T., Stabile E., Burnett M. S., Shou M., Lee C. W., Barr S.*, et al.* Local delivery of marrow-derived stromal cells augments collateral perfusion through paracrine mechanisms. Circulation **109,** 1543, 2004.

94. Kim W. S., Park B. S., Sung J. H., Yang J. M., Park S. B., Kwak S. J.*, et al.* Wound healing effect

of adipose-derived stem cells: a critical role of secretory factors on human dermal fibroblasts. J Dermatol Sci **48,** 15, 2007.

95. Lee E. Y., Xia Y., Kim W. S., Kim M. H., Kim T. H., Kim K. J.*, et al.* Hypoxia-enhanced wound-healing function of adipose-derived stem cells: increase in stem cell proliferation and up-regulation of VEGF and bFGF. Wound Repair Regen **17,** 540, 2009.

96. Hocking A. M., Gibran N. S. Mesenchymal stem cells: paracrine signaling and differentiation during cutaneous wound repair. Exp Cell Res **316,** 2213, 2010.

97. Kwon D. S., Gao X., Liu Y. B., Dulchavsky D. S., Danyluk A. L., Bansal M.*, et al.* Treatment with bone marrow-derived stromal cells accelerates wound healing in diabetic rats. Int Wound J **5,** 453, 2008.

98. Drago D., Cossetti C., Iraci N., Gaude E., Musco G., Bachi A.*, et al.* The stem cell secretome and its role in brain repair. Biochimie **95,** 2271, 2013.

99. Paul G., Anisimov S. V. The secretome of mesenchymal stem cells: Potential implications for neuroregeneration. Biochimie **95,** 2246, 2013.

100. Galindo L. T., Filippo T. R., Semedo P., Ariza C. B., Moreira C. M., Camara N. O.*, et al.* Mesenchymal stem cell therapy modulates the inflammatory response in experimental traumatic brain injury. Neurol Res Int **2011,** 564089, 2011.

101. Chen C.-W., Montelatici E., Crisan M., Corselli M., Huard J., Lazzari L.*, et al.* Perivascular multi-lineage progenitor cells in human organs: regenerative units, cytokine sources or both? Cytokine Growth Factor Rev **20,** 429, 2009.

102. Haynesworth S. E., Baber M. A., Caplan A. I. Cytokine expression by human marrow‐derived mesenchymal progenitor cells in vitro: Effects of dexamethasone and IL‐1α. J Cell Physiol **166,** 585, 1996.

103. Chen J., Zhang Z. G., Li Y., Wang L., Xu Y. X., Gautam S. C.*, et al.* Intravenous administration of human bone marrow stromal cells induces angiogenesis in the ischemic boundary zone after stroke in rats. Circ Res **92,** 692, 2003.

104. Li Y., Chen J., Zhang C. L., Wang L., Lu D., Katakowski M.*, et al.* Gliosis and brain remodeling after treatment of stroke in rats with marrow stromal cells. Glia **49,** 407, 2005.

105. Quesenberry P. J., Aliotta J. M. The paradoxical dynamism of marrow stem cells: considerations of stem cells, niches, and microvesicles. Stem Cell Rev **4,** 137, 2008.

106. Caplan A. Why are MSCs therapeutic? New data: new insight. J Pathol **217,** 318, 2009.

107. Bhatia S. N., Yarmush M. L., Toner M. Controlling cell interactions by micropatterning in co-cultures: hepatocytes and 3T3 fibroblasts. J Biomed Mater Res **34,** 189, 1997.

108. Gerstenfeld L., Barnes G., Shea C., Einhorn T. Osteogenic differentiation is selectively promoted by morphogenetic signals from chondrocytes and synergized by a nutrient rich growth environment.

Connect Tissue Res **44,** 85, 2003.

109. Aplin A. E., Howe A., Alahari S. K., Juliano R. L. Signal transduction and signal modulation by cell adhesion receptors: the role of integrins, cadherins, immunoglobulin-cell adhesion molecules, and selectins. Pharmacol Rev **50,** 197, 1998.

110. Camussi G., Deregibus M. C., Bruno S., Cantaluppi V., Biancone L. Exosomes/microvesicles as a mechanism of cell-to-cell communication. Kidney Int **78,** 838, 2010.

111. Wei C. J., Xu X., Lo C. W. Connexins and cell signaling in development and disease. Annu Rev Cell Dev Biol **20,** 811, 2004.

112. Colombo M., Raposo G., Thery C. Biogenesis, secretion, and intercellular interactions of exosomes and other extracellular vesicles. Annu Rev Cell Dev Biol **30,** 255, 2014.

113. Michael A., Bajracharya S. D., Yuen P. S., Zhou H., Star R. A., Illei G. G.*, et al.* Exosomes from human saliva as a source of microRNA biomarkers. Oral Dis **16,** 34, 2010.

114. Pisitkun T., Shen R.-F., Knepper M. A. Identification and proteomic profiling of exosomes in human urine. Proc Natl Acad Sci U S A **101,** 13368, 2004.

115. Keller S., Rupp C., Stoeck A., Runz S., Fogel M., Lugert S.*, et al.* CD24 is a marker of exosomes secreted into urine and amniotic fluid. Kidney Int **72,** 1095, 2007.

116. van Dommelen S. M., Vader P., Lakhal S., Kooijmans S. A., van Solinge W. W., Wood M. J.*, et al.* Microvesicles and exosomes: opportunities for cell-derived membrane vesicles in drug delivery. J Control Release **161,** 635, 2012.

117. Cocucci E., Racchetti G., Meldolesi J. Shedding microvesicles: artefacts no more. Trends Cell Biol **19,** 43, 2009.

118. Keller S., Sanderson M. P., Stoeck A., Altevogt P. Exosomes: from biogenesis and secretion to biological function. Immunol Lett **107,** 102, 2006.

119. Bruno S., Porta S., Bussolati B. Extracellular vesicles in renal tissue damage and regeneration. European Journal of Pharmacology **790,** 83, 2016.

120. Heijnen H. F., Schiel A. E., Fijnheer R., Geuze H. J., Sixma J. J. Activated Platelets Release Two Types of Membrane Vesicles: Microvesicles by Surface Shedding and Exosomes Derived From Exocytosis of Multivesicular Bodies and -Granules. Blood **94,** 3791, 1999.

121. Elmore S. Apoptosis: a review of programmed cell death. Toxicol Pathol **35,** 495, 2007.

122. Kondo S. Altruistic cell suicide in relation to radiation hormesis. Int J Radiat Biol Relat Stud Phys Chem Med **53,** 95, 1988.

123. Zernecke A., Bidzhekov K., Noels H., Shagdarsuren E., Gan L., Denecke B.*, et al.* Delivery of microRNA-126 by apoptotic bodies induces CXCL12-dependent vascular protection. Sci Signal **2,** ra81, 2009.

124. Gyorgy B., Szabo T. G., Pasztoi M., Pal Z., Misjak P., Aradi B.*, et al.* Membrane vesicles, current

state-of-the-art: emerging role of extracellular vesicles. Cell Mol Life Sci **68,** 2667, 2011.

125. Aliotta J. M., Pereira M., Li M., Amaral A., Sorokina A., Dooner M. S.*, et al.* Stable cell fate changes in marrow cells induced by lung-derived microvesicles. J Extracell Vesicles **1,** 2012.

126. Théry C., Ostrowski M., Segura E. Membrane vesicles as conveyors of immune responses. Nat Rev Immunol **9,** 581, 2009.

127. Mack M., Kleinschmidt A., Brühl H., Klier C., Nelson P. J., Cihak J.*, et al.* Transfer of the chemokine receptor CCR5 between cells by membrane-derived microparticles: a mechanism for cellular human immunodeficiency virus 1 infection. Nat Med **6,** 769, 2000.

128. Sarkar A., Mitra S., Mehta S., Raices R., Wewers M. D. Monocyte derived microvesicles deliver a cell death message via encapsulated caspase-1. PLoS One **4,** e7140, 2009.

129. Sheldon H., Heikamp E., Turley H., Dragovic R., Thomas P., Oon C. E.*, et al.* New mechanism for Notch signaling to endothelium at a distance by Delta-like 4 incorporation into exosomes. Blood **116,** 2385, 2010.

130. Ratajczak J., Miekus K., Kucia M., Zhang J., Reca R., Dvorak P.*, et al.* Embryonic stem cell-derived microvesicles reprogram hematopoietic progenitors: evidence for horizontal transfer of mRNA and protein delivery. Leukemia **20,** 847, 2006.

131. Kogure T., Yan I. K., Lin W. L., Patel T. Extracellular Vesicle-Mediated Transfer of a Novel Long Noncoding RNA TUC339: A Mechanism of Intercellular Signaling in Human Hepatocellular Cancer. Genes Cancer **4,** 261, 2013.

132. Chen X., Liang H., Zhang J., Zen K., Zhang C.-Y. Secreted microRNAs: a new form of intercellular communication. Trends Cell Biol **22,** 125, 2012.

133. Li L., Xie T. Stem cell niche: structure and function. Annu. Rev. Cell Dev. Biol **21,** 605, 2005.

134. Bruno S., Grange C., Deregibus M. C., Calogero R. A., Saviozzi S., Collino F.*, et al.* Mesenchymal stem cell-derived microvesicles protect against acute tubular injury. J Am Soc Nephrol **20,** 1053, 2009.

135. Wetmore B. A., Brees D. J., Singh R., Watkins P. B., Andersen M. E., Loy J.*, et al.* Quantitative analyses and transcriptomic profiling of circulating messenger RNAs as biomarkers of rat liver injury. Hepatology **51,** 2127, 2010.

136. Furuta T., Miyaki S., Ishitobi H., Ogura T., Kato Y., Kamei N.*, et al.* Mesenchymal Stem Cell-Derived Exosomes Promote Fracture Healing in a Mouse Model. Stem Cells Transl Med **5,** 1620, 2016.

137. Hu B., Chen S., Zou M., He Z., Shao S., Liu B. Effect of Extracellular Vesicles on Neural Functional Recovery and Immunologic Suppression after Rat Cerebral Apoplexy. Cell Physiol Biochem **40,** 155, 2016.

138. Kalimuthu S., Gangadaran P., Li X. J., Oh J. M., Lee H. W., Jeong S. Y.*, et al.* In Vivo therapeutic potential of mesenchymal stem cell-derived extracellular vesicles with optical imaging reporter in tumor mice model. Sci Rep **6,** 30418, 2016.

139. Lai R. C., Tan S. S., Teh B. J., Sze S. K., Arslan F., de Kleijn D. P., *et al.* Proteolytic Potential of the MSC Exosome Proteome: Implications for an Exosome-Mediated Delivery of Therapeutic Proteasome. Int J Proteomics **2012,** 971907, 2012.

140. Montemurro T., Vigano M., Ragni E., Barilani M., Parazzi V., Boldrin V., *et al.* Angiogenic and anti-inflammatory properties of mesenchymal stem cells from cord blood: soluble factors and extracellular vesicles for cell regeneration. Eur J Cell Biol **95,** 228, 2016.

141. Kholia S., Ranghino A., Garnieri P., Lopatina T., Deregibus M. C., Rispoli P., *et al.* Extracellular vesicles as new players in angiogenesis. Vascul Pharmacol **86,** 64, 2016.

142. Lai R. C., Arslan F., Lee M. M., Sze N. S., Choo A., Chen T. S., *et al.* Exosome secreted by MSC reduces myocardial ischemia/reperfusion injury. Stem Cell Res **4,** 214, 2010.

143. Bian S., Zhang L., Duan L., Wang X., Min Y., Yu H. Extracellular vesicles derived from human bone marrow mesenchymal stem cells promote angiogenesis in a rat myocardial infarction model. J Mol Med (Berl) **92,** 387, 2014.

144. Kang K., Ma R., Cai W., Huang W., Paul C., Liang J., *et al.* Exosomes Secreted from CXCR4 Overexpressing Mesenchymal Stem Cells Promote Cardioprotection via Akt Signaling Pathway following Myocardial Infarction. Stem Cells Int **2015,** 659890, 2015.

145. Zhang G., Wang D., Miao S., Zou X., Liu G., Zhu Y. Extracellular vesicles derived from mesenchymal stromal cells may possess increased therapeutic potential for acute kidney injury compared with conditioned medium in rodent models: A meta-analysis. Exp Ther Med **11,** 1519, 2016.

146. Nagaishi K., Mizue Y., Chikenji T., Otani M., Nakano M., Konari N., *et al.* Mesenchymal stem cell therapy ameliorates diabetic nephropathy via the paracrine effect of renal trophic factors including exosomes. Sci Rep **6,** 34842, 2016.

147. Doeppner T. R., Herz J., Gorgens A., Schlechter J., Ludwig A. K., Radtke S., *et al.* Extracellular Vesicles Improve Post-Stroke Neuroregeneration and Prevent Postischemic Immunosuppression. Stem Cells Transl Med **4,** 1131, 2015.

148. Hofer H. R., Tuan R. S. Secreted trophic factors of mesenchymal stem cells support neurovascular and musculoskeletal therapies. Stem Cell Res Ther **7,** 131, 2016.

149. Maumus M., Jorgensen C., Noel D. Mesenchymal stem cells in regenerative medicine applied to rheumatic diseases: role of secretome and exosomes. Biochimie **95,** 2229, 2013.

150. Zhang S., Chu W. C., Lai R. C., Lim S. K., Hui J. H., Toh W. S. Exosomes derived from human embryonic mesenchymal stem cells promote osteochondral regeneration. Osteoarthritis Cartilage **24,** 2135, 2016.

151. van Koppen A., Joles J. A., van Balkom B. W., Lim S. K., de Kleijn D., Giles R. H., *et al.* Human embryonic mesenchymal stem cell-derived conditioned medium rescues kidney function in rats with established chronic kidney disease. PLoS One **7,** e38746, 2012.

152. Rustom A., Saffrich R., Markovic I., Walther P., Gerdes H.-H. Nanotubular highways for intercellular organelle transport. Science **303,** 1007, 2004.

153. Koyanagi M., Brandes R. P., Haendeler J., Zeiher A. M., Dimmeler S. Cell-to-Cell Connection of Endothelial Progenitor Cells With Cardiac Myocytes by Nanotubes A Novel Mechanism for Cell Fate Changes? Circ Res **96,** 1039, 2005.

154. Watkins S. C., Salter R. D. Functional connectivity between immune cells mediated by tunneling nanotubules. Immunity **23,** 309, 2005.

155. Wang Y., Cui J., Sun X., Zhang Y. Tunneling-nanotube development in astrocytes depends on p53 activation. Cell Death Differ **18,** 732, 2011.

156. Sowinski S., Jolly C., Berninghausen O., Purbhoo M. A., Chauveau A., Köhler K.*, et al.* Membrane nanotubes physically connect T cells over long distances presenting a novel route for HIV-1 transmission. Nat Cell Biol **10,** 211, 2008.

157. Kwok R. Cell biology: the new cell anatomy. Nature **480,** 26, 2011.

158. Chauveau A., Aucher A., Eissmann P., Vivier E., Davis D. M. Membrane nanotubes facilitate long-distance interactions between natural killer cells and target cells. Proc Natl Acad Sci U S A **107,** 5545, 2010.

159. Kimura S., Hase K., Ohno H. The molecular basis of induction and formation of tunneling nanotubes. Cell Tissue Res **352,** 67, 2013.

160. Önfelt B., Nedvetzki S., Benninger R. K., Purbhoo M. A., Sowinski S., Hume A. N.*, et al.* Structurally distinct membrane nanotubes between human macrophages support long-distance vesicular traffic or surfing of bacteria. J Immunol **177,** 8476, 2006.

161. Wang X., Gerdes H.-H. Long-distance electrical coupling via tunneling nanotubes. Biochim Biophys Acta **1818,** 2082, 2012.

162. Davis D. M., Sowinski S. Membrane nanotubes: dynamic long-distance connections between animal cells. Nat Rev Mol Cell Biol **9,** 431, 2008.

163. Gurke S., Barroso J. F., Gerdes H.-H. The art of cellular communication: tunneling nanotubes bridge the divide. Histochem Cell Biol **129,** 539, 2008.

164. Gerdes H.-H., Carvalho R. N. Intercellular transfer mediated by tunneling nanotubes. Curr Opin Cell Biol **20,** 470, 2008.

165. Sherer N. M., Mothes W. Cytonemes and tunneling nanotubules in cell–cell communication and viral pathogenesis. Trends Cell Biol **18,** 414, 2008.

166. Bukoreshtliev N. V., Wang X., Hodneland E., Gurke S., Barroso J. F., Gerdes H.-H. Selective block of tunneling nanotube (TNT) formation inhibits intercellular organelle transfer between PC12 cells. FEBS Lett **583,** 1481, 2009.

167. Wang X., Veruki M. L., Bukoreshtliev N. V., Hartveit E., Gerdes H.-H. Animal cells connected

by nanotubes can be electrically coupled through interposed gap-junction channels. Proc Natl Acad Sci U S A **107,** 17194, 2010.

168. Galkina S. I., Stadnichuk V. I., Molotkovsky J. G., Romanova J. M., Sud'ina G. F., Klein T. Microbial alkaloid staurosporine induces formation of nanometer-wide membrane tubular extensions (cytonemes, membrane tethers) in human neutrophils. Cell Adh Migr **4,** 32, 2010.

169. Lachambre S., Chopard C., Beaumelle B. Preliminary characterisation of nanotubes connecting T-cells and their use by HIV-1. Biol Cell **106,** 394, 2014.

170. Hase K., Kimura S., Takatsu H., Ohmae M., Kawano S., Kitamura H.*, et al.* M-Sec promotes membrane nanotube formation by interacting with Ral and the exocyst complex. Nat Cell Biol **11,** 1427, 2009.

171. Spees J. L., Olson S. D., Whitney M. J., Prockop D. J. Mitochondrial transfer between cells can rescue aerobic respiration. Proc Natl Acad Sci U S A **103,** 1283, 2006.

172. Kadiu I., Gendelman H. E. Macrophage bridging conduit trafficking of HIV-1 through the endoplasmic reticulum and Golgi network. J Proteome Res **10,** 3225, 2011.

173. Rainy N., Chetrit D., Rouger V., Vernitsky H., Rechavi O., Marguet D.*, et al.* H-Ras transfers from B to T cells via tunneling nanotubes. Cell Death Dis **4,** e726, 2013.

174. He K., Shi X., Zhang X., Dang S., Ma X., Liu F.*, et al.* Long-distance intercellular connectivity between cardiomyocytes and cardiofibroblasts mediated by membrane nanotubes. Cardiovasc Res cvr189, 2011.

175. Rinaldo C. R. HIV-1 Trans Infection of CD4(+) T Cells by Professional Antigen Presenting Cells. Scientifica (Cairo) **2013,** 164203, 2013.

176. Thayanithy V., Dickson E. L., Steer C., Subramanian S., Lou E. Tumor-stromal cross talk: direct cell-to-cell transfer of oncogenic microRNAs via tunneling nanotubes. Transl Res **164,** 359, 2014.

177. Ferrati S., Shamsudeen S., Summers H. D., Rees P., Abbey J. V., Schmulen J.*, et al.* Inter‐endothelial Transport of Microvectors using Cellular Shuttles and Tunneling Nanotubes. Small **8,** 3151, 2012.

178. Vallabhaneni K. C., Haller H., Dumler I. Vascular smooth muscle cells initiate proliferation of mesenchymal stem cells by mitochondrial transfer via tunneling nanotubes. Stem Cells Dev **21,** 3104, 2012.

179. Takahashi A., Kukita A., Li Y. j., Zhang J. q., Nomiyama H., Yamaza T.*, et al.* Tunneling nanotube formation is essential for the regulation of osteoclastogenesis. J Cell Biochem **114,** 1238, 2013.

180. Lou E., Fujisawa S., Barlas A., Romin Y., Manova-Todorova K., Moore M. A.*, et al.* Tunneling Nanotubes: A new paradigm for studying intercellular communication and therapeutics in cancer. Commun Integr Biol **5,** 399, 2012.

181. Lai R. C., Chen T. S., Lim S. K. Mesenchymal stem cell exosome: a novel stem cell-based therapy

for cardiovascular disease. Regen Med **6,** 481, 2011.

182. Wu L., Leijten J., van Blitterswijk C. A., Karperien M. Fibroblast growth factor-1 is a mesenchymal stromal cell-secreted factor stimulating proliferation of osteoarthritic chondrocytes in co-culture. Stem Cells Dev **22,** 2356, 2013.

183. Imberti B., Morigi M., Tomasoni S., Rota C., Corna D., Longaretti L.*, et al.* Insulin-like growth factor-1 sustains stem cell mediated renal repair. J Am Soc Nephrol **18,** 2921, 2007.

184. Asanuma H., Meldrum D. R., Meldrum K. K. Therapeutic applications of mesenchymal stem cells to repair kidney injury. J Urol **184,** 26, 2010.

185. Chen L., Xu Y., Zhao J., Zhang Z., Yang R., Xie J.*, et al.* Conditioned medium from hypoxic bone marrow-derived mesenchymal stem cells enhances wound healing in mice. PLoS One **9,** e96161, 2014.

186. Meisel R., Zibert A., Laryea M., Gobel U., Daubener W., Dilloo D. Human bone marrow stromal cells inhibit allogeneic T-cell responses by indoleamine 2,3-dioxygenase-mediated tryptophan degradation. Blood **103,** 4619, 2004.

187. Sato K., Ozaki K., Oh I., Meguro A., Hatanaka K., Nagai T.*, et al.* Nitric oxide plays a critical role in suppression of T-cell proliferation by mesenchymal stem cells. Blood **109,** 228, 2007.

188. Gupta N., Su X., Popov B., Lee J. W., Serikov V., Matthay M. A. Intrapulmonary delivery of bone marrow-derived mesenchymal stem cells improves survival and attenuates endotoxin-induced acute lung injury in mice. J Immunol **179,** 1855, 2007.

189. Nasef A., Mazurier C., Bouchet S., Francois S., Chapel A., Thierry D.*, et al.* Leukemia inhibitory factor: Role in human mesenchymal stem cells mediated immunosuppression. Cell Immunol **253,** 16, 2008.

190. Spaggiari G. M., Capobianco A., Becchetti S., Mingari M. C., Moretta L. Mesenchymal stem cell-natural killer cell interactions: evidence that activated NK cells are capable of killing MSCs, whereas MSCs can inhibit IL-2-induced NK-cell proliferation. Blood **107,** 1484, 2006.

191. Nemeth K., Leelahavanichkul A., Yuen P. S., Mayer B., Parmelee A., Doi K.*, et al.* Bone marrow stromal cells attenuate sepsis via prostaglandin E(2)-dependent reprogramming of host macrophages to increase their interleukin-10 production. Nat Med **15,** 42, 2009.

192. Spaggiari G. M., Capobianco A., Abdelrazik H., Becchetti F., Mingari M. C., Moretta L. Mesenchymal stem cells inhibit natural killer-cell proliferation, cytotoxicity, and cytokine production: role of indoleamine 2,3-dioxygenase and prostaglandin E2. Blood **111,** 1327, 2008.

193. English K., Ryan J. M., Tobin L., Murphy M. J., Barry F. P., Mahon B. P. Cell contact, prostaglandin E(2) and transforming growth factor beta 1 play non-redundant roles in human mesenchymal stem cell induction of CD4+CD25(High) forkhead box P3+ regulatory T cells. Clin Exp Immunol **156,** 149, 2009.

Chapter 3

Beneficial effects of MSCs on co-cultured chondrocytes are independent of inter-donor variation in chondrogenic differentiation

Yao Fu, Nicole Georgi, Jeroen Leijten, Sanne Both, and Marcel Karperien

Abstract

Co-culturing mesenchymal stem cells (MSCs) with chondrocytes has been reported to result in enhanced proliferation of chondrocytes and matrix deposition by chondrocytes. Although the inter-donor variation of MSCs in differentiation potential is widely recognized, it has remained unknown whether donor variation also influences the beneficial effects of MSCs in chondrocyte-MSC co-cultures. To investigate this, we selected MSCs from 18 distinct donors and investigated their propensity to undergo chondrogenesis. Mono-culture and co-culture micromasses of human MSCs and bovine chondrocytes were cultured in chondrocyte proliferation medium to determine the inter-donor variability and to evaluate whether the beneficial effect of the MSCs is dependent on donor variation. After four weeks, histological analysis of matrix formation and biochemical quantification of glycosaminoglycans (GAGs) were used to detect changes in cartilage matrix deposition. Species-specific qPCR was used to determine the fate and transcriptional profiles of the individual cell populations during co-culture and expression of chondrogenic genes. Human GAPDH expression analysis revealed the near-complete loss of all MSC donors from distinct donors in the co-cultured pellets after four weeks. Average bovine chondrogenic mRNA was expressed at higher levels compared to the bCH group. In the meanwhile, enhanced cartilage matrix deposition in co-culture groups was confirmed by histology staining and GAG quantification assay, which is independent of inter-donor variation and chondrogenic potential of MSCs donors. Interestingly, the pro-chondrogenic co-culture effect was not correlated with the potential of the MSCs to undergo chondrogenic differentiation. These results demonstrate that the beneficial effects of MSC in the chondrocyte-MSC co-culture system are independent of MSCs donor variation in chondrogenic differentiation, which is support for the clinical potential of this approach to boost cartilage tissue regeneration.

3.1 Introduction

Autologous chondrocytes implantation (ACI) has been considered as a golden standard to treat cartilage defects[1-3]. However, the use of autologous chondrocytes has disadvantages that limit its potential clinical applications. These disadvantages include low cell availability and limited cell expansion capability without loss of function[4-7]. Therefore, development of new cell-based tissue engineering strategies is of significant importance for cartilage repair. In this context, the co-culture of articular chondrocytes (ACs) and mesenchymal stem cells (MSCs) is most commonly studied[8-10], which has been shown as effective for cartilage tissue regeneration.

MSCs have emerged as a clinically relevant cell source for cartilage tissue regeneration. The cells can undergo chondrogenesis and are able to deposit a cartilage-specific matrix in a variety of natural and synthetic scaffold materials when exposed to chondrogenic growth factors[11]. In particular, ACs and MSCs cocultures associate with an increased amount of neocartilage formation as compared to either cell type alone[12-14]. Moreover, MSCs can also act as trophic mediators that can guide tissue regeneration[15]. Studies report that in these cocultures, the amount of MSCs significantly decreases over time. This phenomenon is most probably caused by apoptosis, which may play an essential role in the cartilage matrix formation in pellet co-culture system[16]. The beneficial effects of MSCs in the co-culture models were mainly due to increased proliferation of chondrocytes and matrix deposition by chondrocytes that was induced by MSCs rather than by chondrogenic differentiation of MSCs into chondrocytes[8, 16-18]. These studies point to a dominant role of the MSCs in stimulating resident or co-implanted chondrocytes to initiate a regenerative response.

Despite the high translational potential of chondrocyte-MSC co-cultures, the inter-donor variation in this co-culture approach has remained unknown. This is surprising as the considerable inter-donor variation of MSCs is a general and widely known complication for the practical implementation of MSC-based cartilage tissue engineering approaches[19-21]. Researchers have observed striking differences between MSCs of different donors concerning the growth rate, expression of lineage-specific and non-specific markers, and differentiation potential[22-25]. For example, donor age, donor gender, harvest methods, isolation location, and culture conditions are known to determine the differentiation potential of the isolated MSCs[26-28]. In consequence, some researchers have preemptively attempted to

reduce the therapeutic inter-donor variation in chondrocyte-MSC co-cultures *via* the use of mixed donor pools or the selection of highly chondrogenic donors. However, whether the outcome of chondrocyte-MSC co-cultures is affected by inter-donor variability has remained unknown. Therefore, we here compare the potential of MSCs from 18 different individuals on their propensity to undergo chondrogenesis and their ability to stimulate chondrocytes when co-cultured to determine the inter-donor variability of this beneficial effect of MSCs.

3.2 Materials and Methods

3.2.1 Cell culture and expansion

MSCs were isolated from aspirates from 18 human donors as described previously[29]. MSCs from all kinds of donors were cultured in MSC proliferation medium. MSCs were expanded using proliferation medium composed of α-MEM supplemented with 10% FBS, 1% L-glutamine, 0.2 mM Ascorbic acid 2-phosphate (ASAP), 100 U/mL penicillin, 100 µg/mL streptomycin and 1 ng/mL bFGF. Bovine primary chondrocytes (bCHs) were isolated from full-thickness cartilage knee biopsies of 6 months old female calves as previously described[30]. Chondrocytes were expanded in proliferation medium composed of DMEM supplemented with 10% FBS, 1× non-essential amino acid (NEAA), 0.2 mM ASAP, 0.4 mM L-proline, 100 U/mL penicillin and 100 µg/mL streptomycin.

For mono-cultures, 200,000 cells of bCHs (Represented by bCH) or hMSCs (Represented by MSC) were seeded per well of round bottom 96 wells plates. For co-cultures, 200,000 cells were seeded in an 80% hMSC/20% bCH (Represented by Co-culture) ratio. Cells were seeded in chondrocyte proliferation medium and centrifuged for five min at 500 *g*. The medium was refreshed twice a week. Cell pellets were cultured for up to four weeks.

The use of all human materials in this study was approved by a local Medical Ethics Committee. All reagents used for cell culture were purchased from Invitrogen unless otherwise stated. Common chemicals were purchased from Sigma-Aldrich unless otherwise stated.

3.2.2 Histology

Cell pellets were fixed with 10% formalin for 15 min, dehydrated with graded ethanol, and embedded in paraffin using routine procedures. Five µm-thick sections

were cut and stained for sulfated glycosaminoglycans (GAG) using Alcian blue. Nuclei were counterstained with nuclear fast red.

3.3.3 Quantitative GAG

Cell pellets were washed with phosphate-buffered saline (PBS), frozen overnight at -80°C, and digested in digestion buffer (1 mg/mL proteinase K in Tris/EDTA buffer at pH 7.6 containing 185 µg/mL iodoacetamide and 10 µg/mL pepstatin A) for 16 hours at 56°C. The GAG content was quantified with 1,9-dimethyl methylene blue chloride (DMMB) staining in PBE buffer (14.2g/L Na_2HPO_4 and 3.72g/L Na_2EDTA, pH 6.5) using a spectrophotometer (TECAN) at an absorbance of 520 nm. Chondroitin sulfate was used to make a standard curve. Relative cell number was determined by quantification of total DNA using a CyQuant DNA kit (Molecular), according to the manufacturer's instructions.

3.2.4 DNA isolation, RNA isolation, and quantitative polymerase chain reaction

Total DNA was isolated from pellets with the DNA Mini Kit (Promega) according to the manufacturer's protocol. Total RNA was isolated from pellets with the NucleoSpin RNA kit (Machery-Nagel). Total RNA was reverse transcribed into cDNA using the iScript cDNA Synthesis kit (Bio-Rad). Quantitative polymerase chain reaction (qPCR) was performed on genomic DNA or cDNA samples by using the SensiMix SYBE& Fluorescein kit (Bio-Rad). PCR reactions were carried out on the CFX Connect Real-Time PCR Detection System (Bio-Rad) under the following conditions: hot-start for 10 minutes at 95 °C, then 40 cycles consisting of 15 seconds denaturation at 95 °C, 15 seconds annealing at 60 °C and 15 seconds extension at 72 °C, followed by a melting curve. The sequences of the primers for qPCR, either species-specific or cross-species specific, are listed in Supplementary Tables 3.S1 and S2.

3.2.5 Statistical analysis

Statistical analysis of GAG and DNA quantifications were made by using Student's *t*-test. qPCR results were examined for statistical significance with Nonparametric Test, followed by Mann-Whitney Test. *p*-values of < 0.05 were considered statistically significant.

3.3 Results

3.3.1 hMSCs from different donors increase cartilage matrix formation in co-culture with bCHs

To investigate whether donor variation of MSCs would influence the degree of cartilage formation in co-culture pellets, we cultured MSCs from 18 distinct donors with bCHs in 3D pellets. After four weeks of being cultured in the chondrocyte proliferation medium, histology and GAG assays were performed to evaluate cartilage formation. The presence of GAGs was revealed by Alcian blue staining in both mono-culture and co-culture pellets (Fig. 3.1). In line with literature, pure bCH pellet was characterized by relatively low amounts of deposited matrix, which associates with the lack of sufficient amount of chondrogenic growth factors. Similarly, pure MSCs groups demonstrated low levels of differentiation into the chondrogenic lineage, which was associated with substantial inter-donor variation in terms of chondrogenic differentiation. In stark contrast, chondrocyte-MSC co-cultures were characterized by substantially more notable levels of matrix deposition as compared to both pure bCHs and hMSCs groups. Enhanced matrix deposition was actually observed in most of the co-culture groups (Supplementary figure 3.S1).

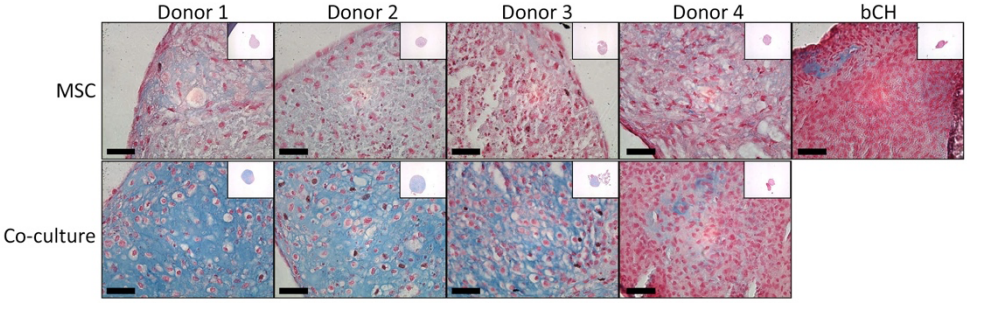

Figure 3.1 *GAG formation in co-culture pellets of bCHs and hMSCs from different donors. Bovine chondrocytes were co-cultured with hMSCs from different donors (hMSC: bCH is 80:20) for 4 weeks in the chondrocyte proliferation medium. Alcian blue staining was performed on cryosections. Nuclei were counterstained with nuclear fast red. Staining results showed various degrees of improved cartilage matrix formation in chondrocyte-MSC co-culture pellets compared to both pure bCHs and different donors of hMSCs groups. Pictures show four representative hMSC donors, in total 18 donors were tested. Data of all donors is presented in supplemental figure 3.S1. Scale bar = 50 µm.*

GAG and DNA contents of each pellet were then determined by chemo-spectrophotometric and fluorescent assays (Fig. 3.2). Both total GAG content and GAG content normalized to DNA increased in most of the co-culture groups comparing to the mono-culture groups (Fig. 3.2A and 2B). The average of 18 donor pairs of hMSCs and bCHs confirmed that co-culture pellets contained more GAG

than mono-culture pellets. In co-culture groups, the average total GAG content was significantly higher than pure MSCs groups with a 6.5-fold change (Fig. 3.2B). The GAG quantification analysis is in line with the histology staining results indicating that the co-culture of hMSCs and bCHs increased cartilage formation. However, no correlation was observed if we pair the GAG content from different hMSCs donors and co-culture groups suggesting that chondrogenic differentiation potential was not correlated with the chondro-induction in co-culture pellets (Fig. 3.2C). Even MSC donors with poor chondrogenic potential sustained GAG production in the co-culture pellets.

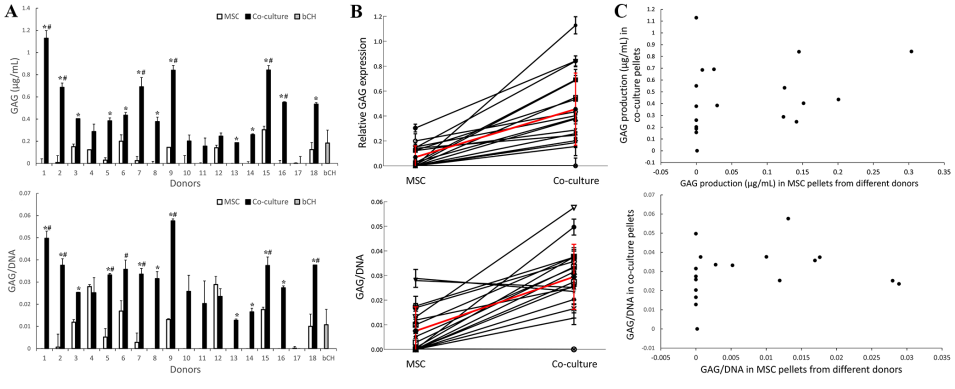

Figure 3.2 *Biochemical assay shows an increase in GAG formation in co-culture pellets. Amount of GAG and DNA in the pellets was measured after a four-week culture period in chondrocyte proliferation medium. Total GAG (top) and GAG/DNA (bottom) are shown, respectively (A). Conditions of hMSCs, bCHs and co-cultures are indicated by the bar colors. * represents p<0,05 compared to values of the pure MSC donor, # represents significance compared to the pure bCH group. Error bar reflects Standard Deviation (S.D.). (B) Correlation of total GAG and GAG/DNA between co-culture group and the respective MSC donor. GAG is expressed higher in co-culture groups compared to the respective hMSC donor. Black lines represent individual donors (n=18). Red line represents the average value. (C) Paired GAG content from different MSCs donors and co-culture groups showed that donor variation of hMSCs does not influence the degree of cartilage formation in co-culture pellets.*

3.3.2 Disappearance of hMSCs in co-culturing with bCHs has no correlation with donor variation

After four weeks of being cultured in chondrocyte proliferation medium, genomic DNA was isolated from cell pellets and species-specific qPCR was used to quantify the genomic GAPDH expression. As shown in Figure 3.3A, after four weeks, the ratio of human genomic DNA decreased from 80% to 1.7% +/- 2.2%. All co-culture

pellets from different hMSCs donors contained predominantly DNA of bovine origin indicating of a loss of human cells during the four-week cell culture period. The same trend appears in mRNA isolated at four weeks. GAPDH mRNA in all the co-culture pellets was from bovine origin, while hardly any human mRNA was detected (Fig. 3.3B). Both the DNA and mRNA analysis of chondrocyte-MSC co-culture pellets demonstrated the near absence of hMSCs in all cell pellets irrespective of donor variation in chondrogenic differentiation.

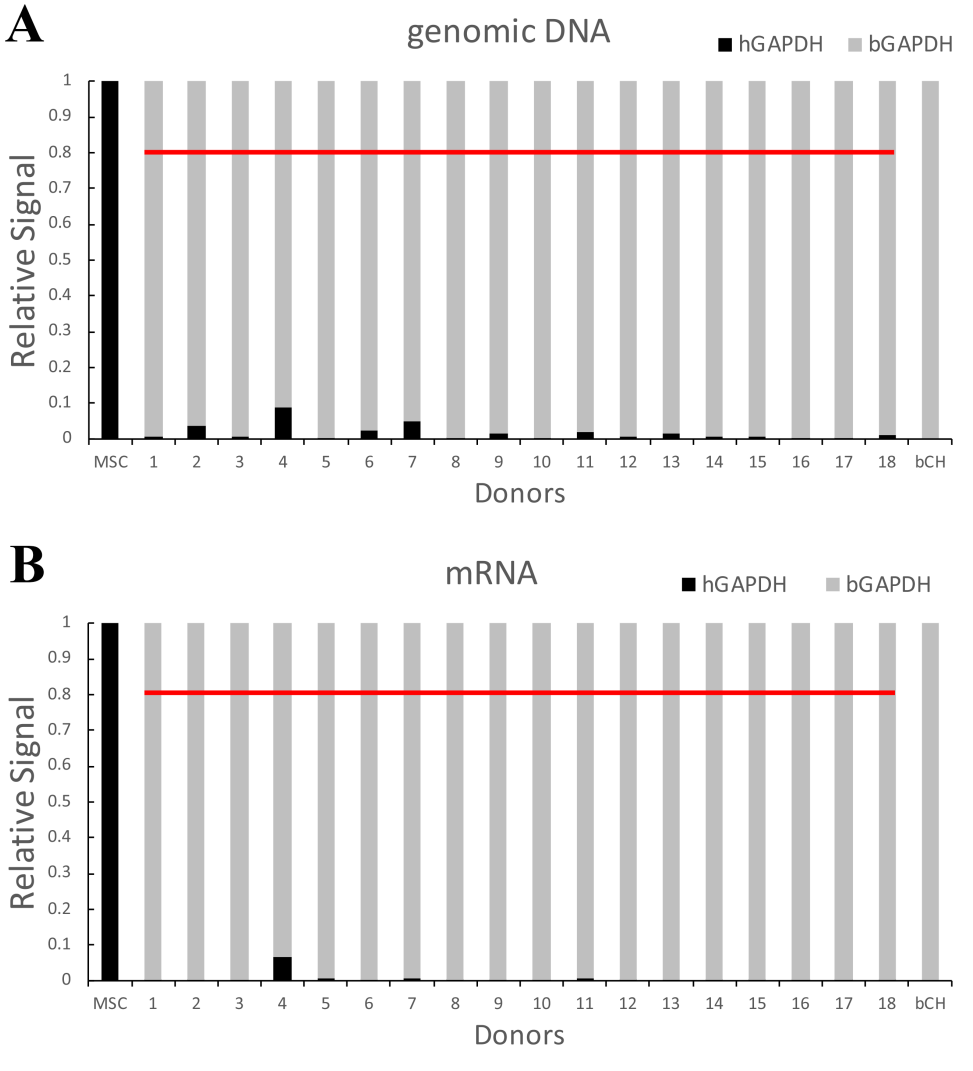

Figure 3.3 *Species-specific qPCR of GAPDH in co-cultures of different donors of hMSCs and bCHs at genomic DNA level (A) and mRNA level (B). Both genomic DNA and RNA were*

extracted from pellets after four weeks in chondrocyte proliferation medium. Data shows a significantly decrease in the percentage of MSCs in pellet co-cultures at four weeks. Red line represents the initial seeding percentage of hMSCs (80%).

3.3.3 Chondrocyte-MSC co-cultures promote matrix formation independently of MSCs donor variation

Both histology staining and biochemical analysis results showed that hMSCs of different donors show distinct chondrogenic potential. Species-specific qPCR was then performed to study the mRNA expression of chondrogenic marker genes in co-culture pellets (Fig. 3.4). After four weeks of being cultured in chondrocyte proliferation medium, average bovine Aggrecan (*Acan*) and Collagen 2 (*Col2a1*) mRNA were expressed at higher levels compared to the bCH group with respectively a 2.2 and 10.8-fold change but with a relatively large spread in data points. When individual co-cultures were examined it was shown that the expression levels of bovine *Acan* and *Col2a1* mRNA in co-culture pellets were either higher or similar to those of pure bCHs pellets (Fig. 3.4A and 4B).

On the other hand, the expression levels of both human *ACAN* and *COL2A1* were much higher in all the co-culture pellets than in pure MSCs pellets (Fig. 3.4C and 4D). This is likely due to the extremely low levels of *hGAPDH* expression in co-culture pellets in comparison with the pure MSCs groups, as measured by species-specific qPCR in figure 3.3 which skews the ratio. The average *Ct* values from different conditions are shown in figure 3.4E demonstrating that *hGAPDH* expression was much lower in the co-cultures. Furthermore, we compared the chondrogenic potential of each condition in depth based on both histochemical and molecular criteria as previously described[39]. Briefly, good chondrogenic differentiation potential was mainly marked by enhanced histological cartilage formation, increased GAG deposition, as well as by significantly higher mRNA expression of *ACAN* and *COL2A1*. Based on these parameters, donors were scored on chondrogenic behavior and divided into three groups: low, moderate, and high chondrogenic potential (Fig. 3.5A). This analysis revealed that none of the MSC donors showed high levels of chondrogenesis and 17 out of the 18 co-cultured donors showed low levels of chondrogenesis when pure MSCs where cultured in growth medium for four weeks (Fig. 3.5B). In contrast, 8 out of the 18 co-cultured donors presented high levels of chondrogenic differentiation while only 4 out of the 18 co-cultured donors were scored as low level chondrogenic performing. Moreover, in line with the paired comparison result (Fig. 3.2C), there was no correlation

between the MSC differentiation potential and the final chondrogenic performance. Taken together, these data indicated that donor variation of MSCs did not influence the degree of cartilage formation in co-culture pellets.

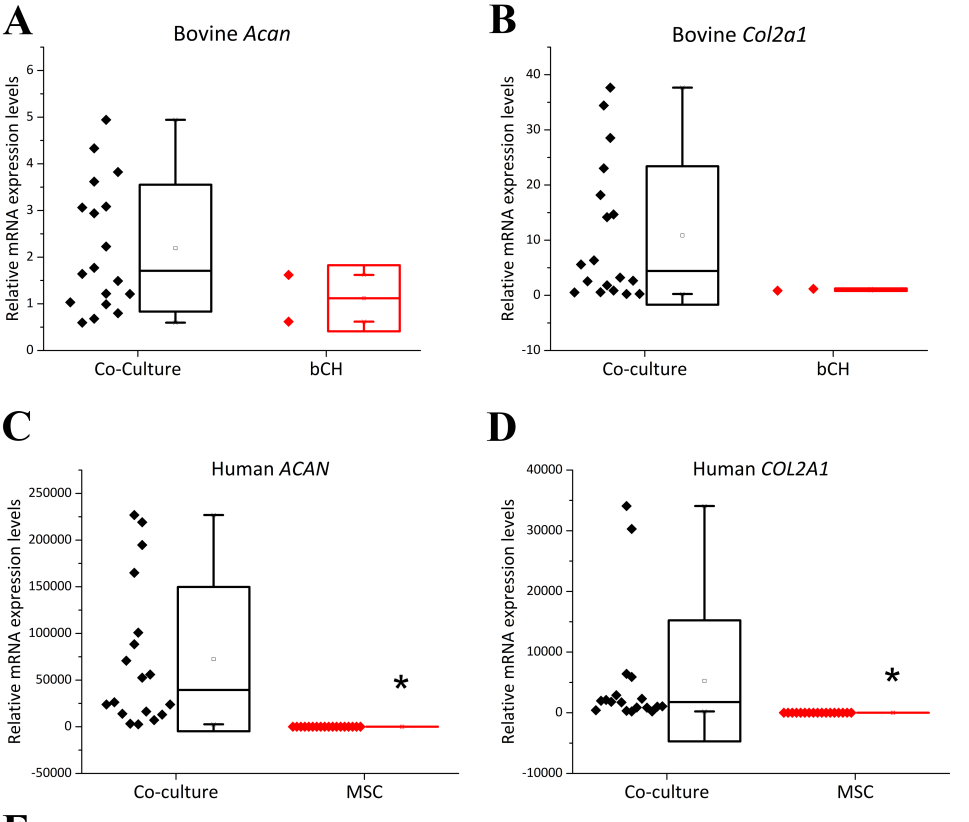

E

	Bovine		Human	
	Co-culture	bCH	Co-culture	MSC
GAPDH	21.88	22.02	31.15	21.82
ACAN	26.84	27.82	27.85	33.63
COL2	26.61	28.74	35.37	36.78

Figure 3.4 *Expression levels of bovine Acan (A) and bovine Col2a1 (B) and human ACAN(C) and human COL2A1 (D) were examined by species-specific qPCR. RNA samples were extracted from pellets cultured in chondrocyte proliferation medium for four weeks. Relative expression levels were obtained by normalization of separate species-specific signals to cross species-specific GAPDH. The values are relative amounts to the pure MSC or*

*chondrocyte groups. Although widely distributed among different donors, average bovine Acan and Col2a1 mRNA were expressed higher compared to bCH group, with respectively a 2.2 and 10.8-fold change. The relative expression levels of human chondrogenic marker genes were much higher in all the co-culture pellets than in pure hMSCs pellets. * represents p<0,05 compared to values of the co-culture pellets. (E) Average Ct values from different conditions showed that human GAPDH expression was much lower in co-culture.*

A

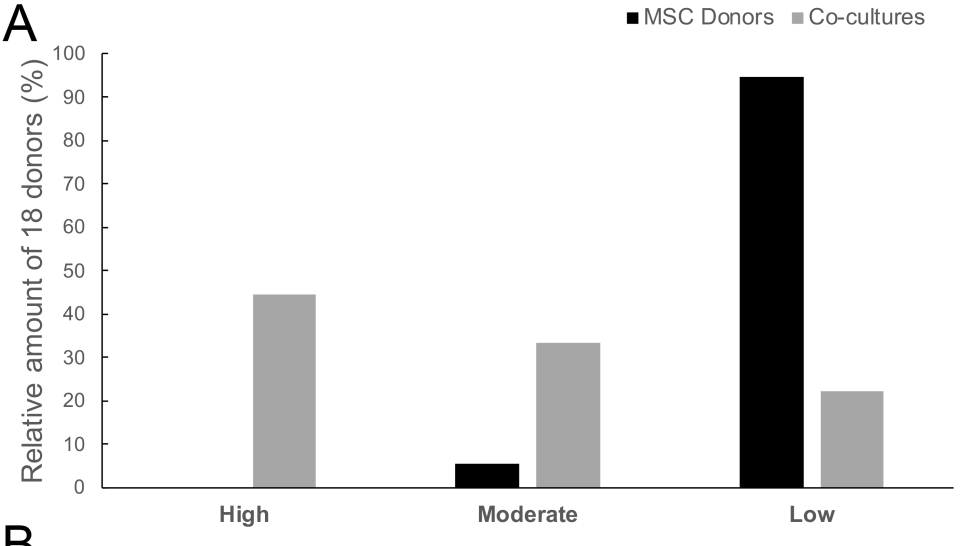

B

Chondrogenic potential	Conditions		Relative amount
High	MSC donors	0	0
	Co-cultures	8	0.44
Moderate	MSC donors	1	0.06
	Co-cultures	6	0.33
Low	MSC donors	17	0.94
	Co-cultures	4	0.22

Figure 3.5 *Scoring of 18 hMSC donors and related co-cultures according to their chondrogenic potential. (A) Scoring was done based on the amount of GAG expression and positive Alcian Blue stain as histological appearance of the cartilage matrix, as well as the mRNA expression levels of chondrogenic marker genes. Scoring donors were separated into high levels, moderate levels, and low levels. Based on the overall score, the percentage of donors in each condition was calculated and plotted (B).*

3.4 Discussion

In this study, we have reported on i) MSCs from distinct donors show a significant decrease in chondrocyte-MSC co-cultures; ii) MSCs from distinct donors could promote cartilage matrix formation in chondrocyte-MSC co-cultures; iii) and that both effects of MSCs are independent of MSC donor variation.

MSCs could serve as a promising cell source for repair of cartilage defects due to the advantages of the noninvasive collection, high proliferative potential, low immunogenicity, and chondrogenic potential *in vitro*[31-34]. However, essential factors deciding on how to use MSCs should not solely be based on their chondrogenic potential and cell phenotype. Although proof of principle exists for cartilage tissue engineering, clinical application is still hampered by considerable donor variation in the ability of MSCs to deposit cartilage matrix *in vivo*[25, 35, 36]. Indeed, in this work, various degree of chondrogenic potential *in vitro* was observed from different donors of hMSCs using histological and biochemical analysis. We should note, however, that in this study the chondrogenic differentiation of the MSCs was performed in suboptimal conditions, e.g. without the addition of pro-chondrogenic factors like TGF-β. The chondrogenic differentiation of these cells in optimal conditions has previously been described[39]. Despite this, pellet culture of the MSCs stimulated a reasonable degree of differentiation into chondrocytes based on histology and GAG staining substantiating the claim that the used panel of MSCs has a high degree of inter-donor variation in chondrogenic differentiation. Previous studies have also observed striking differences between MSCs of different donors concerning the growth rate, expression of both lineage-specific and non-specific markers, and their response to *in vitro* differentiation in the osteoblastic, adipogenic, and chondrogenic cell lineages[22-25]. Whether this difference between donors also affects the beneficial effect of MSCs in the Chondrocyte-MSC co-culture system had remained largely unstudied.

To investigate whether donor variation of MSCs would influence the degree of cartilage formation in co-culture pellets, we cultured MSCs from 18 distinct donors with bCHs in 3D pellets. These donors have previously been characterized in detail with respect to the osteogenic, adipogenic, endothelial cell differentiation potential and expression of CD marker and microRNA[37-39]. These studies showed that the differentiation potential including the chondrogenic potential varied significantly between donors, which is in line with our results. Interestingly, in this study, we have shown that the co-culture effect has no relation with the chondrogenic potential

of the MSCs. Moreover, compared to pure chondrocyte pellets, the expression of bovine chondrogenic genes is enhanced in the co-culture pellets cultured in the proliferation medium. Furthermore, this beneficial effect of MSCs to promote cartilage matrix formation in chondrocyte-MSC co-cultures appears independent of donor variation in chondrogenic differentiation.

Multiple mechanisms have been postulated to explain the increased cartilage matrix formation in the chondrocyte-MSC co-cultures. It was believed that this phenomenon could be explained by the chondrogenic differentiation of MSCs triggered by chondrocytes[40-42]. Although the percentage of MSCs dramatically dropped irrespective of donor from 80% to an only a few percent, the few remaining MSCs expressed *ACAN* and *COL2A1* mRNA at higher levels as compared to pellets of pure MSCs after four weeks of culture. This result indicated that, although the total amount of MSCs will undergo a significant drop, the remaining fraction of MSCs display a stable chondrogenic phenotype. Indeed, studies indicated that chondrocytes could induce the chondrogenic differentiation of MSCs and the addition of the articular chondrocyte-conditioned medium can instigate chondrogenic differentiation of MSCs[41, 43].

Recent studies have demonstrated that increased cartilage formation in co-culture pellets is not mainly due to the chondrogenic differentiation of MSCs, but rather by MSCs exerting a beneficial effect on the chondrocytes stimulating cell proliferation and matrix deposition[8, 16-18]. MSCs accomplish the beneficial effect *via* an indirect mechanism by acting as a trophic mediator. Moreover, the chondrocytes induce apoptosis of the MSCs, which results in a progressive disappearance of MCSs from the original co-culture[16]. The cell death of MSCs in the co-culture pellets further exaggerated the beneficial effects of MSCs. Cell ratio changes in co-culture pellets were studied using species-specific qPCR in our study. In line with previous results, our study demonstrated that the ratio of hMSCs significantly dropped from the initial seeding percentage in co-culture pellets. Although some donor variation was observed in MSC disappearance, the results demonstrated the near absence of human MSCs in all cell pellets. This disappearance showed no correlation with the inter-donor variation in chondrogenic differentiation potential. Combined with the observation that in co-cultures matrix and bovine gene expression was increased during prolonged culturing, this observation indicated that irrespective of the chondrogenic potential of the MSCs, these cells disappear over time in co-cultures and meanwhile stimulate the bovine chondrocytes to produce more cartilage matrix.

At this point in time, little is still known about the exact mechanisms behind the MSC's cell death in co-culture with chondrocytes. Regardless, data has convincingly suggested that the presence of chondrocytes might have contributed to the death of MSCs, which may be caused by secreting apoptosis-inducing cytokines[44, 45]. MSCs expressed detectable cell surface death receptors, which can be activated by apoptosis-inducing ligands. Further investigation is required to demonstrate the precise role of apoptosis-related mechanism that drive the disappearance of MSCs when cocultured with CHs.

When still alive, MSCs continuously secrete factors that promote cell proliferation and matrix formation. Previous studies observed up-regulated expression of *FGF-1* and *BMP-2* genes in chondrocyte-MSC co-culture pellets[46]. These genes have been applied as stimulators to promote chondrogenic induction, cell proliferation and matrix formation[47, 48], which need further study on their cross-talking and regulation. In addition, although species-specific qPCR results indicated that the expression of bovine chondrogenic genes is enhanced in the co-culture pellets, no statistical significance was detected. We believed that this was caused by the limited power in terms of biological replicates. To conclusively demonstrate whether these effects exists, additional studies with higher experimental power are required.

In conclusion, we report for the first time that MSCs, irrespective of their donor variation in chondrogenic differentiation, stimulate cartilage matrix production in co-culture with chondrocytes. Furthermore, we show a similar decrease in the percentage of MSCs in pellet co-cultures over time. Given these remarkably similar observations, we concluded that the MSCs from various donors have likely exerted similar beneficial effects. Taken together, our results demonstrate that the beneficial effects of MSC in Chondrocyte-MSC co-culture system, which are mainly exerted *via* trophic actions, are to a large extent independent of donor variation in chondrogenic differentiation. This supports the potential implications for MSC-based approach to boost cartilage repair strategies.

References

1. Brittberg M., Lindahl A., Nilsson A., Ohlsson C., Isaksson O., Peterson L. Treatment of deep cartilage defects in the knee with autologous chondrocyte transplantation. N Engl J Med **331,** 889, 1994.
2. Peterson L., Minas T., Brittberg M., Lindahl A. Treatment of osteochondritis dissecans of the knee with autologous chondrocyte transplantation - Results at two to ten years. J Bone Joint Surg Am **85A,** 17, 2003.
3. Peterson L., Brittberg M., Kiviranta I., Akerlund E. L., Lindahl A. Autologous chondrocyte transplantation. Biomechanics and long-term durability. Am J Sports Med **30,** 2, 2002.
4. Batty L., Dance S., Bajaj S., Cole B. J. Autologous chondrocyte implantation: an overview of technique and outcomes. ANZ J Surg **81,** 18, 2011.
5. Jakob M., Demarteau O., Schafer D., Stumm M., Heberer M., Martin I. Enzymatic digestion of adult human articular cartilage yields a small fraction of the total available cells. Connect Tissue Res **44,** 173, 2003.
6. Schnabel M., Marlovits S., Eckhoff G., Fichtel I., Gotzen L., Vecsei V*., et al.* Dedifferentiation-associated changes in morphology and gene expression in primary human articular chondrocytes in cell culture. Osteoarthritis Cartilage **10,** 62, 2002.
7. Namba R. S., Meuli M., Sullivan K. M., Le A. X., Adzick N. S. Spontaneous repair of superficial defects in articular cartilage in a fetal lamb model. J Bone Joint Surg Am **80,** 4, 1998.
8. Acharya C., Adesida A., Zajac P., Mumme M., Riesle J., Martin I*., et al.* Enhanced chondrocyte proliferation and mesenchymal stromal cells chondrogenesis in coculture pellets mediate improved cartilage formation. J Cell Physiol **227,** 88, 2012.
9. Bigdeli N., Karlsson C., Strehl R., Concaro S., Hyllner J., Lindahl A. Coculture of Human Embryonic Stem Cells and Human Articular Chondrocytes Results in Significantly Altered Phenotype and Improved Chondrogenic Differentiation. Stem Cells **27,** 1812, 2009.
10. Bian L., Zhai D. Y., Mauck R. L., Burdick J. A. Coculture of human mesenchymal stem cells and articular chondrocytes reduces hypertrophy and enhances functional properties of engineered cartilage. Tissue Eng Part A **17,** 1137, 2011.
11. Yu D. A., Han J., Kim B. S. Stimulation of chondrogenic differentiation of mesenchymal stem cells. Int J Stem Cells **5,** 16, 2012.
12. Dahlin R. L., Kinard L. A., Lam J., Needham C. J., Lu S., Kasper F. K*., et al.* Articular chondrocytes and mesenchymal stem cells seeded on biodegradable scaffolds for the repair of cartilage in a rat osteochondral defect model. Biomaterials **35,** 7460, 2014.
13. Slynarski K., Widuchowski W., Snow M., Weiss W., Kruczynski J., Hendriks J*., et al.* Primary chondrocytes and bone marrow cells on a 3D co-polymer scaffold: 2-year results of a prospective, multicenter, single-arm clinical trial in patients with cartilage defects of the knee. Revue de Chirurgie Orthopédique et Traumatologique **101,** e17, 2015.
14. Yang Y. H., Lee A. J., Barabino G. A. Coculture-Driven Mesenchymal Stem Cell-Differentiated Articular Chondrocyte-Like Cells Support Neocartilage Development. Stem Cells Transl Med **1,** 843, 2012.
15. Fu Y., Karbaat L., Wu L., Leijten J., Both S. K., Karperien M. Trophic Effects of Mesenchymal Stem Cells in Tissue Regeneration. Tissue Eng Part B Rev **23,** 515, 2017.
16. Wu L., Leijten J. C., Georgi N., Post J. N., van Blitterswijk C. A., Karperien M. Trophic effects of mesenchymal stem cells increase chondrocyte proliferation and matrix formation. Tissue Eng Part A **17,** 1425, 2011.
17. Wang M. Q., Rahnama R., Cheng T., Grotkopp E., Jacobs L., Limburg S*., et al.* Trophic Stimulation of Articular Chondrocytes by Late-Passage Mesenchymal Stem Cells in Coculture. J Orthop Res **31,** 1936, 2013.
18. Wu L., Prins H. J., Helder M. N., van Blitterswijk C. A., Karperien M. Trophic effects of mesenchymal stem cells in chondrocyte co-cultures are independent of culture conditions and cell sources. Tissue Eng Part A **18,** 1542, 2012.

19. Siddappa R., Licht R., van Blitterswijk C., de Boer J. Donor variation and loss of multipotency during in vitro expansion of human mesenchymal stem cells for bone tissue engineering. J Orthop Res **25,** 1029, 2007.
20. Kretlow J. D., Jin Y. Q., Liu W., Zhang W. J., Hong T. H., Zhou G.*, et al.* Donor age and cell passage affects differentiation potential of murine bone marrow-derived stem cells. BMC Cell Biol **9,** 60, 2008.
21. Siegel G., Kluba T., Hermanutz-Klein U., Bieback K., Northoff H., Schafer R. Phenotype, donor age and gender affect function of human bone marrow-derived mesenchymal stromal cells. BMC Med **11,** 146, 2013.
22. Mendes S. C., Tibbe J. M., Veenhof M., Bakker K., Both S., Platenburg P. P.*, et al.* Bone tissue-engineered implants using human bone marrow stromal cells: Effect of culture conditions and donor age. Tissue Eng **8,** 911, 2002.
23. Phinney D. G., Kopen G., Righter W., Webster S., Tremain N., Prockop D. J. Donor variation in the growth properties and osteogenic potential of human marrow stromal cells. J Cell Biochem **75,** 424, 1999.
24. Alves H., van Ginkel J., Groen N., Hulsman M., Mentink A., Reinders M.*, et al.* A mesenchymal stromal cell gene signature for donor age. PLoS One **7,** e42908, 2012.
25. Maredziak M., Marycz K., Tomaszewski K. A., Kornicka K., Henry B. M. The Influence of Aging on the Regenerative Potential of Human Adipose Derived Mesenchymal Stem Cells. Stem Cells Int **2016,** 2152435, 2016.
26. Tokalov S. V., Gruner S., Schindler S., Wolf G., Baumann M., Abolmaali N. Age-related changes in the frequency of mesenchymal stem cells in the bone marrow of rats. Stem Cells Dev **16,** 439, 2007.
27. Gallay S. H., Miura Y., Commisso C. N., Fitzsimmons J. S., O'Driscoll S. W. Relationship of donor site to chondrogenic potential of periosteum in vitro. J Orthop Res **12,** 515, 1994.
28. Vacanti V., Kong E., Suzuki G., Sato K., Canty J. M., Lee T. Phenotypic changes of adult porcine mesenchymal stem cells induced by prolonged passaging in culture. J Cell Physiol **205,** 194, 2005.
29. Fernandes H., Dechering K., Van Someren E., Steeghs I., Apotheker M., Leusink A.*, et al.* The role of collagen crosslinking in differentiation of human mesenchymal stem cells and MC3T3-E1 cells. Tissue Eng Part A **15,** 3857, 2009.
30. Hendriks J., Riesle J., Vanblitterswijk C. A. Effect of stratified culture compared to confluent culture in monolayer on proliferation and differentiation of human articular chondrocytes. Tissue Eng **12,** 2397, 2006.
31. Caplan A. I. Adult mesenchymal stem cells for tissue engineering versus regenerative medicine. J Cell Physiol **213,** 341, 2007.
32. Chen W., Liu J., Manuchehrabadi N., Weir M. D., Zhu Z., Xu H. H. Umbilical cord and bone marrow mesenchymal stem cell seeding on macroporous calcium phosphate for bone regeneration in rat cranial defects. Biomaterials **34,** 9917, 2013.
33. Haleem A. M., El Singergy A. A., Sabry D., Atta H. M., Rashed L. A., Chu C. R.*, et al.* The Clinical Use of Human Culture-Expanded Autologous Bone Marrow Mesenchymal Stem Cells Transplanted on Platelet-Rich Fibrin Glue in the Treatment of Articular Cartilage Defects: A Pilot Study and Preliminary Results. Cartilage **1,** 253, 2010.
34. Van Ramshorst J., Bax J. J., Beeres S. L., Dibbets-Schneider P., Roes S. D., Stokkel M. P.*, et al.* Intramyocardial bone marrow cell injection for chronic myocardial ischemia: a randomized controlled trial. JAMA **301,** 1997, 2009.
35. Erickson I. E., van Veen S. C., Sengupta S., Kestle S. R., Mauck R. L. Cartilage Matrix Formation by Bovine Mesenchymal Stem Cells in Three-dimensional Culture Is Age-dependent. Clin Orthop Relat Res **469,** 2744, 2011.
36. Lee J., Lee K. S., Kim C. L., Byeon J. S., Gu N. Y., Cho I. S.*, et al.* Effect of donor age on the proliferation and multipotency of canine adipose-derived mesenchymal stem cells. J Vet Sci **18,** 141, 2017.

37. Mentink A., Hulsman M., Groen N., Licht R., Dechering K. J., van der Stok J.*, et al.* Predicting the therapeutic efficacy of MSC in bone tissue engineering using the molecular marker CADM1. Biomaterials **34,** 4592, 2013.
38. Portalska K. J., Groen N., Krenning G., Georgi N., Mentink A., Harmsen M. C.*, et al.* The effect of donor variation and senescence on endothelial differentiation of human mesenchymal stromal cells. Tissue Eng Part A **19,** 2318, 2013.
39. Georgi N., Taipaleenmaki H., Raiss C. C., Groen N., Portalska K. J., van Blitterswijk C.*, et al.* MicroRNA Levels as Prognostic Markers for the Differentiation Potential of Human Mesenchymal Stromal Cell Donors. Stem Cells Dev **24,** 1946, 2015.
40. Lee J. S., Im G. I. Influence of chondrocytes on the chondrogenic differentiation of adipose stem cells. Tissue Eng Part A **16,** 3569, 2010.
41. Hwang N. S., Im S. G., Wu P. B., Bichara D. A., Zhao X., Randolph M. A.*, et al.* Chondrogenic priming adipose-mesenchymal stem cells for cartilage tissue regeneration. Pharm Res **28,** 1395, 2011.
42. Aung A., Gupta G., Majid G., Varghese S. Osteoarthritic Chondrocyte-Secreted Morphogens Induce Chondrogenic Differentiation of Human Mesenchymal Stem Cells. Arthritis and Rheumatism **63,** 148, 2011.
43. Hwang N. S., Varghese S., Puleo C., Zhang Z., Elisseeff J. Morphogenetic signals from chondrocytes promote chondrogenic and osteogenic differentiation of mesenchymal stem cells. J Cell Physiol **212,** 281, 2007.
44. Secchiero P., Melloni E., Corallini F., Beltrami A. P., Alviano F., Milani D.*, et al.* Tumor Necrosis Factor-Related Apoptosis-Inducing Ligand Promotes Migration of Human Bone Marrow Multipotent Stromal Cells. Stem Cells **26,** 2955, 2008.
45. Wang L., Zhao Y., Shi S. Interplay between Mesenchymal Stem Cells and Lymphocytes: Implications for Immunotherapy and Tissue Regeneration. J Dent Res **91,** 1003, 2012.
46. Wu L., Leijten J., van Blitterswijk C. A., Karperien M. Fibroblast growth factor-1 is a mesenchymal stromal cell-secreted factor stimulating proliferation of osteoarthritic chondrocytes in co-culture. Stem Cells Dev **22,** 2356, 2013.
47. Kozhemyakina E., Lassar A. B., Zelzer E. A pathway to bone: signaling molecules and transcription factors involved in chondrocyte development and maturation. Development **142,** 817, 2015.
48. Ornitz D. M., Marie P. J. Fibroblast growth factor signaling in skeletal development and disease. Genes Dev **29,** 1463, 2015.

3.5 Supplementary material

Figures

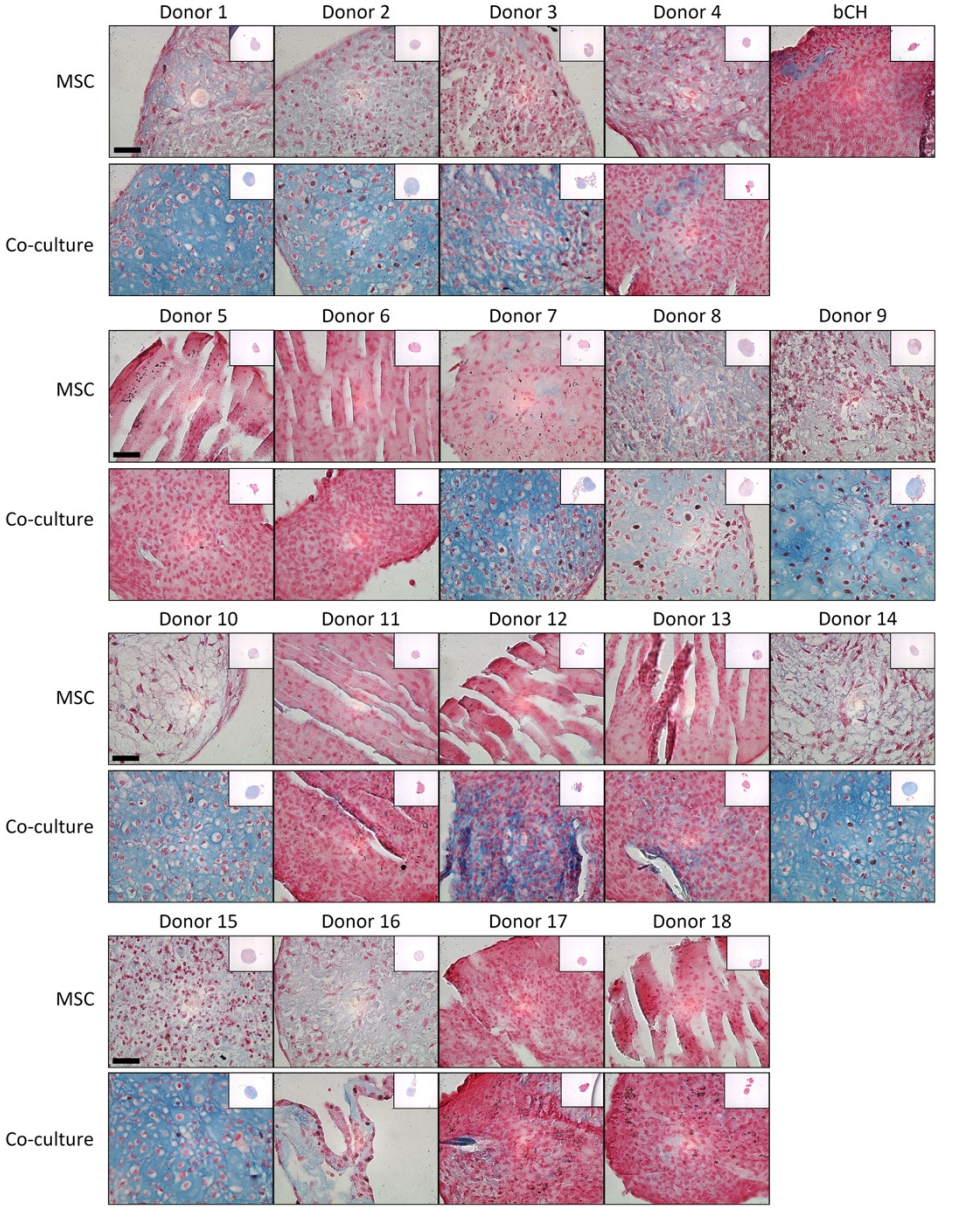

Figure. 3.S1 *Alcian blue staining shows the presence of GAG in pellets from all donors with considerable inter-donor variation. Co-culture of chondrocytes and MSCs improved the*

matrix formation to various degrees compared to both pure bCHs and to the respective hMSCs donor. Moreover, this beneficial effect has no correlation with hMSC donor variation in chondrogenic differentiation. Scale bar = 50 µm.

Table 3.S1 Primers used for quantitative PCR on genomic DNA

Gene Name	Primer Sequence	Product size (bp)
Cross-species GAPDH	F: 5' GCATTGCCCTCAACGACCA 3'	179
	R: 5' CACCACCCTGTTGCTGTAGCC 3'	
Human specific GAPDH	F: 5' TTCCACCCATGGCAAATTCC 3'	131
	R: 5' TTGCCTCCCCAAAGCACATT 3'	
Bovine specific GAPDH	F: 5' AGCCGCATCCCTGAGACAAG 3'	132
	R: 5' CAGAGACCCGCTAGCGCAAT 3'	

Table 3.S2 Primers used for quantitative RT-PCR

Gene Name	Primer Sequence	Product size (bp)
Cross-species GAPDH	F: 5' AGCTCACTGGCATGGCCTTC 3'	116
	R: 5' CGCCTGCTTCACCACCTTCT 3'	
Human specific GAPDH	F: 5' CGCTCTCTGCTCCTCCTGTT 3'	82
	R: 5'CCATGGTGTCTGAGCGATGT 3'	
Bovine specific GAPDH	F: 5' GCCAT CACTG CCACC CAGAA 3'	207
	R: 5' GCGGCAGGTCAGATCCACAA 3'	
Human specific Aggrecan	F: 5' TTCCCATCGTGCCTTTCCA 3'	121
	R: 5' AACCAACGATTGCACTGCTCTT 3'	
Bovine specific Aggrecan	F: 5' CCAAGCTCTGGGGAGGTGTC 3'	98
	R: 5' GAGGGCTGCCCACTGAAGTC 3'	
Human specific Collagen II	F: 5' GGCGGGGAGAAGACGCAGAG 3'	129
	R: 5' CGCAGCGAAACGGCAGGA 3'	
Bovine specific Collagen II	F: 5' AGGTCTGACTGGCCCCATTG 3'	101
	R: 5' CTCGAGCACCAGCAGTTCCA 3'	

Chapter 4

High throughput generated micro-aggregates of MSCs and chondrocytes as a model to investigate cell to cell communication

Yao Fu, Sieger Henke, Sanne Both, Jeroen Leijten, Bram Zoetebier, Marcel Karperien

Abstract

Previous studies showed that mesenchymal stem cells (MSCs) enhance chondrocyte proliferation and matrix production in pellet co-cultures by acting as trophic mediators. The aim of this study was to investigate the mechanism underlying these observations in more detail. In this work, we utilized micro-aggregates of MSCs, chondrocytes, or co-cultures produced in a high throughput platform. These micro-aggregates were embedded in a agarose matrix. Two distinct types of co-cultures in hydrogels were performed: 1) mixtures of monocellular micro-aggregates of MSCs and chondrocytes supporting indirect communication and 2) micro-aggregates composed of both MSCs and chondrocytes supporting direct cell-cell communication. Single cell-seeded constructs were used as a comparison. In the mixed cultures, enhanced cartilage matrix deposition was confirmed in chondrocyte micro-aggregates while simultaneously the micro-aggregates composed of MSC shrunk over time. Also, in the direct cell contact micro-aggregates, cartilage matrix formation was increased by overgrowth of the chondrocytes while the MSCs disappeared. In cultures with indirect cell-cell contact, it was observed that the presence of MSCs promoted the proliferation of chondrocytes. Altogether, our data demonstrated that both direct and indirect MSC-Chondrocyte contacts were involved in the cellular response in micro-aggregate co-cultures. We show that indirect MSC-Chondrocyte contact drives chondrocyte proliferation most likely by secretion of growth factors like FGF1, FGF, and BMP2 and that this effect coincides with the disappearance of MSCs. An enhanced effect on cell proliferation was also shown in the direct micro-aggregate co-cultures. Interestingly in this setup, cartilage matrix production was stimulated in the direct co-cultures suggesting that matrix production in co-cultures is mainly driven by direct cell-cell contact.

4.1 Introduction

Articular cartilage has inadequate regenerative capacity following injury and degradation due to its avascular nature and the low mitotic activity of chondrocytes[1]. Cell-based cartilage repair strategies such as matrix-induced autologous chondrocyte implantation (MACI) could be improved by enhancing cell performance. Aggregation and condensation of cells is a well-studied phenomenon that enhances chondrogenesis and neocartilage formation[2,3]. The traditional way of aggregation is by generating a micromass consisting of 100,000 up to 500,000 cells having diameters ranging from 1-2 mm[3–5]. However, the large length-scale reduces nutrients diffusion, resulting in the chondrogenic matrix deposition vary through the pellet[6–8]. To minimize mass transport limitations, recent studies have focused on the micro-aggregating of progenitor cells to generate a chondrogenic micro-environment[9–12].

Previously, our group has reported on the development of a microwell platform that allows the production of highly controlled micro-aggregates consisting of 50 to 250 cells in high throughput[13,14]. Micro-aggregation of either chondrocytes or progenitor cells enhances chondrogenic differentiation and matrix deposition both *in vitro* and *in vivo,* compared to single cell-seeded constructs. Importantly, micro-aggregates of 100 cells presented higher stability and improved the chondrogenic gene expression profile. These studies indicated that micro-aggregation allows cells to establish a favorable mechanical micro-environment by remodeling their cytoskeleton, depositing ECM, and strengthening adhesion. However, these studies only explored one single type of cell. Presently, pellet co-cultures have been investigated to improve tissue formation in cartilage engineering-based repair strategies[3,15,16]. This data indicates that cartilage matrix deposition increased in co-culture systems of primary chondrocytes and MSCs. Other studies in our group indicated that MSCs enhance chondrocyte proliferation and matrix production by acting as a trophic mediator in co-cultures[17,18]. This data also showed a significant decrease in MSCs in co-culture pellets over time, resulting in an almost homogeneous cartilage tissue

predominantly derived from the initially seeded chondrocytes. The underlying mechanism, how the MSCs exert this beneficial effect in co-cultures is still largely elusive. Thus, this study aims to use this high throughput platform to study the underlying mechanisms that drive increased chondrocyte performance in MSC-Chondrocyte co-cultures.

During the biological process in tissue, cell to cell interaction is known to play a pivotal role in maintaining cell survival and controlling cell signaling and cellular function[19]. Although most studies concluded that direct cell to cell contact is essential for chondrogenesis[20–22], differential effects have been reported whether co-cultures without direct cell to cell contact can achieve similar chondrogenesis as direct co-cultures[23,24]. The mechanism of interaction between MSCs and chondrocytes in co-cultures remains unclear. One approach that can be utilized to assess cell to cell interactions is by using microwell-mediated cell aggregates[25]. Micro-environmental reprogramming *via* cell aggregate formation could provide intact stem cell characteristics and regeneration activity to study cellular function[26]. Compared to the monolayer and conventional pellet cultures, studies on the cell-to-cell interaction and communication are easily addressable in such small pellets. Hence, another aim of this study is to perform more mechanistic studies towards the underlying mechanisms involved in MSC-Chondrocyte communication in co-cultures.

Herein, we utilized a micro-aggregate co-culture system with either direct or indirect cell-cell contact between chondrocytes and MSCs. With the help of this system, we intended to investigate the effect of MSC-Chondrocyte contact on the cell viability and chondro-induction features in co-cultures.

4.2 Materials and methods

4.2.1 Cell culture and expansion

Bovine chondrocytes (bCHs) were isolated from full-thickness cartilage knee biopsies from 6 months old female calves according to the previously reported

protocol[27]. bCHs were expanded in chondrocyte proliferation medium (Dulbecco's modified Eagle's medium (DMEM; Gibco) supplemented with 10% fetal bovine serum (FBS; Gibco), 0.2 mM ascorbic acid 2-phosphate (Sigma), 0.4 mM proline (Sigma),1x nonessential amino acids (Gibco), 100 U/mL penicillin and 100 µg/mL streptomycin (Invitrogen)). Human bone marrow-derived mesenchymal stem cells (hMSCs) were isolated as previously reported[28] and cultured in MSC proliferation medium (α-MEM (Gibco) supplemented with 10% FBS (Gibco), 1% L-glutamine (Gibco), 0.2 mM ASAP (Sigma), 100 U/mL penicillin and 100 µg/mL streptomycin (Invitrogen) and 1 ng/mL bFGF)). The use of human material was approved by a local medical ethical committee. All the medium was refreshed twice a week, and cells at passage 3 were used for the experiments.

4.2.2 Agarose microwell fabrication and micro-aggregates formation

Non-adherent agarose microwells were aseptically fabricated as described previously[14]. Briefly, agarose microwell chips containing ~5000 microwells with a diameter of 200 µm were fabricated by pouring a 3% Ultrapure™ agarose (Invitrogen) solution on convex molds of polydimethylsiloxane (PDMS). After agarose solidification, the agarose chips were separated from the PDMS molds and transferred into 12-well culture plates and covered with PBS. Before cell seeding, the chips were pre-incubated in culture medium overnight at 37°C. For cell aggregate formation, single cells were resuspended in fresh medium and seeded onto the agarose chips at a cell density resulting in sedimentation of 100 cells per microwell. Immediately after seeding, agarose chips were centrifuged at 300g for 3 min to allow the cells to settle down in the microwells and then incubated at 37°C for 24 h to form micro-aggregates. Three types of micro-aggregates were formed, consisting of 100% human MSCs, 100% bovine chondrocytes, or a combination of 80% hMSCs and 20% bCHs (represented by hMSCs, bCHs, and Co-Culture µ-aggregates, respectively).

4.2.3 Cell encapsulation and in vitro chondrogenesis

Micro-aggregates of 100 cells (μ-aggregates) were allowed to form for 24 h in expansion medium. Afterward, the aggregates were flushed out of the micro-wells and mixed with 2% Ultrapure™ agarose (Invitrogen) solution at a concentration of $10x10^6$ cells (approximately 100,000 micro-aggregates) per mL (represented by 10 M/mL). To investigate direct and indirect cell contact during co-culture, two types of experiments were performed. Culture with micro-aggregates composed of both MSCs and chondrocytes (in 4:1 ratio) enabling direct cell-cell contact embedded in agarose (represented by μ-agg-Com). Indirect cell-cell contact was studied in agarose constructs in which monocellular micro-aggregates of either MSCs or chondrocytes (in a 4:1 ratio) were combined (represented by μ-agg-Sep). In total, four groups of micro-aggregates encapsulated in agarose were studied, including μ-agg-MSC, μ-agg-CH, μ-agg-Com, and μ-agg-Sep. Simultaneously, different types of cells (hMSCs, bCHs, and Co-cultures) were also mixed with 2% agarose as single cell suspension at a concentration of 10 million cells/mL, which served as a control. Moreover, for each group, a concentration series of 3, 10, and 20 million cells/mL (M/mL) in agarose were used, effectively decreasing the cell to cell distance with increasing cell seeding density.

After encapsulation of the cells in agarose, they were cultured in chondrogenic differentiation medium (DMEM supplemented with 0.2 mM ascorbic acid 2-phosphate (Sigma), 0.4 mM proline (Sigma), 100 U/mL penicillin and 100 μg/mL streptomycin (Invitrogen), 0.1 μM dexamethasone (Sigma), 100 μg/mL sodium pyruvate (Sigma), 50 μg/mL insulin–transferrin–selenite (ITS; Sigma), 10 ng/mL transforming growth factor β-3 (TGF-β3; R&D Systems)). The medium was refreshed three times every week and at pre-determined time points cultures were analyzed for cell viability, metabolic activity, matrix biosynthesis, and gene expression analysis.

4.2.4 Cell tracking with organic fluorescent dyes

The organic fluorescent dyes CM-DiI and DiO were used for cell tracking in co-cultures. Cells were labeled according to the manufacturer's protocols. All fluorescent images were taken with a Nikon E600 fluorescent microscope.

4.2.5 5-ethynyl-2'-deoxyuridine and TUNEL staining

For labeling of newly synthesized DNA, 5-ethynyl-2'-deoxyuridine (EdU) was added to the culture media at a concentration of 10 mM, 24 h before harvesting the samples. Samples were then washed with phosphate-buffered saline (PBS) and fixed with 10% formalin overnight at 4°C. Samples were embedded in cryomatrix (Thermo-scientific) and cut into 10 µm sections with a cryotome (Shandon). Sections were permeabilized and stained for EdU with Click-iT® EdU Imaging Kit (Invitrogen). Cryosections were also stained for DNA fragments with the DeadEnd Fluorometric TUNEL System (Promega). Nuclei were counterstained with Hoechst 33342.

4.2.6 Histological analyses

Samples were harvested for histological analyses on day 28. Samples were washed with PBS, fixed with 10% formalin at 4°C overnight and then embedded in paraffin using routine procedures. Sections of 5 µm were cut and stained for sulfated glycosaminoglycans (GAG) with Safranin O staining using standard protocol. For immunohistochemistry, cryosections were incubated with 0.3% H_2O_2 and blocked in 5% bovine serum albumin (BSA). Slides were subsequently incubated overnight at 4°C with a rabbit polyclonal antibody against COL II (Abcam). Subsequently, the sections were then incubated with a polyclonal goat-anti-rabbit HRP-conjugated secondary antibody (Dako), followed by development with the DAB Substrate kit (Abcam). Counterstaining was performed with hematoxylin. Non-immune controls underwent the same procedure without primary antibody incubation. Both histology

and immunohistochemistry stained slides were scanned with the NanoZoomer 2.0-RS slide scanner (Hamamatsu).

4.2.7 Quantitative GAG and DNA assay

Samples were washed with PBS and frozen overnight at -80°C. Subsequently, they were digested and measured for GAG quantification as previously reported[3]. The relative cell number was determined by quantification of total DNA using a CyQuant DNA Kit, according to the manufacturer's instructions.

4.2.8 RNA isolation and quantitative polymerase chain reaction

Total RNA was isolated at predefined time points with the TRIzol Reagent (Ambion) according to the manufacturer's protocol. The RNA yields were determined using the Nanodrop2000 (Thermo-scientific). Subsequently, 1 µg of total RNA was reverse-transcribed into cDNA using the iScript cDNA Synthesis kit (Bio-Rad) according to the manufacturer's recommendation. qPCR was performed on cDNA samples by using the SensiMix SYBR& Fluorescein Kit (Bio-Rad). PCR reactions were carried out on CFX Connect™ Real-Time PCR Detection System (Bio-Rad). cDNA was denatured at 95°C for 5 min, followed by 40 cycles. Each cycle consisted of the following conditions: 15s at 95°C, 15s at 60°C, and 30s at 72°C. The sequence of primers for qPCR are listed in table 4.S1. The expression level of aggrecan (*ACAN*) and collagen type II (*COL2*) as well as fibroblast growth factor 1 (*FGF1*), fibroblast growth factor 2 (*FGF2*), and Bone morphogenetic protein 2 (*BMP2*) were investigated, and gene expression was normalized to the expression of species specific *GAPDH* (human or bovine), respectively.

4.2.9 Statistical analysis

Data are presented as mean ± standard deviation with at least three biological replicates per group. Statistical significance between two groups was analyzed using a Student's *t*-test. For three or more groups, a statistical comparison was made using the One-way Analysis of Variance (ANOVA) with Turkey's *post-hoc* analysis. *p*-value of <0.05 was considered statistically significant.

4.3 Results

4.3.1 Encapsulation of micro-aggregates in agarose supports cartilage matrix formation

PDMS molds served as a master mold to generate 3% agarose chips with identically shaped microwells and non-adherent surface for the formation of micro-aggregates (Fig. 4.1). These agarose chips were placed in a well of a 12-well plate and each chip contains 5000 individual microwells with a diameter of 200 μm. Based on previous studies on the stability and formation characteristics of micro-aggregates, as well as the expression of a chondrogenic gene profile, we selected aggregates of 100 cells as the optimal size for further experiments[13,14]. Single-cell suspension of MSC, CH, or the combination were then seeded onto the chips to generate three types of micro-aggregates (Fig. 4.1B). The cells first formed a loose cluster of spherical cells after brief centrifugation. Next, the cell clusters condensed and contracted into smooth spherical micro-aggregates (Fig. 4.1A) in a time span of 24 hours. To further investigate the chondro-induction and cell communication in co-cultures, the micro-aggregates were then embedded in agarose. Notably, two types of co-culture micro-aggregates were generated (Fig. 4.1C).

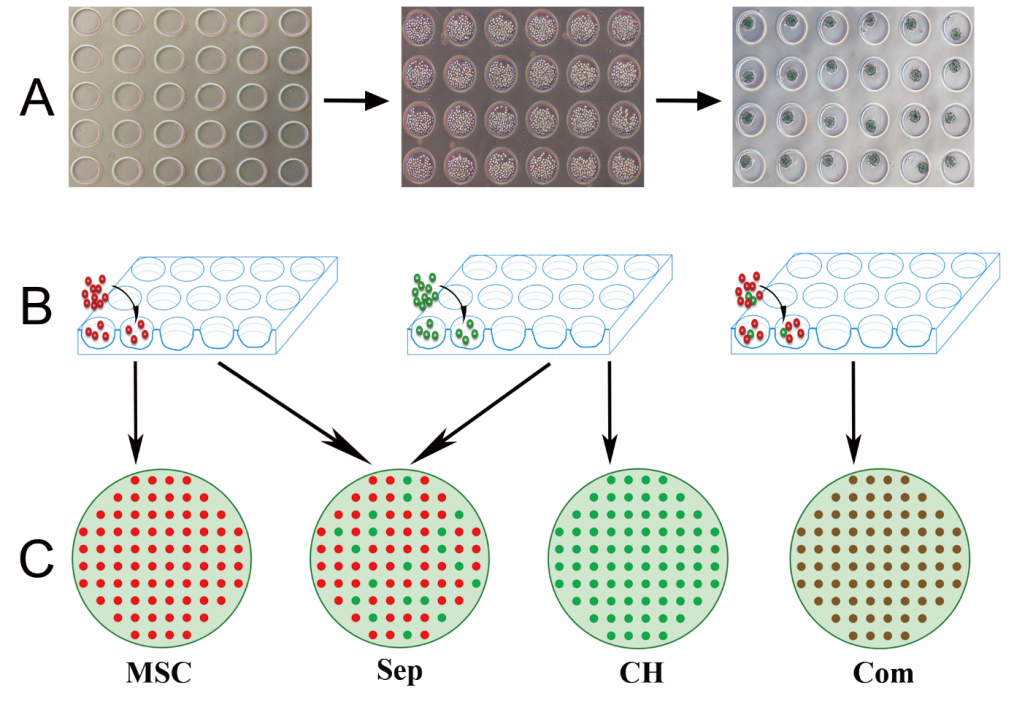

Figure 4.1 *Schematic representation of agarose microwell fabrication, cell aggregation and micro-aggregates encapsulation. A) After cell seeding in the microwell plate, spherical micro-aggregates were formed over 24 hours. B) Three types of micro-aggregates were formed; monocellular MSC and monocellular bovine Chondrocyte micro-aggregates and co-culture micro-aggregates consisting of 80% MSCs and 20% bovine chondrocytes. C) The micro-aggregates were embedded in low melting point agarose in 4 distinct combinations.*

We first compared cartilage formation after embedding bovine chondrocytes either as single cells or as micro-aggregates in agarose at a concentration of $10x10^6$ cells per mL and subsequent culturing in chondrogenic differentiation medium for 28 days. The presence of GAGs was visualized by Safranin O staining (Fig. 4.2A and 2B). As shown in figure 4.2, both spherical aggregates and single cells were homogeneously distributed in the agarose. Histological analyses indicated more intense staining in constructs seeded with micro-aggregates compared to single cell-seeded constructs. The histological analysis was corroborated by gene expression

evaluation. In line with the increased Safranin O staining, mRNA expression of Aggrecan and type II Collagen type was up-regulated in samples with micro-aggregates (Fig. 4.2C).

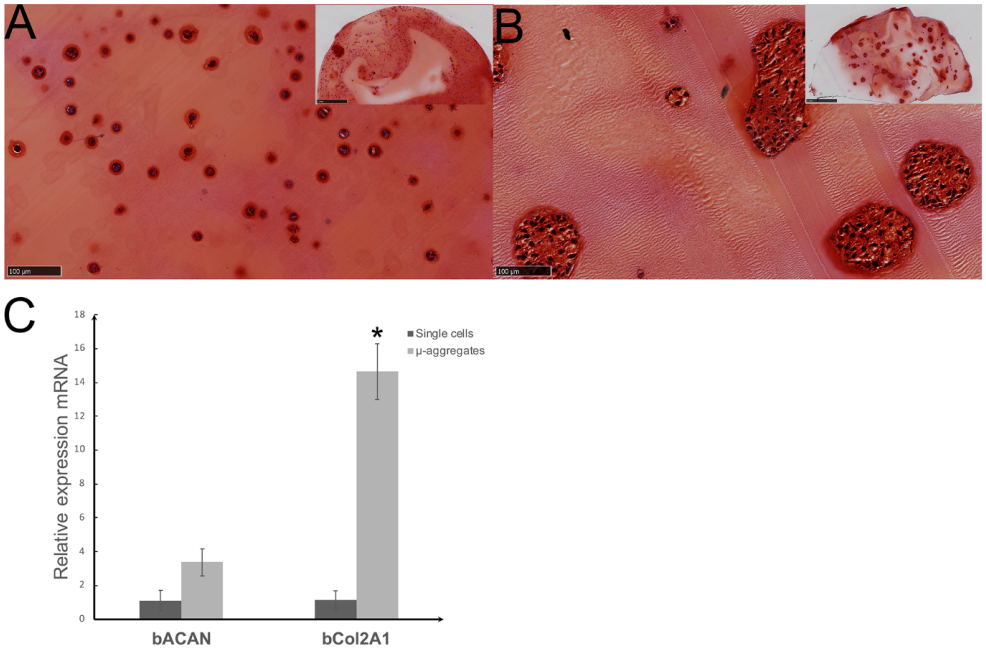

Figure 4.2 *Encapsulation of micro-aggregates of bovine chondrocytes increases cartilage matrix formation compared to single cell-seeded constructs. Safranin O staining in single cell-seeded constructs (A) was substantially lower than monocellular micro-aggregates seeded constructs (B). Inserts indicate the overview of the whole sample; scale bar represents 1 mm. Pictures show the magnified view of sample; scale bar represents 100 µm. (C) Expression levels of ACAN and COL2 were examined by qPCR.*

4.3.2 Direct MSC-Chondrocyte contact induces chondro-induction in micro-aggregate co-cultures

Separated and combined co-culture micro-aggregates (µ-agg-Sep and µ-agg-Com, respectively) were incorporated into agarose at a concentration of 10 x10^6 cells per mL to investigate whether inter micro-aggregate or intra micro-aggregate communication between MSCs and chondrocytes play a role in chondro-induction.

Safranin O staining was performed to show the presence of GAGs in both co-culture systems. As shown in figure 4.3, spherical aggregates were evenly distributed throughout the hydrogel in μ-agg-Sep (Fig. 4.3A) and μ-agg-Com (Fig. 4.3B) conditions. Histological analyses indicated that the μ-agg-Com samples show more intense staining compared to the μ-agg-Sep samples. Additionally, a gradient of GAGs diffusing out of the micro-aggregates and into the hydrogel was observed. Interestingly, in μ-agg-Sep samples intensely stained relatively large micro-aggregates and unstained small micro-aggregates could be observed. Given the overrepresentation of these unstained small micro-aggregates and the resemblance of the larger micro-aggregates with micro-aggregates of pure chondrocytes, the small micro-aggregates likely consist of MSCs (Fig. 4.3A and Supplementary Fig. 4.S1).

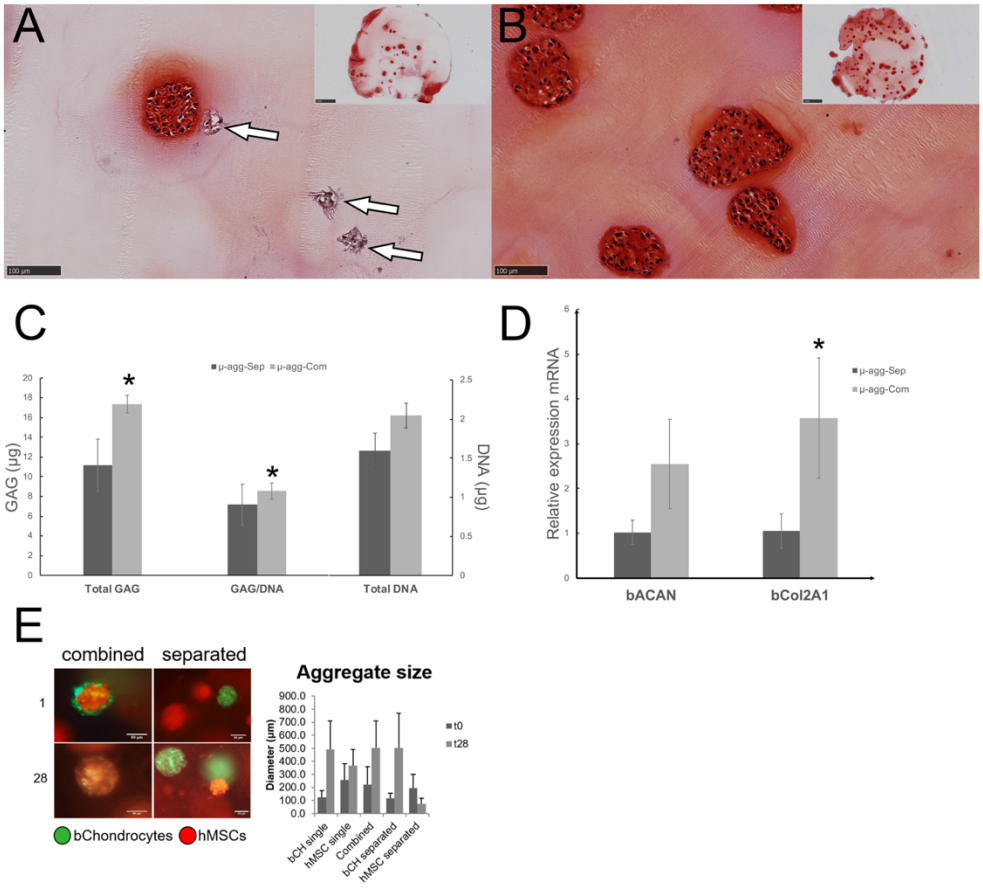

Figure 4.3 *Direct contact improves chondro-induction in micro-aggregate co-cultures. Safranin O staining indicates the presence of GAGs in μ-agg-Sep (A) compared to μ-agg-Com (B). Inserts indicate the overview of the sample. Unstained small micro-aggregates can be seen in the μ-agg-Sep condition (indicated by white arrows); scale bar represents 1 mm. Pictures show the magnified view of the sample; scale bar represents 100 μm. (C) Biochemical assay shows an increase in GAG in μ-agg-Com. Error bars reflect SD. * represents $p<0.05$ compared to the μ-agg-Sep condition. (D) Expression levels of ACAN, and COL2 were examined by species-specific qPCR. * represents $p<0.05$ compared to the μ-agg-Sep condition. (E) Microscopic images of fluorescently labeled micro-aggregates in which chondrocytes were labeled green and MSCs were labeled red and their size quantification at day 1 (D1) and day 28 (D28). The diameter of the aggregates was measured,*

assuming spherical aggregates. Error bars reflect SD. Scale bar represents 100 µm.

The increase of GAG content in the µ-agg-Com group was confirmed by GAG quantification (Fig. 4.3C). The amount of total GAG and GAG/DNA of µ-agg-Com was significantly increased compared to µ-agg-Sep. In line with the histological and biochemical assay, chondrogenic genes expression was also improved in the µ-agg-Com group (Fig. 4.3D). Besides, compared to µ-agg-CH group, safranin O staining result indicated that the presence of GAG was similar in µ-agg-Com (Supplementary Fig. 4.S2A). The GAG quantification showed the results were in line with the histological analysis. The µ-agg-Com displayed increased total GAG while decreased total GAG in µ-agg-Sep compared to µ-agg-CH (Supplementary Fig. 4.S2B). Considering the lower initial seeding percentage of chondrocyte, MSC-Chondrocyte co-cultures in micro-aggregation indeed enhanced the chondro-induction in the system.

Cell tracing experiments, in which chondrocytes were labeled green and MSCs were labeled red were used to follow cell fate of both cell types. Fluorescent labeling showed that MSCs ended up in the center of the micro-aggregates, while the chondrocytes ended up at the periphery 1 day after micro-aggregate formation in line with previous findings (Fig. 4.3E). Overtime, these micro-aggregates grew in size. Due to the mixing of the fluorescent labels it was not possible to distinguish the individual cell types[29]. Monocellular chondrocyte containing micro-aggregates cultured individually or in the µ-agg-Sep increased in size over a 28-day culture period. A comparable increase in size was observed in the µ-agg-Com group. Remarkably, while MCS micro-aggregates cultured without chondrocytes also increased in size, they shrunk when combined with monocellular chondrocyte micro-aggregates in the µ-agg-Sep condition in agreement with data in fig. 4.3A.

We next varied the inter micro-aggregate distance by seeding increasing concentrations of micro-aggregates at 3, 10, and 20 million cells/mL in agarose. Safranin O and immunohistochemistry staining for collagen type II were performed to investigate matrix deposition. As shown in figure 4.4, µ-agg-Com samples (Fig.

4.4B) presented in all groups with more intense GAG staining compared to µ-agg-Sep groups (Fig. 4.4A). GAG staining increased with higher cell concentration. Collagen type 2 staining was detected in all conditions with no obvious differences (Fig. 4.4C and 4D). Altogether, this data suggests that direct cell-cell contact between MSCs and chondrocytes stimulates GAG deposition.

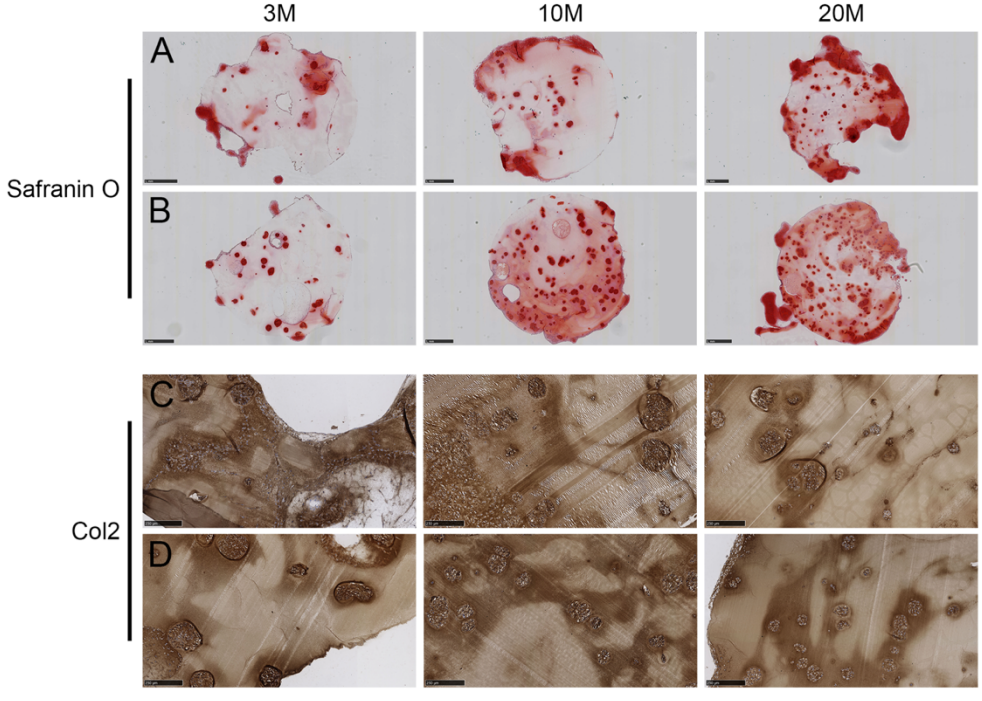

Figure 4.4 *Safranin O staining indicated less intense GAG staining in µ-agg-Sep (A) compared to µ-agg-Com (B). Scale bar represents 1 mm. Immunohistochemistry staining for collagen type II indicated collagen deposition in µ-agg-Sep (C) and µ-agg-Com (D). Scale bar represents 250 µm.*

4.3.3 Direct MSC-Chondrocyte contact induces a sharp decrease in MSCs in micro-aggregate co-cultures, while indirect communication enhances the apoptotic effect

Species-specific qPCR was performed to determine the mRNA expression of GAPDH in co-cultures of micro-aggregates. As shown in Figure 4.5A, the percentage of human MSC-derived GAPDH mRNA in both µ-agg-Com and µ-agg-

Sep gradually reduced over a period of 7 days. The decrease in µ-agg-Com condition was faster than separated co-cultures even though the fold decrease at day 7 was comparable. To determine whether MSCs underwent apoptosis during prolonged cell culture, we performed a fluorescent TUNEL assay (Fig. 4.5B). On Day 7, higher TUNEL-positive cells were found in all micro-aggregate cultures containing MSCs compared to the pure chondrocyte micro-aggregates. Notably, in all conditions TUNEL-positivity reduced at higher cell seeding concentrations, indicating that cell density in hydrogel constructs is critically determines cell viability. Interestingly, in the µ-agg-Sep seeded with 10 million cells/mL significant higher levels of apoptotic cells were found compared to any other condition, suggesting that indirect contact between pure MSC and chondrocyte micro-aggregates may enhance TUNEL positivity in co-cultures. Combined this data suggests that the MSCs die by apoptosis irrespective of the type of co-culture.

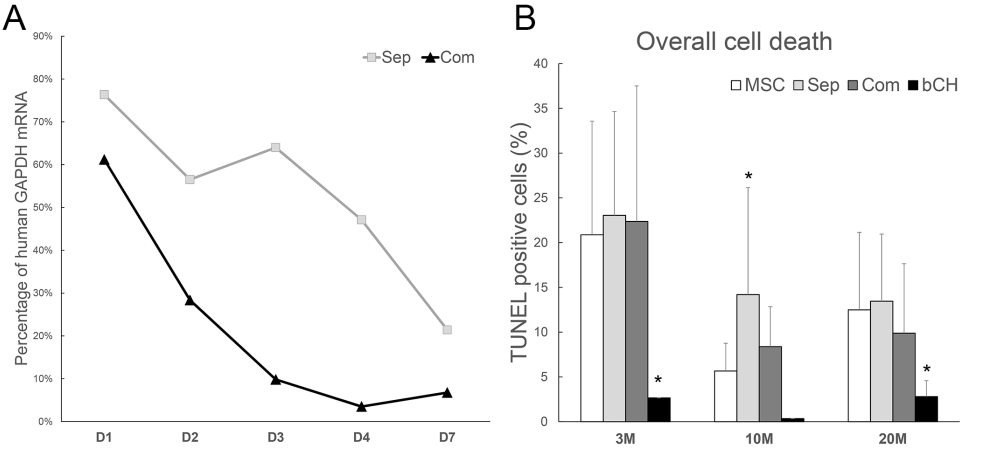

Figure 4.5 *Co-culture induces the loss of MSC in direct and indirect co-cultures. (A) mRNA expression of GAPDH in co-cultures micro-aggregates was determined by using species specific qPCR. (B) Quantification of TUNEL-positive cells in all micro-aggregate groups containing series cell concentration at day 7.*

4.3.4 MSC stimulate chondrocyte proliferation in micro-aggregate co-cultures

We next examined cell proliferation in micro-aggregates using EdU incorporation.

We first determined the percentage of EdU-positive bCHs in µ-agg-CH and µ-agg-Sep (Fig. 4.6A). Interestingly, indirect co-culture increased the proliferation of bCHs irrespective of the cell seeding density. Additionally, decreasing the physical distance by increasing cell seeding density had little effect on the chondrocyte proliferation in µ-agg-Sep groups. The overall cell proliferation in µ-agg-Com and µ-agg-Sep was calculated by the percentage of total EdU-positive cells (Fig. 4.6B). The results indicated that direct MSC-Chondrocyte contact in the µ-agg-Com group significantly enhanced cell proliferation in micro-aggregate co-cultures at day 1 and 3. This data demonstrated that co-culture with MSC stimulated chondrocyte proliferation and showed that this effect was highest in micro-aggregates with direct cell-cell contact.

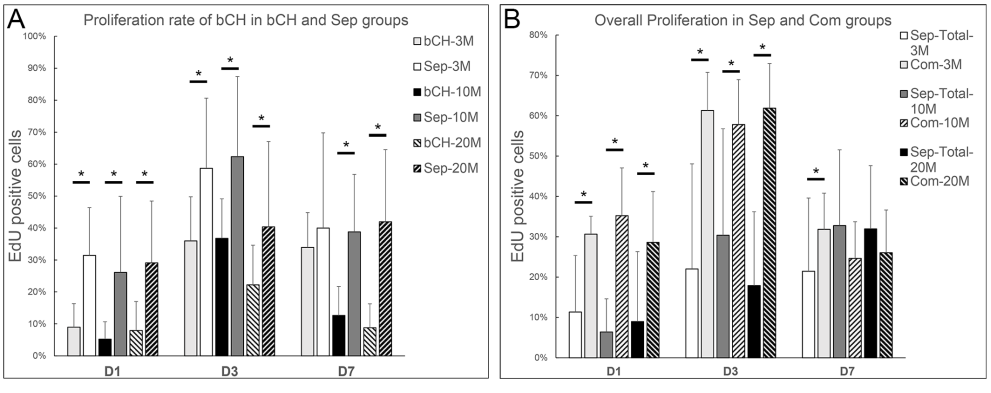

Figure 4.6 *MSCs stimulate chondrocyte proliferation in MSC-CH co-culture micro-aggregates and that this effect was highest in co-cultures with direct cell-cell contact. (A) Quantification of EdU-positive bCHs in µ-agg-CH and µ-agg-Sep. Data from three pellets was analyzed for statistic significance. Error bars reflect SD. (B) Quantification of total EdU-positive cells µ-agg-Sep and µ-agg-Com conditions. Error bars reflect SD.*

4.3.5 Direct MSC-Chondrocyte contact promotes growth factor expression in co-cultures

Species-specific qPCR was performed at day 7 to determine the gene expression of growth factors in micro-aggregate co-cultures (Fig. 4.7). *FGF-1*, *FGF-2*, and *BMP-2* were mostly expressed at higher levels in co-culture

micro-aggregates than in mono-culture micro-aggregates. Remarkably, MSCs expressed significantly higher *FGF2* and *BMP2* levels in the µ-agg-Com group (Fig. 4.7A), while bCHs expressed higher *FGF2* and *BMP2* in the µ-agg-Sep group (Fig. 4.7B). Besides, mRNA expression of these growth factors was increased at higher cell seeding densities in the µ-agg-Com group. This data indicated that direct cell-cell contact improves growth factor mRNA expression in MSC-CH co-cultures.

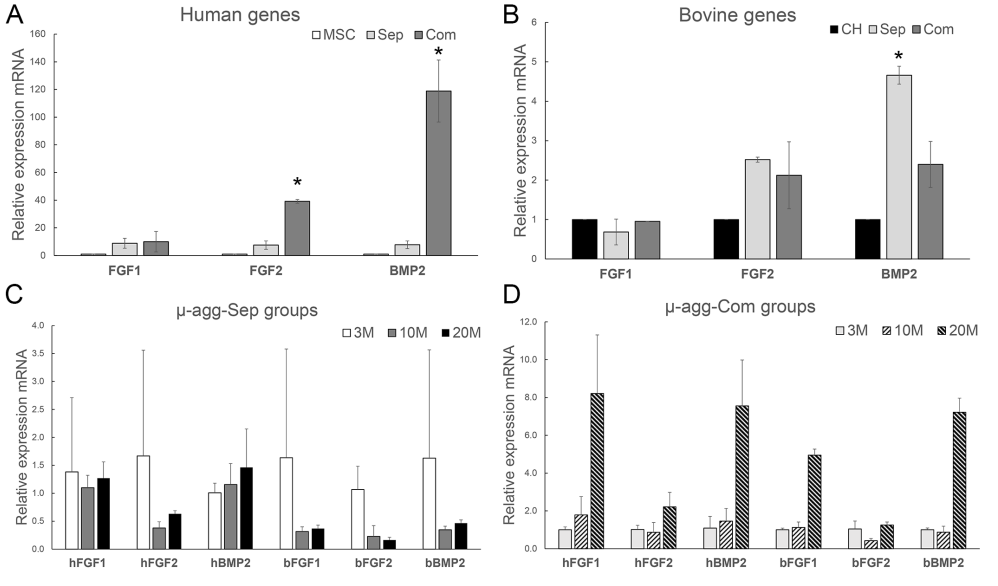

Figure 4.7. *Expression levels of FGF1, FGF2, and BMP2 were examined by species-specific qPCR. Species specific human (A) and bovine (B) mRNA expression in pure MSCs, the µ-agg-Sep (Sep) and µ-agg-Com (Com) micro-aggregates seeded at a density of 10 million cells/mL. C) Human (h) and bovine (b) growth factor mRNA expression in µ-agg-Sep micro-aggregate cultures is dependent on cell seeding density. D) Human (h) and bovine (b) growth factor mRNA expression in µ-agg-Com micro-aggregate cultures is dependent on cell seeding density. Data represent the mean ± standard deviation.*

4.4 Discussion

In this work, micro-aggregates were formed using a high throughput platform to investigate the underlying mechanisms that drive increased chondrocyte

performance in MSC-Chondrocyte co-cultures. Two types of co-culture micro-aggregates were developed to explore the effect of direct and indirect MSC-Chondrocyte contact. The micro-aggregates were subsequently added in an agarose hydrogel. Moreover, we performed a series of cell seeding densities, which allowed us to modify the physical distance between the micro-aggregates. We observed that micro-aggregation is compatible with chondro-induction in micro-aggregate co-cultures. We demonstrate that MSCs promote the proliferation of chondrocytes in co-cultures *via* indirect contact most likely by increasing the expression of FGF1, FGF2, and BMP2. Furthermore, we show that direct cellular contact in co-cultures improves cell viability. Finally, we demonstrate that irrespective of the co-culture method the MSCs die most likely by apoptosis based on TUNEL staining while simultaneously stimulating chondrocytes to proliferate and deposit extracellular matrix.

In our group, we previously reported that micro-aggregation of expanded monocultures of chondrocytes or MSCs boosted cartilage formation both *in vitro* and *in vivo.* A fully controlled high throughput platform was used to reproducibly generate micro-aggregates of a few up to 100 cells[13,14]. This finding was confirmed in this study by enhanced matrix formation as well as chondrogenic related gene expression in the chondrocyte micro-aggregates compared to the single cells seeded constructs. This beneficial effect of chondrocyte micro-aggregation can be partially explained since micro-aggregation allows cells to establish a favorable mechanical micro-environment strengthening adhesion by remodeling their cytoskeleton thereby stimulating the deposition of ECM[13]. Besides by facilitating auto- and paracrine signaling *via* soluble factors[30], micro-aggregation also provides a 3D environment with close cell-cell contact and contraction forces that affect cell behavior[31,32]. Moreover, this microwell-based micro-aggregate culture strategy was also developed to generate *in vitro* micro cartilage tissue[9,12,33].

In this study, we set a micro-aggregates co-culture system using human MSCs and bovine chondrocytes. Both histology and GAG quantification results indicated that

MSC-Chondrocyte co-cultures enhanced the chondro-induction in the micro-aggregate system. This observation is coherent with literature data obtained for the chondrogenic 3D co-culture of mesenchymal stem cells and chondrocytes in pellet co-cultures[17,18,20]. Indeed, chondro-induction was observed in MSC-Chondrocyte pellet co-cultures and superior neocartilage was formed by the combination of two different cell types as compared to either cell type alone. Notably, this system resulted in the enhanced proliferation and matrix deposition of the chondrocytes. Based on species-specific PCR, it was determined that within these direct co-cultures the majority of the chondrogenic expression originated from the chondrocytes[17,34]. The MSCs accomplish this effect by acting as trophic mediators in co-cultures[35]. Moreover, while chondrogenic differentiation of MSCs can be triggered by chondrocytes, it also induces apoptosis in the MSCs[17]. Although the majority of MSCs will undergo apoptosis, the remaining fraction displays a stable chondrogenic phenotype (*Chapter 3* in this thesis). This effect of MSCs is mediated by a yet unidentified communication mechanism.

To understand the underlying mechanism regulating the beneficial effect of MSCs in co-cultures, we developed MSC-Chondrocyte micro-aggregate co-cultures enabling direct and indirect cell-cell contact between the MSCs and the Chondrocytes. Natural tissues are exposed continuously to the environment of cell-cell interactions that affect their function. For instance, pre-cartilage condensation of MSC regulated by cell adhesion molecules[36] is an essential primary step during *in vivo* chondrogenesis[37]. Moreover, it has been reported that cell-cell contact could be a critical factor that controls cell survival and other major cellular functions[25]. In other studies, MSCs revealed that their therapeutic effect in tissue repair strategies may largely depend on their capacity to secrete soluble factors that promote several key biological activities[38,39]. Therefore, how the MSCs exert their beneficial effects in co-cultures was extensively studied. However, the limitation in previously published co-culture studies was that all available platforms could not investigate one factor without influencing the other factors. In this study, we used a unique approach that specifically allowed us to separate the direct cell-cell and cell-matrix

contact from contact by secreted factors. This system benefits from high throughput production of small micro-aggregates as it allows for the analysis of many samples or conditions. When embedded within the biomaterial, the cell types are physically separated by several micrometers preventing cell-cell and cell-matrix contact, while allowing free diffusion of secreted factors. The small construct size keeps the secreted factors approximately constant in the separated and combined co-culture in contrast to transwell or comparable systems. Moreover, by increasing the incorporated cell concentration, we can further regulate the physical distance and cell-cell interaction. Utilizing this system, we can study the cellular interaction during the co-cultures and compare the effect of cell-cell contact with cell-secreted trophic factors on the cell fate and matrix production in co-cultures.

In this study, we first focus on the cellular behavior of these cells in different co-cultures environments. We confirmed that in co-culture micro-aggregates of MSCs and Chondrocytes favoring direct cell-cell contact showed improved chondro-induction compared with an environment where micro-aggregates of pure MSCs and pure Chondrocytes were mixed and seeded in the agarose hydrogel. In this situation, only indirect cell contact between chondrocytes and MSCs is possible. Both histology analysis and GAG quantification indicated that the matrix outputs were significantly enhanced when co-cultures were maintained in direct cell-cell contact conditions. Consistent with the GAG results, chondrogenic gene expression also indicated that the chondro-induction was enhanced in combined micro-aggregate co-cultures. Moreover, when we decrease the physical distance between the cells by increasing cell seeding densities the matrix production was also significantly increased in the separated co-cultures. A previous study[22] suggested that MSCs in direct contact with chondrocytes can communicate through gap junctions, which play a crucial role in cell-cell interaction by the exchange of nutrients such as glucose and amino acids[40]. The discrepancies of previously published studies about the effect of direct and indirect co-cultures may be attributed to the differences in the species from which the cells were isolated, the proportions of stem cells to mature chondrocytes in the cultures and/or the culturing method (2D

culture or 3D biomaterial scaffolds). In the present work, however, we did a comprehensive study that takes different conditions into account and that compares direct and indirect cell-cell separately and adjustably. Altogether, our results suggest that direct cell-cell contact between MSCs and chondrocytes is the most important driver for increased cartilage production in co-cultures.

The decline of MSCs also observed in both co-culture systems. The results clearly showed the morphological changes of the separated aggregates in μ-agg-Sep constructs in which the size of MSC micro-aggregates decreased over time, while the size of CH micro-aggregates increased. However, MSCs performed differently in direct and indirect co-culture with chondrocytes. Direct MSC-Chondrocyte contact presents a shock reaction between the cells, which showed a sharp drop in MSCs mRNA expression. Nevertheless, even in the indirect cell-cell contact co-cultures MSCs decrease over time albeit at a slower pace. The fold change in both direct and indirect co-cultures at day 7 was remarkably similar. Additionally, indirect MSC-Chondrocyte contact enhances the number of TUNEL positive cells in co-cultures.

Previous studies suggested that MSCs can be affected by soluble factors including apoptosis-inducing cytokines, which contribute to the death of MSCs[41]. It was postulated that the mechanism behind the death of the MSCs is likely related to one of the deliberate “suicide” programs present within cells[35]. These suicide programs are usually induced intrinsically or extrinsically by external stimuli such as mechanical stress, oxidative processes, and drug treatments. The programmed suicide death has two primary forms, apoptosis and autophagy[42–44]. Of these two pathways, apoptosis is triggered by biochemical events, which induce characteristic changes in the morphology of the cell. Autophagy, on the contrary, is a catabolic process in which the cell degrades cytoplasmic components essential for survival, thereby leading to a so-called “self-eating” phenomenon. The two pathways of apoptosis and autophagy are intricately interconnected and the upregulation of one of the two consequently leads to downregulation of the other[45]. Further study needs

to be performed to investigate what type of death pathway (autophagy or apoptosis) was predominantly involved in the disappearance of the MSCs in co-cultures with chondrocytes.

Another unresolved question is how MSCs affect the proliferation of chondrocytes in co-cultures. Our results indicated that the presence of MSCs significantly enhanced the proliferation of chondrocytes in co-cultures. Meanwhile, this beneficial effect of MSCs can proceeded through indirect MSC-Chondrocyte contact. However, direct MSC-Chondrocyte contact significantly improved the overall cell proliferation compared to the indirect cell-cell contact constructs. A previous study suggested that the induction of chondrocyte proliferation by MSCs is most likely caused by secreted factors[17]. Indeed, species-specific PCR results indicated that direct MSC-Chondrocyte contact promotes the expression of growth factors. Moreover, the expression of these factors was predominantly expressed by hMSCs. These results are consistent with previous studies that MSC-Chondrocyte co-cultures up-regulated several cytokines and growth factors as well as a variety of matrix remodeling proteins[29]. These factors, including FGF1, FGF2, and BMP2, can contribute to the proliferation of chondrocytes and are partly responsible for the increase of matrix formation in co-cultures[46–51]. Interestingly, higher incorporated cell density, which in turn decreases the physical distance between micro-aggregates, enhances the expression of secreted factors in direct cell-cell contact constructs while having little effect on the indirect group. Altogether, these data suggest that both direct and indirect cell-cell contacts are involved in the increasing proliferation of chondrocytes. The indirect way playing an auxiliary role, while the direct MSC-Chondrocyte contact and secreted factors from MSCs were potent stimulators of chondrocyte proliferation in micro-aggregates co-cultures.

In summary, our data support that micro-aggregation can enhance the chondro-inductive process of chondrocytes. Notably, micro-aggregation can be used to investigate the effects of MSC-Chondrocyte contact on the co-cultures. Our data demonstrated that both direct and indirect MSC-Chondrocyte contact are involved

in cellular behavior changes in the co-cultures. Indirect contact affects the cell viability, especially the cell death, while direct contact more affect the chondro-induction. Otherwise, direct MSC-Chondrocyte contact maintains the cell proliferation and consequently promote matrix production, which is essential for increased chondro-induction in co-cultures. These results suggest that combined micro-aggregates of MSCs and Chondrocytes could be a potential strategy for cartilage tissue regeneration.

References

1. Newman, A. P. Articular Cartilage Repair. *Am. J. Sports Med.* **1998**, *26*, 309–324.

2. Kosher, R. A.; Kulyk, W. M.; Gay, S. W. Collagen Gene Expression during Limb Cartilage Differentiation. *J. Cell Biol.* **1986**, *102*, 1151–1156.

3. Hendriks, J. A. A.; Miclea, R. L.; Schotel, R.; de Bruijn, E.; Moroni, L.; Karperien, M.; Riesle, J.; van Blitterswijk, C. A. Primary Chondrocytes Enhance Cartilage Tissue Formation upon Co-Culture with a Range of Cell Types. *Soft Matter* **2010**, *6*, 5080–5088.

4. Banu, N.; Tsuchiya, T. Markedly Different Effects of Hyaluronic Acid and Chondroitin Sulfate-A on the Differentiation of Human Articular Chondrocytes in Micromass and 3-D Honeycomb Rotation Cultures. *J. Biomed. Mater. Res. Part A* **2007**, *80*, 257–267.

5. Tare, R. S.; Howard, D.; Pound, J. C.; Roach, H. I.; Oreffo, R. O. C. Tissue Engineering Strategies for Cartilage Generation—Micromass and Three Dimensional Cultures Using Human Chondrocytes and a Continuous Cell Line. *Biochem. Biophys. Res. Commun.* **2005**, *333*, 609–621.

6. Hui, T. Y.; Cheung, K. M. C.; Cheung, W. L.; Chan, D.; Chan, B. P. In Vitro Chondrogenic Differentiation of Human Mesenchymal Stem Cells in Collagen Microspheres: Influence of Cell Seeding Density and Collagen Concentration. *Biomaterials* **2008**, *29*, 3201–3212.

7. Giovannini, S.; Diaz-Romero, J.; Aigner, T.; Heini, P.; Mainil-Varlet, P.; Nesic, D. Micromass Co-Culture of Human Articular Chondrocytes and Human Bone Marrow Mesenchymal Stem Cells to Investigate Stable Neocartilage Tissue Formation in Vitro. *Eur Cell Mater* **2010**, *20*, 59.

8. Mueller, M. B.; Tuan, R. S. Functional Characterization of Hypertrophy in Chondrogenesis of Human Mesenchymal Stem Cells. *Arthritis Rheum.* **2008**, *58*, 1377–1388.

9. Kim, B.-C.; Kim, J. H.; An, H. J.; Byun, W.; Park, J.-H.; Kwon, I. K.; Kim, J. S.; Hwang, Y.-S. Microwell-Mediated Micro Cartilage-like Tissue Formation of Adipose-Derived Stem Cell. *Macromol. Res.* **2014**, *22*, 287–296.

10. Markway, B. D.; Tan, G.-K.; Brooke, G.; Hudson, J. E.; Cooper-White, J. J.; Doran, M. R. Enhanced Chondrogenic Differentiation of Human Bone Marrow-Derived Mesenchymal Stem Cells in Low Oxygen Environment Micropellet Cultures. *Cell Transplant.* **2010**, *19*, 29–42.

11. Babur, B. K.; Ghanavi, P.; Levett, P.; Lott, W. B.; Klein, T.; Cooper-White, J. J.; Crawford, R.; Doran, M. R. The Interplay between Chondrocyte Redifferentiation Pellet Size and Oxygen Concentration. *PLoS One* **2013**, *8*, e58865.

12. Babur, B. K.; Futrega, K.; Lott, W. B.; Klein, T. J.; Cooper-White, J.; Doran, M. R. High-Throughput Bone and Cartilage Micropellet Manufacture, Followed by Assembly of Micropellets into Biphasic Osteochondral Tissue. *Cell Tissue Res.* **2015**, *361*, 755–768.

13. Teixeira, L. S. M.; Leijten, J. C. H.; Sobral, J.; Jin, R.; van Apeldoorn, A. A.; Feijen, J.; van Blitterswijk, C.; Dijkstra, P. J.; Karperien, M. High Throughput Generated Micro-Aggregates of Chondrocytes Stimulate Cartilage Formation in Vitro and in Vivo. *Eur. Cell Mater.* **2012**, *23*, 387–399.

14. Leijten, J.; Teixeira, L. S. M.; Bolander, J.; Ji, W.; Vanspauwen, B.; Lammertyn, J.; Schrooten, J.; Luyten, F. P. Bioinspired Seeding of Biomaterials Using Three Dimensional Microtissues Induces Chondrogenic Stem Cell Differentiation and Cartilage Formation under Growth Factor Free Conditions. *Sci. Rep.* **2016**, *6*, 1–12.

15. Hildner, F.; Concaro, S.; Peterbauer, A.; Wolbank, S.; Danzer, M.; Lindahl, A.; Gatenholm, P.; Redl, H.; van Griensven, M. Human Adipose-Derived Stem Cells Contribute to Chondrogenesis in Coculture with Human Articular Chondrocytes. *Tissue Eng. Part A* **2009**, *15*, 3961–3969.

16. Acharya, C.; Adesida, A.; Zajac, P.; Mumme, M.; Riesle, J.; Martin, I.; Barbero, A. Enhanced Chondrocyte Proliferation and Mesenchymal Stromal Cells Chondrogenesis in Coculture Pellets Mediate Improved Cartilage Formation. *J. Cell. Physiol.* **2012**, *227*, 88–97. https://doi.org/10.1002/jcp.22706.

17. Wu, L.; Leijten, J. C. H.; Georgi, N.; Post, J. N.; Van Blitterswijk, C. A.; Karperien, M. Trophic Effects of Mesenchymal Stem Cells Increase Chondrocyte Proliferation and Matrix Formation. *Tissue Eng. - Part A* **2011**, *17*, 1425–1436.

18. Wu, L.; Prins, H. J.; Helder, M. N.; Van Blitterswijk, C. A.; Karperien, M. Trophic Effects of Mesenchymal Stem Cells in Chondrocyte Co-Cultures Are Independent of Culture Conditions and Cell Sources. *Tissue Eng. - Part A* **2012**, *18*, 1542–1551.

19. Pierres, A.; Benoliel, A. M.; Bongrand, P. Cell-Cell Interactions. *Phys. Chem. Biol. interfaces* **2000**, 459–522.

20. Bian, L.; Zhai, D. Y.; Mauck, R. L.; Burdick, J. A. Coculture of Human Mesenchymal Stem Cells and Articular Chondrocytes Reduces Hypertrophy and Enhances Functional Properties of Engineered Cartilage. *Tissue Eng. - Part A* **2011**, *17*, 1137–1145.

21. Zuo, Q.; Cui, W.; Liu, F.; Wang, Q.; Chen, Z.; Fan, W. Co-Cultivated Mesenchymal Stem Cells Support Chondrocytic Differentiation of Articular Chondrocytes. *Int. Orthop.* **2013**, *37*, 747–752.

22. de Windt, T. S.; Saris, D. B. F.; Slaper-Cortenbach, I. C. M.; van Rijen, M. H. P.; Gawlitta, D.; Creemers, L. B.; de Weger, R. A.; Dhert, W. J. A.; Vonk, L. A. Direct Cell–Cell Contact with Chondrocytes Is a Key Mechanism in Multipotent Mesenchymal Stromal Cell-Mediated Chondrogenesis. *Tissue Eng. Part A* **2015**, *21*, 2536–2547.

23. Liu, X.; Sun, H.; Yan, D.; Zhang, L.; Lv, X.; Liu, T.; Zhang, W.; Liu, W.; Cao, Y.; Zhou, G. In Vivo Ectopic Chondrogenesis of BMSCs Directed by Mature Chondrocytes. *Biomaterials* **2010**, *31*, 9406–9414.

24. Levorson, E. J.; Santoro, M.; Kasper, F. K.; Mikos, A. G. Direct and Indirect Co-Culture of Chondrocytes and Mesenchymal Stem Cells for the Generation of Polymer/Extracellular Matrix Hybrid Constructs. *Acta Biomater.* **2014**, *10*, 1824–1835.

25. Bernard, A. B.; Lin, C.-C.; Anseth, K. S. A Microwell Cell Culture Platform for the Aggregation of Pancreatic β-Cells. *Tissue Eng. Part C Methods* **2012**, *18*, 583–592.

26. Higgins, C. A.; Chen, J. C.; Cerise, J. E.; Jahoda, C. A. B.; Christiano, A. M. Microenvironmental Reprogramming by Three-Dimensional Culture Enables Dermal Papilla Cells to Induce de Novo Human Hair-Follicle Growth. *Proc. Natl. Acad. Sci.* **2013**, *110*, 19679–19688.

27. Hendriks, J.; Riesle, J.; Vanblitterswijk, C. A. Effect of Stratified Culture Compared to Confluent Culture in Monolayer on Proliferation and Differentiation of Human Articular Chondrocytes. *Tissue Eng.* **2006**, *12*, 2397–2405.

28. Fernandes, H.; Dechering, K.; Van Someren, E.; Steeghs, I.; Apotheker, M.; Leusink, A.; Bank, R.; Janeczek, K.; Van Blitterswijk, C.; De Boer, J. The Role of Collagen Crosslinking in Differentiation of Human Mesenchymal Stem Cells and MC3T3-E1 Cells. *Tissue Eng. Part A* **2009**, *15*, 3857–3867.

29. Wu, L.; Leijten, J.; van Blitterswijk, C. A.; Karperien, M. Fibroblast Growth Factor-1 Is a Mesenchymal Stromal Cell-Secreted Factor Stimulating Proliferation of Osteoarthritic Chondrocytes in Co-Culture. *Stem Cells Dev.* **2013**, *22*, 2356–2367.

30. Dahlmann, J.; Kensah, G.; Kempf, H.; Skvorc, D.; Gawol, A.; Elliott, D. A.; Dräger, G.; Zweigerdt, R.; Martin, U.; Gruh, I. The Use of Agarose Microwells for Scalable Embryoid Body Formation and Cardiac Differentiation of Human and Murine Pluripotent Stem Cells. *Biomaterials* **2013**, *34*, 2463–2471.

31. DeLise, A. áM; Fischer, L.; Tuan, R. S. Cellular Interactions and Signaling in Cartilage Development. *Osteoarthr. Cartil.* **2000**, *8*, 309–334.

32. Griffith, L. G.; Swartz, M. A. Capturing Complex 3D Tissue Physiology in Vitro. *Nat. Rev. Mol. cell Biol.* **2006**, *7*, 211–224.

33. Babur, B. K.; Kabiri, M.; Klein, T. J.; Lott, W. B.; Doran, M. R. The Rapid Manufacture of Uniform Composite Multicellular-Biomaterial Micropellets, Their Assembly into Macroscopic Organized Tissues, and Potential Applications in Cartilage Tissue Engineering. *PLoS One* **2015**, *10*, e0122250.

34. Meretoja, V. V.; Dahlin, R. L.; Kasper, F. K.; Mikos, A. G. Enhanced Chondrogenesis in Co-Cultures with Articular Chondrocytes and Mesenchymal Stem Cells. *Biomaterials* **2012**, *33*, 6362–6369. https://doi.org/10.1016/j.biomaterials.2012.05.042.

35. Fu, Y.; Karbaat, L.; Wu, L.; Leijten, J.; Both, S. K.; Karperien, M. Trophic Effects of Mesenchymal Stem Cells in Tissue Regeneration. *Tissue Eng. - Part B Rev.* **2017**, *23*, 515–528. https://doi.org/10.1089/ten.teb.2016.0365.

36. Widelitz, R. B.; Jiang, T.; Murray, B. A.; Chuong, C. Adhesion Molecules in Skeletogenesis: II. Neural Cell Adhesion Molecules Mediate Precartilaginous Mesenchymal Condensations and Enhance Chondrogenesis. *J. Cell. Physiol.* **1993**, *156*, 399–411.

37. Goldring, M. B.; Tsuchimochi, K.; Ijiri, K. The Control of Chondrogenesis. *J. Cell. Biochem.* **2006**, *97*, 33–44.

38. Gnecchi, M.; Zhang, Z.; Ni, A.; Dzau, V. J. Paracrine Mechanisms in Adult Stem Cell Signaling and Therapy. *Circ. Res.* **2008**, *103*, 1204–1219.

39. Chen, L.; Tredget, E. E.; Wu, P. Y. G.; Wu, Y. Paracrine Factors of Mesenchymal Stem Cells Recruit Macrophages and Endothelial Lineage Cells and Enhance Wound Healing. *PLoS One* **2008**, *3*, e1886.

40. Mayan, M. D.; Gago-Fuentes, R.; Carpintero-Fernandez, P.; Fernandez-Puente, P.; Filgueira-Fernandez, P.; Goyanes, N.; Valiunas, V.; Brink, P. R.; Goldberg, G. S.; Blanco, F. J. Articular Chondrocyte Network Mediated by Gap Junctions: Role in Metabolic Cartilage Homeostasis. *Ann. Rheum. Dis.* **2015**, *74*, 275–284.

41. Secchiero, P.; Melloni, E.; Corallini, F.; Beltrami, A. P.; Alviano, F.; Milani, D.; D'Aurizio, F.; Di Iasio, M. G.; Cesselli, D.; Bagnara, G. P. Tumor Necrosis Factor-related Apoptosis-inducing Ligand Promotes Migration of Human Bone Marrow Multipotent Stromal Cells. *Stem Cells* **2008**, *26*, 2955–2963.

42. Elmore, S. Apoptosis: A Review of Programmed Cell Death. *Toxicol. Pathol.* **2007**, *35*, 495–516.

43. Levine, B.; Kroemer, G. SnapShot: Macroautophagy. *Cell* **2008**, *132*, 162-e1.

44. Hara, T.; Nakamura, K.; Matsui, M.; Yamamoto, A.; Nakahara, Y.; Suzuki-Migishima, R.; Yokoyama, M.; Mishima, K.; Saito, I.; Okano, H. Suppression of Basal Autophagy in Neural Cells Causes Neurodegenerative Disease in Mice. *Nature* **2006**, *441*, 885–889.

45. Mizushima, N. Autophagy: Process and Function. *Genes Dev.* **2007**, *21*, 2861–2873.

46. Kurth, T.; Hedbom, E.; Shintani, N.; Sugimoto, M.; Chen, F. H.; Haspl, M.; Martinovic, S.; Hunziker, E. B. Chondrogenic Potential of Human Synovial Mesenchymal Stem Cells in Alginate. *Osteoarthr. Cartil.* **2007**, *15*, 1178–1189.

47. Shu, B.; Zhang, M.; Xie, R.; Wang, M.; Jin, H.; Hou, W.; Tang, D.; Harris, S. E.; Mishina, Y.; O'keefe, R. J. BMP2, but Not BMP4, Is Crucial for Chondrocyte Proliferation and Maturation during Endochondral Bone Development. *J. Cell Sci.* **2011**, *124*, 3428–3440.

48. Li, X.; Peng, J.; Wu, M.; Ye, H.; Zheng, C.; Wu, G.; Xu, H.; Chen, X.; Liu, X. BMP2 Promotes Chondrocyte Proliferation via the Wnt/β-Catenin Signaling Pathway. *Mol. Med. Rep.* **2011**, *4*, 621–626.

49. Ornitz, D. M. FGF Signaling in the Developing Endochondral Skeleton. *Cytokine Growth Factor Rev.* **2005**, *16*, 205–213.

50. Khan, I. M.; Palmer, E. A.; Archer, C. W. Fibroblast Growth Factor-2 Induced Chondrocyte Cluster Formation in Experimentally Wounded Articular Cartilage Is Blocked by Soluble Jagged-1. *Osteoarthr. Cartil.* **2010**, *18*, 208–219.

51. Nishida, T.; Kubota, S.; Aoyama, E.; Janune, D.; Maeda, A.; Takigawa, M. Effect of CCN2 on FGF2-Induced Proliferation and MMP9 and MMP13 Productions by Chondrocytes. *Endocrinology* **2011**, *152*, 4232–4241.

4.5 Supplementary Figures

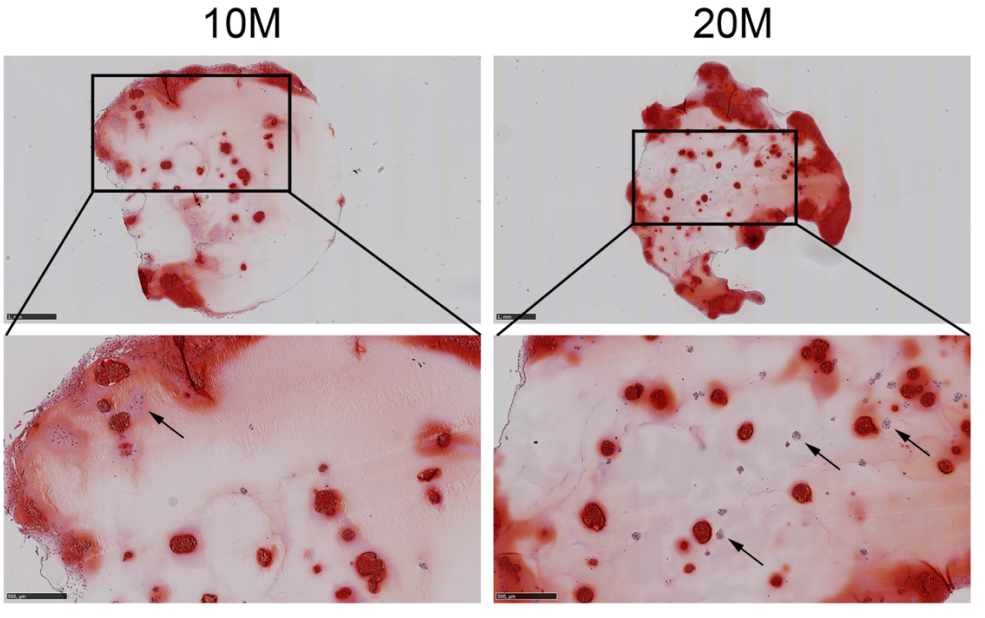

Figure supplementary 4.S1 *Morphology changes of the separated aggregates in μ-agg-Sep conditions. Upper figures show the overview of samples; scale bars represent 1 mm. Lower figures indicate the framed part of sample; scale bars represent 500 μm. The micro-aggregates with changed morphology and decreased bio-function were indicated by black arrows.*

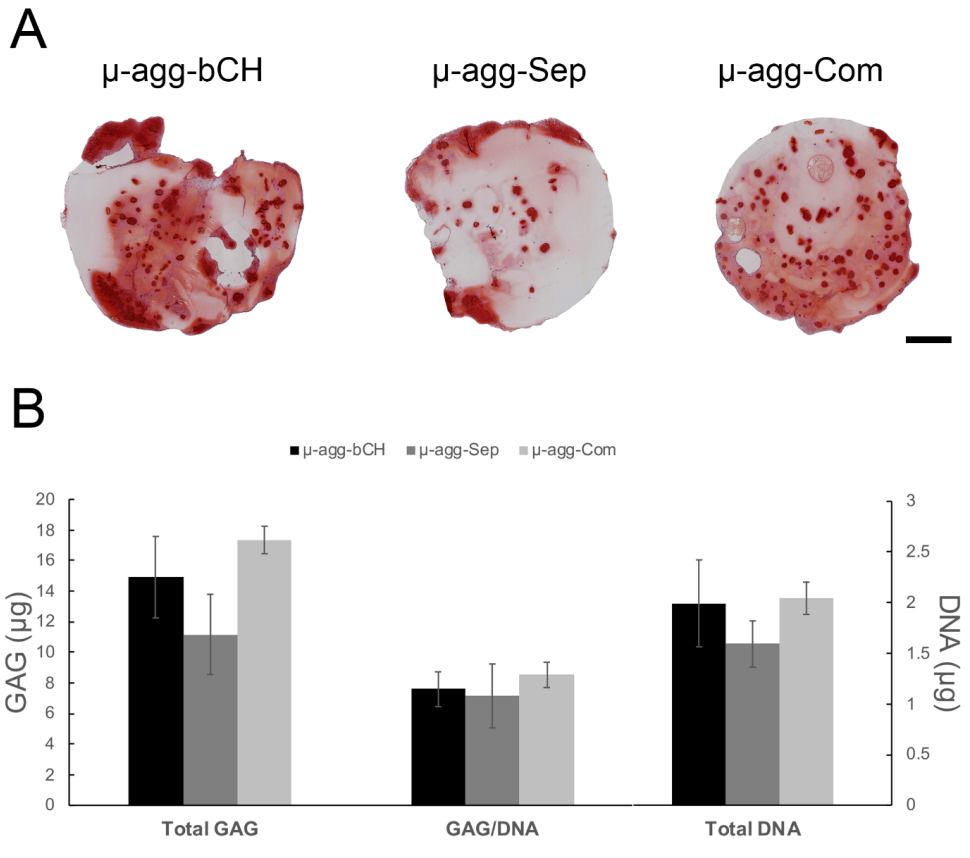

Figure supplementary 4.S2 *Co-cultures enhanced the chondro-induction in micro-aggregates. (A) safranin O staining indicates the presence of GAG in different conditions. Scale bar represents 1 mm. (B) Biochemical assay shows the GAG production in different conditions. Error bars reflect SD.*

Table 4.S1 Primers used for quantitative RT-PCR

Gene Name	Primer Sequence	Product size (bp)
Human specific GAPDH	F: 5' CGCTCTCTGCTCCTCCTGTT 3'	81
	R: 5'CCATGGTGTCTGAGCGATGT 3'	
Bovine specific GAPDH	F: 5' GCCATCACTGCCACCCAGAA 3'	207
	R: 5' GCGGCAGGTCAGATCCACAA 3'	
Cross-species GAPDH	F: 5'AGCTCACTGGCATGGCCTTC 3'	116
	R: 5' CGCCTGCTTCACCACCTTCT 3'	
Human specific Aggrecan	F: 5' TTCCCATCGTGCCTTTCCA 3'	121
	R: 5' AACCAACGATTGCACTGCTCTT 3'	
Bovine specific Aggrecan	F: 5' CCAAGCTCTGGGGAGGTGTC 3'	98
	R: 5' GAGGGCTGCCCACTGAAGTC 3'	
Human specific Collagen II	F: 5' GGCGGGGAGAAGACGCAGAG 3'	129
	R: 5' CGCAGCGAAACGGCAGGA 3'	
Bovine specific Collagen II	F: 5' AGGTCTGACTGGCCCCATTG 3'	101
	R: 5' CTCGAGCACCAGCAGTTCCA 3'	
Human specific FGF1	F: 5' TTAGAAGGAAGAGGTTGGTAG 3'	104
	R: 5' GCTGGCTATGAGACTTACTT 3'	
Bovine specific FGF1	F: 5' GACCAGAAGCTGTGCGAGGA 3'	200
	R: 5' GCCAGATCATCACCACACAG 3'	
Human specific FGF2	F: 5' AGCATTCACACCACTACAA 3'	146
	R: 5' CCAACTCGTAACAATCCATC 3'	
Bovine specific FGF2	F: 5' CTTATCGGAGAAGGCAATG 3'	111
	R: 5' TCGTGTCCAACTCTTAGC 3'	
Human specific BMP2	F: 5' GAGTTCACAAGTTCAAGTCC 3'	165
	R: 5' GCAATGTCTGGTTCTTATCC 3'	
Bovine specific BMP2	F: 5' TGTCCAGTCCGTGAGAAT 3'	162
	R: 5' CTTCCTGTAGGTTCATCGT 3'	

Chapter 5

Autophagy Is Involved in Mesenchymal Stem Cell Death in Coculture with Chondrocytes

Carlo Alberto Paggi*, Yao Fu*, Amel Dudakovic*, Catalina Galeano Garces, Mario Hevesi, Daniela Galeano Garces, Allan B. Dietz, Andre van Wijnen, and Marcel Karperien

**Authors equally contributed to this work*

Abstract

Cartilage formation is stimulated in mixtures of chondrocytes and human adipose-derived mesenchymal stromal cells (MSCs) both in vitro and in vivo. During co-culture, human MSCs perish through an unknown process. The goal of this study is to elucidate the mechanism by which adipose tissue-derived MSC cell death occurs in the presence of chondrocytes. In this work, human primary chondrocytes were co-cultured with human MSCs derived from three donors. The cells were cultured in monoculture or co-culture (20% chondrocytes and 80% MSCs) in pellets (200,000 cell/pellet) for 7 days in chondrocyte proliferation media in hypoxia (2% O_2). RNA sequencing was performed to assess for differences in gene expression between monocultures or co-culture. Immune fluorescence assays were performed to quantify the level of Caspase-3, LC3B and P62. RNA sequencing revealed significant up-regulation of >90 genes in the three co-cultures when compared to monocultures. STRING analysis showed interconnections between >50 of these genes. Remarkably, 75% of these genes play a role in cell death pathways such as apoptosis and autophagy. Immunofluorescence shows a clear up-regulation of the autophagic machinery with no substantial activation of the apoptotic pathway. Collectively, the data suggests that in co-cultures of human MSCs with primary chondrocytes, autophagy is involved in the disappearance of MSCs. We propose that this sacrificial cell death may contribute to the trophic effects of MSCs on cartilage formation.

5.1 Introduction

There is a range of current treatment modalities for symptomatic and focal cartilage defects[1,2]. These include bone marrow stimulation techniques like microfracture or autologous chondrocyte implantation (ACI)[3]. Unfortunately, microfracture generates fibrous cartilaginous scar tissue and therefore provides non-anatomic restoration of articular surface. ACI and related techniques, have demonstrated superior mid- and long-term outcomes as compared with the simpler microfracture process[4,5]. However, culturing of chondrocytes in a 2D environment to obtain sufficient cells for implantation can lead to changes in the chondrocyte phenotype[6,7]. Furthermore, substantial numbers of chondrocytes are harvested from an otherwise intact articular area creating additional damage in the joint surface[6,8].

To reduce the number of chondrocytes (CHs) required for cell implantation, a combination of chondrocytes and mesenchymal stem cells (MSCs) has been studied[9]. Wu *et al.* demonstrated a beneficial effect on cartilage formation over the respective monocultures[10]. MSCs increased chondrocyte proliferation and stimulated deposition of cartilage matrix. However, the trophic effect generated by MSCs is followed by a counter loop where the chondrocytes signal the MSCs to undergo cell death. This mechanism has been confirmed using a variety of MSC sources both *in-vitro* and *in-vivo* and in a clinical trial in which cartilage defects were implanted with a mixture of preoperatively isolated chondrocytes and allogenic bone marrow derived stem cells[11-14].

It was postulated that the mechanism behind the death of the MSCs is likely related to one of the deliberate “suicide” programs present within cells[15].These suicide programs are usually induced intrinsically or extrinsically by external stimuli such as mechanical stress, oxidative processes, and drug treatments. The programmed suicide death has usually two main forms, apoptosis and autophagy[16-18]. These two pathways are intricately interconnected and the up-regulation of one leads to down-regulation of the other[19].

Apoptosis is triggered by biochemical events which induce characteristic changes in the morphology of the cell (i.e. membrane blebbing and nuclear fragmentation). The apoptotic process can be intrinsically activated by the release of cytochrome C from mitochondria or can be activated extrinsically by death receptors. Both pathways lead to the activation of a series of caspases which mediate the cell destruction[16].

Autophagy, is a catabolic process where the cell degrades cytoplasmic components important for survival, thereby leading to a so called “self-eating” phenomenon. This organised degradation and recycle activity uses vesicles, known as autophagosomes, which can contain organelles, proteins, and other components. These autophagosomes subsequently fuse with lysosomes that degrade both the cargo and the vesicles[19].

In light of these results, we decided to investigate which of the two molecular mechanisms was involved in the possible cell death of MSCs in co-cultures. Pellets containing the combination of human chondrocytes and human MSCs were cultured for one week and analyzed for changes in gene and protein expression characteristic for the apoptotic or autophagy pathways. Our data show a clear prevalence in activation of the autophagic pathway. We hypothesize that this mechanism could be a self-sacrifice mechanism of the MSCs which could contributes to the trophic effect of these cells on chondrocytes.

5.2 Materials and Methods

5.2.1 Cell culture and expansion

Human-adipose-tissue-derived-MSCs were extracted from lipoaspirates obtained from consenting two male healthy donors (A211 and A283) and one female donor (A258) (Supplementary Table 5.S1) as previously described. [20-22] Chondrocytes were extracted from healthy looking cartilage of a donor undergoing an amputation. All cells lines collected and used for this study were approved by the Mayo Clinic Institutional Review Board[22].

MSCs were cultured in standard medium (Gilco’s advanced Modified Eagle Medium; MEM) supplemented with 1% penicillin/streptomycin, 1% GLUTAmax, 5% Human Platelet Lysate PLT max and 0.2% heparin. Chondrocytes were cultured in chondrocytes proliferation medium (Gilco’s advance MEM, 10% fetal bovine serum [FBS], 1% penicillin-streptomycin, 1% GLUTAmax, 0.2 mM ascorbic acid 2-phosphate, and 4 mM proline). Both cell types were cultured in normal oxygen conditions (21% oxygen). MSCs were used at passage 5 and primary chondrocytes at passage 4.

5.2.2 Pellet co-culture

Cell pellets were generated by seeding 200,000 cells per well in a 96-well plate. Cells were cultured as monocultures or as co-cultures with a ratio of 80%

MSCs/20% chondrocytes. Both mono- and co-cultures were cultured in chondrogenic proliferation media (same as above) under hypoxia (2% oxygen). Medium was changed every three days. Pellets were harvested at day 7 for RNA-seq and immunofluorescence analysis.

5.2.3 RNA extraction

Total RNA was isolated from the samples using the Direct zol^{TM} RNA kit as instructed by the manufacturer (Zymo Research, Irvine, California). For each condition, 4 to 5 cell pellets were pooled to obtain sufficient RNA yield for downstream analysis. Nanodrop (Thermo Fisher Scientific, Waltham, MA) was used to determine the purity and concentration of the RNA extracted.

5.2.4 RNA sequencing and analysis

RNA sequencing and bioinformatic analysis was performed by the Mayo Clinic RNA sequencing and bioinformatic cores as described previously[22-25]. RNA libraries were prepared using the TruSeq RNA library preparation kit (Illumina, San Diego, CA) following the manufacturer's instructions. The poly-A mRNA of each sample was purified from the total RNA using oligo dT magnetic beads. To multiplex sample loading on the flow cells specific indexes were incorporated at the adaptor ligand using the TruSeq kit. The constructs were purified and enriched using 12 cycles of PCR. Agilent Bioanalyzer DNA 1000 chip and Qubit fluorometry (Invitrogen, Carlsbad, CA) were used to control the quality and the concentration of the samples. Libraries were loaded onto flow cells at concentrations of 8 to 10 pM to generate cluster densities of 700,000/mm^2 following the standard protocol for the Illumina cBot and cBot Paired end cluster-kit version 3. Flow cells were sequenced as 51 X 2 paired end reads on an Illumina HiSeq 2000 using TruSeq SBS sequencing kit version 3 and HCS v2.0.12 data collection software. Base-calling was performed using Illumina's RTA version 1.17.21.3. The RNA-Seq data were analyzed using the standard RNA-Seq workflow by Mayo Bioinformatics Core called MAPRSeq v.1.2.1, which includes alignment with TopHat 2.0.6[26] and quantification of gene expression using the HTSeq software[27]. Normalized gene counts were also obtained from MAPRSeq where expression values for each gene were normalized to 1 million reads and corrected for gene length (Reads Per Kilobase pair per Million mapped reads, RPKM). RNA-seq data were deposited in the Gene Expression Omnibus of the National Center for Biotechnology Information (GSE142831).

5.2.5 Identification of co-culture regulated genes

To estimate the relative RNA contribution of the MSCs in the co-cultures, we used the sex mismatch between the male donors (A211 and A283) and the female chondrocyte donor. The average level of expression of 7 unique male markers in the co-culture was 57% of the levels in the respective monocultures (Table 5.1). As expected, the y-markers were not expressed in the female chondrocytes and MSC (A258). We used these numbers to calculate the expected value of gene expression of a given gene using the following formula for each donor pair and calculated the average of the three donors. Only genes with RPKM values above 0.3 in each of the samples were included in the analysis.

$$(1)\quad RPKM\ Coculture_{expected} = 0.57 * RPKM\ AMSC_{mono} + 0.43 * RPKM\ hCh_{mono}$$

The expected value is valid under the assumption that gene expression in co-cultures is the sum of gene expression in MSCs and chondrocytes and is not influenced by the interaction between both cell types.

The real value was then compared to the expected value to determine the Fold change (Fc) difference.

$$(2)\quad Fc = \frac{RPKM\ Coculture_{real}}{Coculture_{expected}}$$

The majority of genes have a Fc of around 1 indicating that the observed gene expression is the sum of the expression in the MSCs and chondrocytes. Genes with a Fc>2 cut off were considered upregulated genes. Genes with a Fc<0.5 were considered downregulated genes.

Table 5.1 RPKM Values of 7 individual Male genes[a].

Chr	GeneID	A211	A211 + ch	A283	A283 + ch	ch		([A211 + ch]/ A211) * 100	([A283 + ch]/ A283) * 100
chrY	RPS4Y1	108.6745	67.97581	92.28269	43.43297	0.337399		62.54994	47.06513
chrY	DDX3Y	21.43654	11.931	15.98953	8.763549	0.077968		55.6573	54.80805
chrY	PRKY	6.416036	3.24354	4.049743	2.343155	0.056736		50.55364	57.85934
chrY	USP9Y	3.647092	1.915803	1.484446	0.86582	0.023051		52.5296	58.32615
chrY	KDM5D	3.099356	2.289926	2.886254	1.85711	0.00957		73.88392	64.34326
chrY	ZFY	3.287543	1.731643	3.220577	1.739003	0.02219		52.67286	53.99662
chrY	EIF1AY	8.868548	4.7055	8.95836	5.544899	0.038423		53.05829	61.89636
							Average	57.27222	56.89927

RPKM = Reads Per Kilobase pair per Million mapped reads.

[a]The values of the monoculture are compared with the coculture and an average of the 7 genes was obtained. Based on these data, we assumed that 57% of the rPKM in the cocultures was derived from the mesenchymal stromal cells and 43% was derived from chondrocytes.

5.2.6 Immunofluorescence staining

Pellets were harvested for immunofluorescent staining as previously described[28]. Cell-pellets were washed with phosphate-buffered saline (PBS) and fixed with 10% formalin for 15 min. Samples were then embedded in cryomatrix (Thermo Fisher) and cut into 10 μm sections with a cryotome (Shandon). Sections were permeabilized with 0.5% Triton X-100 in PBS for 10 min at room temperature followed by animal serum treatment (5%, 1-hour, room temperature) to block nonspecific binding. Sections were incubated overnight at 4°C in a humidified chamber with antibodies against LC3B (1:500 dilution, MAB85582, R&D System) and SQSTM1/p62 (1:200 dilution, ab56416, Abcam). Subsequently, slides were washed with 0.1% Tween 20 in PBS and incubated with Alexa Fluor-conjugated secondary antibodies (Alexa 568 or Alexa 488, Abcam) for 50 min at room temperature in a humidified chamber. Nuclei were counterstained with 4,6-diamidino-2-phenylindole (DAPI, Molecular Probes) and images were taken with a fluorescence microscope (Nikon Eclipse E400).

5.3 Results

5.3.1 Transcriptome changes in MSCs and chondrocyte co-cultures

The relative contribution of the MSCs in gene expression in the co-cultures dropped from 80% (based on seeding ratio) to 57% after one week in co-culture (Table 5.1). This confirm the disappearance of MSCs from co-cultures and is in agreement with previous observations[9].

Cluster analysis of RNAseq data from monocultured MSCs, chondrocytes and co-cultures at day 7, shows clustering of the distinct conditions in their respective groups (Fig. 5.1b). There is visible variation present in heatmap patterns when comparing the three MSC donors, indicative of inter-donor variation[29]. Moreover, the up- and downregulated genes in the hCHs and MSCs in the monoculture differ greatly from the co-culture suggesting an interaction between the two cells. Based on the similarity in gene expression patterns between the three co-cultures, it is

likely that common pathways are influenced by the interaction between the MSCs and the chondrocytes.

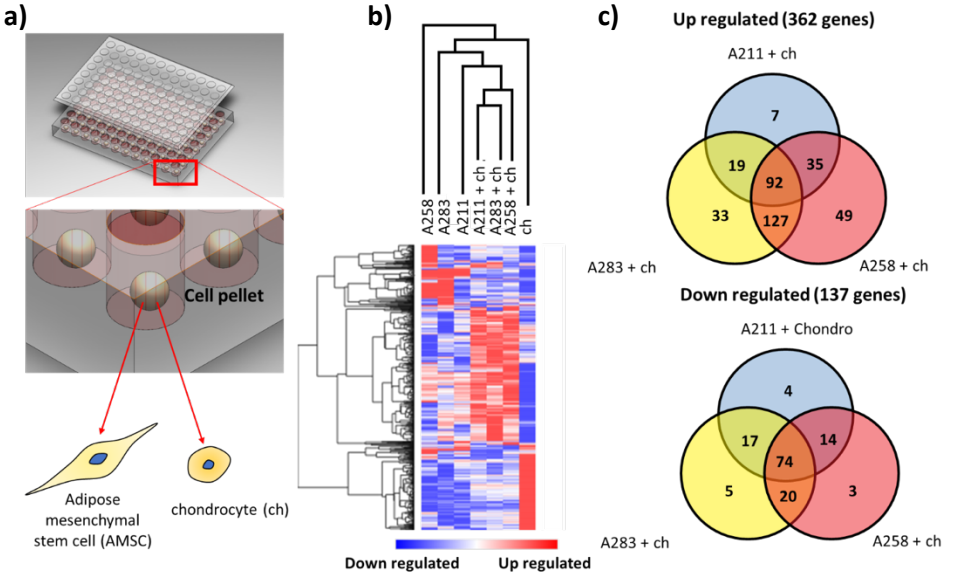

Figure 5.1 *(a) A 96-well plate containing the monoculture or co-culture pellets. (b) Heatmap of the entire genome normalized and clustered using MORPEUS software. the downregulated genes are expressed in blue whereas the upregulated in red. (c) Venn diagrams presenting the similarity between the upregulated (top) or down-regulated (bottom) genes belonging to the different co-cultures.*

A total of 362 genes met the inclusion criteria of >2-fold upregulation and $P < 0{,}05$ in at least one of the co-cultures compared to the expected value assuming no cellular interaction between the MSCs and chondrocytes. In total, 137 genes were down-regulated. The number of upregulated genes was nearly three times higher compared to the downregulated, which may indicate a predominance of pathway activation when cells are placed in co-culture. A Venn diagram was created to identify common up- or down-regulated genes in each of the co-cultures. Co-cultures of chondrocytes with donors A258 and A283 represented a closer pattern of gene up- and down-regulation as compared with the co-culture involving donor A211, which further highlights the presence of inter-donor variability (Fig. 5.1c). In total, 92 genes were more than 2-fold upregulated in all three co-cultures and 74 were more than 2-fold downregulated (Supplementary Figure 5.S1).

5.3.2 Up-regulation of autophagic and apoptotic pathways in MSCs and chondrocyte co-cultures

Among the 92 upregulated genes, 86 were identified (Supplementary Table 5.S6) by the STRING software and 51 were found having known interactions (medium confidence 0.4). Two main clusters were obtained: one consisting of a series of histones (HIST1H2AG, HIST1H2BG, HIST3H2A, HIST1H1E) which may indicate an effect on cell proliferation in line with previous observations[10]. The second, a larger cluster of 51, consisted of a series of genes mainly present in cell death processes like autophagy and apoptosis (37 genes out of 51[16,30]) (Fig. 5.2). The genes identified encode surface (RARRES3[31], TNFRSF10A[32], PIK3R3[33], TRAF1[34]), cytoplasmic (NCF2[35], APOL3[36]) and transporter (TAP1, TAP2)[37] proteins. A literature search of the 51 genes confirmed their role in cell death pathways in more detail (Supplementary Table 5.S2). In general, most of the GO-terms obtained from the ClueGO analysis represented terms like cell stress or death pathways (Fig. 5.2 and Supplementary Table 5.S3). Moreover, 52.17% of the terms GO-pathways detected were related to Ubiquitin-specific processing proteases. Ubiquitination represents a fundamental process in the autophagic machinery[38]. These data suggest that the co-culturing of MSCs and chondrocytes may induce autophagic cell death.

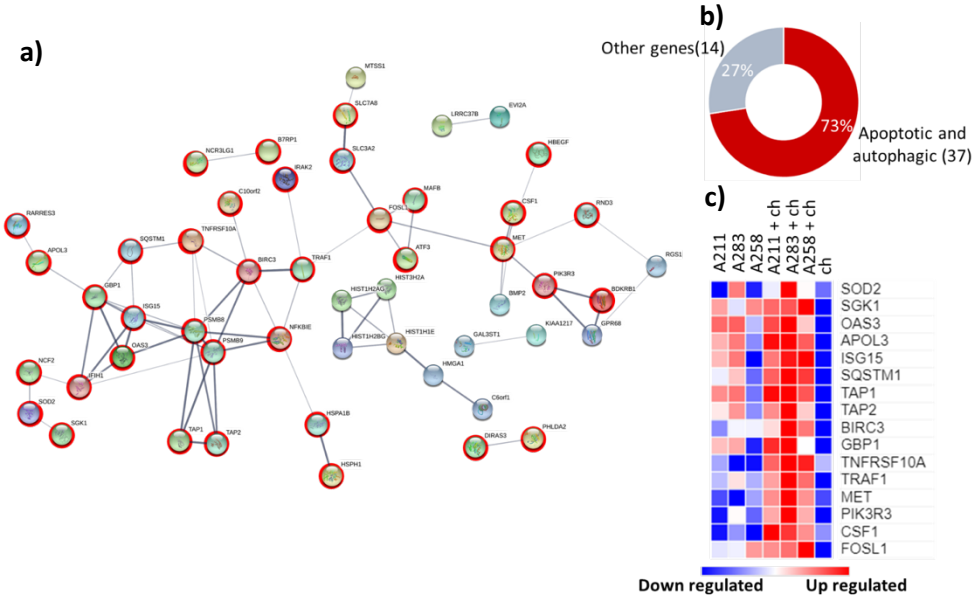

Figure 5.2 *(a) Interconnections of the 51 upregulated genes using STRING software. Red circle symbolizes genes that have previously been annotated to apoptotic or autophagic processes. For other genes insufficient data were present in literature or have been previously annotated to other pathways. (b) Pie chart presenting the percentage of the 51 genes involved in the apoptotic or autophagic pathways based on gene counts in a. (c) Heatmap presenting the normalized (log 2) overexpression (red) levels of 17 upregulated genes using the RPKM values obtained from the RNA sequencing.*

5.3.3 Co-culture treatment induces autophagic flux

To further distinguish whether the MSCs disappear from co-culture by apoptosis or autophagy, the expression of pro-apoptotic, anti-apoptotic, apoptotic and autophagic markers was assessed (Fig. 5.3a-d).

First, we looked at four pro-apoptotic markers (BAD, BAX, BIM, BID) (Fig. 5.3a). These markers belong to the BCL-2 cell-death-regulator-family and they initiate and/or mediate the activation of apoptosis. Here, by comparing the monoculture with the co-culture, the variability among the MSCs donors is clear. Some of the genes are overexpressed in mono- or co-culture depending on the donor. However, the trends between the two conditions do not present any statistical difference which suggest inactivation of the apoptotic pathway (Supplementary Table 5.S4). This is furthermore supported by the gene expression of four of the main caspase pathway regulators (*CASP3, CASP5, CASP8, CASP9*)[16] that did not change or were less expressed in co-cultures (Fig. 5.3c). Moreover, immunofluorescence images were obtained to determine the level of Caspase-3 (Fig. 5.4b). Caspase-3 is the final protein of the apoptotic cascade cycle[39]. During apoptosis, the cells present disrupted nuclei comprising high level of caspase-3 (Fig. 5.4a left). However, in both mono- and co-culture this characteristic is barely present indicating absence of apoptotic activation.

We further checked two of the main anti-apoptotic markers (BCL2 and BCL2L1). Although both did not reach a statistical significance (0,11-BCL2 & 0,15-BCL2L1), both presented, for each of the 3 donors, an increase in expression in co-culture (Fig. 5.3b and Supplementary Table 5.S4). This suggests an activation of anti-apoptotic processes which may cause the in-activation of the caspase cycle.

Furthermore, as regulated necrosis can be triggered by binding of TNF-α and FAS ligand we looked at overexpression of RIPK1, RIPK3, and MLKL. However, none of these genes were significantly upregulated in the cocultured compared with the

monoculture (Supplementary Fig. 5.S4) excluding a role for necrosis in the disappearance of the MSCs.

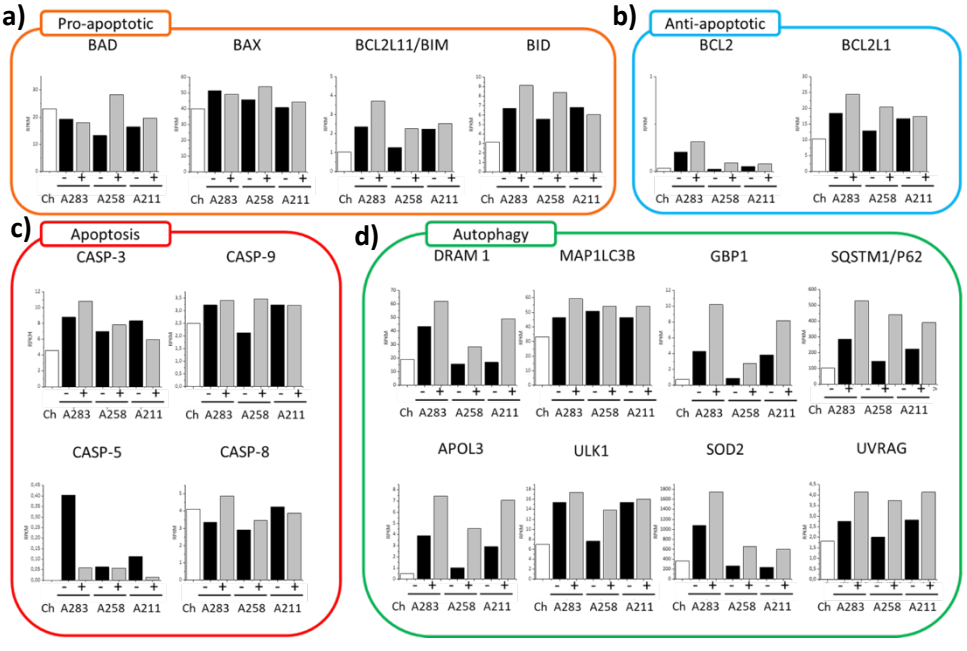

Figure 5.3 *(a) Comparison between the RPKM values of pro-apoptotic markers (BAD, BAX, BCL2l11/BIM, BID); (b) of the antiapoptotic markers (BCL2, BCL2l1); (c) apoptotic markers (CASP-3, CASP-9, CASP-5, CASP-8); (d) of the autophagic markers (DRAM1, MAP1LC3B, GBP1, SQSTM1/P62, APOL3,ULK1, SOD2, UVRAG) obtained from the RNA sequencing.*

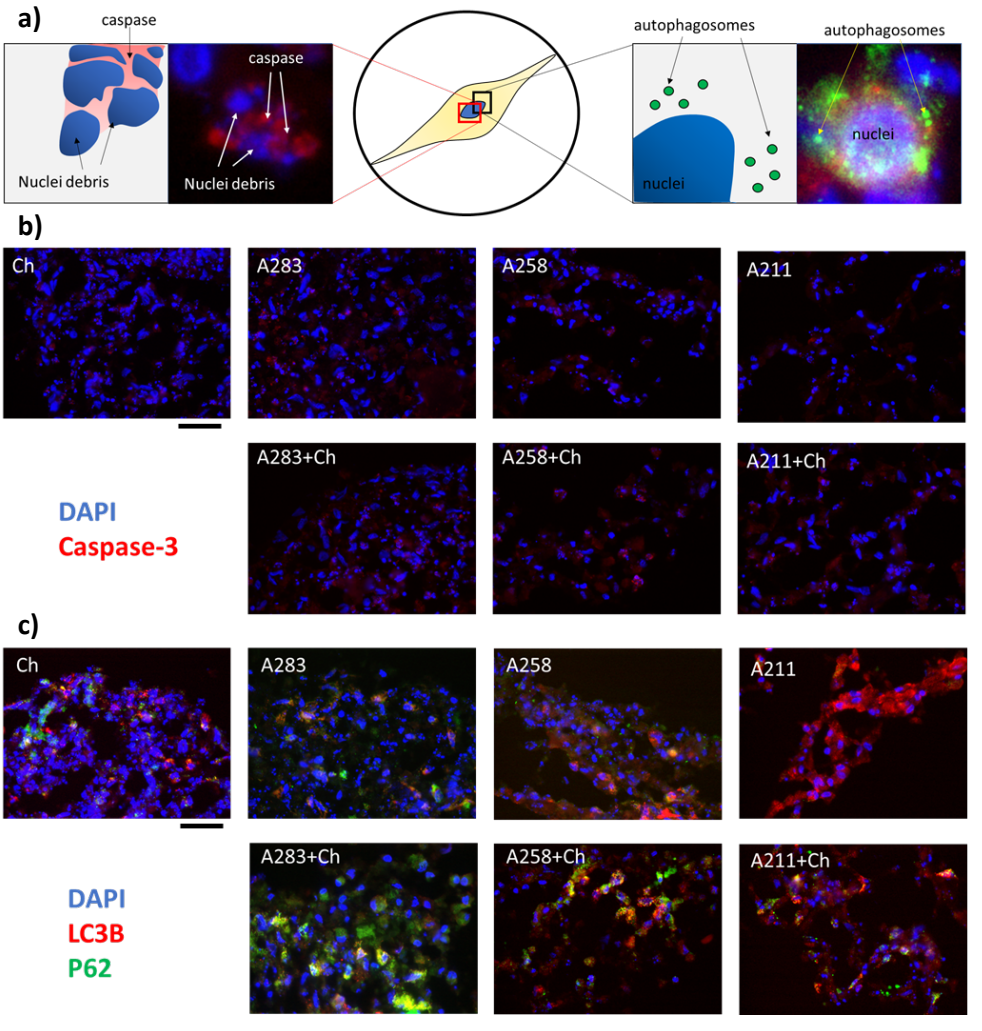

Figure 5.4 *(a) Magnification of a cell undergoing apoptosis (on the left) through caspase-3 (in red) or autophagy (on the right) through LC3B (red) and P62 (green). In blue nuclei; (b) immunofluorescence of the 7 conditions after 7 days of culture of the caspase-3 (in red) and nuclei (in blue); (c) immunofluorescence of the same 7 conditions of lC3B (in red) and P62 (in green). in blue nuclei. Yellow color represents overimposed green and red signals. Scale bars equate to 40 μm.*

We next determined the effects of autophagic markers in the co-cultures (Fig. 5.4). First, we looked at multiple markers highly present during autophagy activation (Fig. 5.3d). Among the 8 individual markers, 7 were statistically up-regulated in the co-culture compared with the monoculture, indicating activation of the autophagic machinery at the gene level. We further looked at the protein level using

immunofluorescence. Here, two well-recognised markers (LC3B and P62) were used. LC3B is conjugated to the autophagosome during autophagosome formation. P62/SQSTM1 protein interacts with both LC3B-II and ubiquitin protein and is degraded in autophagolysosomes[40]. In in-activated autophagy, these two markers can be singularly present (Supplementary Fig. 5.S3 A211) or can be present together but not colocalized (Supplementary Fig. 5.S3 A258). On the contrary, in active autophagy both markers are present and colocalize (Fig. 5.4a), which indicates creation of the autophagosome. Even if the behaviour of the three donors is different, it is clear that the level of combined LC3B and P62 are higher in the co-culture compared with the monoculture for all the donors, indicating upregulation of the autophagic machinery[41]. Taken together, these results suggest that MSCs exhibit enhanced autophagic flux.

5.4 Discussion

In this study, we have studied the mechanism involved in the progressive cell death of the MSCs in coculture with chondrocytes.

We used the sex mismatch between the female chondrocyte and male MSC donors to estimate the relative contribution of the MSCs to the gene expression in the co-cultures. The expression of Y-chromosome-specific RNAs proved stable across donors. By assuming that the expression of Y-specific markers is not influenced by the co-culture conditions, a notion which is supported by previous observations, it is possible to estimate the contribution of the male MSC donors to global RPKM in co-culture with female chondrocytes. Using this approach, we concluded that the relative contribution of MSCs to the RPKM in the co-cultures dropped from 80% to 57% after one week of culture. This supports previous observations where after 4-weeks of culture, MSCs have almost completely disappeared from co-cultures with chondrocytes due to cell death irrespective of the origin of the stem cells[9]. Signs of increased cell death were first noted at day 7 and increased day 14[10]. We reasoned that the 7-day time point marked the beginning of the disappearance of MSCs from co-cultures and selected this time point for an RNA-seq analysis. At this time point, the transcriptome of the co-cultures was substantially and statistically different from the respective monocultures indicating the presence of non-additive interactions between the two cell populations. 362 genes were upregulated of 2-fold in at least 1 of the co-cultures. Of these genes, 92 were consistently upregulated in each of the three co-cultures. The considerable inter-donor variability is in line with previous studies[42]. Interestingly, the donor A258 (female) and A283 (male), presents higher

overlap in terms of both up- and down-regulated genes in co-culture suggesting that the trophic role of MSCs is a generic, sex-independent property of these cells as noted before[43]. We do realize that the method for selecting genes specifically regulated by the interaction between chondrocytes and MSCs has limitations. For example, genes that are inversely regulated in MSCs and chondrocytes may be missed. The genes identified in this study thus represent a snapshot of genes that are regulated in co-cultures.

STRING analysis identified two interconnected networks of which the main included more than half of the total upregulated genes. This network describes genes involved in apoptotic or autophagic processes and comprised proteins involved in subsequent steps of these pathways starting from membrane receptor proteins (TNFRSF10A, PIK3R3, TRAF1) up to fundamental enzymatic components (OAS3). Most of the genes detected are upregulated in one (RARRES3), or both processes (DIRAS3, ISG15, BMP2, PHLDA2). Other genes are involved in the inhibition of one (HBEGF-for apoptosis) or both pathways (ATF3). Moreover, genes such as BIRC3 and NCF2 can upregulate one process while inhibiting the other. Interestingly, these results differ from those of Wu *et al.* where a microarray analysis identified clusters related to intracellular cell cycle regulators, extracellular matrix production and secreted growth factors (FGF1 and BMP2)[44]. This variability could be related to the time points considered. Wu *et al.* performed the analysis at the second day of culture, whereas our study focused on a later time point (day 7)[44]. At this earlier time point, a dominant effect on cell proliferation was found whereas the disappearance of MSCs from the co-cultures was first noted at day 7[9,10]. Also, in our study, we show the upregulation of many proliferation markers, however, this upregulation was modest and consequently did not meet the cutoff of 2-fold used (Supplementary Table 5.S7). No upregulation of cartilage matrix genes was noted, which could be explained by the early time point considered. Interestingly, a decrease in COL10A1 and COL3A1 mRNA expression was visible indicating a reduction in the hypertrophic activity (Supplementary Fig. 5.S5).

Like in the study of Wu *et al.*[44], we have found upregulation of BMP2. This suggests that BMP2 plays a fundamental and prolonged role in the coculture effect. This contrasts FGF1, which in this study was not found upregulated. Combined this data may suggest that FGF-1 functions as trigger in an initial phase in chondrocyte proliferation, whereas BMP-2 is required for longer period of time and may sustain cartilage matrix formation. Indeed, these factors can contribute to the proliferation

of chondrocytes and are partly responsible for the increase of matrix formation in co-cultures[49-52]. Alternatively, the differences could be explained by the use of adipose MSCs versus bone marrow MSCs in the study by Wu *et al.*[44]. This seems, however, unlikely given the consistency in the trophic effect of MSCs from a variety of sources in co-culture with primary chondrocytes[9]. Moreover, the use of a more physiologically relevant hypoxic environment, used in this study, compared to the normoxic environment in the study by Wu *et al.*, may also have contributed to the differences in gene expression.

Due to the crosstalk[53] between the apoptotic and autophagic pathways, it is difficult to draw a conclusion by only looking at the RNA level. Consequently, we looked at the protein expression. Here, because both processes involve a multitude of proteins we looked at key components (LC3B & P62 for autophagy and caspase-3 for apoptosis) of both pathways[41].

Apoptosis can be initiated by an extrinsic or, an intrinsic process both ending with the cleavage of the procaspase-3[16]. Here, the RNA expression data suggested the possible activation of the extrinsic pathway by membrane receptor proteins (TRAF1, TNFRSF10A) rather than the activation of the intrinsic pathway by genes like DIABLO, HTRA2, AIFM1, ENDOG, and CAD (Supplementary Table 5.S5). Since we did not find an in increase or difference in the active form (caspase-3 within the nuclei and nuclei debris) at the protein level, we concluded that the cell death *via* the canonical apoptotic pathway is likely not driving MSCs death.

Autophagy is a cellular degradation pathway that is essential for survival[49]. However, if overexpressed, it could lead to neurodegeneration, cardiomyopathies, abnormalities of skeletal development, and death as shown in mice studies[18,50]. LC3-II is as a quantitative marker of autophagy required for the formation of the autophagosome and its expression is proportional to the amount of autophagosomes in the cell. The P62/SQSTM1 protein serves as a link between LC3 and ubiquitinated substrates[51]. P62/SQSTM1 and P62-bound polyubiquitinated proteins become incorporated into the completed autophagosome. From the data obtained, LC3-II and P62/SQSTM1 were highly expressed, both at the gene and protein level, in the cocultures compared to the monoculture conditions suggesting activation of the autophagic flux. Taken together, our data shows a strong association between the activation of autophagy and the disappearance of MSCs from cocultures with chondrocytes suggesting that the MSCs in coculture preferentially die by autophagy rather than by apoptosis. Formal proof of this hypothesis would require further

studies for example by knocking down genes involved in the autophagic and apoptotic pathways.

This conclusion differs from the previous study performed by Wu *et al.* where high levels of TUNEL positivity staining were detected in the pellets[10]. TUNEL staining detects the DNA breaks formed when DNA fragmentation occurs in the last phase of apoptosis. Normally, this kind of apoptosis is considered as caspase-dependent procedure. However, cell death can proceed in caspase-independent apoptotic pathway, in which TUNEL positive staining is also observed[57]. The mitochondria play a central role in both caspase-dependent and caspase-independent death pathways[58]. It has been recognized that mitochondria can release factors involved in caspase-independent cell death, including apoptosis-inducing factor (AIF) and Endonuclease G (EndoG)[59-61]. In fact, AIF is believed as a key mediator of poly ADP-ribose (PAR) polymerase (PARP) induced caspase-independent cell death[62]. Indeed, it has been reported that autophagy is a cytosolic event that controls caspase-independent macrophage cell death through RARP mediated pathway[63]. Moreover, autophagy activated by DNA damage can kill the cells through the autophagy regulators in the absence of apoptosis[64-66]. However, the major concern with these examples is that they represent a very artificial situation. Regardless, these data may explain the difference in these two studies.

It remains unclear which role MSCs cell death by autophagy plays in the co-culture. We hypothesize that the autophagic extracellular vesicles generated may have an additional trophic effect. During autophagy, cells release a variety of signals, including extracellular vesicles, which after uptake by neighboring cells, induce cellular responses over short- and/or long-range distances[67]. Indeed, researchers proposed the concept of "altruistic cell suicide" based on the observation that dying cells could induce proliferation of neighboring cells[68]. Based on our analysis, it is conceivable that the activation of autophagy in MSCs likely initiates this "altruistic cell death" process in co-culture with chondrocytes. We propose a sequential mechanism where growth factors like FGF1 and BMP2 are released by the MSCs and subsequently are further enhanced by the increased secretion of extracellular vesicles, and their uptake by neighboring chondrocytes. This mechanism can explain how MSCs stimulate cartilage formation while simultaneously disappearing both *in-vitro* and *in-vivo*.

Additional studies should focus on the mechanism behind the initiation of autophagy, the release of extracellular vesicles and their uptake. Particularly

interesting are the studies aimed at analyzing the content of the autophagic vesicles. Activation of autophagy in MSCs might be an efficient way to increase the formation of trophic extracellular vesicles. This may help in optimizing intra-articular injection strategies based on MSC-derived extracellular vesicles rather than MSCs themselves[69-71]. The use of MSC-derived extracellular vesicles rather than the cells themselves may avoid possible long-term phenotype changes of incorporated cells and attenuate many of the safety concerns related to the use of living cells.

In summary, here we provide evidence that MSCs in coculture with primary chondrocytes preferentially die by autophagy. We postulate that this altruistic cell death results in the formation of extracellular vesicles. These extracellular vesicles are an additional mechanism by which the MSCs stimulate chondrocyte proliferation and cartilage matrix formation in pellet co-cultures.

References

1. Sophia Fox, A. J., Bedi, A. & Rodeo, S. A. The basic science of articular cartilage: structure, composition, and function. *Sports Health* **1**, 461-468, doi:10.1177/1941738109350438 (2009).

2. Newman, A. P. Articular cartilage repair. *Am J Sports Med* **26**, 309-324, doi:10.1177/03635465980260022701 (1998).

3. Basad, E. *et al.* Matrix-induced autologous chondrocyte implantation (MACI) in the knee: clinical outcomes and challenges. *Knee Surg Sports Traumatol Arthrosc* **23**, 3729-3735, doi:10.1007/s00167-014-3295-8 (2015).

4. Brittberg, M., Recker, D., Ilgenfritz, J., Saris, D. B. F. & Group, S. E. S. Matrix-Applied Characterized Autologous Cultured Chondrocytes Versus Microfracture: Five-Year Follow-up of a Prospective Randomized Trial. *Am J Sports Med* **46**, 1343-1351, doi:10.1177/0363546518756976 (2018).

5. Saris, D. *et al.* Matrix-Applied Characterized Autologous Cultured Chondrocytes Versus Microfracture: Two-Year Follow-up of a Prospective Randomized Trial. *Am J Sports Med* **42**, 1384-1394, doi:10.1177/0363546514528093 (2014).

6. Batty, L., Dance, S., Bajaj, S. & Cole, B. J. Autologous chondrocyte implantation: an overview of technique and outcomes. *ANZ J Surg* **81**, 18-25, doi:10.1111/j.1445-2197.2010.05495.x (2011).

7. Schnabel, M. *et al.* Dedifferentiation-associated changes in morphology and gene expression in primary human articular chondrocytes in cell culture. *Osteoarthritis Cartilage* **10**, 62-70, doi:10.1053/joca.2001.0482 (2002).

8. Hidvegi, N. C. *et al.* A low temperature method of isolating normal human articular chondrocytes. *Osteoarthritis Cartilage* **14**, 89-93, doi:10.1016/j.joca.2005.08.007 (2006).

9. Wu, L., Prins, H. J., Helder, M. N., van Blitterswijk, C. A. & Karperien, M. Trophic effects of mesenchymal stem cells in chondrocyte co-cultures are independent of culture conditions and cell sources. *Tissue Eng Part A* **18**, 1542-1551, doi:10.1089/ten.TEA.2011.0715 (2012).

10. Wu, L. *et al.* Trophic effects of mesenchymal stem cells increase chondrocyte proliferation and matrix formation. *Tissue Eng Part A* **17**, 1425-1436, doi:10.1089/ten.TEA.2010.0517 (2011).

11. Acharya, C. *et al.* Enhanced chondrocyte proliferation and mesenchymal stromal cells chondrogenesis in coculture pellets mediate improved cartilage formation. *J Cell Physiol* **227**, 88-97, doi:10.1002/jcp.22706 (2012).

12. Wang, M. *et al.* Trophic stimulation of articular chondrocytes by late-passage mesenchymal stem cells in coculture. *J Orthop Res* **31**, 1936-1942, doi:10.1002/jor.22466 (2013).

13. Dahlin, R. L. *et al.* Articular chondrocytes and mesenchymal stem cells seeded on biodegradable scaffolds for the repair of cartilage in a rat osteochondral defect model. *Biomaterials* **35**, 7460-7469, doi:10.1016/j.biomaterials.2014.05.055 (2014).

14. de Windt, T. S. *et al.* Allogeneic Mesenchymal Stem Cells Stimulate Cartilage Regeneration and Are Safe for Single-Stage Cartilage Repair in Humans upon Mixture with Recycled Autologous Chondrons. *Stem Cells* **35**, 256-264, doi:10.1002/stem.2475 (2017).

15. Fu, Y. *et al.* Trophic Effects of Mesenchymal Stem Cells in Tissue Regeneration. *Tissue Eng Part B Rev* **23**, 515-528, doi:10.1089/ten.TEB.2016.0365 (2017).

16. Elmore, S. Apoptosis: a review of programmed cell death. *Toxicol Pathol* **35**, 495-516, doi:10.1080/01926230701320337 (2007).

17. Levine, B. & Kroemer, G. Autophagy in the pathogenesis of disease. *Cell* **132**, 27-42, doi:10.1016/j.cell.2007.12.018 (2008).

18. Hara, T. *et al.* Suppression of basal autophagy in neural cells causes neurodegenerative disease in mice. *Nature* **441**, 885-889, doi:10.1038/nature04724 (2006).

19. Mizushima, N. Autophagy: process and function. *Genes Dev* **21**, 2861-2873, doi:10.1101/gad.1599207 (2007).

20. Crespo-Diaz, R. *et al.* Platelet lysate consisting of a natural repair proteome supports human mesenchymal stem cell proliferation and chromosomal stability. *Cell Transplant* **20**, 797-811, doi:10.3727/096368910X543376 (2011).

21. Mader, E. K. *et al.* Optimizing patient derived mesenchymal stem cells as virus carriers for a phase I clinical trial in ovarian cancer. *J Transl Med* **11**, 20, doi:10.1186/1479-5876-11-20 (2013).

22. Dudakovic, A. *et al.* High-resolution molecular validation of self-renewal and spontaneous differentiation in clinical-grade adipose-tissue derived human mesenchymal stem cells. *J Cell Biochem* **115**, 1816-1828, doi:10.1002/jcb.24852 (2014).

23. Kalari, K. R. *et al.* MAP-RSeq: Mayo Analysis Pipeline for RNA sequencing. *BMC Bioinformatics* **15**, 224, doi:10.1186/1471-2105-15-224 (2014).

24. Dudakovic, A. *et al.* Epigenetic Control of Skeletal Development by the Histone Methyltransferase Ezh2. *J Biol Chem* **290**, 27604-27617, doi:10.1074/jbc.M115.672345 (2015).

25. Hevesi, M. *et al.* Defining the baseline transcriptional fingerprint of rabbit hamstring autograft. *Gene Reports* **15**, doi:UNSP 100363

10.1016/j.genrep.2019.100363 (2019).

26. Kim, D. *et al.* TopHat2: accurate alignment of transcriptomes in the presence of insertions, deletions and gene fusions. *Genome Biol* **14**, R36, doi:10.1186/gb-2013-14-4-r36 (2013).

27. Anders, S., Pyl, P. T. & Huber, W. HTSeq--a Python framework to work with high-throughput sequencing data. *Bioinformatics* **31**, 166-169, doi:10.1093/bioinformatics/btu638 (2015).

28. Zhong, L. *et al.* Endogenous DKK1 and FRZB Regulate Chondrogenesis and Hypertrophy in Three-Dimensional Cultures of Human Chondrocytes and Human Mesenchymal Stem Cells. *Stem Cells Dev* **25**, 1808-1817, doi:10.1089/scd.2016.0222 (2016).

29. Wegmeyer, H. *et al.* Mesenchymal stromal cell characteristics vary depending on their origin. *Stem Cells Dev* **22**, 2606-2618, doi:10.1089/scd.2013.0016 (2013).

30. Tsujimoto, Y. & Shimizu, S. Another way to die: autophagic programmed cell death. *Cell Death Differ* **12 Suppl 2**, 1528-1534, doi:10.1038/sj.cdd.4401777 (2005).

31. Mustafa, N. *et al.* VS-5584 mediates potent anti-myeloma activity via the upregulation of a class II tumor suppressor gene, RARRES3 and the activation of Bim. *Oncotarget* **8**, 101847-101864, doi:10.18632/oncotarget.21988 (2017).

32. He, W. *et al.* Attenuation of TNFSF10/TRAIL-induced apoptosis by an autophagic survival pathway involving TRAF2- and RIPK1/RIP1-mediated MAPK8/JNK activation. *Autophagy* **8**, 1811-1821, doi:10.4161/auto.22145 (2012).

33. Wang, G. *et al.* PIK3R3 induces epithelial-to-mesenchymal transition and promotes metastasis in colorectal cancer. *Mol Cancer Ther* **13**, 1837-1847, doi:10.1158/1535-7163.MCT-14-0049 (2014).

34. Qi, H. *et al.* TRAF Family Proteins Regulate Autophagy Dynamics by Modulating AUTOPHAGY PROTEIN6 Stability in Arabidopsis. *Plant Cell* **29**, 890-911, doi:10.1105/tpc.17.00056 (2017).

35. Italiano, D., Lena, A. M., Melino, G. & Candi, E. Identification of NCF2/p67phox as a novel p53 target gene. *Cell Cycle* **11**, 4589-4596, doi:10.4161/cc.22853 (2012).

36. Smith, E. E. & Malik, H. S. The apolipoprotein L family of programmed cell death and immunity genes rapidly evolved in primates at discrete sites of host-pathogen interactions. *Genome Res* **19**, 850-858, doi:10.1101/gr.085647.108 (2009).

37. Tey, S. K. & Khanna, R. Autophagy mediates transporter associated with antigen processing-independent presentation of viral epitopes through MHC class I pathway. *Blood* **120**, 994-1004, doi:10.1182/blood-2012-01-402404 (2012).

38. Kaminskyy, V. & Zhivotovsky, B. Proteases in autophagy. *Biochim Biophys Acta* **1824**, 44-50, doi:10.1016/j.bbapap.2011.05.013 (2012).

39. Porter, A. G. & Janicke, R. U. Emerging roles of caspase-3 in apoptosis. *Cell Death Differ* **6**, 99-104, doi:10.1038/sj.cdd.4400476 (1999).

40. Bauvy, C., Meijer, A. J. & Codogno, P. Assaying of autophagic protein degradation. *Methods Enzymol* **452**, 47-61, doi:10.1016/S0076-6879(08)03604-5 (2009).

41. Klionsky, D. J. *et al.* Guidelines for the use and interpretation of assays for monitoring autophagy. *Autophagy* **8**, 445-544, doi:10.4161/auto.19496 (2012).

42. Rogue, A., Lambert, C., Spire, C., Claude, N. & Guillouzo, A. Interindividual variability in gene expression profiles in human hepatocytes and comparison with HepaRG cells. *Drug Metab Dispos* **40**, 151-158, doi:10.1124/dmd.111.042028 (2012).

43. Mancuso, P., Raman, S., Glynn, A., Barry, F. & Murphy, J. M. Mesenchymal Stem Cell Therapy for Osteoarthritis: The Critical Role of the Cell Secretome. *Front Bioeng Biotechnol* **7**, 9, doi:10.3389/fbioe.2019.00009 (2019).

44. Wu, L., Leijten, J., van Blitterswijk, C. A. & Karperien, M. Fibroblast growth factor-1 is a mesenchymal stromal cell-secreted factor stimulating proliferation of osteoarthritic chondrocytes in co-culture. *Stem Cells Dev* **22**, 2356-2367, doi:10.1089/scd.2013.0118 (2013).

49. Kurth, T. *et al.* Chondrogenic potential of human synovial mesenchymal stem cells in alginate. *Osteoarthritis Cartilage* **15**, 1178-1189, doi:10.1016/j.joca.2007.03.015 (2007).

50. Shu, B. *et al.* BMP2, but not BMP4, is crucial for chondrocyte proliferation and maturation during endochondral bone development. *J Cell Sci* **124**, 3428-3440, doi:10.1242/jcs.083659 (2011).

51. Li, X. *et al.* BMP2 promotes chondrocyte proliferation via the Wnt/beta-catenin signaling pathway. *Mol Med Rep* **4**, 621-626, doi:10.3892/mmr.2011.474 (2011).

52. Ornitz, D. M. FGF signaling in the developing endochondral skeleton. *Cytokine Growth Factor Rev* **16**, 205-213, doi:10.1016/j.cytogfr.2005.02.003 (2005).

53. Li, M., Gao, P. & Zhang, J. Crosstalk between Autophagy and Apoptosis: Potential and Emerging Therapeutic Targets for Cardiac Diseases. *Int J Mol Sci* **17**, 332, doi:10.3390/ijms17030332 (2016).

54. Mizushima, N. & Klionsky, D. J. Protein turnover via autophagy: implications for metabolism. *Annu Rev Nutr* **27**, 19-40, doi:10.1146/annurev.nutr.27.061406.093749 (2007).

55. Komatsu, M. *et al.* Impairment of starvation-induced and constitutive autophagy in Atg7-deficient mice. *J Cell Biol* **169**, 425-434, doi:10.1083/jcb.200412022 (2005).

56. Bjorkoy, G. *et al.* p62/SQSTM1 forms protein aggregates degraded by autophagy and has a protective effect on huntingtin-induced cell death. *J Cell Biol* **171**, 603-614, doi:10.1083/jcb.200507002 (2005).

57. Kim, S. O., Ono, K., Tobias, P. S. & Han, J. Orphan nuclear receptor Nur77 is involved in caspase-independent macrophage cell death. *J Exp Med* **197**, 1441-1452, doi:10.1084/jem.20021842 (2003).

58. Tsujimoto, Y. Cell death regulation by the Bcl-2 protein family in the mitochondria. *J Cell Physiol* **195**, 158-167, doi:10.1002/jcp.10254 (2003).

59. Cande, C. *et al.* Apoptosis-inducing factor (AIF): a novel caspase-independent death effector released from mitochondria. *Biochimie* **84**, 215-222, doi:10.1016/s0300-9084(02)01374-3 (2002).

60. Li, L. Y., Luo, X. & Wang, X. Endonuclease G is an apoptotic DNase when released from mitochondria. *Nature* **412**, 95-99, doi:10.1038/35083620 (2001).

61. van Loo, G. *et al.* Endonuclease G: a mitochondrial protein released in apoptosis and involved in caspase-independent DNA degradation. *Cell Death Differ* **8**, 1136-1142, doi:10.1038/sj.cdd.4400944 (2001).

62. Yu, S. W. *et al.* Mediation of poly(ADP-ribose) polymerase-1-dependent cell death by apoptosis-inducing factor. *Science* **297**, 259-263, doi:10.1126/science.1072221 (2002).

63. Xu, Y., Kim, S. O., Li, Y. & Han, J. Autophagy contributes to caspase-independent macrophage cell death. *J Biol Chem* **281**, 19179-19187, doi:10.1074/jbc.M513377200 (2006).

64. Shimizu, S. *et al.* Role of Bcl-2 family proteins in a non-apoptotic programmed cell death dependent on autophagy genes. *Nat Cell Biol* **6**, 1221-1228, doi:10.1038/ncb1192 (2004).

65. Yu, L. *et al.* Regulation of an ATG7-beclin 1 program of autophagic cell death by caspase-8. *Science* **304**, 1500-1502, doi:10.1126/science.1096645 (2004).

66. Elgendy, M., Sheridan, C., Brumatti, G. & Martin, S. J. Oncogenic Ras-induced expression of Noxa and Beclin-1 promotes autophagic cell death and limits clonogenic survival. *Mol Cell* **42**, 23-35, doi:10.1016/j.molcel.2011.02.009 (2011).

67. Maas, S. L. N., Breakefield, X. O. & Weaver, A. M. Extracellular Vesicles: Unique Intercellular Delivery Vehicles. *Trends Cell Biol* **27**, 172-188, doi:10.1016/j.tcb.2016.11.003 (2017).

68. Kondo, S. Altruistic cell suicide in relation to radiation hormesis. *Int J Radiat Biol Relat Stud Phys Chem Med* **53**, 95-102 (1988).

69. Furuta, T. *et al.* Mesenchymal Stem Cell-Derived Exosomes Promote Fracture Healing in a Mouse Model. *Stem Cells Transl Med* **5**, 1620-1630, doi:10.5966/sctm.2015-0285 (2016).

70. Hu, B. *et al.* Effect of Extracellular Vesicles on Neural Functional Recovery and Immunologic Suppression after Rat Cerebral Apoplexy. *Cell Physiol Biochem* **40**, 155-162, doi:10.1159/000452533 (2016).

71. Kalimuthu, S. *et al.* In Vivo therapeutic potential of mesenchymal stem cell-derived extracellular vesicles with optical imaging reporter in tumor mice model. *Sci Rep* **6**, 30418, doi:10.1038/srep30418 (2016).

5.5 Supplementary materials

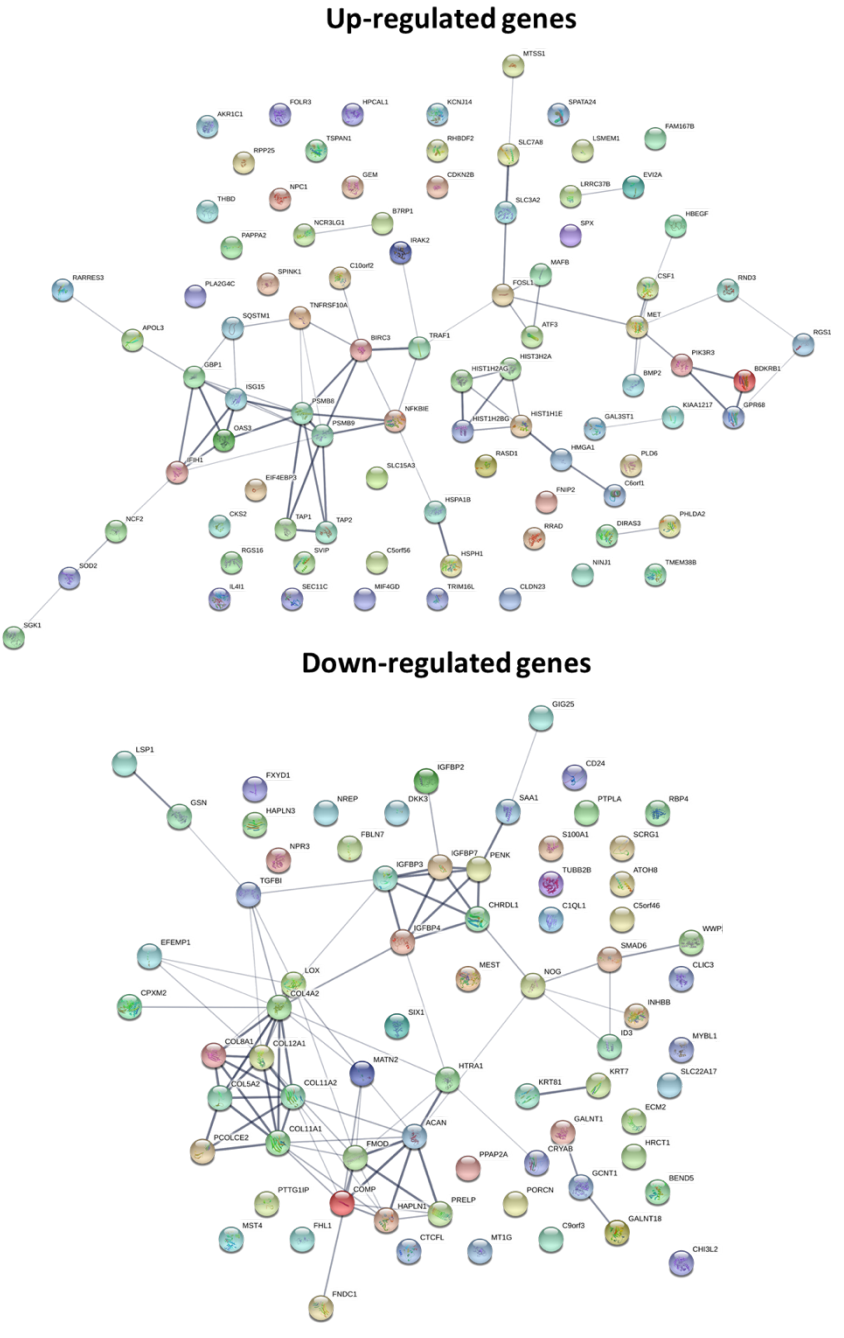

Supplemental Figure 5.S1 *Up- and Down-regulated genes using STRING software.*

Supplemental Table 5.S1 *Scheme of donor variability in terms of sex, age, extraction position and level of diabetes.*

AMSCs	A211	A258	A283
Sex	Male	Female	Male
Age	41	32	54
Position	Abdominal area	Upper thigh	Abdominal area
Diabetes	Normal	Normal	Normal

Supplemental Table 5.S2 *Up-regulated genes having connection detected using STRING software. For each gene a literature search was performed to determine if the gene was actively involved in the autophagic or apoptotic machinery. In green genes enhancing the pathways. In red the genes inhibiting the pathways. In black not fully defined genes, which were shown having an effect in autophagy &/or apoptosis.*

SYMBOL	FULL NAME	AUTOPHAGIC &/OR APOPTOTIC PATHWAY
MTSS1	MTSS I-BAR domain containing 1	--
SLC7A8	Solute Carrier Family 7 Member 8	Apoptosis [1]
SLC3A2	Solute Carrier Family 3 Member 2	Apoptosis [2]
		Apoptosis[3]
		Autophagy (indirect) [4]
		Autophagy (indirect) [5]
MAFB	MAF bZIP transcription factor B	Apoptosis [6]
ATF3	activating transcription factor 3	Autophagy & Apoptosis [7]
		Autophagy [8]
		Autophagy [9]
		Apoptosis [10]
		Apoptosis [11]
		Apoptosis [12]

		Apoptosis [13]
		Apoptosis [14]
LRRC37B	leucine rich repeat containing 37B	--
EVI2A	ecotropic viral integration site 2A	--
HBEGF	heparin binding EGF like growth factor	Apoptosis [15]
		Apoptosis [16]
		Apoptosis [17]
		Apoptosis [18]
RND3	Rho family GTPase 3	Autophagy [19]
		Apoptosis [20]
		Apoptosis [21]
		Apoptosis [22]
RGS1	regulator of G protein signaling 1	Apoptosis [23]
GPR68	G protein-coupled receptor 68	Apoptosis [24]
BDKRB1	bradykinin receptor B1	Apoptosis [25]
KIAA1217		Apoptosis [26]
BMP2	Bone morphogenic protein 2	Autophagy [27]
		Autophagy [28]
		Apoptosis [29]
		Apoptosis [30]
		Apoptosis [31]
		Apoptosis [32]
GAL3ST1	galactose-3-O-sulfotransferase 1	Apoptosis [33]
PHLDA2	pleckstrin homology like domain family A member 2	Apoptosis [34]
		Apoptosis [35]
		Apoptosis [36]
		Apoptosis [37]
		Autophagy [38]
DIRAS3	DIRAS family GTPase 3	Apoptosis & autophagy [39]
		Autophagy [40]
		Autophagy [41]
		Autophagy [42]
		Apoptosis [43]
C6ORF1	small integral membrane protein 29	--
HMGA1	high mobility group AT-hook 1	Autophagy [44]
		Apoptosis [45,46]

HIST1H1E	histone cluster 1 H1 family member e	Apoptosis [47]
		Apoptosis [48]
HIST3H2A	histone cluster 3 H2A	--
HIST1H2AG	histone cluster 1 H2A family member g	--
HIST1H2BG	histone cluster 1 H2B family member g	--
B7RP1	inducible T cell costimulator ligand	Apoptosis [49]
NCR3LG1	natural killer cell cytotoxicity receptor 3 ligand 1	Apoptosis [50]
		Apoptosis [51]
HSPH1	heat shock protein family H (Hsp110) member 1	Apoptosis [52]
		Apoptosis [53]
		Apoptosis [54]
		Apoptosis [55]
		Apoptosis [56]
HSPA1B	heat shock protein family A (Hsp70) member 1B	Apoptosis [57]
		Apoptosis [58]
		Apoptosis [59]
		Apoptosis [60]
RARRES3	phospholipase A and acyltransferase 4	Apoptosis [61]
		Apoptosis [62]
		Apoptosis [63]
IFIH1	interferon induced with helicase C domain 1	Autophagy [64]
		Autophagy [65]
		Apoptosis [66]
		Apoptosis [67]
		Apoptosis [68]
SGK1	glucocorticoid-induced protein kinase 1	Apoptosis & autophagy [69]
		Apoptosis [70]
SOD2	manganese superoxide dismutase (Mn-SOD	Apoptosis & autophagy [71]
		Autophagy [72]
NCF2	Neutrophil Cytosolic Factor 2	Apoptosis & autophagy [73]
TAP1	Antigen peptide transporter 1	Autophagy [74]
		Apoptosis [75]
TAP2	Antigen peptide transporter 2	Autophagy [74]
ISG15	Interferon-stimulated gene 15	Autophagy [76]
		Autophagy [77]

		Apoptosis [78]
GBP1	Guanylate-binding Protein 1	Apoptosis & autophagy [79]
APOL3	Apolipoprotein L3	Apoptosis & autophagy [80]
SQSTM1	Sequestosome 1	Autophagy [81]
		Apoptosis [82]
PSMB8	Proteasome Subunit Beta 8	Apoptosis & autophagy [83]
PSMB9	Proteasome Subunit Beta 9	Apoptosis & autophagy [83]
BIRC3	Baculoviral IAP Repeat Containing 3)	Apoptosis & autophagy [84]
NFKBIE	nuclear factor of kappa light polypeptide gene enhancer in B-cells inhibitor, epsilon	Autophagy [85]
TRAF1	TNF Receptor Associated Factor 1	Autophagy [86]
		Apoptosis [87]
IRAK2	interleukin 1 receptor associated kinase 2	Apoptosis [88]
C10ORF2	chromosome 10 open reading frame 2	Apoptosis [89]
		Apoptosis [90]
FOSL1	Fos-related antigen 1	Autophagy [91]
CSF1	colony stimulating factor 1	Autophagy [92]
		Apoptosis [93]
MET	MET Proto-Oncogene, Receptor Tyrosine Kinase	Autophagy [94]
		Apoptosis[95]
PIK3R3	phosphoinositide-3-kinase regulatory subunit 3	Apoptosis[96]
TNFRSF10A	Tumor necrosis factor receptor superfamily member 10A	Apoptosis & autophagy[3]

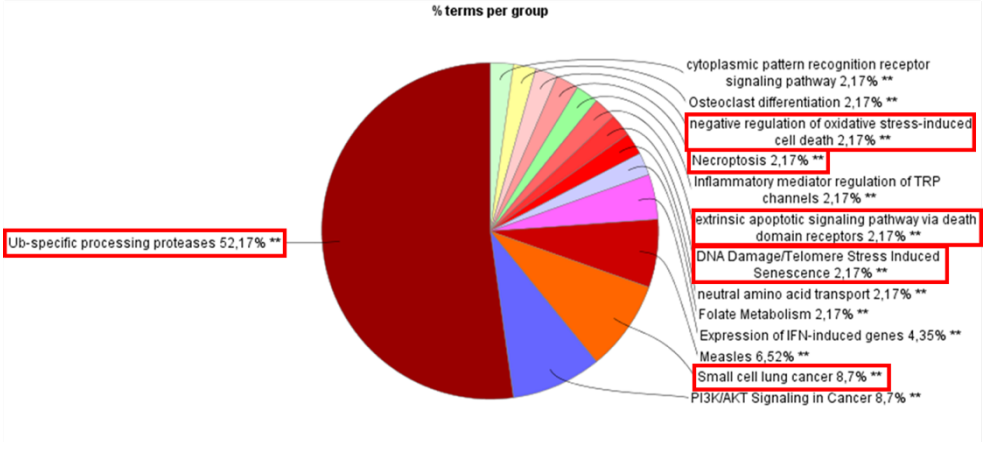

Supplemental Figure 5.S2 *Pie plot showing the % of terms per group of pathways detected. Each group is constituted by a number of GO-pathways (Table 5.3) discovered using ClueGO. The majority of the GO-pathways identified is involved one of the death machinery (red square). The same color is used for the group presented in this pie plot and for table 5.3.*

Supplemental Table 5.S3 *GO-pathways of the 92 up-regulated genes detected using clueGO. The two small red stars above the bars indicate statistical significance (P-value<0.001).*

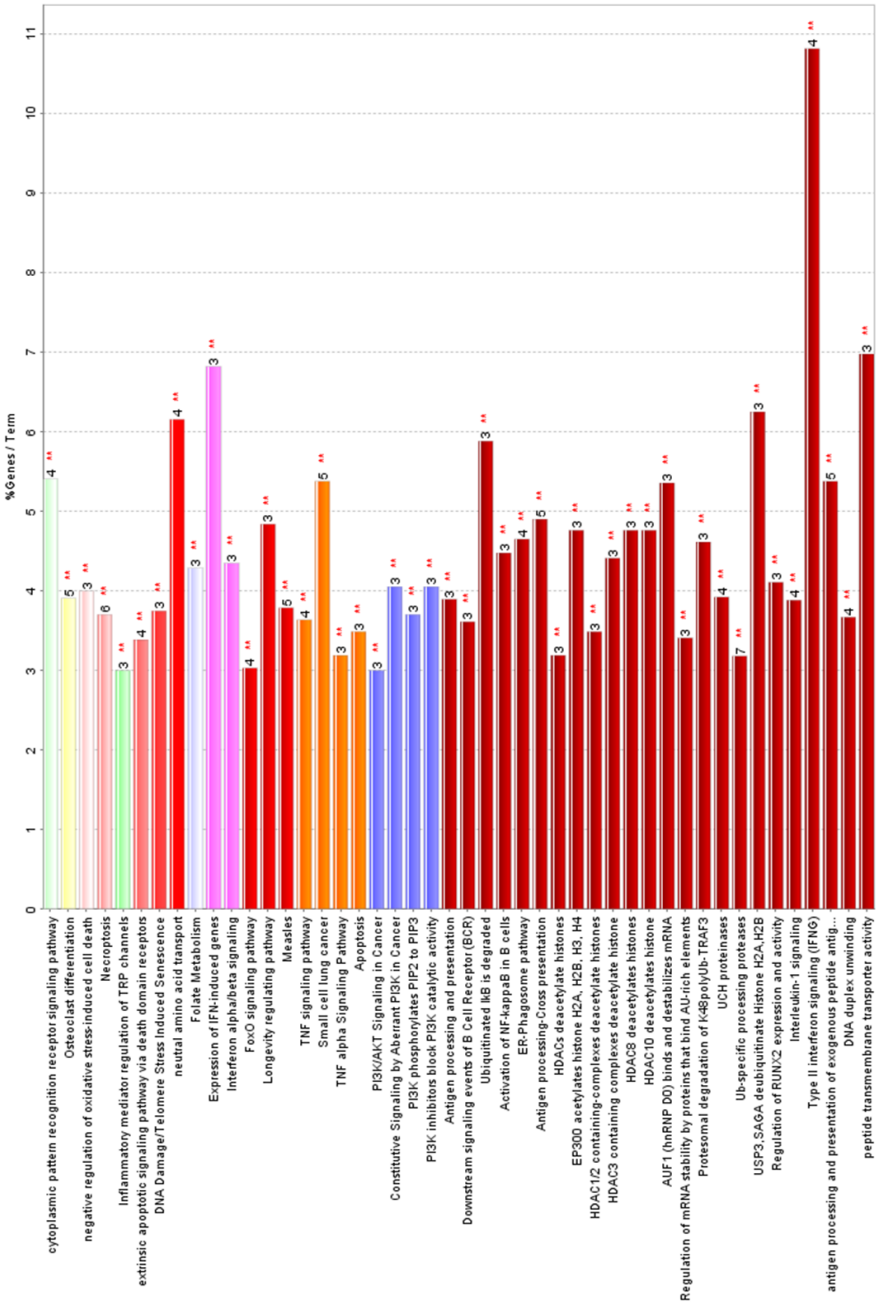

Supplemental Table 5.S4 *RPKM data of 18 individual genes related to autophagy, apoptosis, pro-apoptotic and anti-apoptotic machinery. The data of the MSCs monoculture are then compared to the co-culture using a paired t-test to determine the statistical difference. In yellow, values statistically different (at least below 0.1).*

GeneID	Comment	ch	A211	A283	A258	A211+ch	A283+ch	A258+ch	t-test (PAIRED)
DRAM1	Autophagy	19,19	17,00	43,39	15,94	49,08	62,15	28,27	0,069
SQSTM1/P62	Autophagy	105,40	224,13	284,98	146,92	390,61	529,99	441,07	0,024
MAP1LC3B	Autophagy	33,22	46,46	46,36	50,78	54,16	59,36	54,29	0,099
GBP1	Autophagy	0,75	3,84	4,31	0,88	8,19	10,22	2,76	0,075
APOL3	Autophagy	0,50	2,91	3,89	1,05	7,07	7,47	4,56	0,003
ULK1	Autophagy	6,95	15,43	15,39	7,59	16,07	17,38	13,83	0,222
SOD2	Autophagy	366,97	238,93	1074,04	268,41	603,86	1750,18	656,89	0,041
UVRAG	Autophagy	1,81	2,83	2,76	2,01	4,13	4,15	3,74	0,008
CASP3	Apoptosis	4,58	8,34	8,79	7,00	5,96	10,82	7,82	0,917
CASP5	Apoptosis	0,00	0,11	0,40	0,06	0,01	0,06	0,06	0,277
CASP8	Apoptosis	4,12	4,25	3,36	2,91	3,88	4,88	3,46	0,406
CASP9	Apoptosis	2,50	3,23	3,23	2,14	3,22	3,42	3,47	0,351
BAX	pro-apopotic	40,17	40,81	51,40	45,74	44,42	49,13	54,02	0,404
BAD	pro-apopotic	23,08	16,52	19,33	13,25	19,63	18,01	28,19	0,369
BCL2L11/BIM	pro-apopotic	1,04	2,25	2,37	1,26	2,53	3,72	2,28	0,109
BID	pro-apopotic	3,15	6,81	6,70	5,59	6,03	9,13	8,38	0,321
BCL2	anti-apoptotic	0,03	0,06	0,20	0,02	0,08	0,32	0,09	0,110
BCL2L1	anti-apoptotic	10,33	16,77	18,44	12,94	17,45	24,49	20,45	0,149

Supplemental Figure 5.S3 *Immunofluorescence of the 7 individual conditions. In blue DAPI, in red LC3B and in green P62. Yellow arrow indicates LC3B or P62 in an inactive state. White arrow indicates combination of LC3B and P62 and activation of the autophagic machinery. Scale bar 20 µm.*

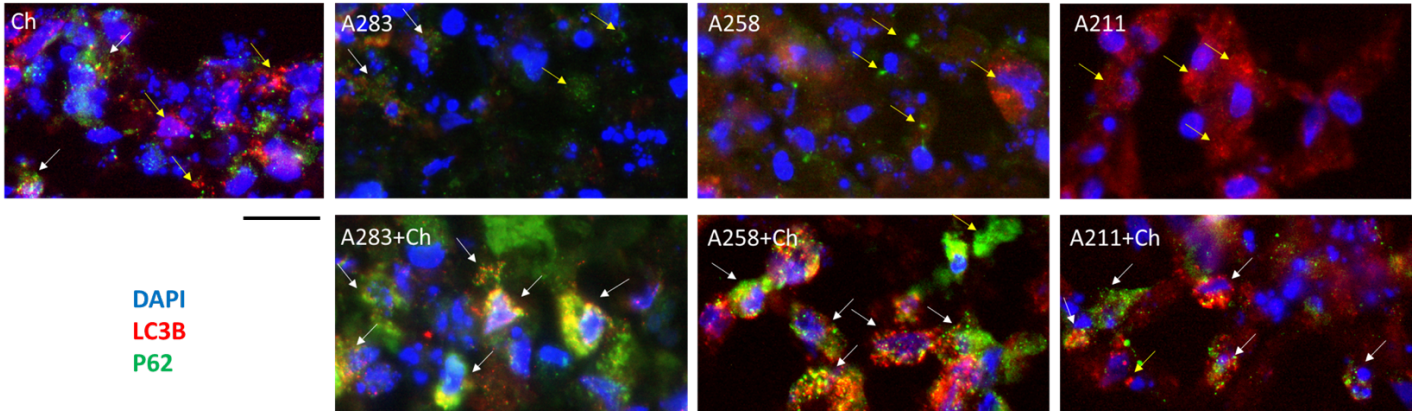

Supplemental Table 5.S5 *RPKM data of 7 individual genes initiating the apoptotic machinery. In light blue the genes initiating apoptosis through an intrinsic pathway in green two receptor genes of the extrinsic pathway. The expected data is the data obtained using equation (1). The fold change is then obtained using the ratio between the real value and the expected value (equation 2). The average for the 3 co-culture is then obtained. In light orange values below the limits used*

GeneID	RPKM data							Expected			Real/Expected (fold change)			Fold change Average
	A211	A211+ch	A283	A283+ch	A258	A258+ch	ch	A211+ch	A283+ch	A258+ch	A211+ch	A283+ch	A258+ch	
ENDOG	2,35	3,23	3,16	3,93	2,82	5,41	4,63	3,33	3,79	3,60	0,97	1,04	1,50	1,17
DIABLO	13,89	16,03	13,40	19,25	12,25	19,48	15,37	14,53	14,25	13,59	1,10	1,35	1,43	1,30
HTRA2	5,51	7,10	8,46	14,04	5,53	9,00	5,93	5,69	7,37	5,70	1,25	1,90	1,58	1,58
CAD	3,15	4,15	3,41	5,97	3,01	4,95	3,12	3,14	3,28	3,06	1,32	1,82	1,62	1,59
AIFM1	3,94	5,09	5,24	7,94	3,25	5,80	3,51	3,75	4,50	3,37	1,36	1,77	1,72	1,62
TNFRSF10A	2,78	5,79	1,67	7,86	1,74	7,15	2,94	2,85	2,22	2,25	2,03	3,55	3,17	2,92
TRAF1	2,32	5,50	3,91	13,29	2,17	7,34	0,83	1,68	2,58	1,59	3,28	5,14	4,61	4,34

Supplemental Table 5.S6 *Description of the 86 up-regulated genes using STRING.*

BDKRB1	*B1 bradykinin receptor; This is a receptor for bradykinin. Could be a factor in chronic pain and inflammation (353 aa)*
TNFRSF10A	*Tumor necrosis factor receptor superfamily member 10A; Receptor for the cytotoxic ligand TNFSF10/TRAIL. The adapter molecule FADD recruits caspase-8 to the activated receptor. The resulting death-inducing signaling complex (DISC) performs caspase-8 proteolytic activation which initiates the subsequent cascade of caspases (aspartate-specific cysteine proteases) mediating apoptosis. Promotes the activation of NF-kappa-B; CD molecules (468 aa)*
RASD1	*Dexamethasone-induced Ras-related protein 1; Small GTPase. Negatively regulates the transcription regulation activity of the APBB1/FE65-APP complex via its interaction with APBB1/FE65 (By similarity); Belongs to the small GTPase superfamily. RasD family (281 aa)*
SLC15A3	*Solute carrier family 15 member 3; Proton oligopeptide cotransporter. Transports free histidine and certain di- and tripeptides (By similarity); Solute carriers (581 aa)*
OAS3	*2'-5'-oligoadenylate synthase 3; Interferon-induced, dsRNA-activated antiviral enzyme which plays a critical role in cellular innate antiviral response. In addition, it may also play a role in other cellular processes such as apoptosis, cell growth, differentiation and gene regulation. Synthesizes preferentially dimers of 2'-5'-oligoadenylates (2-5A) from ATP which then bind to the inactive monomeric form of ribonuclease L (RNase L) leading to its dimerization and subsequent activation. Activation of RNase L leads to degradation of cellular as well as viral RNA, resulting in the inhib [...] (1087 aa)*
HBEGF	*Proheparin-binding EGF-like growth factor; Growth factor that mediates its effects via EGFR, ERBB2 and ERBB4. Required for normal cardiac valve formation and normal heart function. Promotes smooth muscle cell proliferation. May be involved in macrophage-mediated cellular proliferation. It is mitogenic for fibroblasts, but not endothelial cells. It is able to bind EGF receptor/EGFR with higher affinity than EGF itself and is a far more potent mitogen for smooth muscle cells than EGF. Also acts as a diphtheria toxin receptor (208 aa)*
EVI2A	*Protein EVI2A; May complex with itself or/and other proteins within the membrane, to function as part of a cell-surface receptor (259 aa)*
RARRES3	*Retinoic acid receptor responder protein 3; Exhibits PLA1/2 activity, catalyzing the calcium- independent hydrolysis of acyl groups in various phosphotidylcholines (PC) and phosphatidylethanolamine (PE). For most substrates, PLA1 activity is much higher than PLA2 activity. N- and O-acylation activity is hardly detectable; HRAS like suppressor family (164 aa)*
IRAK2	*Interleukin-1 receptor-associated kinase-like 2; Binds to the IL-1 type I receptor following IL-1 engagement, triggering intracellular signaling cascades leading to transcriptional up-regulation and mRNA stabilization (625 aa)*
SPX	*Spexin; Plays a role as a central modulator of cardiovascular and renal function and nociception. Plays also a role in energy metabolism and storage. Inhibits adrenocortical cell proliferation with minor stimulation on corticosteroid release (By similarity) (116 aa)*
PIK3R3	*Phosphatidylinositol 3-kinase regulatory subunit gamma; Binds to activated (phosphorylated) protein-tyrosine kinases through its SH2 domain and regulates their kinase activity. During insulin stimulation, it also binds to IRS-1 (461 aa)*
BIRC3	*Baculoviral IAP repeat-containing protein 3; Multi-functional protein which regulates not only caspases and apoptosis, but also modulates inflammatory signaling and immunity, mitogenic kinase signaling and cell proliferation, as well as cell invasion and metastasis. Acts as an E3 ubiquitin- protein ligase regulating NF-kappa-B signaling and regulates both canonical and non-canonical NF-kappa-B signaling by acting in opposite directions- acts as a positive regulator of the canonical pathway and suppresses constitutive activation of non-canonical NF-kappa-B signaling. The target proteins [...] (604 aa)*
IFIH1	*Interferon-induced helicase C domain-containing protein 1; Innate immune receptor which acts as a cytoplasmic sensor of viral nucleic acids and plays a major role in sensing viral infection and in the activation of a cascade of antiviral responses including the induction of type I interferons and proinflammatory cytokines. Its ligands include mRNA lacking 2'-O- methylation at their 5' cap and long-dsRNA (>1 kb in length). Upon ligand binding it associates with mitochondria antiviral signaling protein (MAVS/IPS1) which activates the IKK-related kinases- TBK1 and IKBKE which phosphorylat [...] (1025 aa)*
FNIP2	*Folliculin-interacting protein 2; Acts as a co-chaperone of HSP90AA1. Inhibits the ATPase activity of HSP90AA1 leading to reduction in its chaperone activity. Facilitates the binding of client protein FLCN to HSP90AA1. May play a role in the signal transduction pathway of apoptosis induced by O6-methylguanine- mispaired lesions (By similarity). May be involved in energy and/or nutrient sensing through the AMPK and mTOR signaling pathways. May regulate phosphorylation of RPS6KB1; DENN/MADD domain containing (1114 aa)*
NPC1	*Niemann-Pick C1 protein; Intracellular cholesterol transporter which acts in concert with NPC2 and plays an important role in the egress of cholesterol from the endosomal/lysosomal compartment. Both NPC1 and NPC2 function as the cellular 'tag team duo' (TTD) to catalyze the mobilization of cholesterol within the multivesicular environment of the late endosome (LE) to effect egress through the limiting bilayer of the LE. NPC2 binds unesterified cholesterol that has been released from LDLs in the lumen of the late endosomes/lysosomes and transfers it to the cholesterol-binding pocket of [...] (1278 aa)*
NFKBIE	*NF-kappa-B inhibitor epsilon; Inhibits NF-kappa-B by complexing with and trapping it in the cytoplasm. Inhibits DNA-binding of NF-kappa-B p50-p65 and p50-c-Rel complexes (500 aa)*
CDKN2B	*Cyclin-dependent kinase 4 inhibitor B; Interacts strongly with CDK4 and CDK6. Potent inhibitor. Potential effector of TGF-beta induced cell cycle arrest; Belongs to the CDKN2 cyclin-dependent kinase inhibitor family (138 aa)*
SPINK1	*Serine protease inhibitor Kazal-type 1; Serine protease inhibitor which exhibits anti-trypsin activity. In the pancreas, protects against trypsin-catalyzed premature activation of zymogens (By similarity); Serine peptidase inhibitors, Kazal type (79 aa)*
GEM	*GTP-binding protein GEM; Could be a regulatory protein, possibly participating in receptor-mediated signal transduction at the plasma membrane. Has guanine nucleotide-binding activity but undetectable intrinsic GTPase activity; RGK type GTPase family (296 aa)*
RRAD	*GTP-binding protein RAD; May play an important role in cardiac antiarrhythmia via the strong suppression of voltage-gated L-type Ca(2+) currents. Regulates voltage-dependent L-type calcium channel subunit alpha- 1C trafficking to the cell membrane (By similarity). Inhibits cardiac hypertrophy through the calmodulin-dependent kinase II (CaMKII) pathway. Inhibits phosphorylation and activation of CAMK2D; Belongs to the small GTPase superfamily. RGK family (308 aa)*
HIST1H1E	*Histone H1.4; Histone H1 protein binds to linker DNA between nucleosomes forming the macromolecular structure known as the chromatin fiber. Histones H1 are necessary for the condensation of nucleosome chains into higher-order structured fibers. Acts also as a regulator of individual gene transcription through chromatin remodeling, nucleosome spacing and DNA methylation (By similarity) (219 aa)*
EIF4EBP3	*Eukaryotic translation initiation factor 4E-binding protein 3; Repressor of translation initiation that regulates EIF4E activity by preventing its assembly into the eIF4F complex- hypophosphorylated form competes with EIF4G1/EIF4G3 and strongly binds to EIF4E, leading to repress translation. In contrast, hyperphosphorylated form dissociates from EIF4E, allowing interaction between EIF4G1/EIF4G3 and EIF4E, leading to initiation of translation (100 aa)*
C10orf2	*Twinkle protein, mitochondrial; Involved in mitochondrial DNA (mtDNA) metabolism. Could function as an adenine nucleotide-dependent DNA helicase. Function inferred to be critical for lifetime maintenance of mtDNA integrity. In vitro, forms in combination with POLG, a processive replication machinery, which can use double-stranded DNA (dsDNA) as template to synthesize single-stranded DNA (ssDNA) molecules. May be a key regulator of mtDNA copy number in mammals (684 aa)*
FOSL1	*Fos-related antigen 1; FOS like 1, AP-1 transcription factor subunit; Belongs to the bZIP family. Fos subfamily (271 aa)*
PLD6	*Mitochondrial cardiolipin hydrolase; Endonuclease that plays a critical role in PIWI- interacting RNA (piRNA) biogenesis during spermatogenesis. piRNAs provide essential protection against the activity of mobile genetic elements (By similarity). piRNA-mediated transposon silencing is thus critical for maintaining genome stability, in particular in germline cells when transposons are mobilized as a consequence of wide-spread genomic demethylation (By similarity). Has been proposed to act as a cardiolipin hydrolase to generate phosphatidic acid at mitochondrial surface (By similarity). A [...] (252 aa)*
MET	*Hepatocyte growth factor receptor; Receptor tyrosine kinase that transduces signals from the extracellular matrix into the cytoplasm by binding to hepatocyte growth factor/HGF ligand. Regulates many physiological processes including proliferation, scattering, morphogenesis and survival. Ligand binding at the cell surface induces autophosphorylation of MET on its intracellular domain that provides docking sites for downstream signaling molecules. Following activation by ligand, interacts with the PI3-kinase subunit PIK3R1, PLCG1, SRC, GRB2, STAT3 or the adapter GAB1. Recruitment of thes [...] (1408 aa)*
RPP25	*Ribonuclease P protein subunit p25; Component of ribonuclease P, a protein complex that generates mature tRNA molecules by cleaving their 5'-ends. Also a component of RNase MRP. This subunit binds to RNA (199 aa)*
HSPH1	*Heat shock protein 105 kDa; Acts as a nucleotide-exchange factor (NEF) for chaperone proteins HSPA1A and HSPA1B, promoting the release of ADP from HSPA1A/B thereby triggering client/substrate protein release. Prevents the aggregation of denatured proteins in cells under severe stress, on which the ATP levels decrease markedly. Inhibits HSPA8/HSC70 ATPase and chaperone activities (By similarity); Heat shock 70kDa proteins (858 aa)*
PHLDA2	*Pleckstrin homology-like domain family A member 2; Plays a role in regulating placenta growth. May act via its PH domain that competes with other PH domain-containing proteins, thereby preventing their binding to membrane lipids (By similarity); Belongs to the PHLDA2 family (152 aa)*
SLC7A8	*Large neutral amino acids transporter small subunit 2; Sodium-independent, high-affinity transport of small and large neutral amino acids such as alanine, serine, threonine, cysteine, phenylalanine, tyrosine, leucine, arginine and tryptophan, when associated with SLC3A2/4F2hc. Acts as an amino acid exchanger. Has higher affinity for L-phenylalanine than LAT1 but lower affinity for glutamine and serine. L-alanine is transported at physiological concentrations. Plays a role in basolateral (re)absorption of neutral amino acids. Involved in the uptake of methylmercury (MeHg) when administe [...] (535 aa)*
RHBDF2	*Inactive rhomboid protein 2; Rhomboid protease-like protein which has no protease activity but regulates the secretion of several ligands of the epidermal growth factor receptor. Indirectly activates the epidermal growth factor receptor signaling pathway and may thereby regulate sleep, cell survival, proliferation and migration (By similarity); Belongs to the peptidase S54 family (856 aa)*

MTSS1	*Metastasis suppressor protein 1; May be related to cancer progression or tumor metastasis in a variety of organ sites, most likely through an interaction with the actin cytoskeleton; I-BAR domain containing (759 aa)*
LSMEM1	*Leucine rich single-pass membrane protein 1 (131 aa)*
CSF1	*Macrophage colony-stimulating factor 1; Cytokine that plays an essential role in the regulation of survival, proliferation and differentiation of hematopoietic precursor cells, especially mononuclear phagocytes, such as macrophages and monocytes. Promotes the release of proinflammatory chemokines, and thereby plays an important role in innate immunity and in inflammatory processes. Plays an important role in the regulation of osteoclast proliferation and differentiation, the regulation of bone resorption, and is required for normal bone development. Required for normal male and female [...] (554 aa)*
C5orf56	*Uncharacterized protein C5orf56; Chromosome 5 open reading frame 56 (126 aa)*
B7RP1	*Inducible T-cell co-stimulator ligand; Ligand for the T-cell-specific cell surface receptor ICOS. Acts as a costimulatory signal for T-cell proliferation and cytokine secretion; induces also B-cell proliferation and differentiation into plasma cells. Could play an important role in mediating local tissue responses to inflammatory conditions, as well as in modulating the secondary immune response by co- stimulating memory T-cell function (By similarity); Belongs to the immunoglobulin superfamily. BTN/MOG family (309 aa)*
LRRC37B	*Leucine-rich repeat-containing protein 37B; Leucine rich repeat containing 37B (947 aa)*
NCR3LG1	*Natural cytotoxicity triggering receptor 3 ligand 1; Triggers NCR3-dependent natural killer cell activation; C1-set domain containing (454 aa)*
ATF3	*Cyclic AMP-dependent transcription factor ATF-3; This protein binds the cAMP response element (CRE) (consensus- 5'-GTGACGT[AC][AG]-3'), a sequence present in many viral and cellular promoters. Represses transcription from promoters with ATF sites. It may repress transcription by stabilizing the binding of inhibitory cofactors at the promoter. Isoform 2 activates transcription presumably by sequestering inhibitory cofactors away from the promoters; Basic leucine zipper proteins (181 aa)*
APOL3	*Apolipoprotein L3; May affect the movement of lipids in the cytoplasm or allow the binding of lipids to organelles; Apolipoproteins (402 aa)*
SVIP	*Small VCP interacting protein; Belongs to the SVIP family (77 aa)*
TAP1	*Antigen peptide transporter 1; Involved in the transport of antigens from the cytoplasm to the endoplasmic reticulum for association with MHC class I molecules. Also acts as a molecular scaffold for the final stage of MHC class I folding, namely the binding of peptide. Nascent MHC class I molecules associate with TAP via tapasin. Inhibited by the covalent attachment of herpes simplex virus ICP47 protein, which blocks the peptide-binding site of TAP. Inhibited by human cytomegalovirus US6 glycoprotein, which binds to the lumenal side of the TAP complex and inhibits peptide translocation [...] (808 aa)*
HIST1H2AG	*Histone cluster 1 H2A family member g; Core component of nucleosome. Nucleosomes wrap and compact DNA into chromatin, limiting DNA accessibility to the cellular machineries which require DNA as a template. Histones thereby play a central role in transcription regulation, DNA repair, DNA replication and chromosomal stability. DNA accessibility is regulated via a complex set of post-translational modifications of histones, also called histone code, and nucleosome remodeling (130 aa)*
HIST3H2A	*Histone H2A type 3; Core component of nucleosome. Nucleosomes wrap and compact DNA into chromatin, limiting DNA accessibility to the cellular machineries which require DNA as a template. Histones thereby play a central role in transcription regulation, DNA repair, DNA replication and chromosomal stability. DNA accessibility is regulated via a complex set of post-translational modifications of histones, also called histone code, and nucleosome remodeling (130 aa)*
NCF2	*Neutrophil cytosol factor 2; NCF2, NCF1, and a membrane bound cytochrome b558 are required for activation of the latent NADPH oxidase (necessary for superoxide production); Tetratricopeptide repeat domain containing (526 aa)*
RGS16	*Regulator of G-protein signaling 16; Regulates G protein-coupled receptor signaling cascades. Inhibits signal transduction by increasing the GTPase activity of G protein alpha subunits, thereby driving them into their inactive GDP-bound form. Plays an important role in the phototransduction cascade by regulating the lifetime and effective concentration of activated transducin alpha. May regulate extra and intracellular mitogenic signals (By similarity) (202 aa)*
PAPPA2	*Pappalysin-2; Metalloproteinase which specifically cleaves insulin- like growth factor binding protein (IGFBP)-5 at the '163-Ser-|- Lys-164' bond. Shows limited proteolysis toward IGFBP-3; Belongs to the peptidase M43B family (1791 aa)*
SGK1	*Serine/threonine-protein kinase Sgk1; Serine/threonine-protein kinase which is involved in the regulation of a wide variety of ion channels, membrane transporters, cellular enzymes, transcription factors, neuronal excitability, cell growth, proliferation, survival, migration and apoptosis. Plays an important role in cellular stress response. Contributes to regulation of renal Na(+) retention, renal K(+) elimination, salt appetite, gastric acid secretion, intestinal Na(+)/H(+) exchange and nutrient transport, insulin-dependent salt sensitivity of blood pressure, salt sensitivity of peri [...] (526 aa)*
GBP1	*Guanylate-binding protein 1; Hydrolyzes GTP to GMP in 2 consecutive cleavage reactions. Exhibits antiviral activity against influenza virus. Promote oxidative killing and deliver antimicrobial peptides to autophagolysosomes, providing broad host protection against different pathogen classes (592 aa)*
DIRAS3	*GTP-binding protein Di-Ras3; RAS type GTPase family (229 aa)*
TSPAN1	*Tetraspanin-1; Tetraspanin 1; Tetraspanins (241 aa)*
MAFB	*Transcription factor MafB; Acts as a transcriptional activator or repressor. Plays a pivotal role in regulating lineage- specific hematopoiesis by repressing ETS1-mediated transcription of erythroid-specific genes in myeloid cells. Required for monocytic, macrophage, osteoclast, podocyte and islet beta cell differentiation. Involved in renal tubule survival and F4/80 maturation. Activates the insulin and glucagon promoters. Together with PAX6, transactivates weakly the glucagon gene promoter through the G1 element. SUMO modification controls its transcriptional activity and ability to [...] (323 aa)*
FAM167B	*Protein FAM167B; Family with sequence similarity 167 member B; Belongs to the FAM167 (SEC) family (163 aa)*
TRAF1	*TNF receptor-associated factor 1; Adapter molecule that regulates the activation of NF- kappa-B and JNK. Plays a role in the regulation of cell survival and apoptosis. The heterotrimer formed by TRAF1 and TRAF2 is part of a E3 ubiquitin-protein ligase complex that promotes ubiquitination of target proteins, such as MAP3K14. The TRAF1/TRAF2 complex recruits the antiapoptotic E3 protein- ubiquitin ligases BIRC2 and BIRC3 to TNFRSF1B/TNFR2; TNF receptor associated factors (416 aa)*
TMEM38B	*Trimeric intracellular cation channel type B; Monovalent cation channel required for maintenance of rapid intracellular calcium release. May act as a potassium counter-ion channel that functions in synchronization with calcium release from intracellular stores; Belongs to the TMEM38 family (291 aa)*
PSMB9	*Proteasome subunit beta type-9; The proteasome is a multicatalytic proteinase complex which is characterized by its ability to cleave peptides with Arg, Phe, Tyr, Leu, and Glu adjacent to the leaving group at neutral or slightly basic pH. The proteasome has an ATP-dependent proteolytic activity. This subunit is involved in antigen processing to generate class I binding peptides. Replacement of PSMB6 by PSMB9 increases the capacity of the immunoproteasome to cleave model peptides after hydrophobic and basic residues (219 aa)*
PSMB8	*Proteasome subunit beta type-8; The proteasome is a multicatalytic proteinase complex which is characterized by its ability to cleave peptides with Arg, Phe, Tyr, Leu, and Glu adjacent to the leaving group at neutral or slightly basic pH. The proteasome has an ATP-dependent proteolytic activity. This subunit is involved in antigen processing to generate class I binding peptides. Replacement of PSMB5 by PSMB8 increases the capacity of the immunoproteasome to cleave model peptides after hydrophobic and basic residues. Acts as a major component of interferon gamma-induced sensitivity. Pla [...] (276 aa)*
TAP2	*Antigen peptide transporter 2; Involved in the transport of antigens from the cytoplasm to the endoplasmic reticulum for association with MHC class I molecules. Also acts as a molecular scaffold for the final stage of MHC class I folding, namely the binding of peptide. Nascent MHC class I molecules associate with TAP via tapasin. Inhibited by the covalent attachment of herpes simplex virus ICP47 protein, which blocks the peptide-binding site of TAP. Inhibited by human cytomegalovirus US6 glycoprotein, which binds to the lumenal side of the TAP complex and inhibits peptide translocation [...] (653 aa)*
NINJ1	*Ninjurin-1; Homophilic cell adhesion molecule that promotes axonal growth. May play a role in nerve regeneration and in the formation and function of other tissues. Cell adhesion requires divalent cations (152 aa)*

HSPA1B	*Heat shock protein family A member 1B (641 aa)*
RND3	*Rho-related GTP-binding protein RhoE; Binds GTP but lacks intrinsic GTPase activity and is resistant to Rho-specific GTPase-activating proteins; Rho family GTPases (244 aa)*
CKS2	*Cyclin-dependent kinases regulatory subunit 2; Binds to the catalytic subunit of the cyclin dependent kinases and is essential for their biological function (79 aa)*
KIAA1217	*Sickle tail protein homolog; Required for normal development of intervertebral disks (1943 aa)*
THBD	*Thrombomodulin; Thrombomodulin is a specific endothelial cell receptor that forms a 1-1 stoichiometric complex with thrombin. This complex is responsible for the conversion of protein C to the activated protein C (protein Ca). Once evolved, protein Ca scissions the activated cofactors of the coagulation mechanism, factor Va and factor VIIIa, and thereby reduces the amount of thrombin generated; C-type lectin domain containing (575 aa)*
SLC3A2	*4F2 cell-surface antigen heavy chain; Required for the function of light chain amino-acid transporters. Involved in sodium-independent, high-affinity transport of large neutral amino acids such as phenylalanine, tyrosine, leucine, arginine and tryptophan. Involved in guiding and targeting of LAT1 and LAT2 to the plasma membrane. When associated with SLC7A6 or SLC7A7 acts as an arginine/glutamine exchanger, following an antiport mechanism for amino acid transport, influencing arginine release in exchange for extracellular amino acids. Plays a role in nitric oxide synthesis in human umbi [...] (631 aa)*
BMP2	*Bone morphogenetic protein 2; Induces cartilage and bone formation. Stimulates the differentiation of myoblasts into osteoblasts via the EIF2AK3-EIF2A- ATF4 pathway. BMP2 activation of EIF2AK3 stimulates phosphorylation of EIF2A which leads to increased expression of ATF4 which plays a central role in osteoblast differentiation. In addition stimulates TMEM119, which upregulates the expression of ATF4; Belongs to the TGF-beta family (396 aa)*
ISG15	*Ubiquitin-like protein ISG15; Ubiquitin-like protein which plays a key role in the innate immune response to viral infection either via its conjugation to a target protein (ISGylation) or via its action as a free or unconjugated protein. ISGylation involves a cascade of enzymatic reactions involving E1, E2, and E3 enzymes which catalyze the conjugation of ISG15 to a lysine residue in the target protein. Its target proteins include IFIT1, MX1/MxA, PPM1B, UBE2L6, UBA7, CHMP5, CHMP2A, CHMP4B and CHMP6. Can also isgylate- EIF2AK2/PKR which results in its activation, DDX58/RIG-I which inhib [...] (165 aa)*
AKR1C1	*Aldo-keto reductase family 1 member C1; Converts progesterone to its inactive form, 20-alpha- dihydroxyprogesterone (20-alpha-OHP). In the liver and intestine, may have a role in the transport of bile. May have a role in monitoring the intrahepatic bile acid concentration. Has a low bile-binding ability. May play a role in myelin formation; Belongs to the aldo/keto reductase family (323 aa)*
SQSTM1	*Sequestosome-1; Autophagy receptor that interacts directly with both the cargo to become degraded and an autophagy modifier of the MAP1 LC3 family. Along with WDFY3, involved in the formation and autophagic degradation of cytoplasmic ubiquitin-containing inclusions (p62 bodies, ALIS/aggresome-like induced structures). Along with SQSTM1, required to recruit ubiquitinated proteins to PML bodies in the nucleus. May regulate the activation of NFKB1 by TNF-alpha, nerve growth factor (NGF) and interleukin-1. May play a role in titin/TTN downstream signaling in muscle cells. May regulate sign [...] (440 aa)*
KCNJ14	*ATP-sensitive inward rectifier potassium channel 14; Inward rectifier potassium channels are characterized by a greater tendency to allow potassium to flow into the cell rather than out of it. Their voltage dependence is regulated by the concentration of extracellular potassium; as external potassium is raised, the voltage range of the channel opening shifts to more positive voltages. The inward rectification is mainly due to the blockage of outward current by internal magnesium. KCNJ14 gives rise to low-conductance channels with a low affinity to the channel blockers Barium and Cesium [...] (436 aa)*
GAL3ST1	*Galactosylceramide sulfotransferase; Catalyzes the sulfation of membrane glycolipids. Seems to prefer beta-glycosides at the non-reducing termini of sugar chains attached to a lipid moiety. Catalyzes the synthesis of galactosylceramide sulfate (sulfatide), a major lipid component of the myelin sheath and of monogalactosylalkylacylglycerol sulfate (seminolipid), present in spermatocytes (By similarity). Also acts on lactosylceramide, galactosyl 1-alkyl-2-sn-glycerol and galactosyl diacylglycerol (in vitro); Belongs to the galactose-3-O-sulfotransferase family (423 aa)*
RGS14	*Regulator of G-protein signaling 14; Regulates G protein-coupled receptor signaling cascades. Inhibits signal transduction by increasing the GTPase activity of G protein alpha subunits, thereby driving them into their inactive GDP-bound form. Besides, modulates signal transduction via G protein alpha subunits by functioning as a GDP-dissociation inhibitor (GDI). Has GDI activity on G(i) alpha subunits GNAI1 and GNAI3, but not on GNAI2 and G(o) alpha subunit GNAO1. Has GAP activity on GNAI0, GNAI2 and GNAI3. May act as a scaffold integrating G protein and Ras/Raf MAPkinase signaling pat [...] (566 aa)*
HMGA1	*High mobility group protein HMG-I/HMG-Y; HMG-I/Y bind preferentially to the minor groove of A+T rich regions in double-stranded DNA. It is suggested that these proteins could function in nucleosome phasing and in the 3'-end processing of mRNA transcripts. They are also involved in the transcription regulation of genes containing, or in close proximity to A+T-rich regions; Canonical high mobility group (107 aa)*
SPATA24	*Spermatogenesis-associated protein 24; Binds DNA with high affinity but does not bind to TATA boxes. Synergises with GMNN and TBP in activation of TATA box-containing promoters and with GMNN and TBPL1 in activation of the NF1 TATA-less promoter. May play a role in cytoplasm movement and removal during spermiogenesis (By similarity) (205 aa)*
C6orf1	*Uncharacterized protein SMIM29; Chromosome 6 open reading frame 1 (159 aa)*
CLDN23	*Claudin-23; Plays a major role in tight junction-specific obliteration of the intercellular space, through calcium- independent cell-adhesion activity; Claudins (292 aa)*
GPR68	*Ovarian cancer G-protein coupled receptor 1; Proton-sensing receptor involved in pH homeostasis. May represents an osteoblastic pH sensor regulating cell-mediated responses to acidosis in bone. Mediates its action by association with G proteins that stimulates inositol phosphate (IP) production or Ca(2+) mobilization. The receptor is almost silent at pH 7.8 but fully activated at pH 6.8. Function also as a metastasis suppressor gene in prostate cancer (By similarity); Belongs to the G-protein coupled receptor 1 family (365 aa)*
HIST1H2BG	*Histone cluster 1 H2B family member g; Core component of nucleosome. Nucleosomes wrap and compact DNA into chromatin, limiting DNA accessibility to the cellular machineries which require DNA as a template. Histones thereby play a central role in transcription regulation, DNA repair, DNA replication and chromosomal stability. DNA accessibility is regulated via a complex set of post-translational modifications of histones, also called histone code, and nucleosome remodeling (126 aa)*
SOD2	*Superoxide dismutase [Mn], mitochondrial; Destroys superoxide anion radicals which are normally produced within the cells and which are toxic to biological systems (222 aa)*
TRIM16L	*Tripartite motif-containing protein 16-like protein; Tripartite motif containing 16 like; Belongs to the TRIM/RBCC family (348 aa)*
MIF4GD	*MIF4G domain-containing protein; MIF4G domain containing (263 aa)*
SEC11C	*Signal peptidase complex catalytic subunit SEC11C; Component of the microsomal signal peptidase complex which removes signal peptides from nascent proteins as they are translocated into the lumen of the endoplasmic reticulum (192 aa)*
IL4I1	*L-amino-acid oxidase; Lysosomal L-amino-acid oxidase with highest specific activity with phenylalanine. May play a role in lysosomal antigen processing and presentation (By similarity); Belongs to the flavin monoamine oxidase family. FIG1 subfamily (589 aa)*
PLA2G4C	*Cytosolic phospholipase A2 gamma; Has a preference for arachidonic acid at the sn-2 position of phosphatidylcholine as compared with palmitic acid; Phospholipases (551 aa)*
FOLR3	*Folate receptor gamma; Binds to folate and reduced folic acid derivatives and mediates delivery of 5-methyltetrahydrofolate to the interior of cells. Isoform Short does not bind folate (245 aa)*
HPCAL1	*Hippocalcin-like protein 1; May be involved in the calcium-dependent regulation of rhodopsin phosphorylation; Belongs to the recoverin family (193 aa)*

Supplemental Table 5.S7 RPKM values of 8 proliferation genes. The expected value of the co-culture is calculated considering the ratio determined with the male markers (43% chondrocytes & 57% MSCs). The value is then compared to the actual value of the co-culture and an average is obtained indicating the fold-change of the real value compared to the expected.

GeneID	A211	A211+ch	A283	A283+ch	A258	A258+ch	ch		211A(57%)+ ch(43%)	283A(57%)+ ch(43%)	258A(57%)+ ch(43%)		A211+ch /211A(57%) + ch(43%)	A283+ch /283A(57%) + ch(43%)	A258+ch /258A(57%) + ch(43%)		average
MKI67	0,86	0,57	0,09	0,26	0,26	0,25	0,15		0,56	0,11	0,22		1,03	2,27	1,18		1,49
MYC	17,18	16,20	12,93	13,07	15,77	15,08	6,41		12,55	10,13	11,75		1,29	1,29	1,28		1,29
PCNA	29,13	35,53	20,49	49,41	18,46	37,86	27,09		28,25	23,33	22,17		1,26	2,12	1,71		1,69
MCM2	3,87	3,68	2,76	3,97	2,61	5,99	3,73		3,81	3,18	3,09		0,97	1,25	1,94		1,38
MCM7	15,88	16,74	11,41	14,44	10,58	16,93	10,36		13,51	10,96	10,49		1,24	1,32	1,61		1,39
CCND1	53,98	63,68	63,10	111,92	159,83	112,17	41,71		48,70	53,90	109,04		1,31	2,08	1,03		1,47
CCNE1	1,39	1,02	1,10	1,74	0,76	1,34	0,59		1,05	0,89	0,69		0,97	1,96	1,95		1,62
CCNB1	2,63	1,91	1,21	2,01	1,20	2,95	0,77		1,83	1,02	1,02		1,04	1,97	2,91		1,97

Supplementary Figure 5.S4 RPKM values of 3 key regulatory markers of the regulated necrosis.

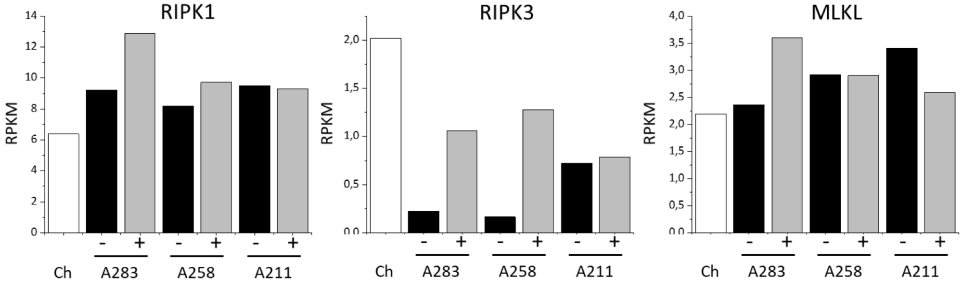

Supplementary Figure 5.S5 Comparison between RPKM values of chondrocytes markers. The first raw shows chondrogenic markers (ACAN, COL2A1, COL1A1). The second raw indicate osteoarthritic markers (COL3A1, COL10A1).

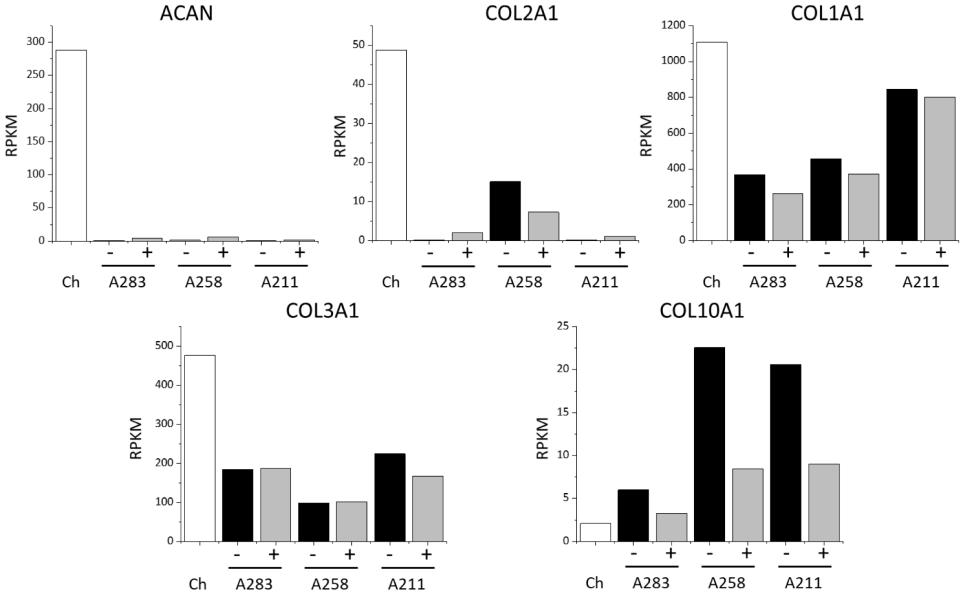

Supplemental References

1. Feng, M. et al. LAT2 regulates glutamine-dependent mTOR activation to promote glycolysis and chemoresistance in pancreatic cancer. J Exp Clin Cancer Res 37, 274, doi:10.1186/s13046-018-0947-4 (2018).

2. Feral, C. C. et al. CD98hc (SLC3A2) mediates integrin signaling. Proc Natl Acad Sci U S A 102, 355-360, doi:10.1073/pnas.0404852102 (2005).

3. He, W. et al. Attenuation of TNFSF10/TRAIL-induced apoptosis by an autophagic survival pathway involving TRAF2- and RIPK1/RIP1-mediated MAPK8/JNK activation. Autophagy 8, 1811-1821, doi:10.4161/auto.22145 (2012).

4. Tattoli, I., Philpott, D. J. & Girardin, S. E. The bacterial and cellular determinants controlling the recruitment of mTOR to the Salmonella-containing vacuole. Biol Open 1, 1215-1225, doi:10.1242/bio.20122840 (2012).

5. Schuster, A. T. et al. Chromosome-associated protein D3 promotes bacterial clearance in human intestinal epithelial cells by repressing expression of amino acid transporters. Gastroenterology 148, 1405-1416 e1403, doi:10.1053/j.gastro.2015.02.013 (2015).

6. Hamada, M. et al. MafB promotes atherosclerosis by inhibiting foam-cell apoptosis. Nat Commun 5, 3147, doi:10.1038/ncomms4147 (2014).

7. Lin, H. et al. Activating transcription factor 3 protects against pressure-overload heart failure via the autophagy molecule Beclin-1 pathway. Mol Pharmacol 85, 682-691, doi:10.1124/mol.113.090092 (2014).

8. Choi, S. R. et al. Activation of autophagic pathways is related to growth inhibition and senescence in cutaneous squamous cell carcinoma. Exp Dermatol 23, 718-724, doi:10.1111/exd.12515 (2014).

9. Sood, V. et al. ATF3 negatively regulates cellular antiviral signaling and autophagy in the absence of type I interferons. Sci Rep 7, 8789, doi:10.1038/s41598-017-08584-9 (2017).

10. Hartman, M. G. et al. Role for activating transcription factor 3 in stress-induced beta-cell apoptosis. Mol Cell Biol 24, 5721-5732, doi:10.1128/MCB.24.13.5721-5732.2004 (2004).

11. Nakagomi, S., Suzuki, Y., Namikawa, K., Kiryu-Seo, S. & Kiyama, H. Expression of the activating transcription factor 3 prevents c-Jun N-terminal kinase-induced neuronal death by promoting heat shock protein 27 expression and Akt activation. J Neurosci 23, 5187-5196 (2003).

12. Nobori, K. et al. ATF3 inhibits doxorubicin-induced apoptosis in cardiac myocytes: a novel cardioprotective role of ATF3. J Mol Cell Cardiol 34, 1387-1397 (2002).

13. Lu, D., Wolfgang, C. D. & Hai, T. Activating transcription factor 3, a stress-inducible gene, suppresses Ras-stimulated tumorigenesis. J Biol Chem 281, 10473-10481, doi:10.1074/jbc.M509278200 (2006).

14. Yin, X., Dewille, J. W. & Hai, T. A potential dichotomous role of ATF3, an adaptive-response gene, in cancer development. Oncogene 27, 2118-2127, doi:10.1038/sj.onc.1210861 (2008).

15. Foo, L. C. et al. Development of a method for the purification and culture of rodent astrocytes. Neuron 71, 799-811, doi:10.1016/j.neuron.2011.07.022 (2011).

16. Armant, D. R. et al. Human trophoblast survival at low oxygen concentrations requires metalloproteinase-mediated shedding of heparin-binding EGF-like growth factor. Development 133, 751-759, doi:10.1242/dev.02237 (2006).

17. Imudia, A. N. et al. Expression of heparin-binding EGF-like growth factor in term chorionic villous explants and its role in trophoblast survival. Placenta 29, 784-789, doi:10.1016/j.placenta.2008.06.013 (2008).

18. Leach, R. E., Kilburn, B. A., Petkova, A., Romero, R. & Armant, D. R. Diminished survival of human cytotrophoblast cells exposed to hypoxia/reoxygenation injury and associated reduction of heparin-binding epidermal growth factor-like growth factor. Am J Obstet Gynecol 198, 471 e471-477; discussion 471 e477-478, doi:10.1016/j.ajog.2008.01.009 (2008).

19. Zhou, J. et al. Chaperone-mediated autophagy regulates proliferation by targeting RND3 in gastric cancer. Autophagy 12, 515-528, doi:10.1080/15548627.2015.1136770 (2016).

20. Ongusaha, P. P. et al. RhoE is a pro-survival p53 target gene that inhibits ROCK I-mediated apoptosis in response to genotoxic stress. Curr Biol 16, 2466-2472, doi:10.1016/j.cub.2006.10.056 (2006).

21. Yue, X. et al. Rnd3 haploinsufficient mice are predisposed to hemodynamic stress and develop apoptotic cardiomyopathy with heart failure. Cell Death Dis 5, e1284, doi:10.1038/cddis.2014.235 (2014).

22. Boswell, S. A., Ongusaha, P. P., Nghiem, P. & Lee, S. W. The protective role of a small GTPase RhoE against UVB-induced DNA damage in keratinocytes. J Biol Chem 282, 4850-4858, doi:10.1074/jbc.M610532200 (2007).

23. Wang, Y., Liu, G., Ren, L., Wang, K. & Liu, A. Long non-coding RNA TUG1 recruits miR29c3p from its target gene RGS1 to promote proliferation and metastasis of melanoma cells. Int J Oncol 54, 1317-1326, doi:10.3892/ijo.2019.4699 (2019).

24. Fang, J. et al. A calcium- and calpain-dependent pathway determines the response to lenalidomide in myelodysplastic syndromes. Nat Med 22, 727-734, doi:10.1038/nm.4127 (2016).

25. Kakoki, M., McGarrah, R. W., Kim, H. S. & Smithies, O. Bradykinin B1 and B2 receptors both have protective roles in renal ischemia/reperfusion injury. Proc Natl Acad Sci U S A 104, 7576-7581, doi:10.1073/pnas.0701617104 (2007).

26. Zhang, C., Lu, J., Liu, B., Cui, Q. & Wang, Y. Primate-specific miR-603 is implicated in the risk and pathogenesis of Alzheimer's disease. Aging (Albany NY) 8, 272-290, doi:10.18632/aging.100887 (2016).

27. Panda, P. K. et al. Abrus agglutinin stimulates BMP-2-dependent differentiation through autophagic degradation of beta-catenin in colon cancer stem cells. Mol Carcinog 57, 664-677, doi:10.1002/mc.22791 (2018).

28. Cao, Y. et al. Noggin attenuates cerulein-induced acute pancreatitis and impaired autophagy. Pancreas 42, 301-307, doi:10.1097/MPA.0b013e31825b9f2c (2013).

29. Hallahan, A. R. et al. BMP-2 mediates retinoid-induced apoptosis in medulloblastoma cells through a paracrine effect. Nat Med 9, 1033-1038, doi:10.1038/nm904 (2003).

30. Kawamura, C. et al. Bone morphogenetic protein-2 induces apoptosis in human myeloma cells with modulation of STAT3. Blood 96, 2005-2011 (2000).

31. Kim, H. K., Oxendine, I. & Kamiya, N. High-concentration of BMP2 reduces cell proliferation and increases apoptosis via DKK1 and SOST in human primary periosteal cells. Bone 54, 141-150, doi:10.1016/j.bone.2013.01.031 (2013).

32. Hyzy, S. L., Olivares-Navarrete, R., Schwartz, Z. & Boyan, B. D. BMP2 induces osteoblast apoptosis in a maturation state and noggin-dependent manner. J Cell Biochem 113, 3236-3245, doi:10.1002/jcb.24201 (2012).

33. Suchanski, J. et al. Sulfatide decreases the resistance to stress-induced apoptosis and increases P-selectin-mediated adhesion: a two-edged sword in breast cancer progression. Breast Cancer Res 20, 133, doi:10.1186/s13058-018-1058-z (2018).

34. Jin, F., Qiao, C., Luan, N. & Li, H. Lentivirus-mediated PHLDA2 overexpression inhibits trophoblast proliferation, migration and invasion, and induces apoptosis. Int J Mol Med 37, 949-957, doi:10.3892/ijmm.2016.2508 (2016).

35. Lee, M. P. & Feinberg, A. P. Genomic imprinting of a human apoptosis gene homologue, TSSC3. Cancer Res 58, 1052-1056 (1998).

36. Dai, H. et al. TSSC3 overexpression associates with growth inhibition, apoptosis induction and enhances chemotherapeutic effects in human osteosarcoma. Carcinogenesis 33, 30-40, doi:10.1093/carcin/bgr232 (2012).

37. Huang, Y., Dai, H. & Guo, Q. N. TSSC3 overexpression reduces stemness and induces apoptosis of osteosarcoma tumor-initiating cells. Apoptosis 17, 749-761, doi:10.1007/s10495-012-0734-1 (2012).

38. Zhao, G. S. et al. TSSC3 promotes autophagy via inactivating the Src-mediated PI3K/Akt/mTOR pathway to suppress tumorigenesis and metastasis in osteosarcoma, and predicts a favorable prognosis. J Exp Clin Cancer Res 37, 188, doi:10.1186/s13046-018-0856-6 (2018).

39. Qiu, J. et al. Distinct subgroup of the Ras family member 3 (DIRAS3) expression impairs metastasis and induces autophagy of gastric cancer cells in mice. J Cancer Res Clin Oncol 144, 1869-1886, doi:10.1007/s00432-018-2708-3 (2018).

40. Zhuo, C., Jiang, R., Lin, X. & Shao, M. LncRNA H19 inhibits autophagy by epigenetically silencing of DIRAS3 in diabetic cardiomyopathy. Oncotarget 8, 1429-1437, doi:10.18632/oncotarget.13637 (2017).

41. Ejaz, A. et al. Weight Loss Upregulates the Small GTPase DIRAS3 in Human White Adipose Progenitor Cells, Which Negatively Regulates Adipogenesis and Activates Autophagy via Akt-mTOR Inhibition. EBioMedicine 6, 149-161, doi:10.1016/j.ebiom.2016.03.030 (2016).

42. Lu, Z. et al. DIRAS3 regulates the autophagosome initiation complex in dormant ovarian cancer cells. Autophagy 10, 1071-1092, doi:10.4161/auto.28577 (2014).

43. Baljuls, A. et al. The tumor suppressor DiRas3 forms a complex with H-Ras and C-RAF proteins and regulates localization, dimerization, and kinase activity of C-RAF. J Biol Chem 287, 23128-23140, doi:10.1074/jbc.M112.343780 (2012).

44. Conte, A. et al. High mobility group A1 protein modulates autophagy in cancer cells. Cell Death Differ 24, 1948-1962, doi:10.1038/cdd.2017.117 (2017).

45. Takaha, N. et al. Expression and role of HMGA1 in renal cell carcinoma. J Urol 187, 2215-2222, doi:10.1016/j.juro.2012.01.069 (2012).

46. Akhter, M. Z. & Rajeswari, M. R. Triplex forming oligonucleotides targeted to hmga1 selectively inhibit its expression and induce apoptosis in human cervical cancer. J Biomol Struct Dyn 35, 689-703, doi:10.1080/07391102.2016.1160257 (2017).

47. Kratzmeier, M., Albig, W., Meergans, T. & Doenecke, D. Changes in the protein pattern of H1 histones associated with apoptotic DNA fragmentation. Biochem J 337 (Pt 2), 319-327 (1999).

48. Happel, N., Doenecke, D., Sekeri-Pataryas, K. E. & Sourlingas, T. G. H1 histone subtype constitution and phosphorylation state of the ageing cell system of human peripheral blood lymphocytes. Exp Gerontol 43, 184-199, doi:10.1016/j.exger.2007.11.008 (2008).

49. Lutz, J. et al. ICOS/B7RP-1 interference in mouse kidney transplantation. Transplantation 84, 223-230, doi:10.1097/01.tp.0000267439.15439.61 (2007).

50. Jiang, T. et al. High expression of B7-H6 in human glioma tissues promotes tumor progression. Oncotarget 8, 37435-37447, doi:10.18632/oncotarget.16391 (2017).

51. Zhang, B. et al. Knockdown of B7H6 inhibits tumor progression in triple-negative breast cancer. Oncol Lett 16, 91-96, doi:10.3892/ol.2018.8689 (2018).

52. Yamagishi, N., Ishihara, K., Saito, Y. & Hatayama, T. Hsp105 family proteins suppress staurosporine-induced apoptosis by inhibiting the translocation of Bax to mitochondria in HeLa cells. Exp Cell Res 312, 3215-3223, doi:10.1016/j.yexcr.2006.06.007 (2006).

53. Zappasodi, R. et al. Serological identification of HSP105 as a novel non-Hodgkin lymphoma therapeutic target. Blood 118, 4421-4430, doi:10.1182/blood-2011-06-364570 (2011).

54. Hosaka, S. et al. Synthetic small interfering RNA targeting heat shock protein 105 induces apoptosis of various cancer cells both in vitro and in vivo. Cancer Sci 97, 623-632, doi:10.1111/j.1349-7006.2006.00217.x (2006).

55. Hatayama, T., Yamagishi, N., Minobe, E. & Sakai, K. Role of hsp105 in protection against stress-induced apoptosis in neuronal PC12 cells. Biochem Biophys Res Commun 288, 528-534, doi:10.1006/bbrc.2001.5802 (2001).

56. Yamagishi, N., Ishihara, K., Saito, Y. & Hatayama, T. Hsp105alpha enhances stress-induced apoptosis but not necrosis in mouse embryonal f9 cells. J Biochem 132, 271-278, doi:10.1093/oxfordjournals.jbchem.a003221 (2002).

57. Ko, S. K. et al. A small molecule inhibitor of ATPase activity of HSP70 induces apoptosis and has antitumor activities. Chem Biol 22, 391-403, doi:10.1016/j.chembiol.2015.02.004 (2015).

58. Kumar, S. et al. Targeting Hsp70: A possible therapy for cancer. Cancer Lett 374, 156-166, doi:10.1016/j.canlet.2016.01.056 (2016).

59. Huang, W. J. et al. Transcriptional upregulation of HSP70-2 by HIF-1 in cancer cells in response to hypoxia. Int J Cancer 124, 298-305, doi:10.1002/ijc.23906 (2009).

60. Kondrikov, D., Fulton, D., Dong, Z. & Su, Y. Heat Shock Protein 70 Prevents Hyperoxia-Induced Disruption of Lung Endothelial Barrier via Caspase-Dependent and AIF-Dependent Pathways. PLoS One 10, e0129343, doi:10.1371/journal.pone.0129343 (2015).

61. Mustafa, N. et al. VS-5584 mediates potent anti-myeloma activity via the upregulation of a class II tumor suppressor gene, RARRES3 and the activation of Bim. Oncotarget 8, 101847-101864, doi:10.18632/oncotarget.21988 (2017).

62. Lotz, K. et al. Suppression of the TIG3 tumor suppressor gene in human ovarian carcinomas is mediated via mitogen-activated kinase-dependent and -independent mechanisms. Int J Cancer 116, 894-902, doi:10.1002/ijc.21127 (2005).

63. Tsai, F. M., Shyu, R. Y. & Jiang, S. Y. RIG1 suppresses Ras activation and induces cellular apoptosis at the Golgi apparatus. Cell Signal 19, 989-999, doi:10.1016/j.cellsig.2006.11.005 (2007).

64. Xu, F. et al. Melanoma differentiation-associated gene 5 is involved in the induction of stress granules and autophagy by protonophore CCCP. Biol Chem 397, 67-74, doi:10.1515/hsz-2015-0195 (2016).

65. Yang, K. et al. Functional RIG-I-like receptors control the survival of mesenchymal stem cells. Cell Death Dis 4, e967, doi:10.1038/cddis.2013.504 (2013).

66. Molineros, J. E. et al. Admixture mapping in lupus identifies multiple functional variants within IFIH1 associated with apoptosis, inflammation, and autoantibody production. PLoS Genet 9, e1003222, doi:10.1371/journal.pgen.1003222 (2013).

67. Besch, R. et al. Proapoptotic signaling induced by RIG-I and MDA-5 results in type I interferon-independent apoptosis in human melanoma cells. J Clin Invest 119, 2399-2411, doi:10.1172/JCI37155 (2009).

68. Lin, L. et al. Activation of Ras/Raf protects cells from melanoma differentiation-associated gene-5-induced apoptosis. Cell Death Differ 13, 1982-1993, doi:10.1038/sj.cdd.4401899 (2006).

69. Liu, W. et al. SGK1 inhibition induces autophagy-dependent apoptosis via the mTOR-Foxo3a pathway. Br J Cancer 117, 1139-1153, doi:10.1038/bjc.2017.293 (2017).

70. Amato, R. et al. IL-2 signals through Sgk1 and inhibits proliferation and apoptosis in kidney cancer cells. J Mol Med (Berl) 85, 707-721, doi:10.1007/s00109-007-0205-2 (2007).

71. Chen, Y., Azad, M. B. & Gibson, S. B. Superoxide is the major reactive oxygen species regulating autophagy. Cell Death And Differentiation 16, 1040, doi:10.1038/cdd.2009.49

https://www.nature.com/articles/cdd200949#supplementary-information (2009).

72. Chen, Y., McMillan-Ward, E., Kong, J., Israels, S. J. & Gibson, S. B. Oxidative stress induces autophagic cell death independent of apoptosis in transformed and cancer cells. Cell Death Differ 15, 171-182, doi:10.1038/sj.cdd.4402233 (2008).

73. Italiano, D., Lena, A. M., Melino, G. & Candi, E. Identification of NCF2/p67phox as a novel p53 target gene. Cell Cycle 11, 4589-4596, doi:10.4161/cc.22853 (2012).

74. Tey, S. K. & Khanna, R. Autophagy mediates transporter associated with antigen processing-independent presentation of viral epitopes through MHC class I pathway. Blood 120, 994-1004, doi:10.1182/blood-2012-01-402404 (2012).

75. Neuzil, J., Dong, L. F., Wang, X. F. & Zingg, J. M. Tocopherol-associated protein-1 accelerates apoptosis induced by alpha-tocopheryl succinate in mesothelioma cells. Biochem Biophys Res Commun 343, 1113-1117, doi:10.1016/j.bbrc.2006.03.052 (2006).

76. Villarroya-Beltri, C., Guerra, S. & Sanchez-Madrid, F. ISGylation - a key to lock the cell gates for preventing the spread of threats. J Cell Sci 130, 2961-2969, doi:10.1242/jcs.205468 (2017).

77. Nakashima, H., Nguyen, T., Goins, W. F. & Chiocca, E. A. Interferon-stimulated gene 15 (ISG15) and ISG15-linked proteins can associate with members of the selective autophagic process, histone deacetylase 6 (HDAC6) and SQSTM1/p62. J Biol Chem 290, 1485-1495, doi:10.1074/jbc.M114.593871 (2015).

78. Zhou, M. J. et al. ISG15 inhibits cancer cell growth and promotes apoptosis. Int J Mol Med 39, 446-452, doi:10.3892/ijmm.2016.2845 (2017).

79. Selleck, E. M. et al. Guanylate-binding protein 1 (Gbp1) contributes to cell-autonomous immunity against Toxoplasma gondii. PLoS Pathog 9, e1003320, doi:10.1371/journal.ppat.1003320 (2013).

80. Smith, E. E. & Malik, H. S. The apolipoprotein L family of programmed cell death and immunity genes rapidly evolved in primates at discrete sites of host-pathogen interactions. Genome Res 19, 850-858, doi:10.1101/gr.085647.108 (2009).

81. Bjorkoy, G. et al. Monitoring autophagic degradation of p62/SQSTM1. Methods Enzymol 452, 181-197, doi:10.1016/S0076-6879(08)03612-4 (2009).

82. Chen, S. et al. Targeting SQSTM1/p62 induces cargo loading failure and converts autophagy to apoptosis via NBK/Bik. Mol Cell Biol 34, 3435-3449, doi:10.1128/MCB.01383-13 (2014).

83. Gomes, A. V. Genetics of proteasome diseases. Scientifica (Cairo) 2013, 637629, doi:10.1155/2013/637629 (2013).

84. Fullgrabe, J., Ghislat, G., Cho, D. H. & Rubinsztein, D. C. Transcriptional regulation of mammalian autophagy at a glance. J Cell Sci 129, 3059-3066, doi:10.1242/jcs.188920 (2016).

85. Xu-Monette, Z. Y. & Young, K. H. The TP53 tumor suppressor and autophagy in malignant lymphoma. Autophagy 8, 842-845, doi:10.4161/auto.19703 (2012).

86. Qi, H. et al. TRAF Family Proteins Regulate Autophagy Dynamics by Modulating AUTOPHAGY PROTEIN6 Stability in Arabidopsis. Plant Cell 29, 890-911, doi:10.1105/tpc.17.00056 (2017).

87. Speiser, D. E. et al. A regulatory role for TRAF1 in antigen-induced apoptosis of T cells. J Exp Med 185, 1777-1783, doi:10.1084/jem.185.10.1777 (1997).

88. Ruckdeschel, K., Mannel, O. & Schrottner, P. Divergence of apoptosis-inducing and preventing signals in bacteria-faced macrophages through myeloid differentiation factor 88 and IL-1 receptor-associated kinase members. J Immunol 168, 4601-4611, doi:10.4049/jimmunol.168.9.4601 (2002).

89. Ai, Z., Lu, Y., Qiu, S. & Fan, Z. Overcoming cisplatin resistance of ovarian cancer cells by targeting HIF-1-regulated cancer metabolism. Cancer Lett 373, 36-44, doi:10.1016/j.canlet.2016.01.009 (2016).

90. Sanchez-Martinez, A. et al. Modeling pathogenic mutations of human twinkle in Drosophila suggests an apoptosis role in response to mitochondrial defects. PLoS One 7, e43954, doi:10.1371/journal.pone.0043954 (2012).

91. Galavotti, S. et al. The autophagy-associated factors DRAM1 and p62 regulate cell migration and invasion in glioblastoma stem cells. Oncogene 32, 699-712, doi:10.1038/onc.2012.111 (2013).

92. Obba, S. et al. The PRKAA1/AMPKalpha1 pathway triggers autophagy during CSF1-induced human monocyte differentiation and is a potential target in CMML. Autophagy 11, 1114-1129, doi:10.1080/15548627.2015.1034406 (2015).

93. Azzam, G., Wang, X., Bell, D. & Murphy, M. E. CSF1 is a novel p53 target gene whose protein product functions in a feed-forward manner to suppress apoptosis and enhance p53-mediated growth arrest. PLoS One 8, e74297, doi:10.1371/journal.pone.0074297 (2013).

94. Lin, X. et al. Targeting autophagy potentiates antitumor activity of Met-TKIs against Met-amplified gastric cancer. Cell Death Dis 10, 139, doi:10.1038/s41419-019-1314-x (2019).

95. Xiao, G. H. et al. Anti-apoptotic signaling by hepatocyte growth factor/Met via the phosphatidylinositol 3-kinase/Akt and mitogen-activated protein kinase pathways. Proc Natl Acad Sci U S A 98, 247-252, doi:10.1073/pnas.011532898 (2001).

96. Wang, G. et al. PIK3R3 induces epithelial-to-mesenchymal transition and promotes metastasis in colorectal cancer. Mol Cancer Ther 13, 1837-1847, doi:10.1158/1535-7163.MCT-14-0049 (2014).

Chapter 6

Interaction between MSCs and Chondrocyte modifies impact of signal modulators

Yao Fu, Sanne Both, and Marcel Karperien

Abstract

In pellet co-cultures of mesenchymal stem cells (MSCs) and primary chondrocytes, MSCs stimulate chondrocyte proliferation and cartilaginous matrix production in a process known as chondro-induction. During this process the MSCs die. Previously we have found evidence that autophagy is the dominant process by which the MSCs disappear from the co-cultures. The significance of MSC cell death in the beneficial effect on cartilage formation in pellet co-cultures is, however, still unclear. In this work, pellet co-cultures were used to investigate the effect of modulators of cell death pathways to obtain more insight in the role of cell death in chondro-induction. Cells were cultured in the starvation environment to analyze the potential activity of cell death pathways in the absence and presence of different signal modulators. The results demonstrated that the starvation environment enhances the activity of autophagy pathway in the monoculture cells, while in co-cultures this effect is reduced. Moreover, interactions between the MSCs and chondrocytes mitigate the impact of signal modulators on the cells in co-cultures. These results suggest that interplay between chondrocytes and MSCs play a beneficial effect on the cellular behavior in the co-cultures, which will contribute to the trophic function of MSCs and further regeneration of cartilage tissue.

6.1 Introduction

Interaction between cells is a crucial component of developmental and physiological functions. Cellular interactions can occur *via* direct cell-to-cell contact, such as by cellular gap junctions that organize cell layers in tissue, or indirectly, as by secreted molecules that bind to receptors expressed on the surface of target cells. The study of cell-cell communication is necessary for both understanding diseases and creating novel biomedical technologies, including immunological interactions, cancer metastasis, stem cell development and so on[1–4].

Understanding the cellular communication pathways and how the cellular interactions are regulated is essential for tissue formation, which could contribute significantly to the engineering of specific tissues *in vitro* and the development of therapies to stimulate tissue repair. However, the mechanisms underlying cellular interaction remain poorly understood, mostly due to the complexity of intercellular communication pathways in multicellular systems, including gap junction signaling, paracrine signaling, endocrine signaling, and synaptic signaling.

Co-culture systems establish an excellent model to study the interaction of heterotypic cell populations. In cartilage tissue engineering, co-culture of primary chondrocytes with Mesenchymal Stromal Cells (MSCs) can potentially overcome many of the problems encountered in basic and clinical applications aimed at restoring a damaged articular cartilage surface, including the dedifferentiation of expanded chondrocytes, hypertrophy of induced MSCs, the limited availability of cartilage cells, and regeneration of both the cartilaginous and osseous layers of osteochondral tissue, thereby potentially improving integration with surrounding tissue[5]. However, the modulation of intercellular interactions in the co-culture system is still unclear. Previously we have shown that in co-cultures of MSCs and primary chondrocytes, the MSCs stimulate chondrocyte proliferation and matrix production while simultaneously these cells die[6,7]. Recently we have found evidence that autophagy is the dominant mechanism for MSC cell death in pellet co-cultures (*Chapter 5*).

There are two major mechanisms driving programmed cell death, namely apoptosis and autophagy. Evidence for both pathways have been found in relation to the death of MSCs in the co-cultures[8,9]. There is an intricate crosstalk network between the signaling pathways leading to activation of both cell death pathways. However, how autophagy and apoptosis are mechanistically interconnected with each other remains unclear and it is also unclear how MSC cell death contributes to or is

involved in chondro-induction. The aim of this study is to address this issue in more detail. Both of these two pathways can be manipulated by external modulators at different stages. In this study, pellet co-cultures were used to investigate the potential activity of apoptosis and autophagy pathways in differentiation medium. Moreover, pellets were also incubated with different external modulators to study how the interaction between cells regulates the response to these modulators of cell death pathways.

6.2 Materials and Methods

6.2.1 Cell culture and expansion

Bovine chondrocytes (bCHs) were isolated from full-thickness cartilage knee biopsies from 6 months old female calves, according to the previously reported protocol[10]. bCHs were expanded in chondrocyte proliferation medium (Dulbecco's modified Eagle's medium (DMEM; Gibco) supplemented with 10% fetal bovine serum (FBS; Gibco), 0.2 mM ascorbic acid 2-phosphate (Sigma), 0.4 mM proline (Sigma),1x nonessential amino acids (Gibco), 100 U/mL penicillin and 100 µg/mL streptomycin (Invitrogen)). Human bone marrow-derived mesenchymal stem cells (hMSCs) were isolated as previously reported[11] and cultured in MSC proliferation medium (α-MEM (Gibco) supplemented with 10% FBS (Gibco), 1% L-glutamine (Gibco), 0.2 mM ASAP (Sigma), 100 U/mL penicillin and 100 µg/mL streptomycin (Invitrogen) and 1 ng/mL bFGF)). The use of human material was approved by a local medical ethical committee. The medium was refreshed twice a week and cells at passage three were used for the experiments.

6.2.2 Cell pellets formation and incubation

To form high-density micromass cell pellets, 200,000 cells per well were seeded in a round-bottom 96-wells plate in the chondrocyte proliferation medium and centrifuged for 3 min at 500×*g* (Supplemental Fig. 6.S1A). For co-cultures, hMSCs and bCHs were mixed at ratios of 80%/20%. Medium was changed to chondrogenic differentiation medium (DMEM supplemented with 0.2 mM ascorbic acid 2-phosphate (Sigma), 0.4 mM proline (Sigma), 100 U/mL penicillin and 100 µg/mL streptomycin (Invitrogen), 0.1 µM dexamethasone (Sigma), 100 µg/mL sodium pyruvate (Sigma), 50 µg/mL insulin–transferrin–selenite (ITS; Sigma), 10 ng/mL transforming growth factor β-3 (TGF-β3; R&D Systems)) one day after seeding when stable pellets were formed.

6.2.3 Modulators incubation

In table 6.1, the modulators of cell death pathways used in this study are listed, including their primary mode of action, their involvement in either autophagy or apoptosis and the concentration at which the compounds were used.

In the first set of experiments, pellets were incubated in chondrogenic differentiation medium with or without Chloroquine (CQ, final concentration at 20 µM, MedChemExpress) in a long-term incubation period. The samples were harvested at the time points of Day 1, 3, 5, and 7.

In the second set of experiments, pellets were incubated in a short-term incubation scenario in the chondrogenic differentiation medium with or without Chloroquine (CQ, final concentration at 20 µM, MedChemExpress), Wortmannin (WM, final concentration at 50 nM, MedChemExpress), Torin1 (final concentration at 250 nM, MedChemExpress), Z-VAD(OMe)-FMK (VAD, final concentration at 20 µM, MedChemExpress), Staurosporine (SS, final concentration at 50 nM, MedChemExpress) as well as with a combination of SS+CQ and Torin1+VAD for 6 hours.

In the third set of experiments, prior to making the co-culture pellets, either the MSCs or the chondrocytes were pre-treated with the signal modulators for 6 hours before mixing with the untreated counterpart cells (Supplemental Fig. 6.S1B). Thereby, two types of co-culture conditions were set up, co-cultures with MSCs pre-treated (Co-MSC+) and co-cultures with CH pre-treated (Co-CH+). After that, pellets were cultured with fresh medium overnight followed by further analysis.

Table 6.1 Modulators treatment details for different experiment setups

Experiment setup	Modulators	Function	Concentration	Incubate period
Set 1	Chloroquine	Autophagy antagonist	20 μM	Up to 7 days
Set 2 and 3	Wortmannin	Autophagy antagonist	50 nM	6 hours
	Chloroquine	Autophagy antagonist	20 μM	
	Torin1	Autophagy agonist	250 nM	
	Z-VAD(OMe)-FMK	Apoptosis antagonist	20 μM	
	Staurosporine	Apoptosis agonist	50 nM	

6.2.4 5-ethynyl-2'-deoxyuridine and TUNEL staining

For labeling of newly synthesized DNA, 5-ethynyl-2'-deoxyuridine (EdU) was added to the culture media at a concentration of 10 mM, 24 h before harvesting the samples. Cell pellets were then washed with phosphate-buffered saline (PBS) and fixed with 10% formalin for 15 min. Samples were embedded in cryomatrix and cut into 10 mM sections with a cryotome (Shandon). Sections were permeabilized and stained for EdU with Click-iT® EdU Imaging Kit (Invitrogen). Cryosections were also stained for DNA fragments with the DeadEnd Fluorometric TUNEL System (Promega). Nuclei were counterstained with Hoechst 33342.

6.2.5 Western blot analysis

Western blotting was performed to assess the presence of LC3B and P62 using protocols adapted from previous studies[12,13]. In brief, all samples were lysed using RIPA buffer (Thermo Fisher) and centrifuged. Protein concentrations were determined by a Pierce BCA protein Assay kit (Thermo Fisher). Equal amounts of

proteins were then separated on gradient (4-15%) Mini-PROTEAN TGX precast gels (Bio-Rad). After electrophoresis, the separated proteins were transferred to PVDF membranes using the Trans-Blot Turbo Transfer System (Bio-Rad). Membranes were blocked with 5% non-fat dry milk in Tris-buffered saline containing 0.1% Tween 20 (TBST, PH 7.5) for 1 hour with gentle shaking. After blocking, membranes were incubated overnight at 4°C with primary antibodies. Antibodies against LC3B (1:5000 dilution, MAB85582, R&D System) as well as SQSTM1/p62 (1:1000 dilution, ab56416, Abcam) were used for analysis. The membranes were then incubated for 1 hour with horseradish peroxidase (HRP)-conjugated goat anti-rabbit IgG or rabbit anti-mouse IgG (1:2000 dilution, Dako) as the secondary antibody. Afterward, immunoreactive bands were developed by the SuperSignal Western Blot Enhancer kit (Thermo Fisher) and visualized with the FluorChem device (ProteinSimple). The expression of β-actin (1:1000 dilution, E7, DSHB) was used as the internal control. Bands were quantified by ImageJ 1.52H software (National Institutes of Health).

6.2.6 Immunofluorescence staining

Pellets were harvested for immunofluorescent staining as previously described[14]. Briefly, cell pellets were washed with PBS and fixed with 10% formalin for 15 min. Samples were then embedded in cryomatrix (Thermo Fisher) and cut into 10 µm sections with a cryotome (Shandon). Sections were permeabilized with 0.5% Triton X-100 in PBS for 10 min at room temperature followed by animal serum treatment (5%, 1 hour, room temperature) to block nonspecific binding. Sections were incubated overnight at 4°C in a humidified chamber with antibodies against LC3B (1:500 dilution, MAB85582, R&D System) and SQSTM1/p62 (1:200 dilution, ab56416, Abcam). Subsequently, slides were washed with 0.1% Tween 20 in PBS and incubated with Alexa Fluor-conjugated secondary antibodies (Alexa 568 or Alexa 488, Abcam) for 50 min at room temperature in a humidified chamber. Nuclei were counterstained with 4,6-diamidino-2-phenylindole (DAPI, Molecular Probes) and images were taken with a fluorescence microscope (Nikon E400).

6.2.7 Statistical analysis

For the experiments using primary human mesenchymal stem cells, three donors were tested, which showed similar results. Each experiment was performed at least in triplicate. So, only data from one representative donor are shown.

Data are presented as mean ± standard deviation. Statistical significance between two groups was analyzed using a Student's *t*-test. For three or more groups, a statistical comparison was made using the One-way Analysis of Variance (ANOVA) with Turkey's *post-hoc* analysis. *p*-value of <0.05 was considered statistically significant.

6.3 Results

6.3.1 The activity of autophagy pathway shows differently in monocultures and co-cultures

Autophagy pathway activity was investigated in the different cell conditions cultured in chondrogenic differentiation medium, representing a starvation environment. The results indicated that monocultures and co-cultures present different autophagic activity in a nutrient-deficient environment. As shown in figure 6.1, during nutrient starvation MSCs showed an up-regulation of an autophagy flux based on the increase in LC3B conversion and the decrease in expression of P62. Interestingly, chondrocyte monocultures responded differently and showed more resistance to nutrient starvation with a marked upregulation of P62 compared to day 1. Compared to monocultures of MSCs the overall protein expression level was quite low. Moreover, all the conditions were also cultured in the presence of the CQ. As shown in figure 6.1, different cell conditions respond distinct to the autophagy inhibitor. In the monoculture condition, CQ presented typical effects on autophagy flux with decreased LC3B conversion and increased P62 expression. The effects were relatively weak in chondrocytes compared to MSCs.

Interestingly, the interaction between MSCs and chondrocytes influences the autophagic activity in the co-cultures. Both LC3B conversion and P62 expression decreased in co-cultures of MSC-Chondrocyte at a 4:1 ratio, an effect which is clearly distinct from the respective pellet monocultures. This suggested that in this time frame autophagy is not fully activated. Furthermore, compared to monocultures, CQ treatment did increase both LC3B and P62 expression, an effect which resembled the monocultures of MSCs rather than of the chondrocytes. According to the quantification results, co-cultures even slightly reduced the protein expression in the presence of CQ.

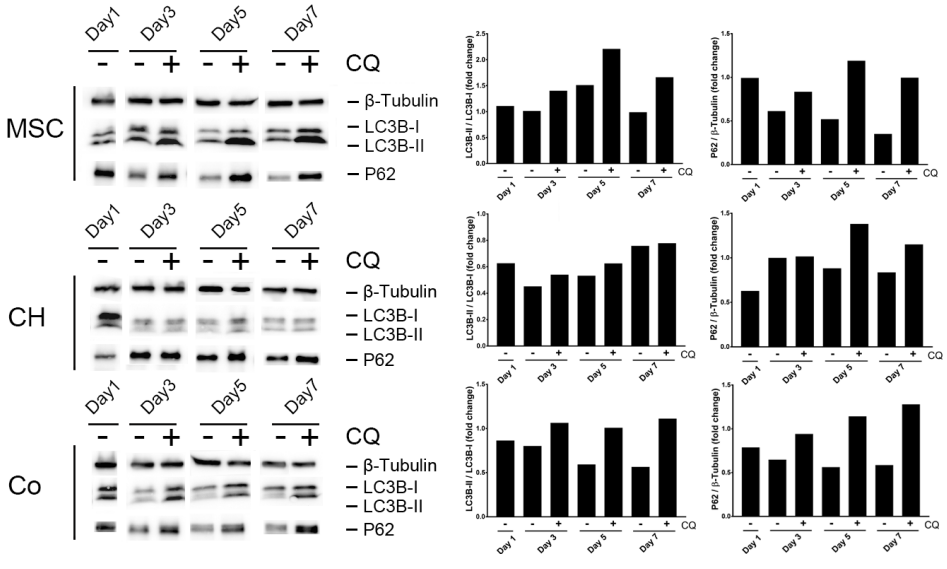

Figure 6.1 *Expression of autophagy markers using Western blot analysis after long-term incubation. Protein expression of LC3B-I, LC3B-II, and P62 in each cell condition in the absence and presence of CQ. β-tubulin is used to normalize the level of proteins among the samples (left panel). Graph of the LCB3-II/ LC3B-I ratio and P62 protein expression after normalization indicating the activity of autophagy (right panel).*

6.3.2 Interactions between cells in the co-cultures enhance cellular behavior

EdU and TUNEL assays were then performed to investigate the overall effect on cell proliferation and death in the different conditions during short-term incubation. As shown in figure 6.2, co-cultures showed clearly beneficial effects on cell proliferation as the overall proliferation in co-culture is higher than the expected values particularly from day 3 onwards. CQ reduced cell proliferation and induced TUNEL positivity in the MSC monoculture. Also, in chondrocyte monoculture, CQ treatment decreased cell proliferation but had only a marginal effect on TUNEL staining. According to the quantification results from TUNEL assay, at day 7, the number of dead cells in the co-cultures in the presence of CQ are less than the expected values, suggesting that the chondrocytes might have a protective effect on TUNEL positivity.

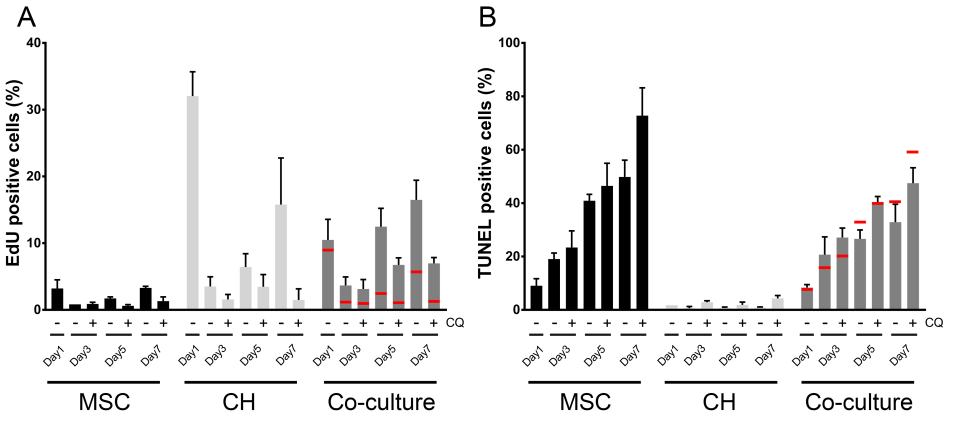

Figure 6.2 *Quantification of EdU-positive (A) and TUNEL-positive (B) cells in each condition culturing in the absence and presence of CQ after long-term incubation. Red lines represent the expected value based on the initial seeding percentage in the co-cultures and is calculated using the formula expected value = 0,8*(EdU or TUNEL MSCs)$_{day\ x}$ + 0,2(EdU or TUNEL pCH)$_{day\ x}$.*

6.3.3 The interplay of cell death pathways in the co-cultures

The above results demonstrated that intercellular communication regulates cellular fate in Chondrocyte-MSC co-cultures and combined cell death pathways involved in the co-cultures in the chondro-induction environment. In the meanwhile, long time treatment of CQ induced high-level cell damage and probably in turn influenced the protein expression. To further investigate the response difference between MSCs and chondrocytes, we exposed the monocultures and co-cultured cells to a panel of external signal modulators in a short-term scenario to check the expression level of autophagy markers. Different cell conditions were cultured in chondrogenic differentiation medium in the presence of all modulators for 6 hours in this section, following overnight incubation in the refreshed medium. Similar to the long-term treatment experiment, starvation induced the autophagy activity in the MSCs while it has rarely an effect on chondrocytes. Moreover, no evident protein expression was observed in the MSC-Chondrocyte co-cultures, no matter whether either MSCs or Chondrocytes were pre-treated. Meanwhile, the autophagy pathway modulators presented typical autophagy regulation effects in the MSCs and chondrocytes monocultures which was not observed in the co-culture conditions. These results, in line with the above observation, indicated that distinct cell types respond differently to the surrounding environment and intercellular interaction in the co-cultures can counteract the activity of the autophagy modulators.

Furthermore, as shown in figure 6.3, this regulatory effect is irrespective of the stimuli and irrespective whether MSCs or Chondrocytes were pre-treated. Meanwhile, the apoptosis pathway presented interplay with the autophagy pathway as LC3B and P62 protein expression was also regulated by the apoptosis modulators. Of note, as an effective apoptosis agonist, Staurosporine strongly promoted the protein expression level of autophagic markers in both MSCs and chondrocytes.

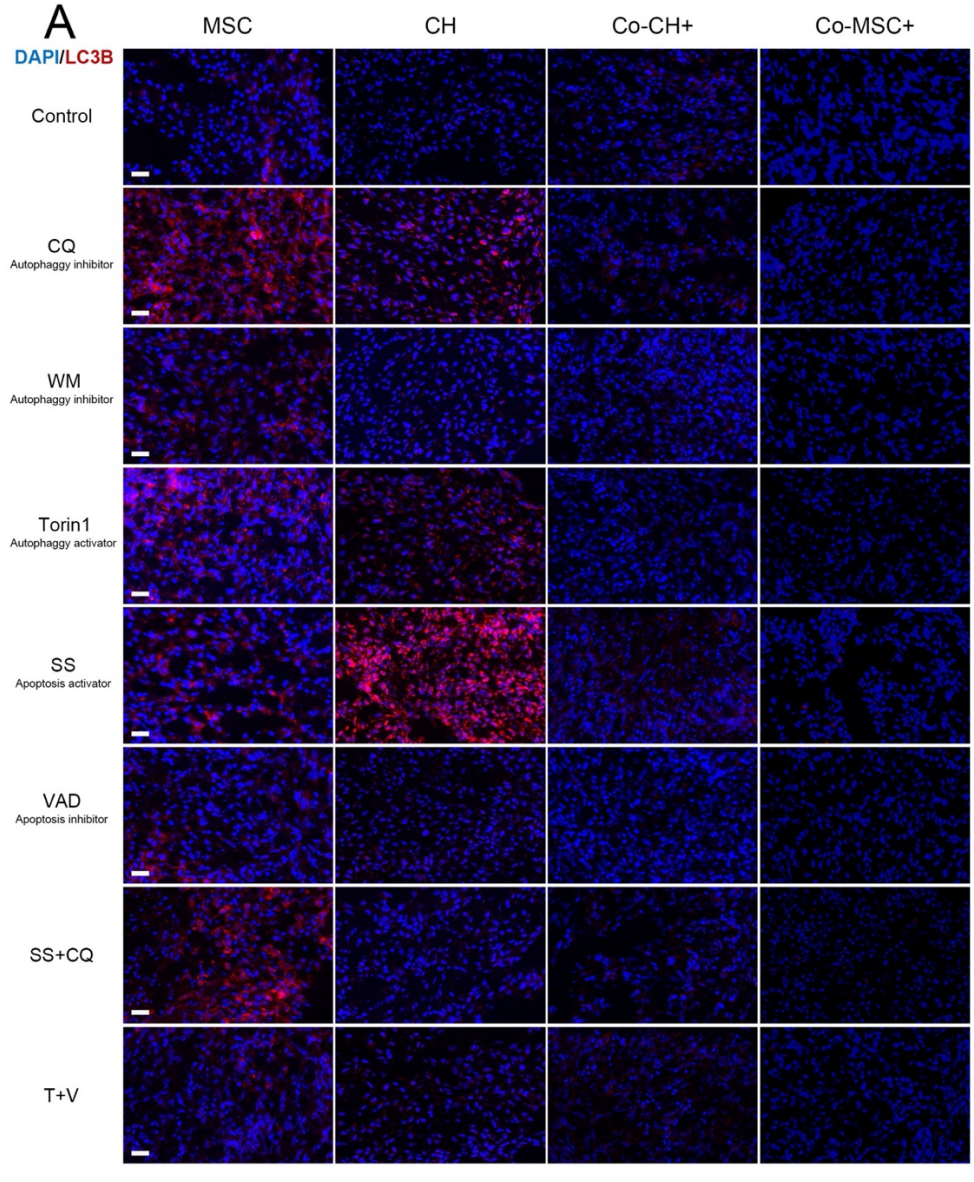

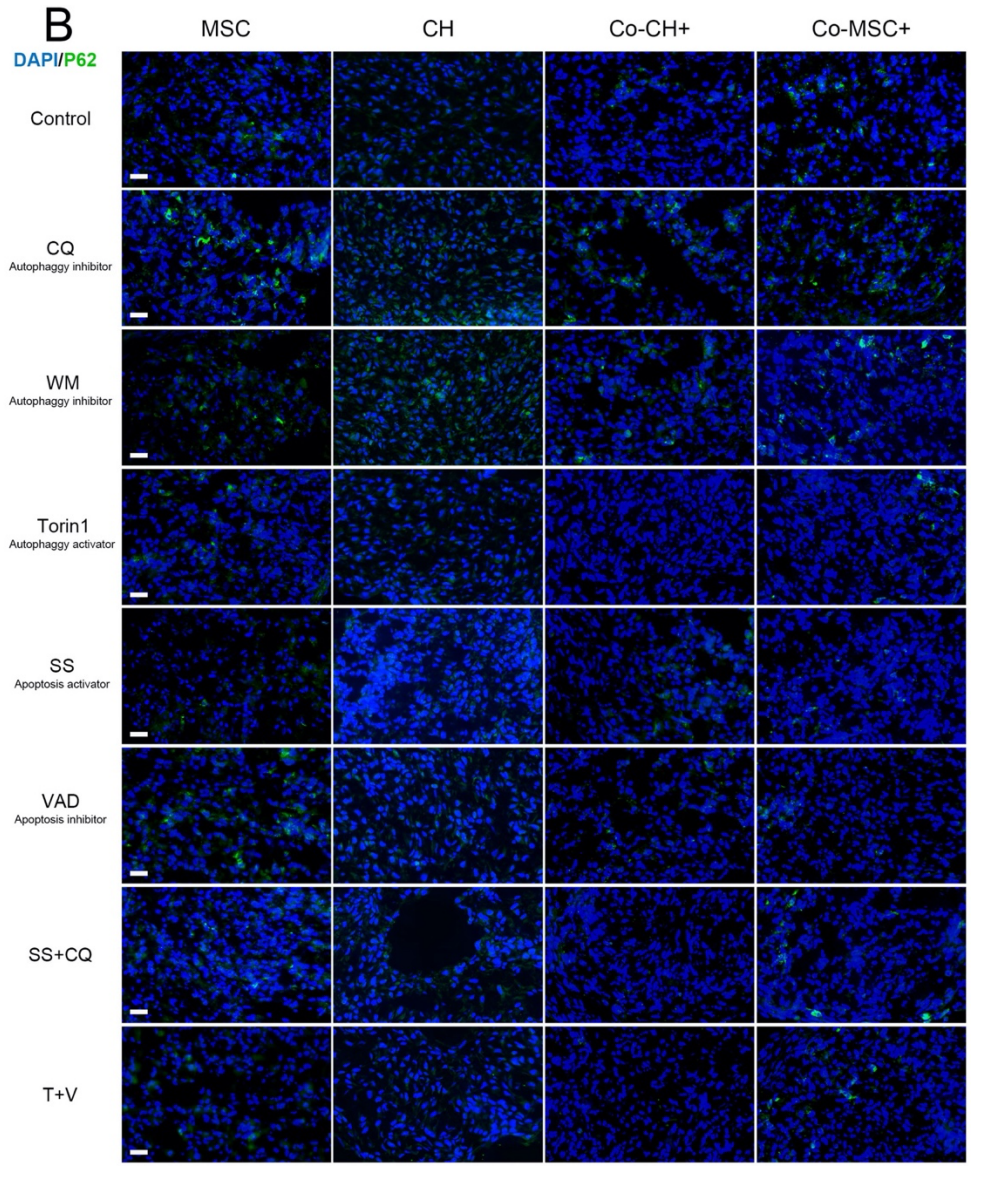

Figure 6.3 *Representative images of immunofluorescent staining of LC3B (A) and P62 (B) puncta. Pellet conditions were cultured in the absence and presence of different signals modulators to show the autophagic flux and interplay between apoptosis and autophagy pathways after short-term incubation. Scale bars represent 25 µm.*

6.3.4 Interaction between cells modifies the response of signal modulators

As shown in figure 6.4, inhibition of the autophagy pathway by CQ and WM increases the cell proliferation of both chondrocyte and MSCs in monoculture. Activation of the autophagy pathway by Torin1 decrease the cell proliferation of MSCs while Torin1 shows less effect on the chondrocyte. For the apoptosis pathway, inhibition of the pathway by VAD increases cell proliferation of chondrocyte and MSCs in monoculture while activation of the apoptosis pathway by SS decreases cell proliferation. Besides, the effects of signal modulators show the opposite direction on TUNEL positivity. Agonists of both death pathways result in an enhancement of overall cell death, while antagonists reduce TUNEL positivity. Remarkably, the pronounced effects on both cell proliferation and TUNEL positivity was blunted in the co-cultures.

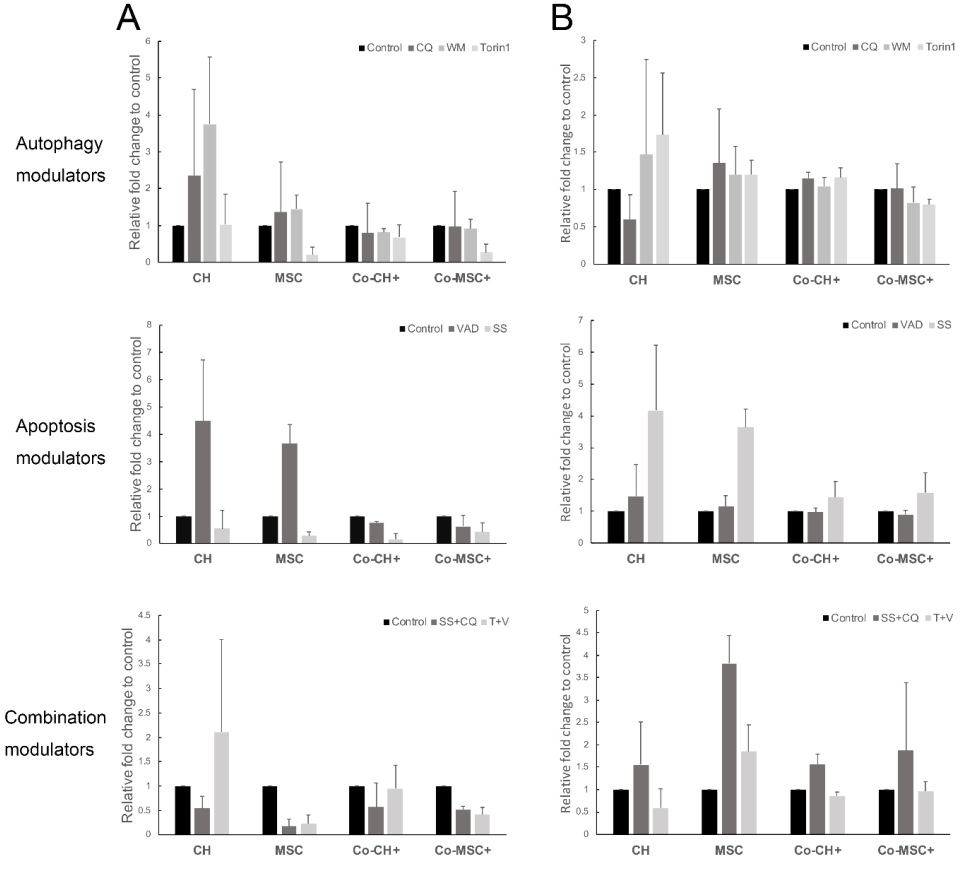

Figure 6.4 *Quantification of EdU-positive (A) and TUNEL-positive (B) cells in each condition cultured in the absence and presence of different signals modulators after short-*

term incubation. Each condition was normalized to the related control group to show the relative fold change.

6.4 Discussion

Cell-cell communication is a crucial component of many biological processes. Cell-to-cell interactions play a vital role in the maintenance of tissue function, regeneration and repair. In this study, we investigated the potential role of cell death pathways in chondro-induction which is observed in pellet co-cultures of MSCs and Chondrocytes using established modulators of either the apoptosis or autophagy pathways. The results showed that the starvation environment induces the activity of autophagy pathway in pellet monocultures, while this effect was mitigated in co-cultures. Moreover, interactions between the MSCs and chondrocytes mitigate the impact of signal modulators on the cells in co-cultures.

The study of cell-cell communication is necessary for understanding many biological functions and diseases. For example, understanding how immune cells and cancer cells interact, both at the immunological synapse and through cytokine secretion, can help us understand and improve cancer immunotherapy. Besides, it forms the basis for a better understanding of cell communications leading to tissue regeneration. Co-culture systems have been established as an indispensable tool for investigating the dynamic interplay between cell populations. Thus, in this work, pellet co-culture systems were used to investigate the potential function and regulation of intercellular communication between the MSCs and chondrocytes.

Our previous work provides evidence that autophagy involved in the cell death of MSCs in pellet co-culture with human chondrocytes under hypoxia (*Chapter 5*). Autophagy, characterized initially as a cytoprotective process initiated upon starvation conditions, underlies various aspects of cellular events by recycling intracellular proteins by lysosomes[15–18]. However, autophagy is now also believed to induce cell death both directly and indirectly[19–21]. In this work, all the pellets start to suffer in starvation since we cultured the cell pellets in the chondrogenic differentiation medium, which is a serum-free environment. Western blot was used to measure autophagic flux in the cells based on LC3B turnover in the absence and presence of autophagy inhibitors[22]. The ratio between LC3-I and LC3-II was then quantified to correlate with autophagy changes, which provide a more accurate measure of autophagic flux[23]. In the meanwhile, the SQSTM1/P62 protein serves as a link between LC3 and ubiquitinated substrates[24]. SQSTM1 and SQSTM1-bound

polyubiquitinated proteins become incorporated into the completed autophagosome and are degraded in autolysosomes, thus serving as an index of autophagic degradation[22]. The inhibition of autophagy correlates with increased levels of SQSTM1, while decreased SQSTM1 levels are associated with autophagy activation[22].

Chloroquine was first used in long-term incubation experiments up to 7 days. CQ can act both as an inhibitor and activator of autophagy. It induces the formation of autophagosomes but blocks their maturation in autophagolysosomes and, hence, is ultimately an inhibitor of autophagy. The results showed that both MSCs and chondrocytes activate the autophagic flux in pellet monocultures, especially in the MSCs while chondrocytes only showed a minor effect. Starvation can induce the activity of the autophagy pathway in the monoculture cells as the autophagic flux can be monitored in the presence of inhibitors. Besides, culturing in the same condition, the activity of pro-autophagic proteins in the MSCs is higher than that in the chondrocytes, suggesting that cells respond differently to the starvation environment. However, contrary to our expectations, co-cultures mitigate the activity of the autophagy pathway as the expression level of LC3B reduced even in the presence of CQ, which suggested a block in autophagy.

Recent studies indicated that apoptosis and autophagy mechanisms are indeed intimately linked while the basis for autophagy influencing cell-fate decisions depends on the death stimulus, cell type, and proteins that are recruited to autophagosomes for lysosomal degradation[25]. Some essential autophagy proteins are targets of caspases, resulting in a reduction of autophagy and an enhancement of apoptosis in the cells[26,27]. Besides, autophagy can also determine whether or not cells die by regulating non-apoptotic cell death directly where there is no need for caspase activation. For example, it was shown that Ras-induced expression of Noxa and Beclin-1 could mediate this autophagic cell death[28]. In this work, culturing in the starvation environment, the reduction of autophagy by the interactions between cells can partly explain the enhanced proliferation in the MSC-Chondrocyte co-cultures, which indicated that autophagy pathway might be involved in the cell proliferation, especially in chondrocytes. Moreover, as shown in the immunofluorescence figures, modulators of the apoptosis pathway can also influence the expression of autophagic markers, suggesting the interplay of these two pathways.

Cellular behavior changes have been detected by the EdU and TUNEL staining to show the cell proliferation and TUNEL positivity in the presence of various pathway modulators during a short-term incubation. These results showed clearly how different cell types respond differently to the stimuli and how the pathway signals regulate cellular fate. Both agonists and antagonists of apoptosis and autophagy pathways present a typical cell behavior regulation effect. However, if we combine MSCs and chondrocyte into the co-culture system, intercellular communication between the cells modifies the response to these signal modulators. This performance is in line with the reduction of autophagy activity and enhanced proliferation in co-cultures. Further studies need to be done to answer some remaining questions. For instance, the specific stimuli and environment that induce autophagy getting more complex, and the functional effect of autophagy on cell death remains unclear. The information transmitted from cells undergoing cell death to neighboring living cells is also warranted further exploration.

Taken together, we have demonstrated that the starvation environment induces the activity of autophagy pathway, but not the apoptosis, in pellet monocultures, while co-cultures mitigate this effect. Interactions between MSCs and chondrocytes modifies the impact of cell death pathway modulators on the cells in the co-cultures.

References

1. Xin, T.; Greco, V.; Myung, P. Hardwiring Stem Cell Communication through Tissue Structure. *Cell* **2016**, *164*, 1212–1225.
2. Malhotra, A.; Shanker, A. NK Cells: Immune Cross-Talk and Therapeutic Implications. *Immunotherapy* **2011**, *3*, 1143–1166.
3. Hennig, S.; Rödel, G.; Ostermann, K. Artificial Cell-Cell Communication as an Emerging Tool in Synthetic Biology Applications. *J. Biol. Eng.* **2015**, *9*, 1–12.
4. Rossello, R. A.; Kohn, D. H. Cell Communication and Tissue Engineering. *Commun. Integr. Biol.* **2010**, *3*, 53–56.
5. Zhang, Y.; Guo, W.; Wang, M.; Hao, C.; Lu, L.; Gao, S.; Zhang, X.; Li, X.; Chen, M.; Li, P. Co-culture Systems-based Strategies for Articular Cartilage Tissue Engineering. *J. Cell. Physiol.* **2018**, *233*, 1940–1951.
6. Wu, L.; Prins, H. J.; Helder, M. N.; Van Blitterswijk, C. A.; Karperien, M. Trophic Effects of Mesenchymal Stem Cells in Chondrocyte Co-Cultures Are Independent of Culture Conditions and Cell Sources. *Tissue Eng. - Part A* **2012**, *18*, 1542–1551. https://doi.org/10.1089/ten.tea.2011.0715.
7. Wu, L.; Leijten, J. C. H.; Georgi, N.; Post, J. N.; Van Blitterswijk, C. A.; Karperien, M. Trophic Effects of Mesenchymal Stem Cells Increase Chondrocyte Proliferation and Matrix Formation. *Tissue Eng. - Part A* **2011**, *17*, 1425–1436. https://doi.org/10.1089/ten.tea.2010.0517.
8. Elmore, S. Apoptosis: A Review of Programmed Cell Death. *Toxicol. Pathol.* **2007**, *35*, 495–516.
9. Levine, B.; Kroemer, G. Autophagy in the Pathogenesis of Disease. *Cell* **2008**, *132*, 27–42.
10. Hendriks, J.; Riesle, J.; Vanblitterswijk, C. A. Effect of Stratified Culture Compared to Confluent Culture in Monolayer on Proliferation and Differentiation of Human Articular Chondrocytes. *Tissue Eng.* **2006**, *12*, 2397–2405.
11. Fernandes, H.; Dechering, K.; Van Someren, E.; Steeghs, I.; Apotheker, M.; Leusink, A.; Bank, R.; Janeczek, K.; Van Blitterswijk, C.; De Boer, J. The Role of Collagen Crosslinking in Differentiation of Human Mesenchymal Stem Cells and MC3T3-E1 Cells. *Tissue Eng. Part A* **2009**, *15*, 3857–3867.
12. Ma, B.; Zhong, L.; van Blitterswijk, C. A.; Post, J. N.; Karperien, M. T Cell Factor 4 Is a Pro-Catabolic and Apoptotic Factor in Human Articular Chondrocytes by Potentiating Nuclear Factor KB Signaling. *J. Biol. Chem.* **2013**, *288*, 17552–17558.
13. Zhong, L.; Schivo, S.; Huang, X.; Leijten, J.; Karperien, M.; Post, J. N. Nitric Oxide Mediates Crosstalk between Interleukin 1β and WNT Signaling in Primary Human Chondrocytes by Reducing DKK1 and FRZB Expression. *Int. J. Mol. Sci.* **2017**, *18*, 2491.
14. Zhong, L.; Huang, X.; Rodrigues, E. D.; Leijten, J. C. H.; Verrips, T.; El Khattabi, M.; Karperien, M.; Post, J. N. Endogenous DKK1 and FRZB Regulate Chondrogenesis and Hypertrophy in Three-Dimensional Cultures of Human Chondrocytes and Human Mesenchymal Stem Cells. *Stem Cells Dev.* **2016**, *25*, 1808–1817.
15. De Duve, C. The Lysosome Turns Fifty. *Nat. Cell Biol.* **2005**, *7*, 847–849.
16. Mindell, J. A. Lysosomal Acidification Mechanisms. *Annu. Rev. Physiol.* **2012**, *74*, 69–86.
17. Forgac, M. Vacuolar ATPases: Rotary Proton Pumps in Physiology and Pathophysiology. *Nat. Rev. Mol. cell Biol.* **2007**, *8*, 917–929.
18. Settembre, C.; Fraldi, A.; Medina, D. L.; Ballabio, A. Signals from the Lysosome: A Control Centre for Cellular Clearance and Energy Metabolism. *Nat. Rev. Mol. cell Biol.* **2013**, *14*, 283–296.
19. Green, D. R.; Galluzzi, L.; Kroemer, G. Mitochondria and the Autophagy–Inflammation–Cell Death Axis in Organismal Aging. *Science (80-.).* **2011**, *333*, 1109–1112.
20. Kroemer, G.; Galluzzi, L.; Vandenabeele, P.; Abrams, J.; Alnemri, E. S.; Baehrecke, E. H.; Blagosklonny, M. V; El-Deiry, W. S.; Golstein, P.; Green, D. R. Classification of Cell Death: Recommendations of the Nomenclature Committee on Cell Death 2009. *Cell death Differ.* **2009**, *16*, 3–11.
21. Green, D. R. The Coming Decade of Cell Death Research: Five Riddles. *Cell* **2019**, *177*, 1094–1107.
22. Klionsky, D. J.; Abdelmohsen, K.; Abe, A.; Abedin, M. J.; Abeliovich, H.; Acevedo Arozena, A.;

Adachi, H.; Adams, C. M.; Adams, P. D.; Adeli, K. Guidelines for the Use and Interpretation of Assays for Monitoring Autophagy. *Autophagy* **2016**, *12*, 1–222.
23. Karim, M. R.; Kanazawa, T.; Daigaku, Y.; Fujimura, S.; Miotto, G.; Kadowaki, M. Cytosolic LC3 Ratio as a Sensitive Index of Macroautophagy in Isolated Rat Hepatocytes and H4-II-E Cells. *Autophagy* **2007**, *3*, 553–560.
24. Bjørkøy, G.; Lamark, T.; Brech, A.; Outzen, H.; Perander, M.; Øvervatn, A.; Stenmark, H.; Johansen, T. P62/SQSTM1 Forms Protein Aggregates Degraded by Autophagy and Has a Protective Effect on Huntingtin-Induced Cell Death. *J. Cell Biol.* **2005**, *171*, 603–614.
25. Fitzwalter, B. E.; Thorburn, A. Recent Insights into Cell Death and Autophagy. *FEBS J.* **2015**, *282*, 4279–4288.
26. Zhu, Y.; Zhao, L.; Liu, L.; Gao, P.; Tian, W.; Wang, X.; Jin, H.; Xu, H.; Chen, Q. Beclin 1 Cleavage by Caspase-3 Inactivates Autophagy and Promotes Apoptosis. *Protein Cell* **2010**, *1*, 468–477.
27. Oral, O.; Oz-Arslan, D.; Itah, Z.; Naghavi, A.; Deveci, R.; Karacali, S.; Gozuacik, D. Cleavage of Atg3 Protein by Caspase-8 Regulates Autophagy during Receptor-Activated Cell Death. *Apoptosis* **2012**, *17*, 810–820.
28. Elgendy, M.; Sheridan, C.; Brumatti, G.; Martin, S. J. Oncogenic Ras-Induced Expression of Noxa and Beclin-1 Promotes Autophagic Cell Death and Limits Clonogenic Survival. *Mol. Cell* **2011**, *42*, 23–35.

6.5 Supplemental Figure

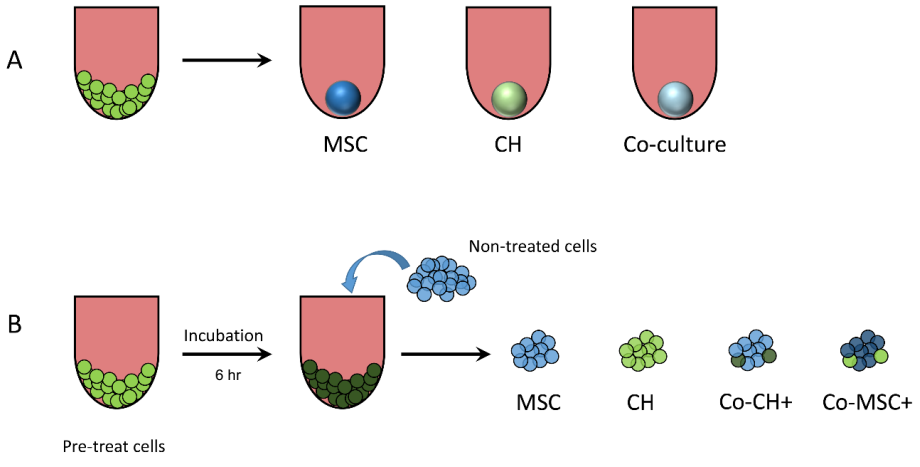

Supplemental Figure 6.S1 *Schematic representation of pellet conditions formation (A) and signal modulators treatments (B).*

Chapter 7

Engineering of optimized hydrogel formulations for cartilage repair

Yao Fu*, Bram Zoetebier*, Sanne Both, Pieter J. Dijkstra, and Marcel Karperien

**Authors equally contributed to this work*

Abstract

The ideal scaffold for cartilage regeneration is expected to provide adequate mechanical strength, has a controlled degradability and provides adhesion, and integration with the surrounding native tissue, while mimicking natural ECMs functions, allowing for nutrient diffusion and promoting cell survival and differentiation. Injectable hydrogels based on tyramine (TA) functionalized hyaluronic acid (HA) and dextran (Dex) are a promising regenerative approach for cartilage repair. The properties of such hydrogels used in this study were adjusted by varying the polymers concentration and ratios. To investigate the changes in properties and their effects on the cellular behavior and cartilage matrix formation, different ratios of HA- and dextran-based hybrid hydrogels at both 5%w/v and 10%w/v were prepared with a designed mold to controll generation. The results indicated that the incorporation of chondrocytes in the hydrogels decreased their mechanical properties. However, rheological and compression analysis indicated that 5%w/v hydrogels laden with cells exhibit a significant increase in the mechanical properties after 21 days when constructs were cultured in chondrogenic differentiation medium. Moreover, compared to 10%w/v hydrogels, the 5%w/v hybrid hydrogels increased the deposition of cartilage matrix, especially in the constructs with a higher Dex-TA content. These results indicate that 5%w/v hybrid hydrogels with 25% HA-TA and 75% Dex-TA have a high potential as an injectable scaffold for cartilage tissue regeneration.

7.1 Introduction

Articular cartilage is a firm and smooth viscoelastic padding of bone ends at the joints to ensure smooth, frictionless and pain-free movemen[1, 2]. Articular cartilage tissue is highly hydrated and consists of approximately of 70% water and 30% extracellular matrix (ECM)[3]. The structure and function of articular cartilage is depends on the molecular composition of its ECM, mainly collagens and proteoglycans[4]. Cartilage has a limited capacity for self-repair due to its avascular nature and the low mitotic activity of chondrocytes[5]. Without proper treatment, damaged articular cartilage will deform, causing chronic pain and joint disability.

Over the past decades, several pharmacological and regenerative therapies have been developed[6]. An ideal scaffold for cartilage regeneration is expected to provide adequate mechanical strength, controlled degradability, adhesion, and integration with the surrounding native tissue. As it does this, it mimicks natural ECMs functions, which allow for nutrient diffusion and the promotion of cell survival and differentiation[7, 8]. It is anticipated that the development of such an effective biomaterial would significantly enhance the potential to develop effective therapies for tissue regeneration and function improvement. One of the promising regenerative therapies is the use of *in situ*-forming (injectable) hydrogels: a three-dimensional (3D) scaffold that mimics the hydrated environment of articular cartilage and facilitates the cell proliferation, differentiation and matrix production by using encapsulated cells[9]. Injectable hydrogels enable a perfect match with irregular cartilage defects and proper alignment with the surrounding tissues[9, 10]. Meanwhile, from the clinical point of view, implantation surgery can be avoided and replaced by a simple minimally invasive injection procedure[9]. Moreover, bioactive molecules or cultured cells can simply be mixed into the hydrogel precursors prior to injection[11]. Therefore, they are promising materials that can function as scaffolds for chondrocyte culture and cartilage regeneration.

The development of injectable hydrogels as scaffolds for cartilage tissue engineering must meet certain essential conditions: bio-compatibility, bio-degradability, bio-functionality, and suitable mechanical strength. In our earlier studies, we developed an injectable hybrid hydrogel composed of a hyaluronic acid (HA) backbone with tyramine conjugated dextran (Dex-TA) sidechains[12]. The hydrogel gelates *in situ* via a biocompatible, enzymatic crosslinking reaction that forms covalent TA-TA bonds and has been shown to support the survival and

growth of the incorporated chondrocytes and mesenchymal stem cells as well as the deposition of a new matrix *in vitro*[13, 14]. Using a similar mechanism, we also showed efficient gel formation after mixing of HA-TA and Dex-TA conjugates[15]. The advantage of these hybrid, injectable hydrogels is that multiple functionalities can be included in one gel system to fine-tune physical properties, proteolytic degradation, and extracellular matrix production. Moreover, these hydrogels can be tailored for stiffness and degradation rate by varying the polymers concentration and ratios. In this study, we determined the optimal concentration and ratio for cell growth and matrix formation in HA-TA and Dex-TA hybrid hydrogels. To obtain these results, hydrogels at different conjugate concentrations and ratios were laden with bovine chondrocytes (bCHs), and the cartilaginous specific matrix formed in the cell/gel constructs over time was analyzed. Furthermore, physical properties like storage moduli and morphology of the hydrogels were examined.

7.2 Materials and Methods

7.2.1 Materials

Dextran (40 kDa, pharmaceutical grade) was purchased from Pharmacosmos, Denmark. Sodium hyaluronate (27 kDa, pharmaceutical grade) was purchased from Contipro Pharma, Czech Republic. Tyramine (99%), DMF (anhydrous, 99.8%), LiCl (99.0%), p-nitrophenyl chloroformate (PNC, 96%), pyridine (anhydrous, 99.8%), DMSO-d6 (99.9%), NaCl (≥99.0%), D2O (99.9 atom % D), horseradish peroxidase (HRP, 325 units/mg solid), and hydrogen peroxide (30%) were purchased from Sigma-Aldrich. Tyramine·HCl salt (99%) was obtained from Acros Organics. 4-(4,6-Dimethoxy-1,3,5-triazin-2-yl)-4-methylmorpholinium Chloride (DMTMM, 97%) was purchased from Fluorochem Ltd. UK. Ethanol (≥99.9%) and Diethyl ether (≥99.7%) were purchased from Merck. Milli-Q water was used from the Milli-Q Advantage A10 system equipped with a 0.22µm Millipak®-40 Express filter.

7.2.2 Synthesis of dextran-tyramine and hyaluronic acid-tyramine

Dextran-tyramine was synthesized by the activation of dextran with PNC and subsequent aminolysis with tyramine adapted from Ramirez *et al.*[16]. Hyaluronic acid-tyramine was prepared by amidation of the carboxyl groups of HA with tyramine, the procedure was adapted from Rydergren[17] and D'Este *et al.*[18]. Detailed description of polymers synthesis can be found in the Supplementary Methods. Synthesis and characterization of Dex-TA and HA-TA polymers are described in

Supplementary Figure 7.S1. The Dex-TA used in this study had a substitution degree of 10%, i.e. 10% of the monosaccharides of dextran have been modified. HA-TA had a substitution degree of 10%, i.e. 10% of the carboxylic acid groups of hyaluronic acid have been modified.

7.2.3 Cell culture and expansion

Bovine chondrocytes (bCHs) were isolated from cartilage knee biopsies of full-thickness from six-month old female calves according to the previously reported protocol[19]. bCHs were expanded in chondrocyte proliferation medium (Dulbecco's modified Eagle's medium (DMEM; Gibco) supplemented with 10% fetal bovine serum (FBS; Gibco), 0.2 mM ascorbic acid 2-phosphate (Sigma), 0.4 mM proline (Sigma),1x nonessential amino acids (Gibco), 100 U/mL penicillin and 100 µg/mL streptomycin (Invitrogen)). The medium was refreshed twice a week, and cells at passage 3 were used for the experiments.

7.2.4 Hydrogel formation

To prepare identical hydrogel samples, we designed a mold (Supplementary Figure 7.S2). In brief, the hydrogels were prepared in a PTFE mold to produce six identical hydrogels of 8 mm diameter and 1.5 mm height. After dissolving the tyramine-conjugated polymers in sterile phosphate buffered saline (PBS), the polymer solution with horseradish peroxidase (HRP, 40units/mL; Sigma-Aldrich) was incubated overnight at 4°C on a roller bank. The mixture was then combined with bCHs in a concentration of 10 million cells/mL. Cell free controls were also prepared. Freshly prepared hydrogen peroxide (H_2O_2) was added to the mixture and immediately transferred to the mold using a 1 mL pipette after a brief vortex. The final gel concentrations were a 10%w/v or 5%w/v polymer, 10 million/mL bCHs, 4 U/mL HRP and 0.03% H_2O_2 (for 10%w/v polymer) or 0.015% H_2O_2 (for 5%w/v polymer). HA-TA and Dex-TA were combined in 5 ratios (100:0, 75:25, 50:50, 25:75, and 0:100, represented by groups A, B, C, D, and E respectively).

7.2.5 Hydrogel incubation

After gelation, the gels were transferred to six-well plates and incubated in chondrogenic differentiation medium (DMEM supplemented with 0.2 mM ascorbic acid 2-phosphate (Sigma), 0.4 mM proline (Sigma), 100 U/mL penicillin and 100 µg/mL streptomycin (Invitrogen), 0.1 µM dexamethasone (Sigma), 100 µg/mL sodium pyruvate (Sigma), 50 µg/mL insulin-transferrin-selenite (ITS; Sigma), 10 ng/mL transforming growth factor β-3 (TGF-β3; R&D Systems)). The medium was

refreshed three times every week, and the gels were harvested at the time points of Day 0, 7, and 21.

7.2.6 Rheological analysis

Rheological experiments were carried out using an MCR301 rheometer (Anton Paar) using parallel plates (8 mm diameter) at 20°C under a 0.05N normal force in the oscillatory mode with 0.5% strain and 1.0 Hz, which was in the LVE range according to the measured frequency and strain sweeps. The cylindrical hydrogels were prepared in 8 mm wide, 1.5 mm high molds and measured after equilibrating overnight in medium. At least three specimens were tested for each sample.

7.2.7 Hydrogel Swelling Ratio

The swelling ratio was based on the weight of the hydrogel samples:

$$Swelling\ ratio = \frac{w_{wet} - w_{dry}}{w_{dry}} \quad (1)$$

To assess swelling, the hydrogels were measured after equilibrating overnight in medium and compared to their dry weight. At least three specimens were tested for each composition.

7.2.8 Compression tests

Compression testing was performed on the cylindrical gels as prepared and equilibrated for the rheological testing using a Texture Analyser TA-HD plus (StableMicro Systems Ltd., Surrey, UK) fitted with a 50 kg load cell. The hydrogels underwent three compression cycles with a maximum strain of 50% using a compression speed of 0.05 mm/s. The compression tests were conducted at room temperature, and at least three specimens were tested for each sample.

The following data was derived from the stress-strain curves. Maximum stress is the stress needed to compress the sample until 50% strain is reached. The high strain compressive modulus was calculated from the stress-strain curves using a linear slope at a strain ranging from 40 to 49.5%. The percentage of energy dissipated during a compression-relaxation cycle was calculated by dividing the surface of the hysteresis loop by the surface under the compression trace.

7.2.9 Histology and Immunohistochemistry staining

The samples were fixed in 10% formalin and then incubated in OCT (Thermo-scientific) overnight at 4°C. The samples embedded in OCT were then snap frozen

using liquid nitrogen. Cryosections of 10 µm were cut using cryotome (Leica CM1100) and stained for sulfated glycosaminoglycan (GAG) with Alcian blue and Safranin O staining. For immunohistochemistry, cryosections were incubated with 0.3% H_2O_2 and blocked in 5% bovine serum albumin. Slides were subsequently incubated overnight at 4°C with a rabbit polyclonal antibody against COL II (Abcam). The sections were then incubated with polyclonal goat-anti-rabbit HRP-conjugated secondary antibody (Dako), followed by development with the DAB Substrate kit (Abcam). Counterstaining was performed with hematoxylin. Non-immune controls underwent the same procedure without primary antibody incubation. Both histology and immunohistochemistry stained slides were scanned with the NanoZoomer 2.0-RS slide scanner (Hamamatsu).

7.2.10 Live-dead staining

The effect of the hydrogel's composition on cell viability was studied using a Live-dead assay. At day 0 and 21, the hydrogel constructs were rinsed with PBS and stained with calcein AM/ethidium homodimer using the Live-dead assay Kit (Invitrogen), according to the manufacturer's instructions. Hydrogel/cell constructs were visualized using fluorescence microscopy (Leica DM IRB) and different areas were randomly selected. As a result, living cells fluoresce green and the nuclei of dead cells red. Image J software was used for cell counting. The cell viability was calculated by the percentage of live cells (green) in the total cells (green + red) from each area. Values represent the mean +/− standard deviation of at least three biological replicates.

7.2.11 RNA isolation and quantitative polymerase chain reaction

The 5%w/v hydrogels were prepared for species-specific quantitative polymerase chain reaction (qPCR) analysis. At day 0 and day 21, hydrogel samples were first homogenized by gentleMACS Dissociator according to the manufacturer's instructions (Miltenyi Biotec). Total RNA was then isolated with the TRIzol Reagent (Ambion) according to the manufacturer's protocol and reverse-transcribed into cDNA using the iScript cDNA Synthesis kit (Bio-Rad). qPCR was performed on cDNA samples by using the SensiMix SYBR& Fluorescein Kit (Bio-Rad). PCR reactions were carried out on CFX Connect™ Real-Time PCR Detection System (Bio-Rad). cDNA was denatured at 95°C for 10min followed by 40 cycles. Each cycle consisted of following conditions: 15s at 95°C, 15s at 60°C, and 30s at 72°C. The sequence of primers for qPCR are listed in Table 7.1. The expression level of

aggrecan (*ACAN*), collagen type I, II and IX (*COL1*, *COL2*, and *COL9*) and Osteopontin (*OPN*) were investigated.

Table 7.1 Primers used for quantitative RT-PCR

Gene Name	Primer Sequence	Product size (bp)
Bovine specific GAPDH	F: 5' GCCATCACTGCCACCCAGAA 3' R: 5' GCGGCAGGTCAGATCCACAA 3'	207
Bovine specific Aggrecan	F: 5' GACCAGAAGCTGTGCGAGGA 3' R: 5' GCCAGATCATCACCACACAG 3'	319
Bovine specific Collagen II	F: 5' ATCAACGGTGGCTTCCACT 3' R: 5' TTCGTGCAGCCATCCTTCAG 3'	263
Bovine specific Collagen IX	F: 5' GGACTCAACACGGGTCCACA 3' R: 5' ACAGGTCCAGCAGGGCTTTG 3'	102
Bovine specific Collagen I	F: 5' GCGGCTACGACTTGAGCTTC 3' R: 5' CACGGTCACGGACCACATTG 3'	102
Bovine specific Osteopontin	F: 5' ACTGGACTCTTCTCGCCGCC 3' R: 5' CGGAGGCAATGCCCAAGAGGC 3'	90

7

7.2.12 Statistical analysis

Data were presented as mean ± standard deviation. Statistical significance between two groups was analyzed using a Student's *t*-test. For three or more groups, a statistical comparison was done using the One-way Analysis of Variance (ANOVA) with Turkey's *post-hoc* analysis. *P*-value of <0.05 was considered statistically significant.

7.3 Results

7.3.1 Hydrogel formation and morphology

In this study, the hydrogels were formed by dissolving the functionalized polymers (Dex-TA DS10% and HA-TA DS10%) and HRP in PBS (mixed with cells where desired) and adding minute quantities of H_2O_2 as an oxidizing agent. Upon the addition of H_2O_2, the crosslinking of tyramine was initiated. Precooling the

solutions on ice and using a final concentration of 4.0 U/mL, HRP gave us a working time (*i.e.* gelation time) of about 30 sec, after which the solution gelated in the mold. The quantity of H_2O_2 was adapted to the molar amount of tyramine groups, ensuring the complete consumption of the oxidizing agent in all conditions within the different weight concentrations. The overview figures of the hydrogels (shown in Supplementary Figure 7.S3) reveal that the size of the hydrogels decreased after the dextran concentration was increased from 0 to 100%. Both the hydrogels with and without cells show the same trend; however, the addition of cells increased the gel size.

7.3.2 Cell viability of chondrocytes in different hydrogels

Cell viability of the bovine chondrocytes in the hydrogels was evaluated using a live-dead assay, in which living cells stained green and dead cells stained red (Fig. 7.1a). We counted the amount of alive and dead cells and calculated the percentage of live cells (Fig. 7.1b and 1c). The results showed that the chondrocytes were distributed homogeneously inside hydrogels, and over 90% of the cells remained viable in most of the conditions at day 0. After 21 days of culturing in the chondrogenic medium, as shown in the figure, chondrocytes maintained their characteristic round shapes, while the cell viability decreased in all conditions over time. Groups B and C (75%:25% and 50%:50% HA-TA: Dex:TA, respectively) show greater cell viability than under other conditions in both 5%w/v and 10%w/v hydrogels. Meanwhile, groups D and E, which had a higher dextran concentration, presented lower cell viability in 5%w/v conditions compared to that in 10%w/v, especially in pure dextran hydrogels (group E). On the other hand, the other groups show similar cell viability between 5%w/v and 10%w/v hydrogels. However, after 21 days, there is still around 70% to 90% cell survival, indicating that these biomimetic hydrogels could provide a supportive environment for chondrocyte proliferation and differentiation as well as matrix deposition.

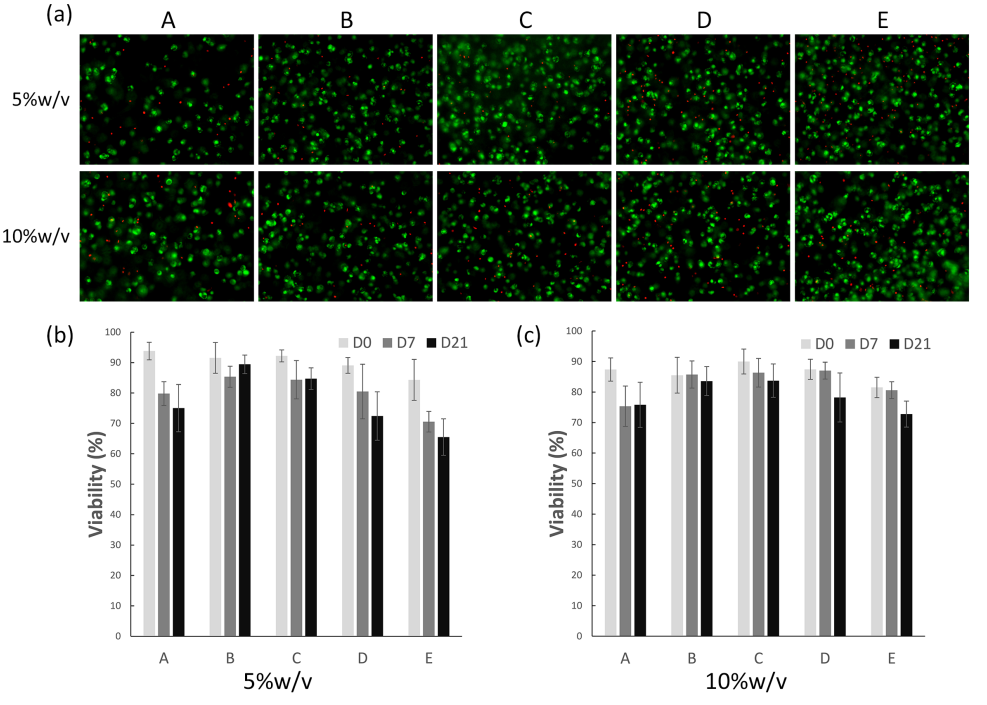

Figure 7.1 *Representative figures show live/dead staining of 5%w/v and 10%w/v hydrogels encapsulated with chondrocytes after culturing for 21 days in the chondrogenic medium (a). Condition A to E represent different mix ratios of HA and Dex (100:0, 75:25, 50:50, 25:75, 0:100). Cell viability was then quantified based on the live/dead staining figures of 5%w/v (b) and 10%w/v (c) hydrogels at Day 0, 7 and 21.*

7.3.3 Mechanical properties

The rheological properties and equilibrium swelling of the hydrogels on day 0 are shown in Figure 7.2. As expected, increasing the polymer concentration of the hydrogels increased the storage modulus. Similarly, the equilibrium swelling ratio of the constructs with a lower polymer concentration was higher than for those with higher polymer concentration. The inclusion of cells in our hydrogel constructs generally decreased the storage modulus and increased the swelling of the hydrogels, suggesting the decrease of crosslink density for these constructs. The average decrease in crosslink density was calculated to be 40% upon inclusion of cells. The calculations were based on the classical rubber elasticity theory and are provided in the Supplementary information (Table 7.S1 and Equation (S1)).

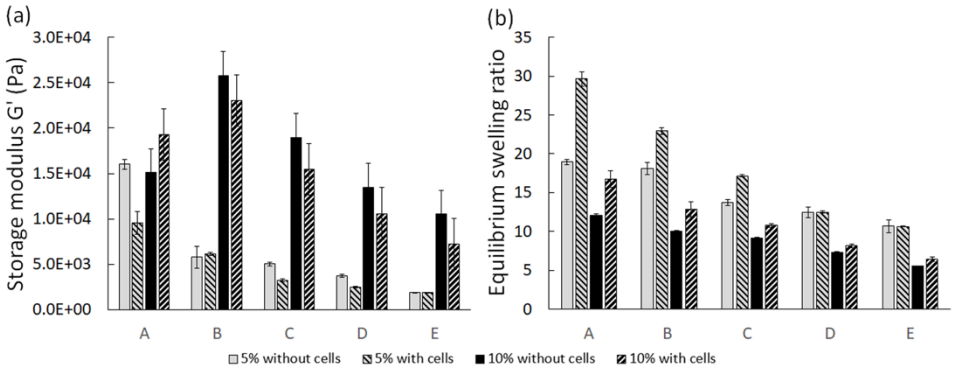

Figure 7.2 *Rheological properties (a) and equilibrium swelling (b) of the hydrogels on day 0. A to E represent different mix ratios of HA:Dex (100:0, 75:25, 50:50, 25:75, 0:100).*

The mechanical properties of the hydrogels were measured after 7 and 21 days of incubation in chondrogenic differentiation medium. Although the hydrogels with cells are weaker, upon culturing they become stronger and more elastic. After 21 days, we saw an increase in the storage modulus measured by rheology, which indicated that the hydrogel could store more deformation energy in an elastic manner that it could on day 0 and day 7. It would indicate an increase in network density, which is related to the deposition of cartilage ECM proteins as confirmed by histology. This increase in storage modulus was most prominent for 5%w/v hydrogels, indicating that the weaker, more open structure of the hydrogel is preferred for the deposition of cartilaginous matrix (Figure 7.3 a1-a4). This observation was confirmed by texture analysis showing that the maximum pressure needed to compress the hydrogels to 50% strain (Figure 7.3 b1-b4) and the E-modulus under high strain (Figure 7.3 c1-c4) were increased in the 5%w/v hydrogels. Next to that, the elasticity of the hydrogels was also increased after 21 days, which we derived by the hysteresis in the stress-strain curves recorded (Figure 7.3 d1-d4).

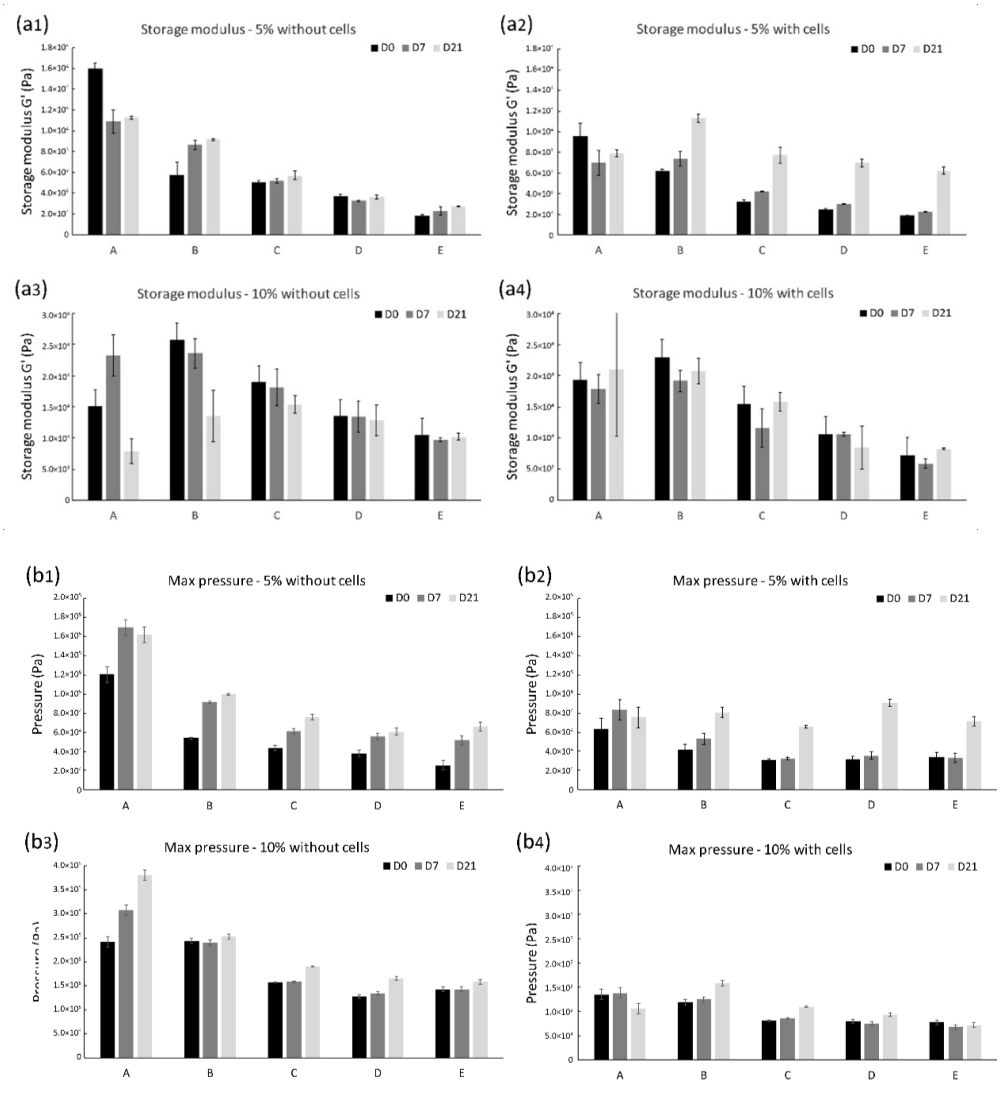

Figure 7.3 *Cont*

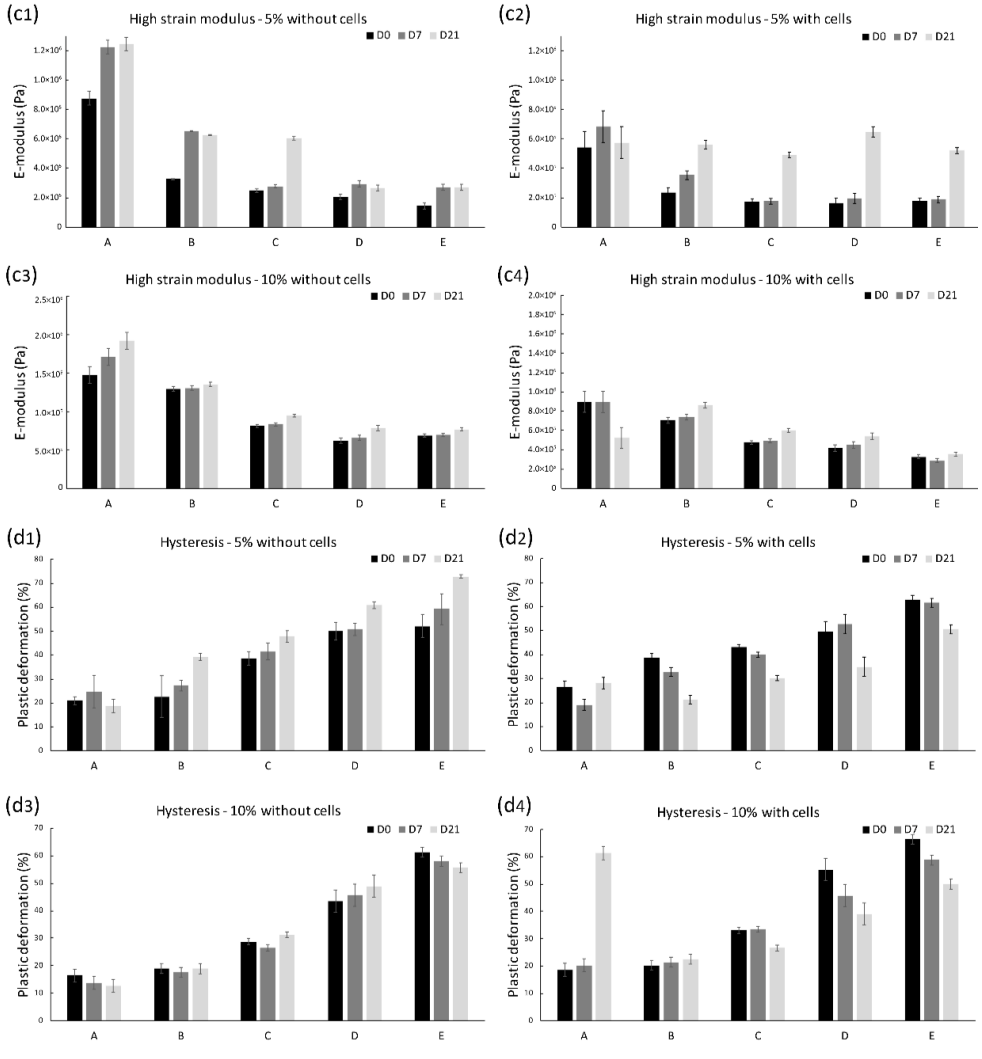

Figure 7.3 *Mechanical properties of the hydrogels after 0, 7, and 21 days of culture. Conditions A to E represent different ratios of HA and Dex (100:0, 75:25, 50:50, 25:75, 0:100).* ***(a1-a4)*** *the storage modulus of the hydrogels,* ***(b1-b4)*** *the pressure needed for 50% deformation of the hydrogels,* ***(c1-c4)*** *the high strain Young's modulus of the hydrogels,* ***(d1-d4)*** *the elasticity of hydrogels.*

7.3.4 Higher Dextran concentration of hydrogels enhanced matrix deposition

GAG production by chondrocytes in all conditions was examined by histology using Safranin O staining (Supplementary Fig. 7.S4, only Day 21 Safranin O staining results are shown). The staining results of HA hydrogel without cells showed that pure HA gel is stained by the dyes as expected (data not shown), which indicate that histology staining is not specific enough to distinguish the matrix production in these hydrogels. Nonetheless, histological staining supported that the chondrocytes incorporated in these hydrogels produced abundant ECM rich in GAGs after 21 days, as confirmed by the dense GAG staining in these gels. These results demonstrated that the incorporation of HA would improve the performance of Dex-TA gels in cartilage tissue engineering and that 5%w/v hydrogels show better matrix production than did 10%w/v hydrogels.

Collagen type II is the primary type of collagen present in articular cartilage[20]. Consequently, we performed immunohistochemistry staining to detect the specific production of collagen type II (Fig. 7.4 and Supplementary Fig. 7.S5). After 21 days, cartilage matrix was deposited inside different hydrogel conditions. Moreover, it is clearly shown that 5%w/v hybrid hydrogels encapsulated with chondrocytes exhibited greater deposition of type II collagen than the 10%w/v groups did. Besides, the condition that was composed of 25% HA and 75% dextran (condition D) displayed the most intense staining of all the 5%w/v hybrid hydrogels. The histochemical analysis also reveals that the cartilage matrix formation is more dominant at the periphery of the hydrogels, especially in hydrogels of 10%w/v groups.

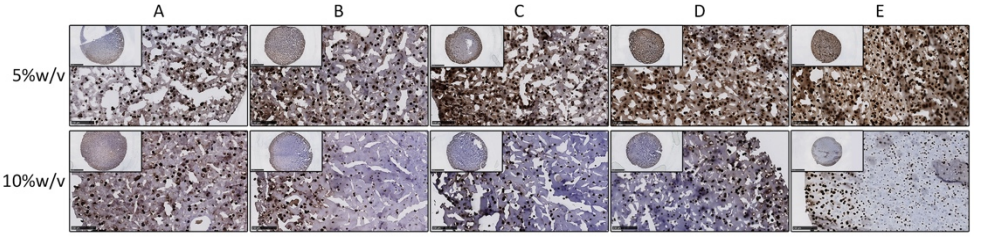

Figure 7.4 *Immunohistochemistry staining of collagen type II for 5%w/v and 10%w/v hydrogels encapsulated with chondrocytes after culturing for 21 days in chondrogenic medium. From condition A to E represent the different conditions with different mix ratio of HA and Dex (100:0, 75:25, 50:50, 25:75, 0:100). Inserts indicate the overview of each hydrogel; scale bar = 2.5 mm. Pictures show the magnified view of each hydrogel; scale bar = 250 μm.*

Next, we performed qPCR to study the mRNA expression of chondrogenic genes in 5%w/v hydrogels combined with bCHs that were cultured in the chondrogenic differentiation medium for 21 days. The histochemical results were corroborated by gene expression analysis (Fig. 7.5). The relative fold expression of chondrogenic related genes such as *ACAN*, *COL2A1*, and *COL9A1* was up-regulated in hydrogels containing higher Dextran concentration (Fig. 7.5a to 5c). The expression of *SOX9* was also measured in this study, which showed a similar trend as these genes (data not shown). However, the overall mRNA expression level of *SOX9* remained low in all conditions. Additionally, a decrease in the expression of *COL1A1* and *OPN* in conditions with a higher dextran content was observed compared to the pure HA group (Fig. 7.5d and 5e).

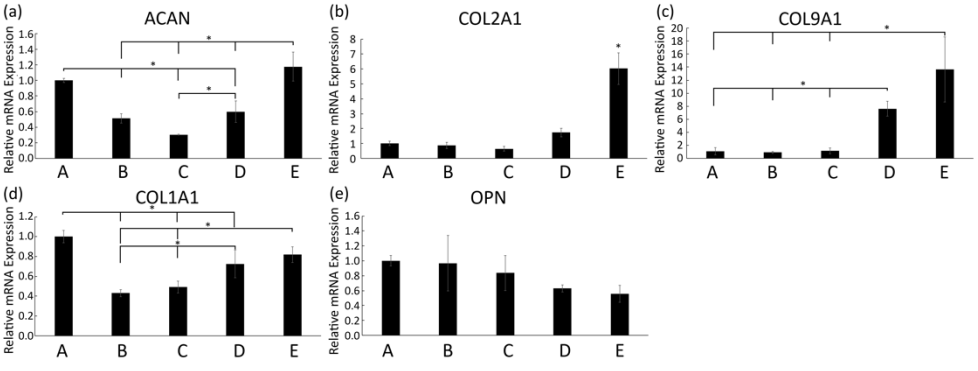

Figure 7.5 *Relative mRNA expression levels for ACAN (a), COL2A1 (b), COL9A1 (c), COL1A1 (d), and OPN (e), expressed by bovine chondrocytes incorporated into 5%w/v hydrogels, after 21 days in culturing in the chondrogenic medium. Assignments A to E represent the different conditions with different mix ratio of HA:Dex (100:0, 75:25, 50:50, 25:75, 0:100). Error bars reflect SD and * represents $p < 0.05$ compared to other indicated conditions.*

7.4 Discussion

In this work, different ratios of HA and dextran-based hybrid hydrogels at both 10%w/v and 5%w/v were prepared with a mold to determine physical property changes and their effects on the cellular behavior and cartilage matrix formation. Our results indicated that the incorporation of chondrocytes in the hydrogels introduced soft pockets in the hydrogel matrix, which decreased their mechanical properties on a macroscopic level. Interestingly, the rheological and compression analysis indicated that 5%w/v hydrogels laden with cells showed a significant

increase in the mechanical properties after culturing for 21 days. Moreover, compared to 10%w/v hydrogels, the 5%w/v hybrid hydrogels showed enhanced deposition of cartilage matrix, especially in the constructs with higher Dex-TA concentrations.

The chondrocytes encapsulated inside hydrogels retained a round shape at 21 days in culture. However, compared to previously reported HA-*g*-Dex-TA hydrogels, hydrogels in this study showed decreased cell viability[12], which can be firstly explained by the difference in measured time points. Initially, over 90% of the incorporated cells were alive, demonstrating the cytocompatibility of the hybrid hydrogels. Decreased cell viability after 21 days could also be explained by the procedure of hydrogel formation. To make sure all components were incorporated homogeneously, the solution was mixed by vortexing after the addition of H_2O_2. The shear forces during vortexing could damage the incorporated cells. Further studies need to address the force effect on the cells and determine the proper vortexing speed. Moreover, the relatively low cell viability observed for the Dex-TA hydrogel may be attributed to the increasing crosslinking density of the constructs. The limited exchange of nutrients and waste products to the surrounding culture media can reduce cell viability[21].

With the help of the mold we designed, highly controlled cylindrical hydrogels were formed by dissolving the polymers and HRP in PBS and adding H_2O_2 as an oxidizing agent. Compared to pure hydrogels without cells, the inclusion of cells increased the hydrogel swelling, which could have indicated a decrease incrosslink density for these constructs. The increased size of hydrogels with higher HA concentration can be explained by an increase in water uptake resulting from the electrostatic repulsion of negatively charged HA chains at pH 7.4[12]. This swelling behavior also suggests a decrease in network density as a result of degradation[22]. HA is an essential component of the ECM in cartilage tissue, which is biodegradable *via* enzymatic hydrolysis using hyaluronidase (HAse)[23, 24]. HA degraded by the HAse expressed by the incorporated chondrocytes in the hybrid hydrogels could have been another reason for this behavior[25].

In the design of hydrogels as scaffolds for cartilage repair, adequate mechanical support is a critical requirement. The scaffold should be mechanically stable in order to protect the seeded cells and the developing tissue and to withstand the physiologic load[26]. On a cellular scale, the mechanical properties of a scaffold are potent regulators of cell migration and their phenotypes[27]. The mechanical properties of

the studied hydrogels could be adjusted by varying the ratio of dextran and hyaluronic acid and the polymer concentration. The evaluation of these properties is an essential parameter in predicting the possibility in tissue production and construct quality. Rheological studies on the constructs were performed to determine storage and loss moduli, which are values for elasticity and viscosity respectively[28]. Compression of cylindrical hydrogel samples between two plates yields a stress-strain curve, from which the elastic modulus and other mechanical properties can be derived[29]. Therefore, physical properties were determined by rheology and texture analysis at different time points to investigate how gel composition and mechanical properties could influence the cell behavior and how the cells consequently would influence the hydrogel characteristics.

In line with the previous report, increasing the polymer concentration in the hydrogels increased the storage modulus because hydrogels prepared at a concentration of 10%w/v showed higher storage modulus compared to 5%w/v hydrogels. Furthermore, by encapsulating the chondrocytes, the corresponding storage modulus *G'* values decreased, suggesting the decrease of crosslink density of these constructs.

However, upon culturing in differentiation medium for 21 days, these gels become stronger and more elastic. Compared to pure gels without cells, chondrocytes laden constructs showed enhanced storage moduli after 21 days. Especially in cell laden 5%w/v hydrogels, a significantly increased storage modulus was observed in rheological measurements. This improvement was most evident in constructs with higher Dex-TA concentration. However, the 10%w/v hydrogels showed only moderate changes compare to the initial values. This observation was confirmed by the rheological analysis. Previous reports indicated that the compressive modulus for articular cartilage is 0.24 to 0.85 MPa[30] which is substantially higher than the compressive modulus, which was obtained after three weeks of culture of the hydrogel constructs. The compressive modulus of the latter constructs approached the mechanical properties of the chondron which has a modulus of around 70 kPa[31]. This suggested that in 21 days of being cultured the chondrocytes created an environment that resembled at least some of the properties of the native chondron. These results also suggested that the increased network density in the hydrogels is related to ECM deposition and that the 5%w/v hydrogels, which are weaker and have a more open structure, were preferred for the deposition of cartilaginous matrix. Furthermore, a higher Dex-TA concentration was shown to promote this.

This hypothesis was confirmed by the cartilage matrix-related staining. Compared to day 0 constructs, abundant deposition of cartilage matrix was observed inside different hydrogel conditions after 21 days, which can partly explain the increased stiffness and elasticity of the cell-laden hydrogels. Interestingly, it was clearly shown that 5%w/v hybrid hydrogels laden with chondrocytes exhibited a denser deposition of cartilage matrix compared to the 10%w/v constructs. These data were consistent with the significantly increased mechanical properties in 5%w/v hydrogels from rheology and compression analysis. It was likely caused by greater diffusion of nutrients and growth factors in the 5%w/v hydrogels than in the 10%w/v hydrogels since 10%w/v hydrogels showed higher mechanical strength, which is known to compromise diffusion capability[32]. Besides, a higher polymer concentration also resulted in a decreased accumulation of matrix components such as proteoglycans and collagen type II[33]. Indeed, in 10%w/v hydrogels, the formation of cartilage matrix was dominantly observed at the periphery of the hydrogels.

Moreover, 5%w/v hybrid hydrogels with a higher Dex-TA content produced an abundant, homogeneously distributed cartilage matrix, which was corroborated by the up-regulated expression of chondrogenic related genes. Considering that HA is present in native cartilage and plays a role in influencing the cell phenotype and matrix production[34, 35], incorporation of HA in hybrid hydrogel would improve the performance of hybrid hydrogels in cartilage tissue engineering. Concludingly, these results indicated that 5%w/v hydrogels showed better matrix production than 10%w/v hydrogels and that a combination of 25% HA and 75% Dex is probably the optimal hybrid condition for cell growth and matrix formation.

In summary, we prepared different ratios of HA and dextran-based hybrid hydrogels of controlled size and shape at both 10%w/v and 5%w/v using a designed mold. The behavior of chondrocytes incorporated in the hybrid hydrogels demonstrated that the gel systems had proper biocompatibility. Our data demonstrates that the presence of chondrocytes decreased the hydrogels' initial mechanical properties. Nonetheless, chondrocyte-laden constructs showed an enhanced storage modulus after 21 days. Rheological and compression analysis indicated that 5%w/v hydrogels laden with cells particularly showed a significant increase in mechanical properties. Moreover, compared to 10%w/v hydrogels, the 5%w/v hybrid hydrogels induced an enhanced matrix deposition (increased glycosaminoglycan and collagen production). This observation was most evident in constructs with a higher Dex-TA

concentration. Altogether, these data suggest that a 5%w/v hybrid hydrogel with 25% HA and 75% Dex is a promising construct for cartilage repair approaches.

References

1. Hayes, W. C.; Mockros, L. F. Viscoelastic Properties of Human Articular Cartilage. *J. Appl. Physiol.* **1971**, *31*, 562–568.

2. Pearle, A. D.; Warren, R. F.; Rodeo, S. A. Basic Science of Articular Cartilage and Osteoarthritis. *Clin. Sports Med.* **2005**, *24*, 1–12.

3. Barrere, F.; Mahmood, T. A.; De Groot, K.; Van Blitterswijk, C. A. Advanced Biomaterials for Skeletal Tissue Regeneration: Instructive and Smart Functions. *Mater. Sci. Eng. R Reports* **2008**, *59*, 38–71.

4. Akkiraju, H.; Nohe, A. Role of Chondrocytes in Cartilage Formation, Progression of Osteoarthritis and Cartilage Regeneration. *J. Dev. Biol.* **2015**, *3*, 177–192.

5. Newman, A. P. Articular Cartilage Repair. *Am. J. Sports Med.* **1998**, *26*, 309–324.

6. Zhang, W.; Ouyang, H.; Dass, C. R.; Xu, J. Current Research on Pharmacologic and Regenerative Therapies for Osteoarthritis. *Bone Res.* **2016**, *4*, 1–14.

7. Drury, J. L.; Mooney, D. J. Hydrogels for Tissue Engineering: Scaffold Design Variables and Applications. *Biomaterials* **2003**, *24*, 4337–4351.

8. Qiu, Y.-S.; Shahgaldi, B. F.; Revell, W. J.; Heatley, F. W. Observations of Subchondral Plate Advancement during Osteochondral Repair: A Histomorphometric and Mechanical Study in the Rabbit Femoral Condyle. *Osteoarthr. Cartil.* **2003**, *11*, 810–820.

9. Van Tomme, S. R.; Storm, G.; Hennink, W. E. In Situ Gelling Hydrogels for Pharmaceutical and Biomedical Applications. *Int. J. Pharm.* **2008**, *355*, 1–18.

10. Jeong, B.; Kim, S. W.; Bae, Y. H. Thermosensitive Sol–Gel Reversible Hydrogels. *Adv. Drug Deliv. Rev.* **2012**, *64*, 154–162.

11. Yu, L.; Ding, J. Injectable Hydrogels as Unique Biomedical Materials. *Chem. Soc. Rev.* **2008**, *37*, 1473–1481.

12. Jin, R.; Moreira Teixeira, L. S.; Dijkstra, P. J.; van Blitterswijk, C. A.; Karperien, M.; Feijen, J. Enzymatically-Crosslinked Injectable Hydrogels Based on Biomimetic Dextran-Hyaluronic Acid Conjugates for Cartilage Tissue Engineering. *Biomaterials* **2010**, *31*, 3103–3113. https://doi.org/10.1016/j.biomaterials.2010.01.013.

13. Jin, R.; Hiemstra, C.; Zhong, Z.; Feijen, J. Enzyme-Mediated Fast in Situ Formation of Hydrogels from Dextran-Tyramine Conjugates. *Biomaterials* **2007**, *28*, 2791–2800. https://doi.org/10.1016/j.biomaterials.2007.02.032.

14. Jin, R.; Moreira Teixeira, L. S.; Dijkstra, P. J.; Zhong, Z.; Van Blitterswijk, C. A.; Karperien, M.; Feijen, J. Enzymatically Crosslinked Dextran-Tyramine Hydrogels as Injectable Scaffolds for Cartilage Tissue Engineering. *Tissue Eng. - Part A* **2010**, *16*, 2429–2440. https://doi.org/10.1089/ten.tea.2009.0764.

15. Wang, R.; Leber, N.; Buhl, C.; Verdonschot, N.; Dijkstra, P.J.; Karperien, M. Cartilage adhesive and mechanical properties of enzymatically crosslinked polysaccharide tyramine conjugate hydrogels. Polym. Adv. Technol. 2014, 25, 568–574.

16. Ramirez, J. C.; Sánchez-Chaves, M.; Arranz, F. Dextran Functionalized by 4-nitrophenyl Carbonate Groups. Aminolysis Reactions. *Die Angew. Makromol. Chemie Appl. Macromol. Chem. Phys.* **1995**, *225*, 123–130.

17. Rydergren, S. Chemical Modifications of Hyaluronan using DMTMM-Activated Amidation. In

Synthetical Organic Chemistry; Uppsala University: Uppsala, Sweden, 2013; Available online: https://www.diva-portal.org/smash/get/diva2:640661/FULLTEXT02.pdf (accessed on 1 April 2021).

18. D'Este, M.; Eglin, D.; Alini, M. A systematic analysis of DMTMM vs EDC/NHS for ligation of amines to hyaluronan in water. Carbohydr. Polym. 2014, 108, 239–246.

19. Hendriks, J.; Riesle, J.; Vanblitterswijk, C. A. Effect of Stratified Culture Compared to Confluent Culture in Monolayer on Proliferation and Differentiation of Human Articular Chondrocytes. *Tissue Eng.* **2006**, *12*, 2397–2405.

20. Aigner, T.; Stöve, J. Collagens—Major Component of the Physiological Cartilage Matrix, Major Target of Cartilage Degeneration, Major Tool in Cartilage Repair. *Adv. Drug Deliv. Rev.* **2003**, *55*, 1569–1593.

21. Burdick, J. A.; Chung, C.; Jia, X.; Randolph, M. A.; Langer, R. Controlled Degradation and Mechanical Behavior of Photopolymerized Hyaluronic Acid Networks. *Biomacromolecules* **2005**, *6*, 386–391.

22. Lee, F.; Chung, J. E.; Kurisawa, M. An Injectable Enzymatically Crosslinked Hyaluronic Acid–Tyramine Hydrogel System with Independent Tuning of Mechanical Strength and Gelation Rate. *Soft Matter* **2008**, *4*, 880–887.

23. Akmal, M.; Singh, A.; Anand, A.; Kesani, A.; Aslam, N.; Goodship, A.; Bentley, G. The Effects of Hyaluronic Acid on Articular Chondrocytes. *J. Bone Joint Surg. Br.* **2005**, *87*, 1143–1149.

24. Menzel, E. J.; Farr, C. Hyaluronidase and Its Substrate Hyaluronan: Biochemistry, Biological Activities and Therapeutic Uses. *Cancer Lett.* **1998**, *131*, 3–11.

25. Tanimoto, K.; Suzuki, A.; Ohno, S.; Honda, K.; Tanaka, N.; Doi, T.; Nakahara-Ohno, M.; Yoneno, K.; Nakatani, Y.; Ueki, M. Hyaluronidase Expression in Cultured Growth Plate Chondrocytes during Differentiation. *Cell Tissue Res.* **2004**, *318*, 335–342.

26. Lu, L.; Zhu, X.; Valenzuela, R. G.; Currier, B. L.; Yaszemski, M. J. Biodegradable Polymer Scaffolds for Cartilage Tissue Engineering. *Clin. Orthop. Relat. Res.* **2001**, *391*, S251–S270.

27. Breuls, R. G. M.; Jiya, T. U.; Smit, T. H. Scaffold Stiffness Influences Cell Behavior: Opportunities for Skeletal Tissue Engineering. *Open Orthop. J.* **2008**, *2*, 103.

28. Malda, J.; Visser, J.; Melchels, F. P.; Jüngst, T.; Hennink, W. E.; Dhert, W. J. A.; Groll, J.; Hutmacher, D. W. 25th Anniversary Article: Engineering Hydrogels for Biofabrication. *Adv. Mater.* **2013**, *25*, 5011–5028.

29. Wong, M.; Carter, D. R. Articular Cartilage Functional Histomorphology and Mechanobiology: A Research Perspective. *Bone* **2003**, *33*, 1–13.

30. Little, C. J.; Bawolin, N. K.; Chen, X. Mechanical Properties of Natural Cartilage and Tissue-Engineered Constructs. *Tissue Eng. Part B Rev.* **2011**, *17*, 213–227.

31. Alexopoulos, L.G.; Haider, M.A.; Vail, T.P.; Guilak, F. Alterations in the mechanical properties of the human chondrocyte pericellular matrix with osteoarthritis. J. Biomech. Eng. **2003**, 125, 323–333.

32. Nicodemus, G. D.; Bryant, S. J. Cell Encapsulation in Biodegradable Hydrogels for Tissue Engineering Applications. *Tissue Eng. Part B Rev.* **2008**, *14*, 149–165.

33. Söntjens, S. H. M.; Nettles, D. L.; Carnahan, M. A.; Setton, L. A.; Grinstaff, M. W. Biodendrimer-Based Hydrogel Scaffolds for Cartilage Tissue Repair. *Biomacromolecules* **2006**, *7*, 310–316.

34. Chung, C.; Burdick, J. A. Influence of Three-Dimensional Hyaluronic Acid Microenvironments

on Mesenchymal Stem Cell Chondrogenesis. *Tissue Eng. Part A* **2009**, *15*, 243–254.

35. Liao, E.; Yaszemski, M.; Krebsbach, P.; Hollister, S. Tissue-Engineered Cartilage Constructs Using Composite Hyaluronic Acid/Collagen I Hydrogels and Designed Poly (Propylene Fumarate) Scaffolds. *Tissue Eng.* **2007**, *13*, 537–550.

7.5 Supplementary materials

7.5.1 Methods

7.5.1.1 Synthesis of dextran-p-nitrophenyl carbonate

LiCl (4.0 g, dried at 115 °C) and dextran (5.00 g, 30.8 mmol repeating units (r.u.)) are weighed into a 500 mL three necked round bottom flask equipped with a stirrer bar. The flask is evacuated and refilled with nitrogen 3 times, after which it is left under vacuum at 95 °C for 1.5h. After thoroughly drying, the flask was filled with nitrogen and 200 mL of anhydrous DMF was added *via* a cannula while stirring. The flask was then equipped with a thermometer and the mixture was heated to 95 °C while stirring the solution. Once the dextran was completely dissolved, the solution was cooled to 0 °C and anhydrous pyridine (2.0 ml, 25.8 mmol) was added. Subsequently, freshly sublimed para-nitrophenyl chloroformate (2.5 g, 12.4 mmol) was added in small portions, while keeping the temperature below 2 °C. After 1 hour, the reaction mixture was poured into 1 L of ice-cold ethanol. The precipitate was filtered off (Por 4) and washed with cold ethanol (3×100 mL) and subsequently with diethyl ether (3×100 mL). After drying under vacuum, the product was obtained as a white powder (6.00 g, 30.7 mmol r.u., 99 % yield, DS20%). 1H-NMR (400 MHz, DMSO-d6): δ(ppm) = 3.0-4.0 (saccharide ring protons, m, 6H); 4.2-5.8 (anomeric and hydroxyl protons, m, 4H); 7.58 (Ar o-CH, d, 2H); 8.34 (Ar m-CH, d, 2H).

7.5.1.2 Synthesis of dextran-tyramine

Dextran-PNC (6.00 g, 30.7 mmol r.u., 6.15 mmol p-nitrophenyl carbonate) was weighed into a 250 mL three necked round bottom flask equipped with a stirrer bar. The flask was evacuated and refilled with nitrogen 3 times, after which the flask was filled with nitrogen and 100 mL of anhydrous DMF was added via a cannula while stirring. Once the dextran was completely dissolved, tyramine (1.69 g, 12.3 mmol) was added. After 1 hour, the reaction mixture was poured into 1 L of ice-cold ethanol. The precipitate was filtered off (Por 4) and washed with cold ethanol (3×100 mL) and subsequently with diethyl ether (3×100 mL). After drying under vacuum, the crude product was obtained as a white powder. The crude product was dissolved in 75 mL of Milli-Q water and dialysed against Milli-Q water for 3 days (MWCO 3500 Da), followed by filter sterilization and freeze-drying yielding the product as a white foam (5.04 g, 28.0 mmol, 92 % yield, DS10%). 1H-NMR (400

MHz, DMSO-d6): δ(ppm) = 3.0-4.0 (saccharide ring protons, m, 6H); 4.2-5.8 (anomeric and hydroxyl protons, m, 4H); 6.67 (Ar m-CH, d, 2H); 6.99 (Ar o-CH, d, 2H).
The calculation of the DS of dextran-TA and dextran-PNC is based on the integrals of 4.2-5.8 ppm (corresponding to the 4 anomeric protons from dextran), compared with the integral of the aromatic protons of tyramine (6.60-6.75 and 6.90-7.07) or para-nitrophenyl (7.40-7.65 and 8.20-8.40). The DS of dextran is given as the percentage of saccharide units modified in dextran.

7.5.1.3 Synthesis of hyaluronic acid-tyramine

Sodium hyaluronate (5.00 g, 12.5 mmol r.u.) was dissolved in 500 mL Milli-Q water in a 1 L round bottom flask equipped with a stirrer bar. While stirring at room temperature, 4-(4,6-dimethoxy-1,3,5-triazin-2-yl)-4-methylmorpholinium chloride (DMTMM, 3.46 g, 12.5 mmol, 1eq) and tyramine hydrochloride (TA·HCl, 2.17 g, 12.5 mmol, 1eq) were added subsequently. The addition of DMTMM and TA·HCl was repeated after 24 and 48 hours. After 72 hours, 40 mL NaCl (sat) was added to the reaction mixture and the reaction mixture was poured into 2.5 L cold ethanol. The crude product was isolated by centrifugation at 5000 rpm followed by drying in vacuo. The crude product was dissolved in 75 mL Milli-Q water and dialysed against Milli-Q water for 3 days (MWCO 1000 Da). Filter sterilization and lyophilization yielded the product as a white foam (5.10 g, 12.4 mmol, 99 % yield, DS10%). 1H-NMR (400 MHz, D2O): δ(ppm) = 1.98 (acetyl-CH3, s, 3H); 2.75 (2-CH2, s, 2H); 2.90 (1-CH2, s, 2H); 3.2-4.2 (saccharide ring, m, 10H); 4.34 (s, 1H); 4.43 (d, 1H); 6.84 (Ar m-CH, d, 2H); 7.16 (Ar o-CH, d, 2H).
The degree of substitution (DS) was calculated based on the integral of the methyl group at 1.98 ppm is compared to the integral of the tyramine signals at 6.80-6.87 and 7.10-7.21 ppm. The DS of hyaluronic acid is given as the percentage of COOH groups modified in hyaluronic acid (*i.e.* per disaccharide).

7.5.1.4 Crosslinking density

The crosslink density was calculated based on the classical rubber elasticity theory:

$$G' = v_e RT\vartheta^{1/3} \qquad \text{(eq. S1)}$$

With the effective crosslink density, $\boldsymbol{\nu_e}$, the shear storage modulus, G', and the polymer volume fraction, $\boldsymbol{\vartheta}$.

Table 7.S1 Effective crosslink density, ν_e (mM).

	A	B	C	D	E
D0 5%	2.46	0.91	0.86	0.66	0.35
D0 5% cells	1.27	0.89	0.51	0.44	0.35
D0 10%	2.70	5.01	4.25	3.11	2.37
D0 10% cells	3.10	4.03	2.87	2.16	1.60

7.5.2 Supplemental Figures

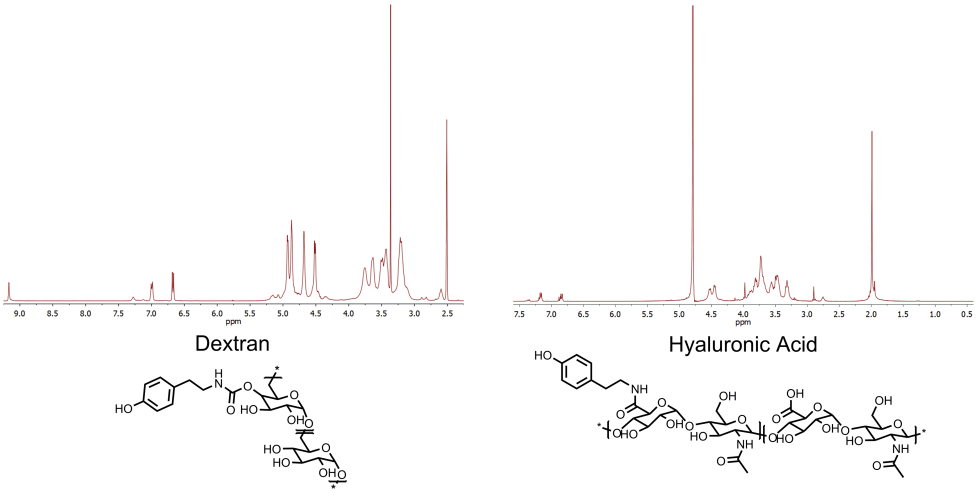

Figure 7.S1 *^{1}H NMR spectra of dextran and hyaluronic acid tyramine conjugates (Dex-TA and HA-TA). (a) Dextran-tyramine conjugates were successfully prepared by subsequent activation of dextran by PNC and reaction with tyramine. The final product had a substitution degree of 10%, i.e. 10% of the monosaccharides of dextran have been modified, which was confirmed by 1H-NMR. (b) HA was conjugated in a single step amidation, and the carboxyl group was activated by DMTMM producing an ester, which can be converted into an amide in the presence of tyramine. DMTMM as single step amidation agent was first described by Kunishima et al [1]. HA-TA had a substitution degree of 10%, i.e. 10% of the carboxylic acid groups (i.e. disaccharides) of hyaluronic acid have been modified, which was confirmed by 1H-NMR.*

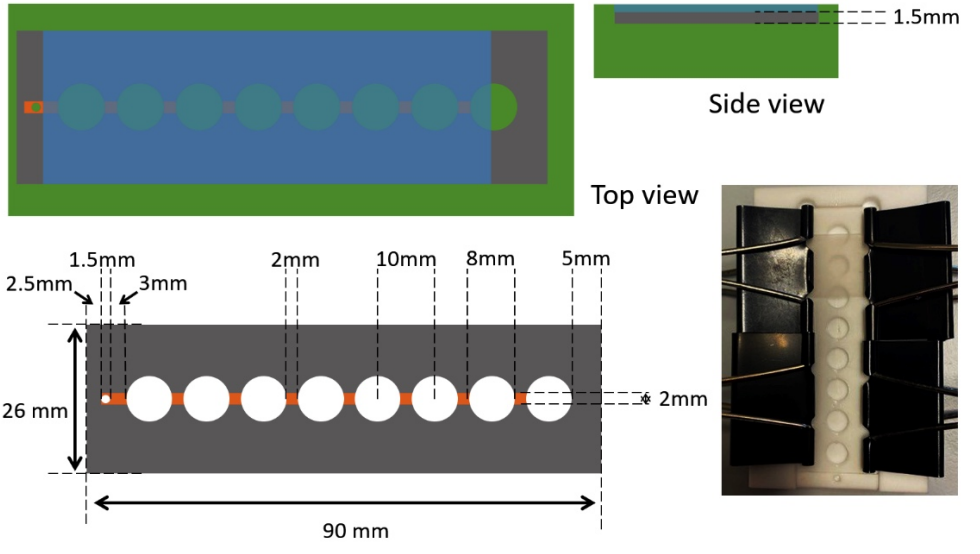

Figure 7.S2 *Sketches of the prepared hydrogel molds, composed of a Teflon base (green), a 1.5mm think Teflon insert (grey) with a 0.75 mm deep groove (orange) connecting the 8mm diameter holes for the hydrogels. The mold is covered with a glass slide leaving the inlet (left) and outlet (right) uncovered.*

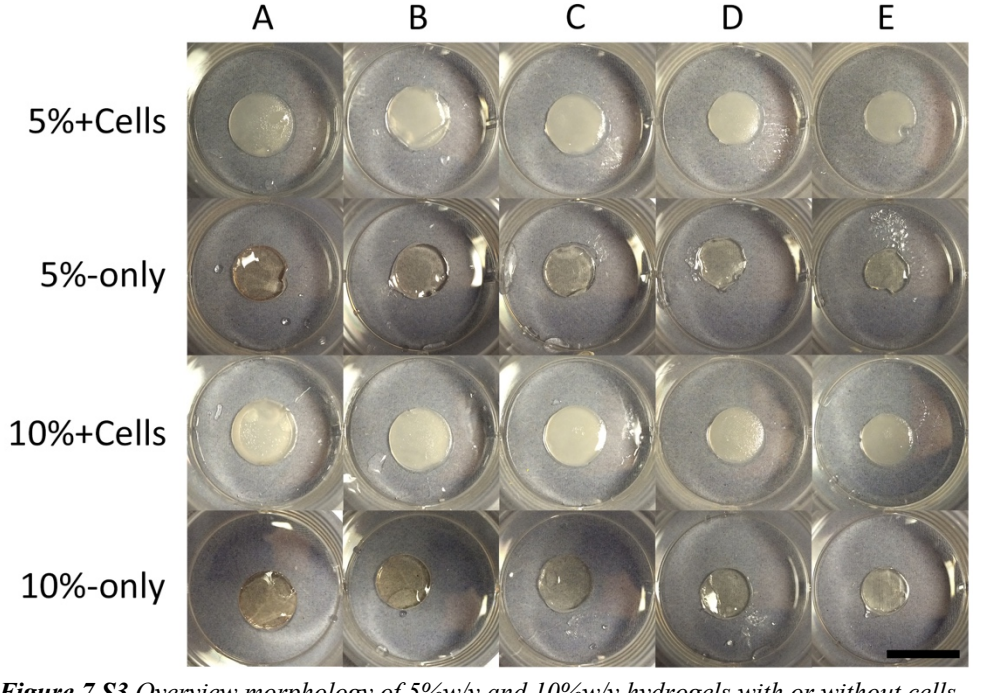

Figure 7.S3 *Overview morphology of 5%w/v and 10%w/v hydrogels with or without cells.*

From condition A to E show the different mix ratio of HA and Dex (100:0, 75:25, 50:50, 25:75, 0:100). The size of hydrogels decreased from condition A to E in both with and without cell groups, while the combination of cells increases the gel size. Scale bar = 10 mm.

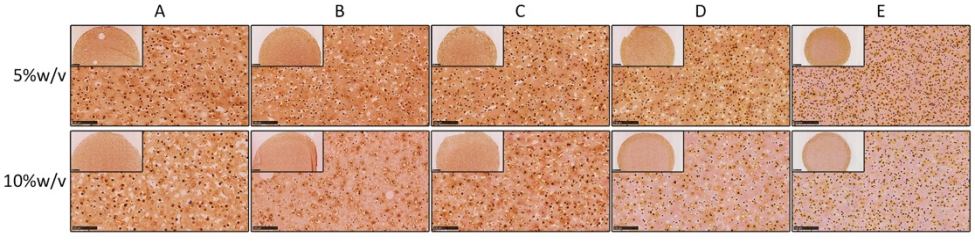

Figure 7.S4 *Safranin O staining of 5%w/v and 10%w/v hydrogels encapsulated with chondrocytes after culturing for 21 days in the chondrogenic medium. Inserts indicate the overview of each hydrogel; scale bar = 1 mm. Pictures show the magnified view of each hydrogel; scale bar = 250 µm.*

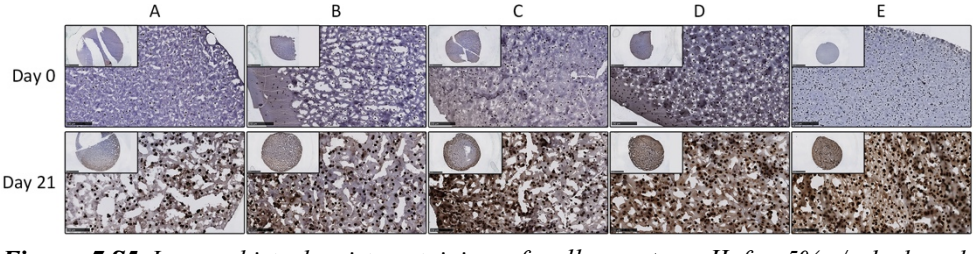

Figure 7.S5 *Immunohistochemistry staining of collagen type II for 5%w/v hydrogels encapsulated with chondrocytes after 0- or 21-days culturing in the chondrogenic medium. Inserts indicate the overview of each hydrogel; scale bar = 2.5 mm. Pictures show the magnified view of each hydrogel; scale bar = 250 µm.*

Supplementary References

1. Kunishima, M.; Kawachi, C.; Monta, J.; *et al*. 4-(4, 6-dimethoxy-1, 3, 5-triazin-2-yl)-4-methyl-morpholinium chloride: an efficient condensing agent leading to the formation of amides and esters. *Tetrahedron*, **1999**, 55: 13159-13170.

Chapter 8

Preliminary *in vivo* evaluation: Hyaluronic acid and Dextran hybrid injectable hydrogels for cartilage tissue engineering application

Yao Fu, Sanne Both, Jacqueline Plass, Bram Zoetebier, Piet Dijkstra, and Marcel Karperien

Abstract

Previously, 5%w/v Hyaluronic acid tyramine (HA-TA) and Dextran-tyramine (Dex-TA) hybrid hydrogels were demonstrated to provide a mechanically stable environment, maintain the cell viability, and promote the cartilaginous specific matrix deposition *in vitro*. In this study, 5%w/v hybrid hydrogels were combined with human Mesenchymal Stem Cells (MSCs), bovine chondrocytes or a combination of both in a 4:1 ratio and were subcutaneously implanted in the back of male and female nude rats to assess the performance of cell-laden hydrogels in tissue formation. Subcutaneous implantation of these biomaterials showed signs of integration of the gels within the host tissue. Histological analysis showed residual fibrotic capsules four weeks after implantation. However, enhanced tissue invasion and some giant cells infiltration were observed in the HA/Dex hydrogels laden with either human MSCs or bovine chondrocytes but not with the co-culture. Moreover, Chondrocyte-MSC co-cultures show beneficial interaction with the biomaterials, for instance in enhanced cell proliferation and matrix deposition. In addition, we provide evidence that host gender has an impact on the performance of chondrocytes encapsulated in HA/Dex-TA hydrogels. This preliminary investigation revealed that hydrogels laden with different types of cells resulted in distinct host responses. Taken together all these results, along with previous data, it can be concluded that 5%w/v hydrogels with a higher concentration of Dex-TA encapsulated with Chondrocyte-MSC co-cultures are adequate for injectable applications and *in situ* cell delivery in cartilage regeneration approaches.

8.1 Introduction

Articular cartilage injuries may occur as a result of either traumatic mechanical destruction or progressive mechanical degeneration. The combination of the lack of blood supply and low mitotic activity of chondrocytes leads to a limited ability to repair and regeneration of articular cartilage[1–3]. At the moment, injectable *in situ* forming hydrogels have emerged as promising cartilage tissue engineering strategies due to the ability to form three-dimensional, highly hydrated scaffolds after injection in an aqueous form[4–6].

Injectable materials enable localized and straightforward delivery of cells and biomolecules *via* minimally invasive procedures without the associated risks of surgical implantation. These materials allow for the ability to fill irregular-shaped defects, avoiding the difficulty of prefabricating patient-specific shapes[7,8]. Moreover, hydrogels with different physical properties can also be designed and implanted in non-self-healing critical size defects, temporarily replacing the extracellular matrix and assisting the healing process[9]. Previously, our group has developed an injectable hybrid hydrogel composed of hyaluronic acid-tyramine (HA-TA) and tyramine conjugated dextran (Dex-TA)[10]. The hydrogel is formed *in situ* using a biocompatible enzymatic cross-linking reaction and supports survival and tissue formation chondrocytes and mesenchymal stem cells *in vitro* (*Chapter 7* of this thesis).

Tissue exposure to biomaterials triggers a foreign body response (FBR), a non-specific immune response process which may result in a persistent chronic inflammation and fibrotic encapsulation of the material[11–13]. In this inflamed environment, macrophages, lymphocytes, and their granular products contribute to the infiltration of foreign body giant cells (multinucleated fused macrophages) into the implantation site and the development of a collagen rich fibrotic connective tissue layer surrounding the implant[13–16]. The degree of host response depends on the extent of homeostasis that is disturbed in the host by the injury and the subsequent implantation of the foreign material as well as the properties of the material itself. Previously, an implant was considered to be biocompatible if it was encapsulated by an avascular layer of collagen without affecting its intended performance[17]. However, the impermeable nature of the fibrous capsule, in some cases, results in poor mass transport and electrolyte diffusion between the implant and the tissue, which impairs the function, safety, and biocompatibility of cell laden

implants[18–20]. This is particularly relevant when these constructs are used in a tissue regeneration strategy.

In a previous study (*Chapter 7*), we have demonstrated that 5%w/v Hyaluronic acid and Dextran (HA/Dex) hybrid hydrogels encapsulated with chondrocytes provide a mechanically stable environment, maintain the cell viability, and promote the cartilaginous specific matrix deposition *in vitro*. In this study, 5%w/v hybrid hydrogels were combined with different types of cells and then subcutaneously implanted in the back of male and female nude rats for a four-week period. The main objective was aimed to assess the response of the cell laden hydrogels with respect of tissue formation and to characterize the reaction of the neighboring tissues, and investigate the interaction between hybrid hydrogels and co-cultures or mono-cultures. In second objective, we also investigate the effect of host gender differences on these outcomes by implanting samples (HA/Dex hydrogels encapsulated with chondrocytes or MSCs, respectively) subcutaneously in the back of female and male nude rats.

8.2 Materials and Methods

8.2.1 Materials

Dextran (40 kDa, pharmaceutical grade) was purchased from Pharmacosmos, Denmark. Sodium hyaluronate (27 kDa, pharmaceutical grade) was purchased from Contipro Pharma, Czech Republic. Tyramine (99%), DMF (anhydrous, 99.8%), LiCl (99.0%), p-nitrophenyl chloroformate (PNC, 96%), pyridine (anhydrous, 99.8%), DMSO-d6 (99.9%), NaCl (≥99.0%), D2O (99.9 atom % D), horseradish peroxidase (HRP, 325 units/mg solid), hydrogen peroxide (30%) were purchased from Sigma-Aldrich. Tyramine·HCl salt (99%) was obtained from Acros Organics. 4-(4,6-Dimethoxy-1,3,5-triazin-2-yl)-4-methylmorpholinium Chloride (DMTMM, 97%) was purchased from Fluorochem Ltd. UK. Ethanol (≥99.9%) and Diethyl ether (≥99.7%) were purchased from Merck. Milli-Q water was used from the Milli-Q Advantage A10 system equipped with a 0.22µm Millipak®-40 Express filter.

8.2.2 Cell culture and expansion

Bovine chondrocytes (bCHs) were isolated from full-thickness cartilage knee biopsies from ~6 months old calves according to the previously reported protocol[21]. bCHs were expanded in chondrocyte proliferation medium (Dulbecco's modified Eagle's medium (DMEM; Gibco) supplemented with 10% fetal bovine serum (FBS;

Gibco), 0.2 mM ascorbic acid 2-phosphate (ASAP; Sigma), 0.4 mM proline (Sigma), 1x nonessential amino acids (Gibco), 100 U/mL penicillin and 100 µg/mL streptomycin (Invitrogen)). Human bone marrow-derived mesenchymal stem cells (hMSCs) were isolated as previously reported[22] and cultured in MSC proliferation medium (α-MEM (Gibco) supplemented with 10% FBS (Gibco), 1% L-glutamine (Gibco), 0.2 mM ASAP (Sigma), 100 U/mL penicillin and 100 µg/mL streptomycin (Invitrogen) and 1 ng/mL bFGF)). The use of human material was approved by a local medical ethical committee. The medium was refreshed twice a week, and cells were at passage 3 used for the experiments.

8.2.3 Synthesis of polymers

Dextran-tyramine (Dex-TA) and hyaluronic acid-tyramine (HA-TA) were synthesized as previously reported (see *Materials and Methods* section in *Chapter 7*). Briefly, Dextran-tyramine was synthesized by the activation of dextran with PNC and subsequent amino lysis with tyramine adapted from Ramirez et al[23]. Hyaluronic acid-tyramine was prepared by amidation of the carboxyl groups of HA by tyramine, the procedure was adapted from Yu et al[24]. Detailed description of polymers synthesis can be found in the Supplementary Methods.

8.2.4 Hydrogel formation

Hydrogel samples were prepared as previously reported (see *Hydrogel formation* section in *Chapter 7*). Briefly, the hydrogels were prepared in a newly designed PTEE mold to produce identical hydrogels of 5 mm in diameter and 2.5 mm in height. After dissolving the tyramine-conjugated polymers in sterile phosphate buffered saline (PBS), polymer solutions were prepared and incubated with horseradish peroxidase (HRP, 40units/mL; Sigma-Aldrich) overnight at 4°C. The mixture was then combined with different types of cells (MSCs, CHs, and co-cultures) in the concentration of 10 million cells/mL. For co-cultures (represented as group Co), hMSCs and bCHs were mixed at a ratio of 80%/20%. Freshly prepared 0.3% hydrogen peroxide (H_2O_2) was added to the mixture and immediately transferred to the mold using a 1mL pipette after a brief vortex. The final concentrations of the gels were 5%w/v polymer, 10 million cells/mL, 4 U/mL HRP and 0.015% H_2O_2. HA-TA and Dex-TA were combined in three ratios (100:0, 50:50, and 0:100, represented by group HA, HA/Dex, and Dex, respectively). All the conditions are listed in Table 8.1.

8.2.5 Hydrogel implantation

After incubating in medium overnight, the hydrogel samples described above were implanted subcutaneously in the back of 14-week old nude rats (Crl:NIH-Foxn1rnu) (Fig. 8.1A). Each rat received Carprofen (4mg/kg) as an analgesic before the start of the procedure. The rats were induced with 4% isoflurane and maintained at 1.5-2% during the procedure. The skin was cleaned with 70% ethanol and four subcutaneous pockets were created on each lateral side of the spine on the backs of 10 male rude rats (eight implants in total per rat). In each pocket, one hydrogel was inserted randomly. Simultaneously, two samples (HA/Dex hydrogels encapsulated with chondrocytes or MSCs, respectively) were also implanted subcutaneously randomly in the back of another 10 female nude rats.

This experiment was approved by the local animal experimental committee. After 28 days, the implants and respective surrounding tissue were harvested and fixed with 10% formalin and then incubated in cryomatrix (Thermo-scientific) overnight at 4°C. The samples embedded in cryomatrix were snap frozen using liquid nitrogen and stored at -80°C.

8.2.6 Histology

Cryosections of 10 µm were cut using a cryotome (Thermo-scientific) and processed for histological evaluation with different staining methods. Hematoxylin-eosin (H&E) staining was performed using a standard protocol. Masson-Goldner Trichrome staining was performed to detect connective tissue and fibrous capsule thickness following the instruction of manufacture (Merck). Briefly, samples were first placed in Weigert's hematoxylin staining solution for 5 min and washed in tap water for 10 min. Sections were then shortly rinsed in 1% acetic acid and incubated in an Azophloxine solution for 10 min, rinsed in 1% acetic acid followed by incubation in Tungstophosphoric acid orange G solution for 1 min. Sections were again rinsed in 1% acetic acid for 30 s followed by incubation in light green for 2 min and another wash in 1% acetic acid. The thickness of the fibrous capsule and the inflammatory cell layer were measured for sections of all the conditions. For each section, four points on each capsule around the implant were measured (n=10). The peri-implant fibrotic capsule thickness was defined as the distance between the border of the fibrotic tissue adjacent to the implant, and the muscle or fat tissue adjacent to the fibrotic capsule at the other end.

8.2.7 Naphthol AS-D Chloroacetate esterase staining

Naphthol AS-D staining was performed to stain granular cells, like neutrophils and mast cells. The chloroacetate esterase staining was performed following the instruction of manufacture (Sigma). Briefly, the chloroacetate esterase staining solution was first prepared as the protocol described. The cryosections were then incubated with the staining solution for 20 min at 37°C in the dark. Sections were subsequently washed in distilled water and mounted with Faramount aqueous mounting medium (Dako). All cells containing red granules were regarded as positive.

8.2.8 Immunohistochemistry staining

For immunohistochemistry, endogenous peroxidase was blocked by incubating the cryosections with 0.3% H_2O_2. After washing with PBS, the sections were blocked in 5% bovine serum albumin to prevent nonspecific binding. Slides were subsequently incubated overnight at 4°C with a rabbit polyclonal antibody against COL II (Abcam). Thereafter, sections were incubated with polyclonal goat-anti-rabbit HRP-conjugated secondary antibody (Dako) for 30 minutes at room temperature, followed by development with DAB Substrate kit (Abcam). Counterstaining was performed with hematoxylin. Non-immune controls underwent the same procedure without primary antibody incubation.

8.2.9 Image analysis and statistical analysis

All the stained slides were scanned with the NanoZoomer 2.0-RS slide scanner (Hamamatsu). Stained sections were scored by three blinded individuals, independently to assess the tissue response. Fibrous capsule thickness and inflammatory cells were evaluated semi-quantitatively using NanoZoomer Digital Pathology software. The data is presented as mean ± standard deviation. Statistical significance was analyzed using the One-way Analysis of Variance (ANOVA) with Turkey's *post-hoc* analysis. p-value of <0.05 was considered statistically significant.

8.3 Results

8.3.1 In vivo implantation in nude rats

Cell-based hydrogel constructs were subcutaneously implanted in the back of nude rats for 28 days to investigate cartilage matrix formation and tissue responses *in vivo*. Macroscopic observation of constructs, in all animals, shows proper integration with host tissue and no signs of edema or toxicity in the tissue surrounding the implants (Fig. 8.1B). All the hydrogel samples were clearly visible under the skin and

maintained their structural integrity, indicating that they had not yet degraded significantly. Also, no evident macroscopic inflammation of the implanted constructs was observed.

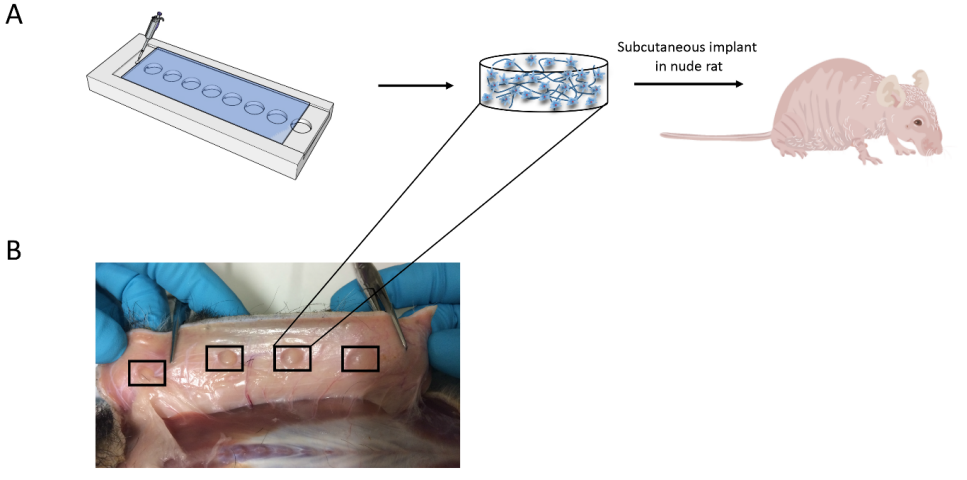

Figure 8.1 *Experimental setup. (A) Schematic illustration of the outline of the experiment. Identical cell laden hydrogels containing different types of cells were formed using a PTEE mold. Next, the prepared hydrogel constructs were implanted subcutaneously in the back of 10 nude rats for 28 days. (B) Macroscopic observation of the different groups after 28 days post-implantation. From left to right are representative pictures of groups HA-TA & Co, Dex-TA & CH, HA/Dex & MSC, HA/Dex & CH, respectively. Frames denote the location of the implanted hydrogels.*

To investigate the *in vivo* innate inflammatory response, the explanted samples as well as the surrounding tissues were histologically assessed (Figs. 8.2, 3, and 4). Representative histological images of sections stained with hematoxylin and eosin (H&E) to examine the presence of tissue response are shown in Fig. 8.2. The histological sections were evaluated *via* light microscopy and scored for tissue reaction, presence of giant cells, nuclei visibility, neutrophils and cell clusters. The variable degrees of the inflammatory components are summarized in Table 8.1. The presence of the above inflammatory components was scored from (-), absence to (+++), profound presence. The stained sections show that the HA hydrogels with encapsulated CHs do not display a solid block of gel, but a more maze-like structure, which could be caused by the degradation of the gel. Mixing in Dextran-TA

progressively decreased the maze-like structure. Remarkable it was not present in the HA hydrogels laden with a mixture of MSCs and bCH.

Conditions		Tissue reaction	Giant cells	Nuclei visibility	Neutrophil	Cell Clusters
CH1	HA	+±	+	++±	±	-
	HA/Dex	++	+	+	-	+
	Dex	+	±	++±	-	-
MSC	HA/Dex	++	+±	+	±	-
	Dex	+	+	++	±	+
Co-Cultures	HA	-	-	+++	-	-
	HA/Dex	-	±	+	-	-
	Dex	-	±	++	±	++

Table 8.1 *Histological scoring of the in vivo sections. Twenty-eight days after subcutaneous implantation in male nude rats (n=10 rats in each group) the sections were assessed via various markers to evaluate the tissue response. The presence of the above inflammatory components was scored from (-), absence to (+++), profound presence.*

A new interface consisting of inflammatory cells (*e.g.*, macrophages) was generated between the hydrogels and host tissues after implantation, but no acute inflammatory reaction was observed in all types of samples. Stained figures show that most of the explanted constructs displayed smooth edges in the material-tissue interface. Hydrogel samples containing pure chondrocytes or MSCs resulted in a more abundant chronic tissue reaction, especially in the cell-based HA/Dex conditions. Enhanced tissue invasion and some giant cells infiltration were observed in the HA/Dex hydrogels either encapsulated with bCH or hMSCs. However, tissue reaction was barely noticeable in the co-culture encapsulated hydrogels irrespective of the hydrogel composition. In terms of giant cells concentration, the normal presence of giant cells was observed in the constructs containing either bCH or hMSCs. On the contrary, giant cells were barely presented in the co-culture encapsulated hydrogels.

Regarding cell morphology, similar results were found in most of the implanted samples. Encapsulated cells showed a round morphology and homogeneous

distribution throughout the constructs. However, proliferating cells were found in the conditions of HA/Dex with CHs, Dex with MSCs, and Dex with co-cultures generated cell clusters. Especially in the Dex encapsulated co-cultures, enhanced newly formed cell clusters were observed. Of interest, cellularity analysis showed that in HA/Dex constructs nuclei visibility significantly decreased compared to other conditions. Most of the cells in the HA/Dex samples stained pink so no nuclei were visible, regardless of the cell type encapsulated.

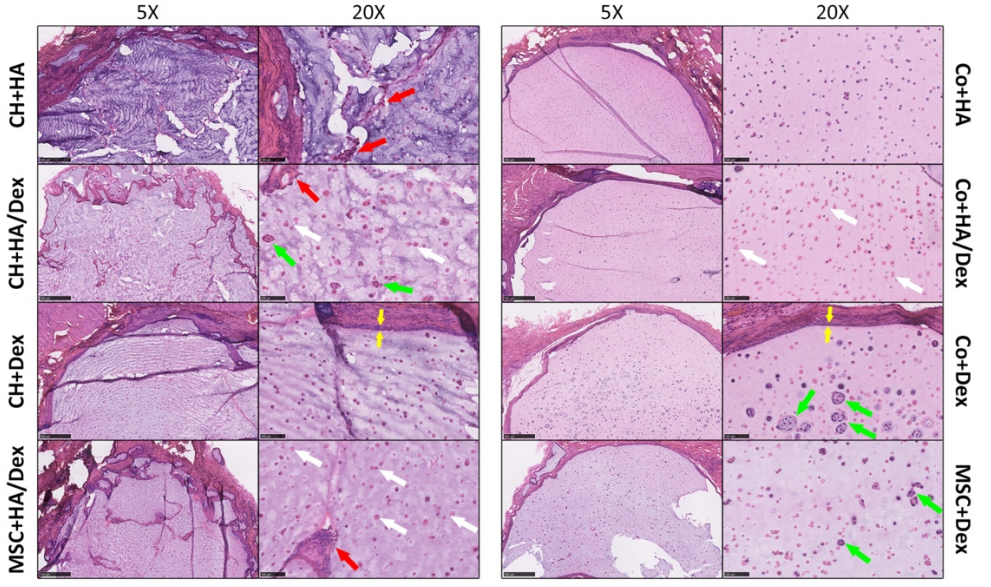

Figure 8.2 *Histological analysis of in vivo response after 28 days of subcutaneous implantation. Representative histological sections of hydrogel samples stained with H&E. The left panel in each condition shows 5× magnification pictures (scale bars represent 500 µm), whereas the right panel shows 20× (scale bars represent 100 µm). The red arrows in the stained sections show giant cells, the green arrows show cell clusters, and the white arrows show the cells without nuclei respectively. Yellow arrows at the material/host interface indicate the layer of inflammatory cells.*

Next, we checked for the presence of neutrophile granulocytes surrounding the implantation site. Neutrophile granulocytes, which represent the abundant cell type in peripheral blood and normally arrive as first immune cells at an implant site and disappear in the course of the following days. Chloroacetate esterase histochemistry is a well-known method to detect granular cells, like neutrophils and mast cells. Positively stained granular cells, which were mostly identified as mast cells, were only sporadically present in the outside of the gel-tissue boundary and seldom into

the implant. These results demonstrate the absence of significant inflammation processes.

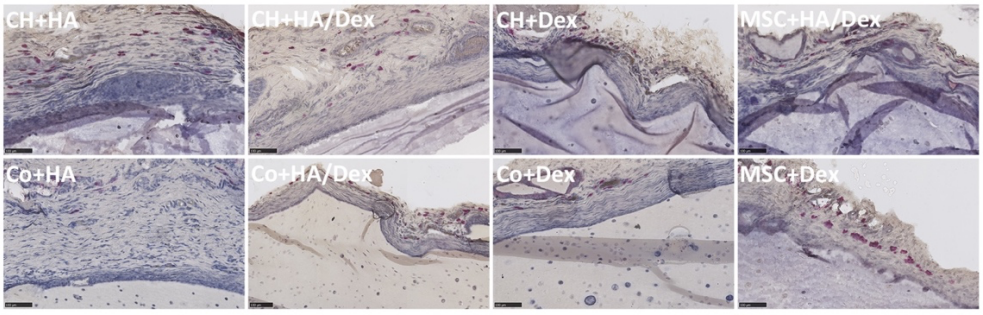

Figure 8.3 *Neutrophile granulocytes staining after 28 days of subcutaneous implantation. Representative figures of hydrogel samples with positive cells stained with Chloroacetate esterase histochemistry. Positively stained cells displayed red granulation. Scale bars represent 100 µm.*

The trichromatic Masson-Goldner staining is most suitable to depict the structure of connective tissues and cells and to assess the fibrous capsule formation by collagen deposition. Representative Masson-Goldner trichrome staining of the cell-based hydrogel samples at 28 days post-implantation is shown in Fig. 8.4A. This staining revealed that all samples were surrounded by a fibrous capsule. Additionally, a semi-quantitative assessment of capsule thickness and inflammatory cells at the implant surface is shown in Fig. 8.4B and C. The average thickness of the peri-implant capsule in all conditions ranged from 40 µm to 48 µm and no significant differences were observed between the different hydrogels (Fig. 8.4B). A layer of inflammatory cells was present at the material-tissue interface (Fig. 8.2). The layer thickness was highest around HA hydrogels with co-cultures compared to others (Fig. 8.4C).

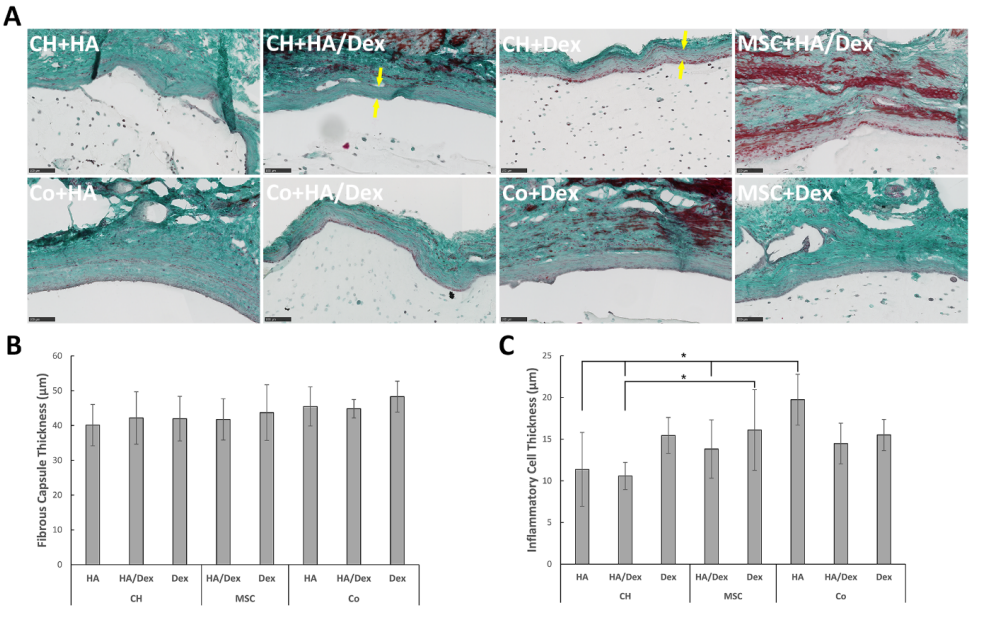

Figure 8.4 *Histological characteristics of implant fibrous capsule after 28 days of subcutaneous implantation. (A) Representative Masson-Goldner trichrome staining of all hydrogels. All images show the interface between the host tissues (at top of images) and the implant. As a result of staining according to the protocol, nuclei will be stained in dark brown to black, cytoplasm and muscles will appear brick red, the connective tissue will appear green and erythrocytes will be bright orange. Yellow arrows in the stained sections indicate the fibrous capsule at the material/host interface. The thickness of the fibrous capsule (B) and the inflammatory cell layer (C, shown in figure 8.2 with yellow arrows) were measured for sections of all the conditions. Data is presented as mean with standard deviation as error bars for n=10 biological replicates per hydrogel condition. Scale bars represent 100 µm.*

8.3.2 Co-cultures encapsulated hydrogels present positively deposition of cartilage matrix

The immunohistochemistry was performed to investigate the expression of proteins that indicate cartilage matrix production. Collagen type II, which is the primary type of collagen present in articular cartilage, was chosen in this study. We rarely observed the expression of COL II in the constructs encapsulated with MSCs after subcutaneous implantation. We did observe some pericellular staining for COL II within the hydrogels loaded with CHs. Positively stained protein expression was more apparent in co-culture laden hydrogels. Notably, intense deposition of type II

collagen was observed in Dex hydrogels laden with co-cultures. Besides, the histochemical analysis also revealed that the cartilage matrix formation was more dominant at the periphery of the hydrogels. These results indicate that the co-culture system and Dex-TA hydrogel could effectively promote the appropriate interactions or stimulations for chondrogenesis, leading to the facilitated secretion of chondrogenic extracellular matrix and cartilaginous tissue formation during *in vivo* subcutaneous implantation.

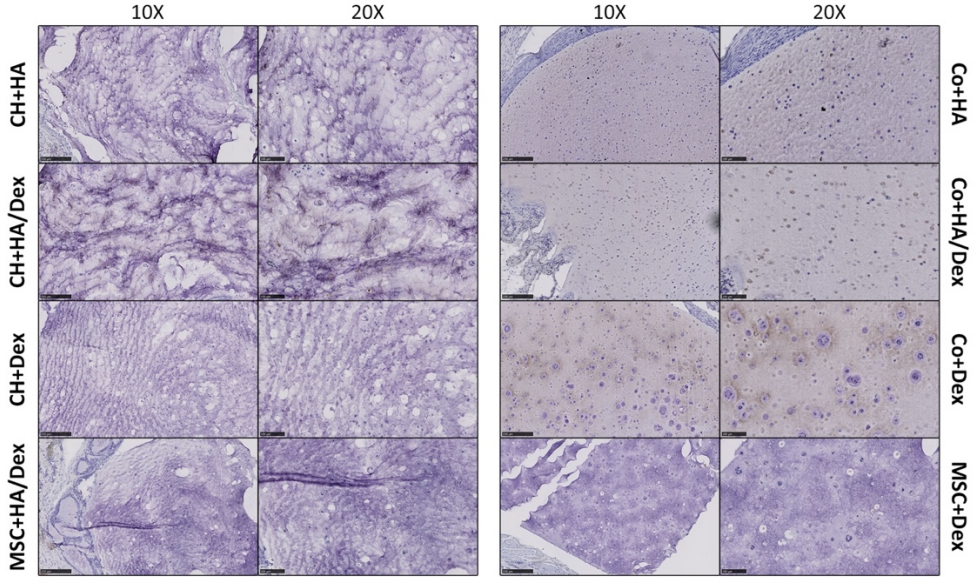

Figure 8.5 *Matrix deposition after 28 days of subcutaneous implantation. Representative immunohistochemical staining of the hydrogel samples for COL II. The positive protein expression stained in dark brown. The left panel in each condition shows 10× magnification pictures (scale bars represent 250 µm), whereas the right panel shows 20× (scale bars represent 100 µm).*

8.3.3 Gender difference shows impact on the performance of chondrocyte laden hydrogels

To investigate the impact of gender differences on the outcomes, we implanted HA/Dex hydrogels laden with chondrocytes or MSCs, respectively subcutaneously in the back of another 10 female nude rats. The histological analysis results were summarized in the table 8.2. Surprisingly, we found gender differences in the performance of implanted hydrogels, however, this impact was mainly observed for hydrogels laden with chondrocytes but not with MSCs. Irrespective of gender, all

the samples formed a clear thin fibrous capsule surrounding the hydrogels while no sign of acute inflammatory response was observed. In the MSCs encapsulated samples, most of the assessed markers were present similarly in samples from both male and female. However, as shown in the figure 8.6, the outcomes from chondrocytes encapsulated hydrogels clearly show gender differences. Compared to samples from female rats, the *in vivo* environment in male rats increased the size of encapsulated chondrocytes, depressed the nuclei visibility of encapsulated chondrocytes and promoted the formation of cell clusters.

Samples	Gender	Tissue reaction	Giant cells	Nuclei visibility	Cell Size (μm)	Collagen capsule	Capsule thickness (μm)	Neutrophil	Cell Clusters
CH+HA/Dex	M	++	+	+	17.81	+	40.66	-	+
	F	+	+	++±	12.21	+	44.79	-	-
MSC+HA/Dex	M	++	+±	+	17.65	+	42.54	±	-
	F	+±	+	+	17.42	+	45.20	±	-

Table 8.2 *Histological analysis of the in vivo sections from different genders. Twenty-eight days after subcutaneous implantation in different genders nude rats (n=10 rats in each group) the sections were assessed via various markers to evaluate impact of gender difference on the performance of cell encapsulated hydrogels. M represents male and F represents female.*

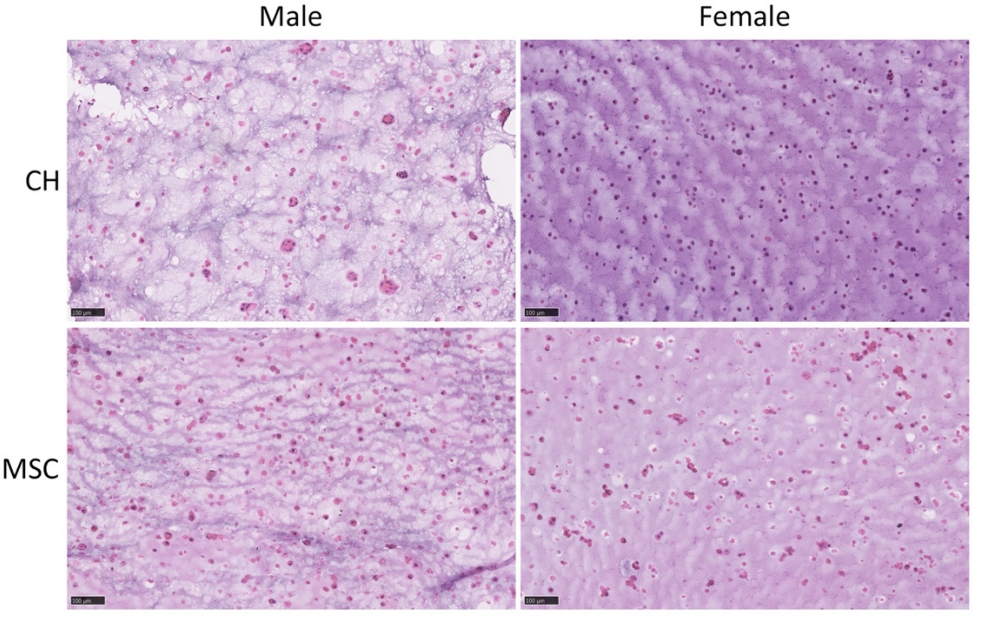

Figure 8.6 *Histological analysis comparing implants laden with chondrocytes or MSCs in either male (left) or female (right) nude rats. 5%w/v HA/Dex hydrogels encapsulated with MSCs or chondrocytes were implanted subcutaneously into the back of both male and female rude rats. Representative histological sections of hydrogel samples stained with H&E. Scale bars represent 100 μm.*

8.4 Discussion

Previously, we have developed and characterized an injectable hydrogel system suitable for the encapsulation of cells for applications in cartilage tissue regeneration *in vitro*. We utilized different conditions of Hyaluronic acid and Dextran hybrid hydrogels and demonstrated that 5%w/v hydrogels showed enhanced deposition of cartilage matrix, thereby significantly increasing the mechanical properties. In this work, the safety and biocompatibility of the above hybrid hydrogels encapsulated with different types of cells were tested by subcutaneously implantation in the back of nude rats for four weeks. This study demonstrated that, as a major result, both hydrogels present limited immune response and small fibrotic capsule surrounding the material. As the second major aspect, Chondrocyte-MSC co-cultures show beneficial interaction with the biomaterials. Finally, this preliminary investigation revealed that hydrogels with different types of cells resulted in distinct tissue responses, which indicated the possibility of personalized regeneration approaches based on the situation of individual patients. Of interest, gender appeared to influence the performance of chondrocyte laden hydrogels after subcutaneous implantation.

The utilization of injectable hydrogels in cartilage regeneration is considered to be a promising strategy due to the minimally invasive processing. The gelation *in situ* enables the formed hydrogel to quickly set its volume and easily adapt to the shape of the defect site, establishing an efficient integration with the host tissue. Besides, this system can deliver cells and/or bioactive agents of interest in a non-harsh way and keep them at the implantation site[25]. However, implantation of biomaterials triggers a series of host reactions at the injury site that include material/tissue interactions, acute and chronic inflammation, granulation tissue development, foreign body reaction, and fibrous capsule development[15,16]. Accordingly, this body response to the foreign material compromises the *in vivo* functionality and durability of the implanted material[13]. To evaluate the response of a host to a first contact with this biomaterial, 5%w/v hybrid hydrogels encapsulated with different types of cells were subcutaneously implanted in the back of nude rat, and histological analysis

was conducted to assess the inflammatory processes associated with the implantation, as well as the integration into the host tissue.

After four weeks, all the implanted samples show proper integration with host tissue and no signs of granulation tissue development or toxicity in the tissue surrounding the implants. Histological analysis revealed that all hydrogels conditions elicited no acute inflammatory response. H&E staining of histological sections also revealed a homogeneous distribution of the cells within the matrix, with the cells exhibiting the common round-shaped phenotype characteristic. While no signs of acute inflammation response could be detected, a thin (40-48 μm) fibrotic capsule, as an indication of chronic inflammation, was observed around all the implants. However, there were no polymorphonuclear and mononuclear cells visible, and no significant differences were observed between the different hydrogel conditions. The *in vivo* performance of these hydrogels, along with previous data, suggests that both HA, Dex, and the hybrid hydrogels are suitable for injectable applications in cartilage regeneration approaches with good *in vivo* safety and biocompatibility.

However, it should be noticed that some differences in foreign body reaction to the hydrogel matrix was observed after four weeks. For instance, hydrogels laden with either chondrocytes or MSCs induced some tissue reaction, particularly in the hydrogels composed of HA-TA only. Moreover, the foreign body giant cells, a typical feature of the foreign body reaction, were only observed in somewhat larger numbers in mono-culture cells encapsulated hydrogels with HA. In this case, the encapsulation of MSCs did not elicit the formation of foreign body giant cells, as previously reported[26,27]. Nevertheless, pure Dextran-TA hydrogels encapsulated with mono-culture cells showed moderate tissue reaction in the matrix and less giant cells formation. Besides, hydrogels with HA showed a maze-like structure in the mono-culture environment. This performance can be explained by the degradation of HA *in vivo*. HA is a major component of the cartilage extracellular matrix and exhibits rapid erosion and degradation behaviors *in vivo* due to its high water-absorbing properties and enzymatic degradation[28]. The space left after HA degradation promotes the surrounding tissue invasion and may explain the infiltration of foreign body giant cells. Moreover, HA/Dex constructs show significantly depressed nuclei visibility compared to other conditions. Most of the cells in the HA/Dex gels stained pink while nuclei were barely visible, regardless of the cell type encapsulated. This performance can be explained by different reasons. First, HA/Dex hydrogels may have had a negative impact on the viability

of encapsulated cells, regardless of the cell type. Cellularity analysis indeed show that a lot of cells with damaged nuclei are present in the HA/Dex constructs. Second, the *in vivo* environment in the male rats probably increased the size of encapsulated cells in HA/Dex constructs, which impacts the sectioning and in turn affects the staining results.

Interestingly, all these performances were attenuated in the co-culture environment. No tissue reaction and giant cell formation was observed in hydrogels laden with both bCH and hMSCs. Our previous studies demonstrated the beneficial interactions between the cells in Chondrocyte-MSC co-cultures. The *in vivo* performance indicated that this beneficial interaction also affects the performance of hydrogels compared to hydrogels laden with either MSCs or bCH. The underlying mechanism and potential role of this interplay between cells and biomaterials need further investigation.

Moreover, enhanced newly formed cell clusters were observed in pure Dextran-TA encapsulated co-cultures, which indicated that Dex-TA hydrogel provides the environment to support the beneficial interactions in Chondrocyte-MSC co-cultures. Besides, only hydrogels encapsulated with co-cultures present positively deposition of cartilage matrix. Notably, coherent with the *in vitro* study, intense deposition of type II collagen was observed in pure Dextran-TA hydrogels with co-cultures. In conclusion, together with previous studies results, modification of HA with a higher concentration of Dextran-TA provides the opportunity to create optimal biomaterials for the cartilage tissue regeneration and Chondrocyte-MSC co-cultures stimulate interaction with these hydrogels. These data suggest that further study *in situ* is needed for the development of a fully functional cartilage tissue-engineered construct that can be applied clinically. It should be noted though that the subcutaneous implantation site may have influenced the outcome in cartilage matrix production. It seems feasible that orthotopic implantation may facilitate cartilage matrix production over the subcutaneous implantation site. Additionally, different combinations of hydrogel and cells showed distinct differences in mechanical properties, degradation, and chondro-induction features. These properties are important considerations in the design of precision biomaterials to enable the survival, differentiation, and transplantation of biomaterial-cell-based combination approaches. With the growing interest in personalized therapeutic approaches[29,30], combination therapies have vital potential for their ability to sense and respond to the therapeutic needs of individual patients. The different outcomes of the *in vivo*

performance in this work highlight the potential application in personalized regeneration based on the situation of individual patients.

Animal models are essential to assess the value of current and future tissue-engineering therapies, which play a critical role in many domains of study in medicine and biology[31]. Multiple factors need to be considered in selecting an appropriate animal model, such as animal size, age, gender, economic cost, ethical concerns, and potential of clinic transition. In this work, we investigate the impact of gender differences on our injectable hydrogels for cartilage tissue engineering. The histological assessment indicated that the gender of the host has an effect on the performance of the implanted hydrogels. However, the impact is mainly on the hydrogels encapsulated with chondrocytes but not the MSCs. Due to the space limitation in this study, we only chose cell laden HA/Dex hydrogels. Further studies need to process on the animals with normal immune system and other hybrid hydrogels to check if there's any outcomes change.

In this work, the evaluation of the *in vivo* response upon subcutaneous implantation of Hyaluronic acid and Dextran hybrid hydrogels was conducted in nude rats, revealing proper integration with the surrounding tissues and the presence of a residual fibrotic capsule. Moreover, the *in vivo* performance revealed the interaction of Chondrocyte-MSC co-cultures with biomaterials, suggesting their further study towards the development of functional cartilage tissue-engineered constructs for personalized application. Taken together, the results from this work, along with previous data, has shown that 5%w/v Dex-TA hydrogels laden with Chondrocyte-MSC co-cultures provide an adequate support matrix for chondro-induction between MSC and bCH co-cultures stimulating cartilage matrix formation.

References

1. Mankin, H.J. The response of articular cartilage to mechanical injury. JBJS. LWW, **64**, 460, 1982.
2. Hunter, W. Of the structure and disease of articulating cartilages. Clin Orthop Relat Res. LWW, **317**, 3, 1995.
3. Newman, A.P. Articular cartilage repair. Am J Sports Med. Sage Publications Sage CA: Los Angeles, CA, **26**, 309, 1998.
4. Ekenseair, A.K., Kasper, F.K., and Mikos, A.G. Perspectives on the interface of drug delivery and tissue engineering. Adv Drug Deliv Rev. Elsevier, **65**, 89, 2013.
5. Klouda, L., and Mikos, A.G. Thermoresponsive hydrogels in biomedical applications. Eur J Pharm Biopharm. Elsevier, **68**, 34, 2008.
6. Tan, H., and Marra, K.G. Injectable, biodegradable hydrogels for tissue engineering applications. Materials (Basel). Molecular Diversity Preservation International, **3**, 1746, 2010.
7. Van Tomme, S.R., Storm, G., and Hennink, W.E. In situ gelling hydrogels for pharmaceutical and biomedical applications. Int J Pharm. Elsevier, **355**, 1, 2008.
8. Jeong, B., Kim, S.W., and Bae, Y.H. Thermosensitive sol–gel reversible hydrogels. Adv Drug Deliv Rev. Elsevier, **64**, 154, 2012.
9. Neffe, A.T., Pierce, B.F., Tronci, G., Ma, N., Pittermann, E., Gebauer, T., et al. One step creation of multifunctional 3D architectured hydrogels inducing bone regeneration. Adv Mater. Wiley Online Library, **27**, 1738, 2015.
10. Jin, R., Moreira Teixeira, L.S., Dijkstra, P.J., van Blitterswijk, C.A., Karperien, M., and Feijen, J. Enzymatically-crosslinked injectable hydrogels based on biomimetic dextran-hyaluronic acid conjugates for cartilage tissue engineering. Biomaterials [Internet]. Elsevier Ltd, **31**, 3103, 2010.
11. Sheikh, Z., Brooks, P.J., Barzilay, O., Fine, N., and Glogauer, M. Macrophages, foreign body giant cells and their response to implantable biomaterials. Materials (Basel). Multidisciplinary Digital Publishing Institute, **8**, 5671, 2015.
12. Babensee, J.E., Anderson, J.M., McIntire, L. V, and Mikos, A.G. Host response to tissue engineered devices. Adv Drug Deliv Rev. Elsevier, **33**, 111, 1998.
13. Morais, J.M., Papadimitrakopoulos, F., and Burgess, D.J. Biomaterials/tissue interactions: possible solutions to overcome foreign body response. AAPS J. Springer, **12**, 188, 2010.
14. Anderson, J.M., and McNally, A.K. Biocompatibility of implants: lymphocyte/macrophage interactions. Semin Immunopathol. Springer, pp. 221–33, 2011.
15. Luttikhuizen, D.T., Harmsen, M.C., and Luyn, M.J.A. Van. Cellular and molecular dynamics in the foreign body reaction. Tissue Eng. Mary Ann Liebert, Inc. 2 Madison Avenue Larchmont, NY 10538 USA, **12**, 1955, 2006.
16. Anderson, J.M., Rodriguez, A., and Chang, D.T. Foreign body reaction to biomaterials. Semin Immunol. Elsevier, pp. 86–100, 2008.
17. Sharkawy, A.A., Klitzman, B., Truskey, G.A., and Reichert, W.M. Engineering the tissue which encapsulates subcutaneous implants. II. Plasma–tissue exchange properties. J Biomed Mater Res An Off J Soc Biomater Japanese Soc Biomater Aust Soc Biomater. Wiley Online Library, **40**, 586, 1998.
18. Ratner, B.D. Reducing capsular thickness and enhancing angiogenesis around implant drug release systems. J Control Release. Elsevier, **78**, 211, 2002.
19. Zhang, L., Cao, Z., Bai, T., Carr, L., Ella-Menye, J.-R., Irvin, C., et al. Zwitterionic hydrogels implanted in mice resist the foreign-body reaction. Nat Biotechnol. Nature Publishing Group, **31**, 553, 2013.
20. Langer, R. Perspectives and challenges in tissue engineering and regenerative medicine. Adv Mater. Wiley Online Library, **21**, 3235, 2009.
21. Hendriks, J., Riesle, J., and Vanblitterswijk, C.A. Effect of stratified culture compared to confluent culture in monolayer on proliferation and differentiation of human articular chondrocytes. Tissue Eng. Mary Ann Liebert, Inc. 2 Madison Avenue Larchmont, NY 10538 USA, **12**, 2397, 2006.
22. Fernandes, H., Dechering, K., Van Someren, E., Steeghs, I., Apotheker, M., Leusink, A., et al. The role of collagen crosslinking in differentiation of human mesenchymal stem cells and MC3T3-E1 cells. Tissue Eng Part A. Mary Ann Liebert, Inc. 140 Huguenot Street, 3rd Floor New Rochelle, NY 10801

USA, **15**, 3857, 2009.
23. Ramirez, J.C., Sánchez-Chaves, M., and Arranz, F. Dextran functionalized by 4-nitrophenyl carbonate groups. Aminolysis reactions. Die Angew Makromol Chemie Appl Macromol Chem Phys. Wiley Online Library, **225**, 123, 1995.
24. Yu, F., Cao, X., Li, Y., Zeng, L., Yuan, B., and Chen, X. An injectable hyaluronic acid/PEG hydrogel for cartilage tissue engineering formed by integrating enzymatic crosslinking and Diels–Alder "click chemistry." Polym Chem. The Royal Society of Chemistry, **5**, 1082, 2013.
25. Hoffman, A.S. Hydrogels for biomedical applications. Adv Drug Deliv Rev. Elsevier, **64**, 18, 2012.
26. Bartosh, T.J., Ylöstalo, J.H., Mohammadipoor, A., Bazhanov, N., Coble, K., Claypool, K., et al. Aggregation of human mesenchymal stromal cells (MSCs) into 3D spheroids enhances their antiinflammatory properties. Proc Natl Acad Sci. National Acad Sciences, **107**, 13724, 2010.
27. Aggarwal, S., and Pittenger, M.F. Human mesenchymal stem cells modulate allogeneic immune cell responses. Blood. American Society of Hematology, **105**, 1815, 2005.
28. Burdick, J.A., and Prestwich, G.D. Hyaluronic acid hydrogels for biomedical applications. Adv Mater. Wiley Online Library, **23**, H41, 2011.
29. Oliva, N., Unterman, S., Zhang, Y., Conde, J., Song, H.S., and Artzi, N. Personalizing biomaterials for precision nanomedicine considering the local tissue microenvironment. Adv Healthc Mater. Wiley Online Library, **4**, 1584, 2015.
30. Aguado, B.A., Grim, J.C., Rosales, A.M., Watson-Capps, J.J., and Anseth, K.S. Engineering precision biomaterials for personalized medicine. Sci Transl Med. American Association for the Advancement of Science, **10**, 2018.
31. Ahern, B.J., Parvizi, J., Boston, R., and Schaer, T.P. Preclinical animal models in single site cartilage defect testing: a systematic review. Osteoarthr Cartil. Elsevier, **17**, 705, 2009.

8.5 Supplementary materials

8.5.1 Synthesis of dextran-p-nitrophenyl carbonate

LiCl (4.0 g, dried at 115 °C) and dextran (5.00 g, 30.8 mmol r.u.) are weighed into a 500 mL three necked round bottom flask equipped with a stirrer bar. The flask is evacuated and refilled with nitrogen 3 times, after which it is left under vacuum at 95 °C for 1.5h. After thoroughly drying, the flask was filled with nitrogen and 200 mL of anhydrous DMF was added *via* a cannula while stirring. The flask was then equipped with a thermometer and the mixture was heated to 95 °C while stirring the solution. Once the dextran was completely dissolved, the solution was cooled to 0 °C and anhydrous pyridine (2.0 ml, 25.8 mmol) was added. Subsequently, freshly sublimed para-nitrophenyl chloroformate (2.5 g, 12.4 mmol) was added in small portions, while keeping the temperature below 2 °C. After 1 hour, the reaction mixture was poured into 1 L of ice-cold ethanol. The precipitate was filtered off (Por 4) and washed with cold ethanol (3×100 mL) and subsequently with diethyl ether (3×100 mL). After drying under vacuum, the product was obtained as a white powder (6.00 g, 30.7 mmol r.u., 99 % yield, DS20%). 1H-NMR (400 MHz, DMSO-d6): δ(ppm) = 3.0-4.0 (saccharide ring protons, m, 6H); 4.2-5.8 (anomeric and hydroxyl protons, m, 4H); 7.58 (Ar o-CH, d, 2H); 8.34 (Ar m-CH, d, 2H).

8.5.2 Synthesis of dextran-tyramine

Dextran-PNC (6.00 g, 30.7 mmol r.u., 6.15 mmol p-nitrophenyl carbonate) was weighed into a 250 mL three necked round bottom flask equipped with a stirrer bar. The flask was evacuated and refilled with nitrogen 3 times, after which the flask was filled with nitrogen and 100 mL of anhydrous DMF was added via a cannula while stirring. Once the dextran was completely dissolved, tyramine (1.69 g, 12.3 mmol) was added. After 1 hour, the reaction mixture was poured into 1 L of ice-cold ethanol. The precipitate was filtered off (Por 4) and washed with cold ethanol (3×100 mL) and subsequently with diethyl ether (3×100 mL). After drying under vacuum, the crude product was obtained as a white powder. The crude product was dissolved in 75 mL of Milli-Q water and dialysed against Milli-Q water for 3 days (MWCO 3500 Da), followed by filter sterilization and freeze-drying yielding the product as a white foam (5.04 g, 28.0 mmol, 92 % yield, DS10%). 1H-NMR (400 MHz, DMSO-d6): δ(ppm) = 3.0-4.0 (saccharide ring protons, m, 6H); 4.2-5.8 (anomeric and hydroxyl protons, m, 4H); 6.67 (Ar m-CH, d, 2H); 6.99 (Ar o-CH, d, 2H).

The calculation of the DS of dextran-TA and dextran-PNC is based on the integrals of 4.2-5.8 ppm (corresponding to the 4 anomeric protons from dextran), compared with the integral of the aromatic protons of tyramine (6.60-6.75 and 6.90-7.07) or para-nitrophenyl (7.40-7.65 and 8.20-8.40). The DS of dextran is given as the percentage of saccharide units modified in dextran.

8.5.3 Synthesis of hyaluronic acid-tyramine

Sodium hyaluronate (5.00 g, 12.5 mmol r.u.) was dissolved in 500 mL Milli-Q water in a 1 L round bottom flask equipped with a stirrer bar. While stirring at room temperature, 4-(4,6-dimethoxy-1,3,5-triazin-2-yl)-4-methylmorpholinium chloride (DMTMM, 3.46 g, 12.5 mmol, 1eq) and tyramine hydrochloride (TA·HCl, 2.17 g, 12.5 mmol, 1eq) were added subsequently. The addition of DMTMM and TA·HCl was repeated after 24 and 48 hours. After 72 hours, 40 mL NaCl (sat) was added to the reaction mixture and the reaction mixture was poured into 2.5 L cold ethanol. The crude product was isolated by centrifugation at 5000 rpm followed by drying in vacuo. The crude product was dissolved in 75 mL Milli-Q water and dialysed against Milli-Q water for 3 days (MWCO 1000 Da). Filter sterilization and lyophilization yielded the product as a white foam (5.10 g, 12.4 mmol, 99 % yield, DS10%). 1H-NMR (400 MHz, D2O): δ(ppm) = 1.98 (acetyl-CH3, s, 3H); 2.75 (2-CH2, s, 2H); 2.90 (1-CH2, s, 2H); 3.2-4.2 (saccharide ring, m, 10H); 4.34 (s, 1H); 4.43 (d, 1H); 6.84 (Ar m-CH, d, 2H); 7.16 (Ar o-CH, d, 2H).

The degree of substitution (DS) was calculated based on the integral of the methyl group at 1.98 ppm is compared to the integral of the tyramine signals at 6.80-6.87 and 7.10-7.21 ppm. The DS of hyaluronic acid is given as the percentage of COOH groups modified in hyaluronic acid (*i.e.* per disaccharide).

Chapter 9

Reflection and Outlook

9.1 Cell communication between Mesenchymal Stem Cells and chondrocytes

9.1.1 Cellular interactions in Chondrocyte-MSC co-cultures

It is vital to develop and improve the quality of tissue obtained during tissue engineering. Meanwhile, tissue development, repair, and regeneration are the results of cellular interactions, which most likely involves cell-cell communication. Cells do communicate with each other in the cellular environment, and cellular behaviors are integrated to maintain tissue homeostasis and perform physiological functions. Cell-cell interactions mediated between the different cell types, secreted paracrine factors, and extracellular matrix components are vital in new tissue formation mechanisms. However, the basic principle that lies in these cellular interactions is not clear. One of the most definite tools for studying the cellular interaction during normal physiology, homeostasis, repair, and regeneration is the co-culture system. The co-culture system aims to mimic the organization and complexity of the *in vivo* cellular environment, thereby facilitating the bio-stimulation of cells and influencing their biological function and behavior. In cartilage tissue engineering, the amount of cartilage matrix produced in Chondrocyte-MSC co-cultures is at least equal or even higher than that in monoculture of chondrocyte or MSCs. Co-culture can overcome many problems for basic and clinical applications, including the dedifferentiation of expanded chondrocytes, hypertrophy of induced MSCs, and regeneration of both cartilaginous and surrounding tissue[1]. However, the co-culture approach for cartilage tissue engineering is not fully ready for clinical use since the underlying mechanisms of intercellular interactions are still unclear.

When different types of cells are co-cultured, they can communicate in various ways, depending on their neighboring cells and mutual ability to interact. Cellular communication can be performed by direct connection (cell to cell physically contact) between adjacent cells, through membrane molecules and gap junctions, along with indirect contact (paracrine signaling), which requires diffusible factors spreading through the extracellular matrix. Understanding the cellular communication pathways in co-cultures and how cellular interactions are regulated is essential for tissue formation. It could contribute significantly to the cartilage engineering and help to the improvement of existing therapies and development of new regenerative strategies. Therefore, in the first part of this thesis, we tried to discuss the cellular interactions in Chondrocyte-MSC co-cultures and improve our fundamental understanding of the mechanisms leading to chondral regeneration.

Numerous questions remain about what happens in the co-culture systems, including i) how the cells perform the indirect interaction in the co-culture system? ii) what the role is of the disappearance of MSCs in Chondrocyte-MSC co-cultures? iii) whether direct cellular communication or trophic factors only or a combination of the above, play the predominant role in co-cultures?

9.1.2 Extracellular vesicles in Chondrocyte-MSC communication

In *Chapter 3*, along with previous works from our group, we demonstrated that MSCs act as trophic mediators through secreted factors to promote proliferation and delay the dedifferentiation of chondrocytes in co-cultures. Moreover, these features are independent of the sources, growth environment, and donor variation of the cells. Recent studies indicated that the secreted factors, including peptides/proteins, lipids, DNA, mRNAs, miRNAs, and LncRNAs, are conveyed by extracellular vesicles (EVs). As reviewed in *Chapter 2*, EVs are cytosol fragments with spherical morphology, surrounded by a membrane composed of a lipid bilayer and hydrophilic proteins, similar to the cell plasma membrane. EVs are a heterogeneous group of vesicles and include exosomes, microvesicles, and apoptotic bodies. Cell communication utilizing EVs is considered a universal way for cells to interact with each other and influence the behavior of other neighboring cells by exchanging material and information. Indeed, EVs can stimulate target cells and induce alterations in the phenotype and behavior of recipient cells.

In the Chondrocyte-MSC co-cultures, EVs have been widely considered an essential factor in cell-to-cell communication[2]. EVs secreted by MSCs were shown to modulate the microenvironment of the synovial cavity and mediate chondrocyte migration, proliferation, and matrix deposition[3,4]. MSC-EVs could increase the expression of typical chondrogenic markers while inhibiting catabolic and inflammatory markers *in vitro*[5,6]. Moreover, MSC-EVs stimulated repair of osteochondral defects in animal models and protected mice from joint damage, which involved increased cellular proliferation and infiltration[6,7]. MicroRNA (miR)-140-5p and miR-135b transferred by MSC-EVs were demonstrated to stimulate chondrocyte proliferation and migration *in vitro* and attenuate symptoms of osteoarthritis (OA) *in vivo*[3,8]. In line with the enhanced proliferation of chondrocytes in co-culture, MSC-EVs were also shown to protect chondrocytes from apoptosis and inhibit macrophage activation[6,7,9]. MSC-EVs could activate AKT/ERK pro-survival signaling pathway for tissue regeneration by rapid phosphorylation of AKT/ERK in chondrocytes and subsequently promoting cell

proliferation as well as migration[7,10]. Meanwhile, MSC-EVs have been reported that inhibit the expression of the pro-apoptosis protein Bcl-2-associated X protein (BAX) and pro-inflammatory cytokines, tumor necrosis factor-α (TNF-α) and interleukin (IL)-1β, while enhancing the expression of the anti-apoptosis protein B-cell lymphoma 2 (BCL2)[5,11].

In the second scenario, as shown in *Chapter 3*, MSCs might still be induced into chondrogenic differentiation by the chondro-induction of chondrocytes, which indicated that the interaction between the cells could be bidirectional. Indeed, chondrocytes were shown to release EVs to nearby MSCs, which induce the synergistic effect of co-culture and promote functional differentiation and improved matrix production[12]. Moreover, bidirectional EVs treatments increased proliferation of both chondrocytes and MSCs, and similar bidirectional influences, including enhanced chondrogenic differentiation and promoted cartilage matrix deposition in both cell populations[13]. However, the effects of EVs released by chondrocytes on other cells depend on the state of the chondrocyte[14], which raises the question whether the release of EVs is cell-type specific and influenced by the state of the donor cell, the stimuli that modulate their production, and the molecular mechanism that leads to their biogenesis.

EVs isolated from MSCs have been reported to have therapeutic and regenerative potentials and may be more advantageous for therapeutic use. Compared with MSCs, EVs are more stable and reservable, avoid the potential safety, regulatory and practicality issues of cellular incorporation, with a lower possibility of immune rejection following allogeneic administration[15]. However, many questions still remain that need to be investigated. Further studies need to explore whether the secretion of EVs is a selective on-demand secretion or rather the consequence of a random release. To dig detailed mechanisms at the molecular level, it will be essential to determine the specific molecular factors mediating the co-culture effect, and which of these are conveyed exclusively by EVs.

Furthermore, long-distance, which probably reduces communication efficiency, is still a limiting factor for intercellular interaction. Thus, there are still opposite opinions about the role of direct and indirect contact in cellular communication. To understand the mechanisms of recognition and internalization of EVs by recipient cells, future experiments are necessary to identify whether the EVs influence cell functionality directly (by providing missing components to the recipient cells) or

indirectly (by reactivating related pathways). Besides, it would be better to develop a practical approach for standardized sample processing and EVs isolation.

9.1.3 Cell death pathways in Chondrocyte-MSC communication

The decreasing amount of MSCs is also an interesting and still poorly understood observation in the co-culture system. Our studies indicated that the decrease in MSCs is a general phenomenon, which is also independent of cell source, growth conditions, and donor variation. There are two major mechanisms involved in the regulation of cell death, apoptosis and autophagy, which have shown cross-talking network between the signaling pathways of both these processes. Nevertheless, how autophagy and apoptosis are mechanistically interconnected with each other remains unclear.

Apoptosis is one of the most fundamental cellular behaviors that remove unnecessary or potentially harmful cells by activating a genetically encoded suicide program. Apoptosis can be driven by either intrinsic or extrinsic pathways in mammals. Mitochondria secrete cytochrome c (Cyt c), which interacts with Apaf-1 and pro-caspase-9 to form an apoptosome to activate effector caspases, such as Caspase-3 and Caspase-7. Extrinsic apoptosis occurs *via* initiator caspase-8 and requires the activation of cell death ligand and receptor signaling (such as TNFα and Fas). Recent *in vivo* genetic studies have revealed that apoptotic cells actively modulate the proliferation of surrounding cells and morphogenetic changes of neighbors. These interactions between apoptotic cells and surrounding cells contribute to the maintenance of tissue homeostasis[16,17]. Apoptotic bodies, as one type of EVs mentioned above, have been suggested to have similar characteristics to EVs formed from healthy cells in terms of cargo delivery to recipient cells, such as apoptotic byproducts from apoptotic clearance, and immune regulation concerning what molecular cargoes are carried.

Autophagy is a conserved intracellular degradation pathway that traffics substrates, including bulk cytoplasm, damaged organelles, long-lived proteins, and infectious agents to lysosomes[18]. Autophagy serves as a regulator of homeostasis, effectively preserving the balance between cellular components' production, and the breakdown of damaged or unnecessary organelles and other cellular constituents[19,20]. There is an interplay network between apoptosis and autophagy processes[21,22]. Apoptosis regulators, such as BCL family proteins, can regulate the autophagy process, while autophagy can also control the timing and efficiency of apoptosis[23,24].

Of note, autophagy can also determine whether cells die by regulating non-apoptotic cell death directly where there is no need for caspase activation.

Recent studies indicated that apoptosis and autophagy mechanisms are indeed intimately linked while the basis for autophagy influencing cell-fate decisions depends on the death stimulus, cell type, and proteins that recruited to autophagosomes for lysosomal degradation[21]. The complex crosstalk between apoptosis and autophagic cell death underlies the pathogenesis of multiple diseases. In this thesis, only limited work has been done to investigate the cell death network in the Chondrocyte-MSC co-cultures. We found that both apoptosis and autophagy pathways are involved in the death of MSCs in co-culture with chondrocytes. Meanwhile, the interaction between these two types of cells modifies the cell response to the pathway modulators. There is much more that needs to be done and many remaining questions to be answered. For instance, does the autophagy induced by cell death stimuli have a functional effect on cell death? What are the consequences of inhibiting early- or late-stage autophagy on cell death? What type of information is transmitted from cells undergoing cell death to live cells in the vicinity?

9.1.4 cell-laden microgel system for cellular interaction investigation

Cellular communication between cells can be performed through direct or indirect contact pathways. The trophic effects of MSCs demonstrated that cell-cell communication between MSC and chondrocyte without direct contact could activate cellular responses and subsequently influence cartilage tissue regeneration. In opposite, some researchers believe that physical contact of the cells is predominant in co-cultures.

In *Chapter 4*, with the help of a micro-aggregates co-culture system, we have shown that both interaction pathways are involved in the cell-cell communication in Chondrocyte-MSC co-cultures, while each of them focuses on different cellular behavior changes. Micro-aggregates of cells presented enhanced chondrogenic gene expression and matrix deposition, compared to single cell seeded constructs. High stability and formation characteristics micro-aggregates encapsulations can be harvested utilizing a high throughput platform. Different co-culture models can be formed to study the cellular interactions among the systems.

However, during the experiment period, some drawbacks of this model were identified. First, the harvest efficiency of micro-aggregates is not guaranteed since the cell aggregations are tightly attached to the surface of the agarose chip. Second, we encapsulated the micro-aggregated into 3% agarose, following the previous guidelines in our group. However, agarose is a thermosensitive hydrogel which sets fast preventing homogenous distribution of the micro-aggregates in the gel. This obstacle limits the application of micro-aggregate co-culture system in the cellular interaction investigation and the further application in the cartilage tissue regeneration.

To overcome these limitations, a cell-laden microgel system serves as an approach to study the cellular response. Microgel can promote efficient mass transport and improves cell-matrix interactions, thereby maintaining the long-term viability of the encapsulated cells. The cell-laden microgels have been utilized as building blocks for a wide range of studies, including those seeking to understand cell differentiation, cell-cell communications, cell-matrix interactions, external shear stress imposed on cells, and the functioning of mesoscale tissue structures[25,26]. Besides, growth factors that influence the cellular behavior and cellular interactions can be incorporated into the microgels to investigate the functions of such factors in a relevant microenvironment. Utilizing injectable biomaterials, aggregates or even single cell can be easily incorporated into the microgels by using the microfluidic methods.

Microfluidics is the process of precise manipulation of fluids in channels and chambers at micron-level sizes[27]. With this method, it is possible to produce composite microgels that carry different cell types. Indeed, microfluidic technologies have been used to generate monodisperse cell-laden microgels with varying properties in a high throughput manner. Moreover, microfluidic technologies offer the ability to control the encapsulation process, the desired number of cells per particle, cellular spatial manipulation, cellular morphological and dimensional properties[28]. To conclude, microfluidics-generated cell-laden microgel will be a powerful tool and set of techniques for controlling and investigating cell-cell interactions on different levels of complexity, such as single cells as well as small populations.

9.2 Modification of injectable hydrogels for cartilage tissue regeneration

Injectable hydrogels have attracted increasing attention due to convenient clinical operation, non-invasive surgical procedures, and seamless filling of irregular

defects[29]. In the meanwhile, injectable scaffolds can also sustain drug release and extend the drug retention time. As investigated in *Chapter 7*, molecular weight and precursor concentration significantly affected physiochemical properties and biological functions of hydrogels. An ideal injectable scaffold for cartilage regeneration is expected to provide adequate mechanical strength, has a controlled degradability and provides adhesion, and integration with the surrounding native tissue, while mimicking natural ECMs functions, allowing for nutrient diffusion and promoting cell survival and differentiation. Thus, the modification of the injectable hydrogel system, including suitable incorporation composites and suitable cell encapsulation method for mechanical properties and biological functions of hydrogels, is vital for the application of injectable hydrogel in the cartilage tissue regeneration.

Native cartilage is one of the most chondro-inductive scaffolds for cell differentiation. Recent studies have demonstrated that decellularized ECM is a more appropriate scaffold for tissue engineering and regenerative medicine applications[30,31]. Decellularized ECM, which containing growth factors, GAGs as well as proteins, could provide a suitable microenvironment for cultured cells comparable to that of native tissues. The injectable hydrogel obtained from decellularized ECM can promote cell viability, proliferation, and differentiation. Moreover, as a major component of the cartilage ECM, collagens have adequate biocompatibility, biodegradability, and a low immunogenic profile. The collagen type I (Col I) could improve cell adhesion and proliferation and enhance multiple gene expression levels associated with hyaline cartilage formation[32,33]. Col I had been incorporated into hydrogels to induce MSCs differentiation and secretion of a large amount of collagen type II, and promote hyaline cartilage formation and regeneration[34,35]. The results indicated that Col I hydrogel could provide a suitable microenvironment and aggregate the signal molecules for chondrogenesis. Hence, injectable hydrogel combined with Col I to construct biomimetic hybrid hydrogel would be a potential strategy for cartilage tissue regeneration.

MSC differentiation was shown to depend on the stiffening induction time of hydrogels with earlier stiffening times favoring osteogenesis and later times favoring adipogenesis[36]. Nanocomposites have been utilized to vary the mechanical properties of hydrogel scaffolds[37]. To improve the mechanical property, biological activity, and biomimetic function, functional nanoparticles (NPs) or nanostructures

have been incorporated into the injectable bulk hydrogel[38,39]. Several nanomaterials have been developed as injectable scaffolds to mimic the ECM of cartilage[40–43]. Nanocomposites with large surface area-to-volume ratios can not only provide enhanced mechanical properties but also improve the surface reactivity and components encapsulating efficiencies. In this regard, nanoparticles have also been investigated in scaffolds for the controllable delivery of drugs and growth factors to enhance the efficiency and duration of delivery[44–47].

Microencapsulation of cells, as microparticles in hydrogels, is another strategy to deliver cells for long-term therapeutic delivery successfully. The controlled release of bioactive factors from microgels has demonstrated their capabilities as transporters for essential bioactive molecules for guiding tissue reconstruction[48]. Thus, microgels combination with bulk hydrogels or directly injectable microgels alone have attracted attention due to microgel can provide a suitable environment for the cells[49,50]. Microgels containing stem cells can protect the encapsulated cells from shear stress damage during injection, facilitate efficient nutrient and waste exchange, and provide a suitable environment for tissue regeneration. Microgels can also serve as a platform for microscale tissue culturing in a 3D microenvironment, which can mimic *in vivo* native tissues more accurately and is more suitable for upregulating cell functionality. As mentioned in the above section, microfluidic techniques have been applied to encapsulate cells within microgels in a high throughput manner, making cell-laden microgel as suitable building blocks that can be assembled into tissue constructs with functions that closely mimic those of native tissue[51,52]. Cells in the microgels have exhibited high mobility, long-term viability, and enhanced chondrogenic gene and protein expression. The use of microgels in tissue regeneration could be a promising approach for clinical scenarios where complex biomaterial structures and various cells and factors delivery modulation may be required.

As another type of microencapsulation, extracellular vesicles (EVs) act as messengers and transfer various biomolecules to regulate the function of neighboring cells, as mentioned above in the context of intercellular communication. These vesicles can induce cell migration and homing when they were encapsulated into PLGA scaffolds. However, a major problem with this application is limitations in engraftment and rapid clearance rate of the EVs in the target site. In this regard, injectable hydrogels have recently been utilized to encapsulate a large amount of EVs and release them in a controllable manner to the target site[53]. Hydrogel-

encapsulated EVs delivery system has provided a new approach for tissue regeneration therapy. However, further studies need to be performed to answer some other questions, such as which hydrogels are suitable for delivering the EVs? Or what composites in the hydrogel are suitable to load and release them in a desirable manner? Moreover, to dig detailed mechanisms, as mentioned in the above section, it is essential to determine the specific growth factors conveying exclusively by EVs that mediate the biofunction.

The role of growth factors (GFs) is crucial in encouraging stem cell differentiation, maintaining cell viability, and promoting matrix synthesis and deposition[54]. Most cartilage tissue engineering approaches rely on the pre-culture of scaffolds in medium containing growth factors such as Transforming growth factor (TGF)-β, which are crucial for cartilage formation and homeostasis. A system where the GF is unbound and quickly diffuses into the surrounding environment may not provide sufficient chondrogenic stimulation. Thus, in all of the above advances in injectable hydrogels, controlled supplementation and delivery of the GFs is required to ensure their bioavailability. Advanced biomaterials or compositions capable of binding suitable GFs would be beneficial for the application of injectable hydrogel. There are several strategies for loading GFs on a scaffold for delivery[55,56]. Bioactive factors can be loaded directly by physical crosslinking, which is probably leading to a burst release, or encapsulated into a carrier such as particles, microgels, and EVs to obtain the desired sustained release profile. Meanwhile, there are various types of GF families involved in cartilage tissue regeneration, which is already summarized in previous literatures[57,58]. Several studies have shown that hydrogels loaded with GFs would promote cell proliferation and migration and cartilage regeneration[59–62]. Synthetic peptides could also be introduced into the system to mimic the desirable signals provided by growth factors and induce chondrogenesis without the need for a tissue-derived matrix[63]. Besides, natural materials such as ECM and Platelet lysate (PL)[64], which contains a cocktail of autologous growth factors and biochemical signals, would be autologous sources of growth factors and stimuli.

Reference

1. Zhang, Y.; Guo, W.; Wang, M.; Hao, C.; Lu, L.; Gao, S.; Zhang, X.; Li, X.; Chen, M.; Li, P. Co-culture Systems-based Strategies for Articular Cartilage Tissue Engineering. *J. Cell. Physiol.* **2018**, *233*, 1940–1951.
2. Van Niel, G.; d'Angelo, G.; Raposo, G. Shedding Light on the Cell Biology of Extracellular Vesicles. *Nat. Rev. Mol. cell Biol.* **2018**, *19*, 213.
3. Tao, S.-C.; Yuan, T.; Zhang, Y.-L.; Yin, W.-J.; Guo, S.-C.; Zhang, C.-Q. Exosomes Derived from MiR-140-5p-Overexpressing Human Synovial Mesenchymal Stem Cells Enhance Cartilage Tissue Regeneration and Prevent Osteoarthritis of the Knee in a Rat Model. *Theranostics* **2017**, *7*, 180.
4. Zhu, Y.; Wang, Y.; Zhao, B.; Niu, X.; Hu, B.; Li, Q.; Zhang, J.; Ding, J.; Chen, Y.; Wang, Y. Comparison of Exosomes Secreted by Induced Pluripotent Stem Cell-Derived Mesenchymal Stem Cells and Synovial Membrane-Derived Mesenchymal Stem Cells for the Treatment of Osteoarthritis. *Stem Cell Res. Ther.* **2017**, *8*, 1–11.
5. Vonk, L. A.; van Dooremalen, S. F. J.; Liv, N.; Klumperman, J.; Coffer, P. J.; Saris, D. B. F.; Lorenowicz, M. J. Mesenchymal Stromal/Stem Cell-Derived Extracellular Vesicles Promote Human Cartilage Regeneration in Vitro. *Theranostics* **2018**, *8*, 906.
6. Cosenza, S.; Ruiz, M.; Toupet, K.; Jorgensen, C.; Noël, D. Mesenchymal Stem Cells Derived Exosomes and Microparticles Protect Cartilage and Bone from Degradation in Osteoarthritis. *Sci. Rep.* **2017**, *7*, 1–12.
7. Zhang, S.; Chuah, S. J.; Lai, R. C.; Hui, J. H. P.; Lim, S. K.; Toh, W. S. MSC Exosomes Mediate Cartilage Repair by Enhancing Proliferation, Attenuating Apoptosis and Modulating Immune Reactivity. *Biomaterials* **2018**, *156*, 16–27.
8. Tofiño-Vian, M.; Guillén, M. I.; del Caz, M. D. P.; Silvestre, A.; Alcaraz, M. J. Microvesicles from Human Adipose Tissue-Derived Mesenchymal Stem Cells as a New Protective Strategy in Osteoarthritic Chondrocytes. *Cell. Physiol. Biochem.* **2018**, *47*, 11–25.
9. Qi, H.; Liu, D.-P.; Xiao, D.-W.; Tian, D.-C.; Su, Y.-W.; Jin, S.-F. Exosomes Derived from Mesenchymal Stem Cells Inhibit Mitochondrial Dysfunction-Induced Apoptosis of Chondrocytes via P38, ERK, and Akt Pathways. *Vitr. Cell. Dev. Biol.* **2019**, *55*, 203–210.
10. Zhang, S.; Teo, K. Y. W.; Chuah, S. J.; Lai, R. C.; Lim, S. K.; Toh, W. S. MSC Exosomes Alleviate Temporomandibular Joint Osteoarthritis by Attenuating Inflammation and Restoring Matrix Homeostasis. *Biomaterials* **2019**, *200*, 35–47.
11. Ni, H.; Yang, S.; Siaw-Debrah, F.; Hu, J.; Wu, K.; He, Z.; Yang, J.; Pan, S.; Lin, X.; Ye, H. Exosomes Derived from Bone Mesenchymal Stem Cells Ameliorate Early Inflammatory Responses Following Traumatic Brain Injury. *Front. Neurosci.* **2019**, *13*, 14.
12. Kim, M.; Steinberg, D. R.; Burdick, J. A.; Mauck, R. L. Extracellular Vesicles Mediate Improved Functional Outcomes in Engineered Cartilage Produced from MSC/Chondrocyte Cocultures. *Proc. Natl. Acad. Sci.* **2019**, *116*, 1569–1578.
13. Kim, Y. G.; Park, U.; Park, B. J.; Kim, K. Exosome-Mediated Bidirectional Signaling between Mesenchymal Stem Cells and Chondrocytes for Enhanced Chondrogenesis. *Biotechnol. Bioprocess Eng.* **2019**, *24*, 734–744.
14. Liu, X.; Shortt, C.; Zhang, F.; Bater, M. Q.; Cowman, M. K.; Kirsch, T. Extracellular Vesicles Released From Articular Chondrocytes Play a Major Role in Cell–Cell Communication. *J. Orthop. Res.* **2020**, *38*, 731–739.
15. Liao, Z.; Luo, R.; Li, G.; Song, Y.; Zhan, S.; Zhao, K.; Hua, W.; Zhang, Y.; Wu, X.; Yang, C. Exosomes from Mesenchymal Stem Cells Modulate Endoplasmic Reticulum Stress to Protect against Nucleus Pulposus Cell Death and Ameliorate Intervertebral Disc Degeneration in Vivo. *Theranostics* **2019**, *9*, 4084.
16. Eroglu, M.; Derry, W. B. Your Neighbours Matter–Non-Autonomous Control of Apoptosis in Development and Disease. *Cell Death Differ.* **2016**, *23*, 1110–1118.
17. Pérez-Garijo, A.; Steller, H. Spreading the Word: Non-Autonomous Effects of Apoptosis during Development, Regeneration and Disease. *Development* **2015**, *142*, 3253–3262.
18. Klionsky, D. J.; Abdelmohsen, K.; Abe, A.; Abedin, M. J.; Abeliovich, H.; Acevedo Arozena, A.;

Adachi, H.; Adams, C. M.; Adams, P. D.; Adeli, K. Guidelines for the Use and Interpretation of Assays for Monitoring Autophagy. *Autophagy* **2016**, *12*, 1–222.
19. Mindell, J. A. Lysosomal Acidification Mechanisms. *Annu. Rev. Physiol.* **2012**, *74*, 69–86.
20. Settembre, C.; Fraldi, A.; Medina, D. L.; Ballabio, A. Signals from the Lysosome: A Control Centre for Cellular Clearance and Energy Metabolism. *Nat. Rev. Mol. cell Biol.* **2013**, *14*, 283–296.
21. Fitzwalter, B. E.; Thorburn, A. Recent Insights into Cell Death and Autophagy. *FEBS J.* **2015**, *282*, 4279–4288.
22. Noguchi, M.; Hirata, N.; Tanaka, T.; Suizu, F.; Nakajima, H.; Chiorini, J. A. Autophagy as a Modulator of Cell Death Machinery. *Cell Death Dis.* **2020**, *11*, 1–12.
23. Thorburn, J.; Andrysik, Z.; Staskiewicz, L.; Gump, J.; Maycotte, P.; Oberst, A.; Green, D. R.; Espinosa, J. M.; Thorburn, A. Autophagy Controls the Kinetics and Extent of Mitochondrial Apoptosis by Regulating PUMA Levels. *Cell Rep.* **2014**, *7*, 45–52.
24. Pattingre, S.; Tassa, A.; Qu, X.; Garuti, R.; Liang, X. H.; Mizushima, N.; Packer, M.; Schneider, M. D.; Levine, B. Bcl-2 Antiapoptotic Proteins Inhibit Beclin 1-Dependent Autophagy. *Cell* **2005**, *122*, 927–939.
25. McGuigan, A. P.; Sefton, M. V. Design and Fabrication of Sub-Mm-Sized Modules Containing Encapsulated Cells for Modular Tissue Engineering. *Tissue Eng.* **2007**, *13*, 1069–1078.
26. Yanagawa, F.; Kaji, H.; Jang, Y.; Bae, H.; Yanan, D.; Fukuda, J.; Qi, H.; Khademhosseini, A. Directed Assembly of Cell-laden Microgels for Building Porous Three-dimensional Tissue Constructs. *J. Biomed. Mater. Res. Part A* **2011**, *97*, 93–102.
27. Whitesides, G. M. The Origins and the Future of Microfluidics. *Nature* **2006**, *442*, 368–373.
28. Mohamed, M. G. A.; Ambhorkar, P.; Samanipour, R.; Yang, A.; Ghafoor, A.; Kim, K. Microfluidics-Based Fabrication of Cell-Laden Microgels. *Biomicrofluidics* **2020**, *14*, 21501.
29. Ren, K.; He, C.; Xiao, C.; Li, G.; Chen, X. Injectable Glycopolypeptide Hydrogels as Biomimetic Scaffolds for Cartilage Tissue Engineering. *Biomaterials* **2015**, *51*, 238–249.
30. Xu, Y.; Li, D.; Yin, Z.; He, A.; Lin, M.; Jiang, G.; Song, X.; Hu, X.; Liu, Y.; Wang, J. Tissue-Engineered Trachea Regeneration Using Decellularized Trachea Matrix Treated with Laser Micropore Technique. *Acta Biomater.* **2017**, *58*, 113–121.
31. Tang, P.; Chauhan, A. Decellular Nerve Allografts. *JAAOS-Journal Am. Acad. Orthop. Surg.* **2015**, *23*, 641–647.
32. Yang, J.; Liu, Y.; He, L.; Wang, Q.; Wang, L.; Yuan, T.; Xiao, Y.; Fan, Y.; Zhang, X. Icariin Conjugated Hyaluronic Acid/Collagen Hydrogel for Osteochondral Interface Restoration. *Acta Biomater.* **2018**, *74*, 156–167.
33. Chen, Y.; Sui, J.; Wang, Q.; Yin, Y.; Liu, J.; Wang, Q.; Han, X.; Sun, Y.; Fan, Y.; Zhang, X. Injectable Self-Crosslinking HA-SH/Col I Blend Hydrogels for in Vitro Construction of Engineered Cartilage. *Carbohydr. Polym.* **2018**, *190*, 57–66.
34. Cai, H.; Wang, P.; Xu, Y.; Yao, Y.; Liu, J.; Li, T.; Sun, Y.; Liang, J.; Fan, Y.; Zhang, X. BMSCs-Assisted Injectable Col I Hydrogel-Regenerated Cartilage Defect by Reconstructing Superficial and Calcified Cartilage. *Regen. Biomater.* **2020**, *7*, 35–45.
35. Zhang, L.; Yuan, T.; Guo, L.; Zhang, X. An in Vitro Study of Collagen Hydrogel to Induce the Chondrogenic Differentiation of Mesenchymal Stem Cells. *J. Biomed. Mater. Res. Part A* **2012**, *100*, 2717–2725.
36. Guvendiren, M.; Burdick, J. A. Stiffening Hydrogels to Probe Short-and Long-Term Cellular Responses to Dynamic Mechanics. *Nat. Commun.* **2012**, *3*, 1–9.
37. Song, F.; Li, X.; Wang, Q.; Liao, L.; Zhang, C. Nanocomposite Hydrogels and Their Applications in Drug Delivery and Tissue Engineering. *J. Biomed. Nanotechnol.* **2015**, *11*, 40–52.
38. Jeznach, O.; Kołbuk, D.; Sajkiewicz, P. Injectable Hydrogels and Nanocomposite Hydrogels for Cartilage Regeneration. *J. Biomed. Mater. Res. Part A* **2018**, *106*, 2762–2776.
39. Coburn, J. M.; Gibson, M.; Monagle, S.; Patterson, Z.; Elisseeff, J. H. Bioinspired Nanofibers Support Chondrogenesis for Articular Cartilage Repair. *Proc. Natl. Acad. Sci.* **2012**, *109*, 10012–10017.
40. Radhakrishnan, J.; Manigandan, A.; Chinnaswamy, P.; Subramanian, A.; Sethuraman, S. Gradient

Nano-Engineered in Situ Forming Composite Hydrogel for Osteochondral Regeneration. *Biomaterials* **2018**, *162*, 82–98.
41. Boyer, C.; Figueiredo, L.; Pace, R.; Lesoeur, J.; Rouillon, T.; Le Visage, C.; Tassin, J.-F.; Weiss, P.; Guicheux, J.; Rethore, G. Laponite Nanoparticle-Associated Silated Hydroxypropylmethyl Cellulose as an Injectable Reinforced Interpenetrating Network Hydrogel for Cartilage Tissue Engineering. *Acta Biomater.* **2018**, *65*, 112–122.
42. Kuang, L.; Ma, X.; Ma, Y.; Yao, Y.; Tariq, M.; Yuan, Y.; Liu, C. Self-Assembled Injectable Nanocomposite Hydrogels Coordinated by in Situ Generated CaP Nanoparticles for Bone Regeneration. *ACS Appl. Mater. Interfaces* **2019**, *11*, 17234–17246.
43. Wang, J.; Li, B.; Pu, X.; Wang, X.; Cooper, R. C.; Gui, Q.; Yang, H. Injectable Multicomponent Biomimetic Gel Composed of Inter-Crosslinked Dendrimeric and Mesoporous Silica Nanoparticles Exhibits Highly Tunable Elasticity and Dual Drug Release Capacity. *ACS Appl. Mater. Interfaces* **2020**, *12*, 10202–10210.
44. Santo, V. E.; Gomes, M. E.; Mano, J. F.; Reis, R. L. Controlled Release Strategies for Bone, Cartilage, and Osteochondral Engineering—Part II: Challenges on the Evolution from Single to Multiple Bioactive Factor Delivery. *Tissue Eng. Part B Rev.* **2013**, *19*, 327–352.
45. Lim, S. M.; Oh, S. H.; Lee, H. H.; Yuk, S. H.; Im, G. Il; Lee, J. H. Dual Growth Factor-Releasing Nanoparticle/Hydrogel System for Cartilage Tissue Engineering. *J. Mater. Sci. Mater. Med.* **2010**, *21*, 2593–2600.
46. Park, J. S.; Yang, H. N.; Woo, D. G.; Chung, H.-M.; Park, K.-H. In Vitro and in Vivo Chondrogenesis of Rabbit Bone Marrow–Derived Stromal Cells in Fibrin Matrix Mixed with Growth Factor Loaded in Nanoparticles. *Tissue Eng. Part A* **2009**, *15*, 2163–2175.
47. Shi, D.; Xu, X.; Ye, Y.; Song, K.; Cheng, Y.; Di, J.; Hu, Q.; Li, J.; Ju, H.; Jiang, Q. Photo-Cross-Linked Scaffold with Kartogenin-Encapsulated Nanoparticles for Cartilage Regeneration. *ACS Nano* **2016**, *10*, 1292–1299.
48. Newsom, J. P.; Payne, K. A.; Krebs, M. D. Microgels: Modular, Tunable Constructs for Tissue Regeneration. *Acta Biomater.* **2019**, *88*, 32–41.
49. Bian, L.; Zhai, D. Y.; Tous, E.; Rai, R.; Mauck, R. L.; Burdick, J. A. Enhanced MSC Chondrogenesis Following Delivery of TGF-B3 from Alginate Microspheres within Hyaluronic Acid Hydrogels in Vitro and in Vivo. *Biomaterials* **2011**, *32*, 6425–6434.
50. Sandker, M. J.; Duque, L. F.; Redout, E. M.; Klijnstra, E. C.; Steendam, R.; Kops, N.; Waarsing, J. H.; Van Weeren, R.; Hennink, W. E.; Weinans, H. Degradation, Intra-Articular Biocompatibility, Drug Release, and Bioactivity of Tacrolimus-Loaded Poly (Dl-Lactide-PEG)-b-Poly (l-Lactide) Multiblock Copolymer-Based Monospheres. *ACS Biomater. Sci. Eng.* **2018**, *4*, 2390–2403.
51. Zhao, X.; Liu, S.; Yildirimer, L.; Zhao, H.; Ding, R.; Wang, H.; Cui, W.; Weitz, D. Injectable Stem Cell-laden Photocrosslinkable Microspheres Fabricated Using Microfluidics for Rapid Generation of Osteogenic Tissue Constructs. *Adv. Funct. Mater.* **2016**, *26*, 2809–2819.
52. Li, F.; Truong, V. X.; Thissen, H.; Frith, J. E.; Forsythe, J. S. Microfluidic Encapsulation of Human Mesenchymal Stem Cells for Articular Cartilage Tissue Regeneration. *ACS Appl. Mater. Interfaces* **2017**, *9*, 8589–8601.
53. Liu, X.; Yang, Y.; Li, Y.; Niu, X.; Zhao, B.; Wang, Y.; Bao, C.; Xie, Z.; Lin, Q.; Zhu, L. Integration of Stem Cell-Derived Exosomes with in Situ Hydrogel Glue as a Promising Tissue Patch for Articular Cartilage Regeneration. *Nanoscale* **2017**, *9*, 4430–4438.
54. Fortier, L. A.; Barker, J. U.; Strauss, E. J.; McCarrel, T. M.; Cole, B. J. The Role of Growth Factors in Cartilage Repair. *Clin. Orthop. Relat. Res.* **2011**, *469*, 2706–2715.
55. Qu, M.; Jiang, X.; Zhou, X.; Wang, C.; Wu, Q.; Ren, L.; Zhu, J.; Zhu, S.; Tebon, P.; Sun, W. Stimuli-Responsive Delivery of Growth Factors for Tissue Engineering. *Adv. Healthc. Mater.* **2020**, *9*, 1901714.
56. Qasim, M.; Chae, D. S.; Lee, N. Y. Bioengineering Strategies for Bone and Cartilage Tissue Regeneration Using Growth Factors and Stem Cells. *J. Biomed. Mater. Res. Part A* **2020**, *108*, 394–411.
57. Gugjoo, M. B.; Amarpal, G. T.; Aithal, H. P.; Kinjavdekar, P. Cartilage Tissue Engineering: Role

of Mesenchymal Stem Cells along with Growth Factors & Scaffolds. *Indian J. Med. Res.* **2016**, *144*, 339.
58. Augustyniak, E.; Trzeciak, T.; Richter, M.; Kaczmarczyk, J.; Suchorska, W. The Role of Growth Factors in Stem Cell-Directed Chondrogenesis: A Real Hope for Damaged Cartilage Regeneration. *Int. Orthop.* **2015**, *39*, 995–1003.
59. Levinson, C.; Lee, M.; Applegate, L. A.; Zenobi-Wong, M. An Injectable Heparin-Conjugated Hyaluronan Scaffold for Local Delivery of Transforming Growth Factor B1 Promotes Successful Chondrogenesis. *Acta Biomater.* **2019**, *99*, 168–180.
60. Fan, W.; Yuan, L.; Li, J.; Wang, Z.; Chen, J.; Guo, C.; Mo, X.; Yan, Z. Injectable Double-Crosslinked Hydrogels with Kartogenin-Conjugated Polyurethane Nano-Particles and Transforming Growth Factor B3 for in-Situ Cartilage Regeneration. *Mater. Sci. Eng. C* **2020**, *110*, 110705.
61. Vayas, R.; Reyes, R.; Arnau, M. R.; Évora, C.; Delgado, A. Injectable Scaffold for Bone Marrow Stem Cells and Bone Morphogenetic Protein-2 to Repair Cartilage. *Cartilage* **2019**, 1947603519841682.
62. Silva, C.; Carretero, A.; da Costa, D. S.; Reis, R. L.; Novoa-Carballal, R.; Pashkuleva, I. Design of Protein Delivery Systems by Mimicking Extracellular Mechanisms for Protection of Growth Factors. *Acta Biomater.* **2017**, *63*, 283–293.
63. Mahzoon, S.; Detamore, M. S. Chondroinductive Peptides: Drawing Inspirations from Cell–Matrix Interactions. *Tissue Eng. Part B Rev.* **2019**, *25*, 249–257.
64. Jooybar, E.; Abdekhodaie, M. J.; Alvi, M.; Mousavi, A.; Karperien, M.; Dijkstra, P. J. An Injectable Platelet Lysate-Hyaluronic Acid Hydrogel Supports Cellular Activities and Induces Chondrogenesis of Encapsulated Mesenchymal Stem Cells. *Acta Biomater.* **2019**, *83*, 233–244.

Acknowledgments

First of all, I want to thank Marcel Karperien for offering me the PhD position. Marcel, you have been a great supervisor to me. I particularly appreciated your courage and inspiration on my work. I have learned a lot on both professional and personal fronts from you. I am convinced your advice will be continuously support during my future professional career.

I would also like to thank my daily supervisor Sanne Both. Sanne, your passional, bright, and creative mind is really inspiring. The time that you drive me around to get me familiar with this place is still so vivid to me. You taught me most of the written and unwritten lessons contributing my development as a scientist. This is of great value to me. It's my honor to have you as daily supervisor and friend during my PhD training.

It has been a great time in the department of Developmental BioEngineering, therefore, I would like to thank all my direct and indirect colleagues. Many thanks to Bram Zoetebier. I really enjoyed the time to work on the hydrogels together with you. It has been a great pleasure to walk around the campus and the city in the Nottingham with you and Barbara and Casper. Carlo Paggi, I am grateful for our intensive collaboration. You are a smart, optimistic, and hardworking scientist. I thank you for all your enthusiasm shared with me and the talking between us. In bocca al lupo! Kannan Govindaraj, as my longest officemate, I really enjoyed all the

discussions and laughs with both you and Sakshi. I also would like to thank Jacqueline for lab introduction and technical support and advise; Janine Post for the motivated discussion and meetings; Piet Dijkstra for valuable input on my work; Janneke Alers for giving me the opportunity to tutor some excellent students; Ingrid van der Schoor for great administrative support; and of course Bas, Brenda, Elaheh, Jan, Joao, Lisanne, Maik, Michelle, Milou, Sieger, and Tom, for all the enjoyable discussions, laughs, coffee times, and group outings.

I would also like to acknowledge all members of my graduation committee. During my PhD training, I was constantly inspired by your scientific work. It is an honor to present this thesis to you.

Please allow me to express my thanks in Chinese in the following part.
感谢果哥，无法想象如果没有你最初几个月的做伴，我会以怎样艰难的开局打开这个新的地图。也因着果哥的关系，认识了在恩村的第一个朋友，奎哥。从我抵荷伊始的结识到送我上车踏上归国的行程，奎哥贯穿了我在恩村的整个旅途。真的非常感谢奎哥作为朋友的陪伴和作为大哥的交心，也感谢熊总对我无数次叨扰的热心招待，衷心希望你们能够一直幸福认真的生活。另外这段时间最幸运的事情之一，就是结识了愿意收留我给我提供堪称完美住所的荣姐和小林。无论在工作还是生活上，我都从荣姐那里学习到了很多东西，希望荣姐能够继续开创自己的事业，同时跟小林继续幸福美好的生活。蕾蕾和晓斌哥，感谢你们在工作和生活上对我的莫大帮助，也是晓斌哥让我晓得了什么是真正的勤奋和忘我工作。宇昕，你的英伦范儿让我欣羡你的生活

态度让我欣赏，希望你能拥抱未来美好的生活。正潮，每次跟你谈心都会让我大有收获，希望你能抛开过去开启新的篇章。敏敏和洪林，谢谢你们一直以来的陪伴和生活上的帮助。钟林，感谢你们多次的款待，希望你们在荷兰的生活一切顺利，古一小朋友能够健康活泼地成长。韩进，谢谢你对我在生活上的耐心，相信你工作上的努力终会有回报。另外还有文龙、王灿、文博、曾丹、若楠等小伙伴，谢谢与你们一起度过的愉快时光。感谢林云锋老师为我提供的机会和支持。谢谢娜姐和琴姐对我工作的督促和生活的关心。此外，也要感谢郭德纲和于谦两位老师在无数个日夜中的陪伴。

感谢父母多年来的养育之恩。从大学算起，已是离家十载有余，多是聚少离多，不能随侍膝下，而立之后，每念及此思虑良多，希望我的表现能够让你们骄傲，也以此告慰爷爷与外公。

愿健康与幸福陪伴我的家人与朋友。也祝我自己拥有美好的明天。

Love you, Cecilia.

Live Long and Prosper.

Yao Fu

Biography

Yao Fu was born on the 24th of March in Suzhou, Anhui province of China. In 2011 he received his Bachelor of Veterinary Medicine degree from the Anhui Science and Technology University, China. In September 2011 he started his master project under the supervision of Prof. Dr. Yunfeng Lin at the Sichuan University, China. During his studies he focused on the proliferation and osteogenic differentiation of iPS cells derived from murine adipose stem cells. In the meanwhile, he pursued the study of osteoporosis disease, including compare the adipogenic potential of adipose tissue-derived stem cells obtained from ovariectomized mice with that of control ADSCs, and analyze the pathological mechanism from the point of functional changes of ADSCs. He also participated in some other research works, including the experiment of different biomaterials combined stem cells to repair cartilage defects. He obtained his master of Preclinical Stomatology degree in 2014. And then he started his PhD training at the department of Developmental BioEngineering within the MIRA Institute for Biomedical Technology and Technical Medicine at the University of Twente under the supervision of Prof. Dr. Marcel Karperien. The project of his research was investigating the cellular interactions in cell-based cartilage repair. For part of the work described in this thesis, he received travel grant to promote the continuance of this project.

Scientific Output

Publications

Y Fu, L Karbaat, L Wu, J Leijten, SK Both, M Karperien. Trophic effects of mesenchymal stem cells in tissue regeneration; Tissue Engineering Part B: Reviews 23 (6), 515-528

CA Paggi*, A Dudakovic*, **Y Fu***, CG Garces, M Hevesi, D Galeano Garces, A B Dietz, A J van Wijnen, M Karperien. Autophagy Is Involved in Mesenchymal Stem Cell Death in Coculture with Chondrocytes. CARTILAGE. July 2020.

Y Fu*, B Zoetebier*, S Both, PJ Dijkstra, M Karperien. Engineering of Optimized Hydrogel Formulations for Cartilage Repair. Polymers 13 (9), 1526

Y Fu, N Georgi, J Leijten, S Both, M Karperien. Beneficial effects of MSCs on co-cultured chondrocytes are independent of inter-donor chondrogenesis variation; *Submitted*.

Y Fu, S Henke, S Both, J Leijten, B Zoetebier, M Karperien. High throughput generated micro-aggregates of MSCs and primary chondrocytes as a model to investigate cell to cell communication; *In Preparing*.

Y Fu, Marcel Karperien, et al. Preliminary in vivo evaluation Hyaluronic acid and Dextran hybrid injectable hydrogels for cartilage tissue engineering application. *In Preparing*.

Y Fu, S Both, M Karperien. Interaction between MSCs and Chondrocyte modifies impact of signal modulators. *In Preparing*.

Wang R, Que I, **Y Fu**, Both S., Chan A., Dijkstra P. J., Karperien, M. Non-invasive near-infrared fluorescence in vivo imaging of biodegradable enzymatically crosslinked polysaccharide hydrogels. *In preparing*.

Y Fu, Yunfeng Lin, et al. Adipogenic differentiation potential of adipose derived mesenchymal stem cells from ovariectomized mice; Cell Proliferation, 47 (6), 604-614

Y Fu, Yunfeng Lin, et al. Potential Replication of Induced Pluripotent Stem Cells for Craniofacial Reconstruction; Current Stem Cell Research & Therapy, 2014, 9 (3), 205-214

Book Chapter

Y Fu, CA Paggi, A Dudakovic, AJ van Wijnen, JN Post, M Karperien. Book Chapter: Engineering cartilage tissue by co-culturing of chondrocytes and mesenchymal stromal cells. Osteoporosis and Osteoarthritis, 53-70

Abstracts

Y Fu, R Wang, S Both, P Dijkstra, M Karperien. Tracking the degradation of polysaccharide hydrogels by non-invasive near-infrared fluorescence imaging (Oral presentation). NBTE, 2015, Lunteren, NL

Y Fu, S Henke, S Both, J Leijten, B Zoetebier, M Karperien. High throughput generated micro-aggregates of MSCs and chondrocytes as a model to investigate cell-cell communication (Poster presentation). NBTE, 2016, Lunteren, NL

Y Fu, R Wang, S Both, P Dijkstra, M Karperien. Tracking the degradation of polysaccharide hydrogels by non-invasive near-infrared fluorescence imaging; Osteoarthritis and Cartilage 2016; 24(1):S150. OARSI, 2016, Amsterdam, NL

CA Paggi*, **Y Fu***, A Dudakovic, C Galeano Garces, M Hevesi, D Galeano Garces, A J. van Wijnen, M Karperien. Autophagy drives the therapeutic

effect of MSCs in single-stage cell-based cartilage regeneration. ICRS, 2019.

B Zoetebier, K Sivasubramaniyan, M Puricelli, **Y Fu**, J Hendriks, L Kock, GJVM van Osch, M Karperien. ENZYMATICALLY CROSSLINKED NATURAL POLYMERS FOR CARTILAGE REPAIR. Orthopaedic Proceedings 103 (SUPP_4), 109-109